SEA
GRANT
PROJECT
OFFICE

A MATHEMATICAL MODEL FOR THE PREDICTION OF UNSTEADY SALINITY INTRUSION IN ESTUARIES

By

M. Llewellyn Thatcher

and

Donald R. F. Harleman

Massachusetts Institute of Technology

Cambridge, Massachusetts 02139

Report No. MITSG 72-7

February 25, 1972

A MATHEMATICAL MODEL FOR THE PREDICTION OF UNSTEADY SALINITY INTRUSION IN ESTUARIES

By

M. Llewellyn Thatcher

and

Donald R. F. Harleman

Report No. MITSG 72-7

Index No. 72-307-Ccb

ABSTRACT

The salinity structure of a tidal estuary fed by upstream fresh water sources is an important factor of water quality. In addition, this structure is intimately related to the circulation of the estuary because of density currents induced by the salt-fresh water relation.

Previous investigations in two and three dimensions have been limited to extremely simplified geometrical and steady-state assumptions. One-dimensional studies have considered the variable area case, but have been limited to descriptive rather than predictive methods because of the difficulty of handling the downstream boundary condition for the one-dimensional salt balance equation and because of the necessity to specify a longitudinal dispersion coefficient based on field data for the estuary being studied.

This study presents a predictive numerical model of unsteady salinity intrusion in estuaries by formulating the problem in finite-difference terms using the one-dimensional, tidal time, variable area equations for the conservation of water mass, conservation of momentum and conservation of salt. Tidal time means a time scale of calculation larger than that defining turbulence, but much smaller than a tidal period in order to correctly represent the tidal advection within a tidal period. The tidal dynamic equations are coupled to the conservation of salt equation through a salinity-density relationship, and the ocean boundary condition for salt is formulated in a manner which depends on the direction of flow at the entrance to the estuary.

The longitudinal dispersion coefficient has been shown to be proportional to the magnitude of the local, time-varying longitudinal salinity gradient, and this constant of proportionality has been shown to depend on a dimensionless parameter which expresses the degree of vertical stratification of the estuary. This relationship has been established for a wide range of stratification conditions.

The mathematical model has been verified using data from the Waterways Experiment Station salinity flume and field data from the Delaware, the Potomac, and the Hudson. By specifying initial conditions, fresh water hydrographs, and tidal elevations at the ocean, it is possible to predict the time-varying salinity using this model.

ACKNOWLEDGEMENT

Primary support for this study came from the Office of Sea Grant, National Oceanic and Atmospheric Administration, U.S. Department of Commerce, Coherent Area Project Grant GH-88 and 2-35150, under the Estuary Modeling Program underway at the Ralph M. Parsons Laboratory for Water Resources and Hydrodynamics of the Department of Civil Engineering. Partial support was also provided by a grant from the Henry L. and Grace Doherty Charitable Foundation, Inc. This program is under the administrative and technical supervision of Professor Arthur T. Ippen and Professor Donald R.F. Harleman (DSR 72602 and DSR 73479). The purpose of the Estuary Modeling Program is to develop analytical and numerical techniques for modeling the behavior of estuaries and coastal embayments in order to extend the basic understanding of estuarine dynamics and the ability to make predictions relating to the estuarine environment.

The study of one of the test cases, the Hudson Estuary, was supported by the consulting firm of Quirk, Lawler & Matusky Engineers under DSR 73308.

The study of the Delaware Estuary would not have been possible without the cooperation and helpfulness in providing field data by Mr. W. H. Bobb of the Waterways Experiment Station, Corps of Engineers, and by Mr. J. F. Phillips and Mr. E. L. Dodson of the Philadelphia District, Corps of Engineers, Department of the Army.

The writers wish to express their appreciation to Dr. Arthur T. Ippen, Institute Professor, to Dr. Frank E. Perkins, Associate Professor of Civil Engineering, and to Dr. John D. Ditmars, Visiting Assistant Professor of Civil Engineering, for their interest and many helpful suggestions. Miss Alician Quinlan, Mr. Dennis Mahoney and Mr. David Najarian, Research Assistants, have provided valuable assistance in preparing the Hudson Estuary test case. Typing was done by Miss Susanna Natti.

The major part of the computer work was done at the M.I.T. Information Processing Center.

The material contained in this report was submitted by Mr. Thatcher in partial fulfillment of the requirements for the degree of Doctor of Science at M.I.T. Initial support for his study was received in the form of a National Science Foundation Traineeship.

TABLE OF CONTENTS

I. Introduction

1.1 The Tidal Estuary, Definitions

Definitions of estuaries are very broad and include almost any body of water which joins the ocean at the coast. Usually an estuary is defined by the fact that a land mass confines it in some way; for example, a marine biologist may consider salt marshes estuaries. However, for the purpose of this study additional restrictions will be imposed upon this broad definition.

This study is concerned with those bodies of water which are connected to the ocean at one end and fed by sources of fresh water as the water body's boundaries extend landward. The behavior of the estuary in terms of circulation and salinity is dependent upon many factors, but principally upon the tidal variation at the ocean, the estuarine geometry, and the inflows of fresh water.

The circulation in such a tidal estuary is three-dimensional and is complicated by the fact that as fresh water enters the estuary it is lighter than the water coming from the ocean and consequently a tendency to stratify is inherent. Thus the circulation and salinity regimes are intimately related and a detailed investigation of one by necessity involves the other.

Fortunately, it is possible to take advantage of the distinct characteristics of individual estuaries and to introduce certain assumptions about their behavior, thus making the study of the salinity regime and the circulation possible. These assumptions also serve as a means of classifying individual estuaries. Pritchard (1955) has

classified estuaries in terms of steady-state considerations of the principal advective and dispersive transport processes.

Starting with a three-dimensional representation of the salt balance equation, one can write for the steady-state, time-averaged-over-a-tidal-cycle condition:

$$\bar{u}\frac{\partial \bar{s}}{\partial x} + \bar{v}\frac{\partial \bar{s}}{\partial y} + \bar{w}\frac{\partial \bar{s}}{\partial z} = \frac{\partial}{\partial x}\left[\bar{e}_x \frac{\partial \bar{s}}{\partial x}\right] + \frac{\partial}{\partial y}\left[\bar{e}_y \frac{\partial \bar{s}}{\partial y}\right] + \frac{\partial}{\partial z}\left[\bar{e}_z \frac{\partial \bar{s}}{\partial z}\right] \quad (1\text{-}1$$

where the time-averaged-over-a-tidal-cycle quantities are:

1) $\bar{u}$, $\bar{v}$, and $\bar{w}$, the fluid velocities in the longitudinal, vertical and lateral directions x, y, and z,

2) $\bar{s}$, the local salinity at coordinates x, y, and z, and

3) $\bar{e}_x$, $\bar{e}_y$, $\bar{e}_z$, the turbulent diffusion coefficients for this time-averaged equation.

In the case of a laterally homogeneous, highly stratified or salt-wedge situation as produced by small tidal action with respect to strong fresh water discharge, Pritchard shows that the salt balance Equation 1-1 can be approximated by

$$\bar{u}\frac{\partial \bar{s}}{\partial x} + \bar{v}\frac{\partial \bar{s}}{\partial y} = 0 \quad (1\text{-}2)$$

Thus a classification of type A is assigned to the salt wedge type as shown in Figure 1.1a. As the tidal action increases in proportion to fresh water discharge, the salt-fresh interface of the type A estuary breaks down and the vertical transport of salt becomes important. In mathematical terms Equation 1-1 is now approximated by

Note: Circulation represented is time-averaged over a tidal cycle.

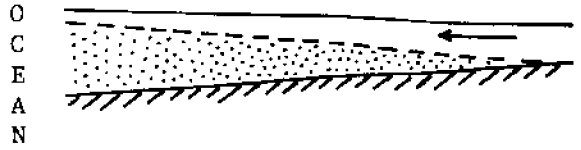

Salt wedge, stratified.
Weak tidal action and strong fresh water discharge.
Laterally homogeneous.

(a) Type A

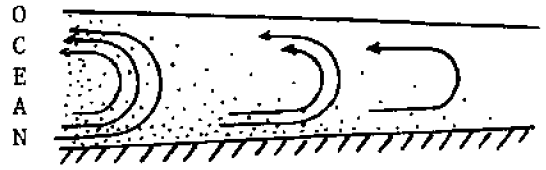

Moderate stratification or partially mixed.
Laterally homogeneous.

(b) Type B

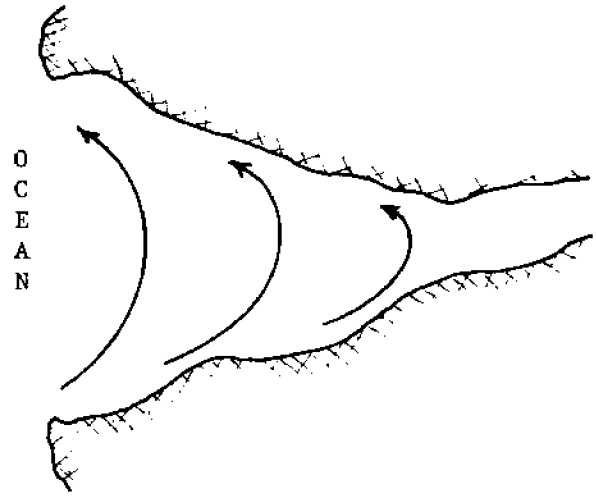

Circulation due to Coriolis effects.
Vertically homogeneous.

(c) Type C

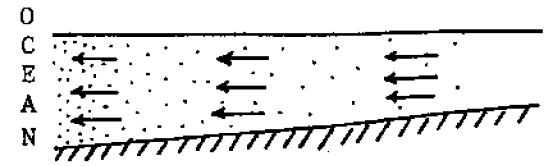

Well mixed.
Vertically and laterally homogeneous.

(d) Type D

Pritchard's Classification of Estuaries

Figure 1.1

$$\bar{u}\frac{\partial \bar{s}}{\partial x} + \bar{v}\frac{\partial \bar{s}}{\partial y} = \frac{\partial}{\partial y}\left[\bar{e}_y \frac{\partial \bar{s}}{\partial y}\right] \tag{1-3}$$

and the estuary is called type B (Figure 1.1b).

As vertical mixing reaches the point where the estuary is both vertically and laterally homogeneous the downstream advective flux becomes balanced by an upstream dispersive flux. Equation 1-1 is approximated by

$$\bar{u}\frac{\partial \bar{s}}{\partial x} = \frac{\partial}{\partial x}\left[\bar{e}_x \frac{\partial \bar{s}}{\partial x}\right] \tag{1-4}$$

and the estuary called type D (Figure 1.1d). In the case of a wide estuary not laterally homogeneous, but vertically homogeneous, the Coriolis effect may produce a lateral salinity gradient. Under these conditions Pritchard approximates the steady-state by

$$\bar{u}\frac{\partial \bar{s}}{\partial x} + \bar{w}\frac{\partial \bar{s}}{\partial z} = \frac{\partial}{\partial z}\left[\bar{e}_z \frac{\partial \bar{s}}{\partial z}\right] \tag{1-5}$$

and designates the estuary type C (Figure 1.1c).

This study pertains to estuaries wherein lateral homogeneity is assumed, but where vertical homogeneity is not necessarily present. In terms of Pritchard's classification, this study treats class B (partially mixed or moderately stratified) estuaries with class D being included as the limiting case. The degree of stratification which can be treated by the method to be described in this study is difficult to establish a priori, because the accuracy of the method will decrease as stratification becomes extreme. The results described

in Chapter 7 show that class B estuaries have been successfully treated. It is not intended to treat class A or wedge type estuaries.

1.2 Predominant Influences on Salinity Intrusion

The geometry of each estuary has its effect on the circulation and salinity distribution; however, given a particular geometry, the two primary factors influencing the salinity intrusion are the time history of the fresh water inflows and the range and mean tidal elevation at the ocean entrance. The manner in which these two boundary conditions determine the time varying salinity distribution is the subject of this study.

Cohen and McCarthy (1962) have made observations of the salinity distribution in the Delaware Estuary. Figure 1.2 shows the interrelation between the source of fresh water and the source of salt water in the Delaware. July, 1954 was a period of low fresh water flow for the Delaware as indicated by the fresh water inflow hydrograph of Figure 1.2. The effect of this long period of low fresh water discharge is clearly demonstrated in terms of the maximum and minimum chlorides which show the salinity front advancing upstream. As an example of the effect of the tidal elevation at the ocean entrance, Cohen and McCarthy point out that the peak chloride on October 15 was the result of an abnormally high tide as reflected in the mean river level peak for the same day. In general there is a quick response to the ocean boundary condition as in the October 15th peak, and a slower response to changes in the fresh water discharge boundary conditions as evidenced by the gradual increase of salinity during the July low

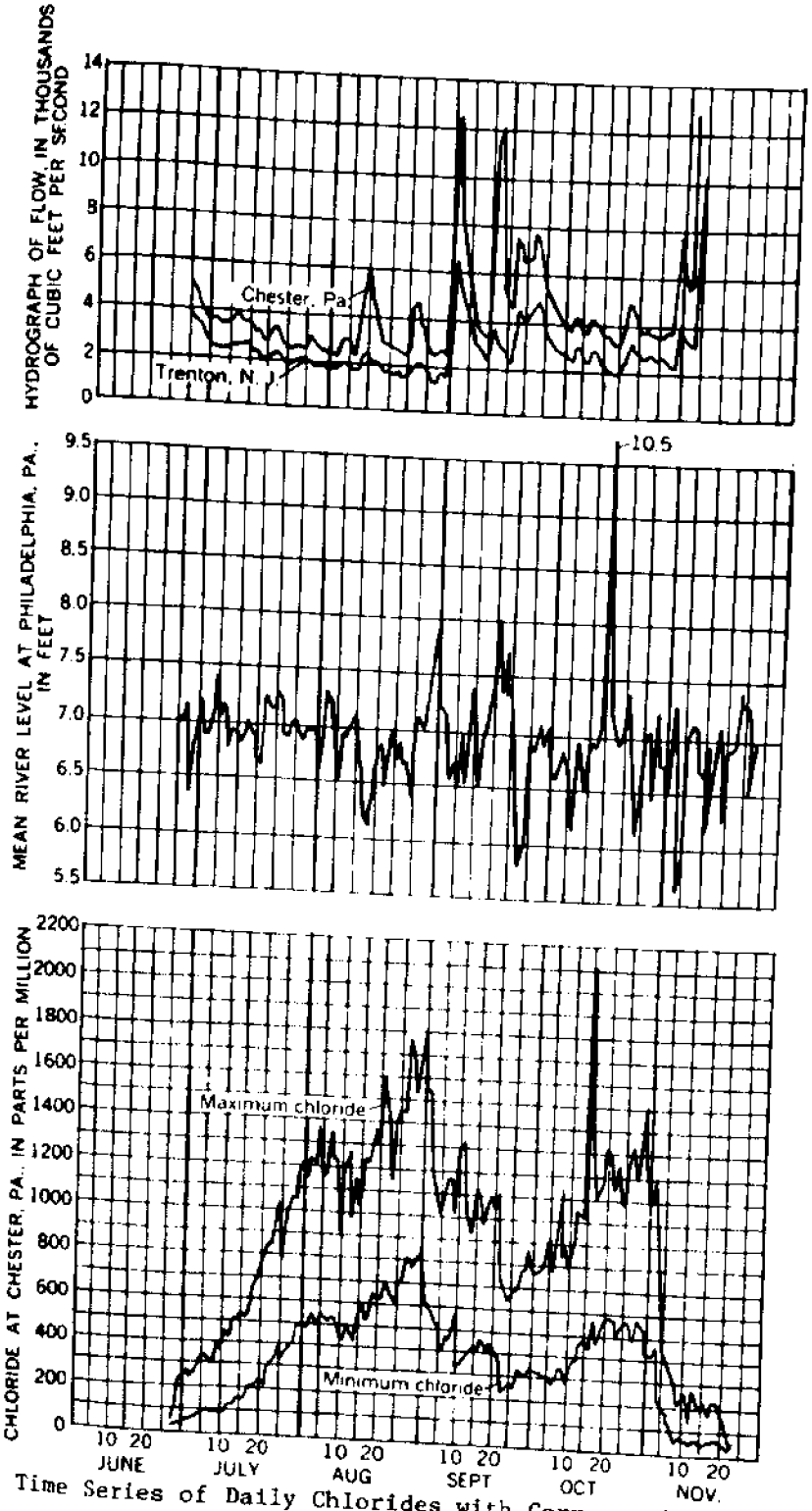

Time Series of Daily Chlorides with Corresponding Hydrograph and Mean River Level (from Cohen and McCarthy, 1962)

Figure 1.2

flow period.

1.3 Descriptions and Predictions of Salinity Intrusion

In the most general sense a description or prediction of the salinity intrusion would be in terms of the salinity at all points in the estuary at any time 't'. Such a three-dimensional specification is beyond the state of the art at this time. Even two-dimensional studies in which the salinity varies in the longitudinal and vertical directions have been restricted to descriptive mathematical models limited by steady-state assumptions, simple geometric configurations, and simplified boundary conditions. Thus descriptions and predictions of salinity intrusion have been primarily limited to the one-dimensional formulation wherein salinity at a longitudinal position 'x' is assumed to be representative of the entire cross-section.

To predict the salinity distribution in a tidal estuary the one-dimensional salt balance equation in tidal time becomes the appropriate mathematical model. The expression "tidal time" refers to a time scale much less than that of a tidal cycle but greater than that defining turbulence (for example, a time scale of the order of minutes in the case of a 12-hour diurnal tide). The one-dimensional tidal time salt balance equation for a variable area estuary, which will be discussed in detail in Chapter 3, is:

$$\frac{\partial s}{\partial t} + u \frac{\partial s}{\partial x} = \frac{1}{A} \frac{\partial}{\partial x} \left[EA \frac{\partial s}{\partial x} \right] \qquad (1\text{-}6)$$

where

$s(x,t)$ is the salinity representative of the entire cross-section at x,

$u(x,t)$ is the cross-sectional average longitudinal velocity, including tidal and fresh water components,

$A(x,t)$ is the cross-sectional area, and

$E(x,t)$ is the longitudinal dispersion coefficient.

In order to solve Equation 1-6 by numerical or other techniques the variables u, A and E must be specified. The velocity, $u(x,t)$ and the area $A(x,t)$ can be determined only if the tidal hydraulics are known. Such knowledge can be obtained by numerically solving the equations of continuity and momentum at the same time that one solves the salt balance Equation 1-6.

The longitudinal dispersion coefficient $E(x,t)$ must also be specified in order to solve Equation 1-6. Although $E(x,t)$ can be defined in terms of available hydraulic and geometric parameters for a completely mixed estuary, its definition in the partially mixed region has long been one of the major difficulties in the study of salinity intrusion. Usually field data is resorted to in order to obtain some estimate of $E(x,t)$. Such studies are expensive and the results do not make the mathematical model a predictive one because the solutions obtained are valid only for the conditions under which the data was taken.

In earlier studies, the difficulties of dealing with the tidal motion were circumvented by the development of two basic simplifications of Equation 1-6, both of which replace the tidal time velocity, u, by a non-tidal advective velocity u_f, this latter velocity being the

average fresh water velocity during the tidal cycle.

The first of these simplifications is obtained by averaging Equation 1-6 over a tidal cycle. The resulting equation is

$$\frac{\partial \bar{s}}{\partial t} + u_f \frac{\partial \bar{s}}{\partial x} = \frac{1}{\bar{A}} \frac{\partial}{\partial x} \left[E^{TA} \bar{A} \frac{\partial \bar{s}}{\partial x} \right] \qquad (1\text{-}7)$$

This is similar in form to Equation 1-6 but the velocity is no longer in tidal time but is u_f, the average fresh water velocity during the tidal cycle and the salinity, $\bar{s}$, is the salinity of the cross-section averaged over a tidal cycle. The area, $\bar{A}$, being averaged over a tidal cycle, no longer reflects tidal variations in the water surface. The dispersion coefficient $E^{TA}(x)$ is not the same as the $E(x,t)$ of Equation 1-6 and is not equal to the average value of $E(x,t)$ over a tidal cycle. In fact, the $E^{TA}(x)$ distribution must be determined by fitting solutions of Equation 1-7 to known physical data in terms of time-averaged salinities.

The second simplification of the tidal time salt balance equation is obtained by the slack tide approximation. This approximation assumes that, at a time near that of slack water, the salt balance in the estuary can be described by

$$\frac{\partial s}{\partial t} + u_f \frac{\partial s}{\partial x} = \frac{1}{A} \frac{\partial}{\partial x} \left[E^{SL} A \frac{\partial s}{\partial x} \right] \qquad (1\text{-}8)$$

wherein the salinity $s(x,t_{SL})$ is the salinity at slack tide, $A(x,t_{SL})$ is the area at slack tide, and $E^{SL}(x)$ is a new dispersion coefficient

which must be determined from physical slack tide data and is neither related to $E^{TA}(x)$ nor to the $E(x,t)$ of Equation 1-6. The similarity of the slack tide approximation to the average-over-a-tidal-cycle approximation is easily seen by comparison of the two Equations 1-7 and 1.8. This similarity does not imply that the dispersion coefficients are in any way related. In fact they are quite different as is shown in Figure 1.3. This figure was constructed by backfiguring the dispersion coefficient $E(x)$ from data presented by Stigter and Siemons (1967) using the time-averaged-over-a-tidal-cycle, the high water slack, and the low water slack salinity distributions. The difference exhibited points out the problem of relating continuing studies of a particular estuary to previous dispersion coefficients. If the assumptions of such studies are not consistent, the dispersion coefficients resulting from one study will not be valid in terms of another.

The elimination of the direct effects of tidal motion by these non-tidal approaches has simplified greatly the mathematical model, however this simplification has introduced additional difficulties and restrictions.

The requirement of a boundary condition on salinity at the ocean end of the estuary is especially difficult using these approaches. First of all, under the time-average-over-a-tidal-cycle approach one simply does not know the salinity or enough about the salinity to specify this boundary condition. Consequently, applications have required measurements of the salinity at the ocean boundary, or statistical predictions derived from such measurements, thereby making the

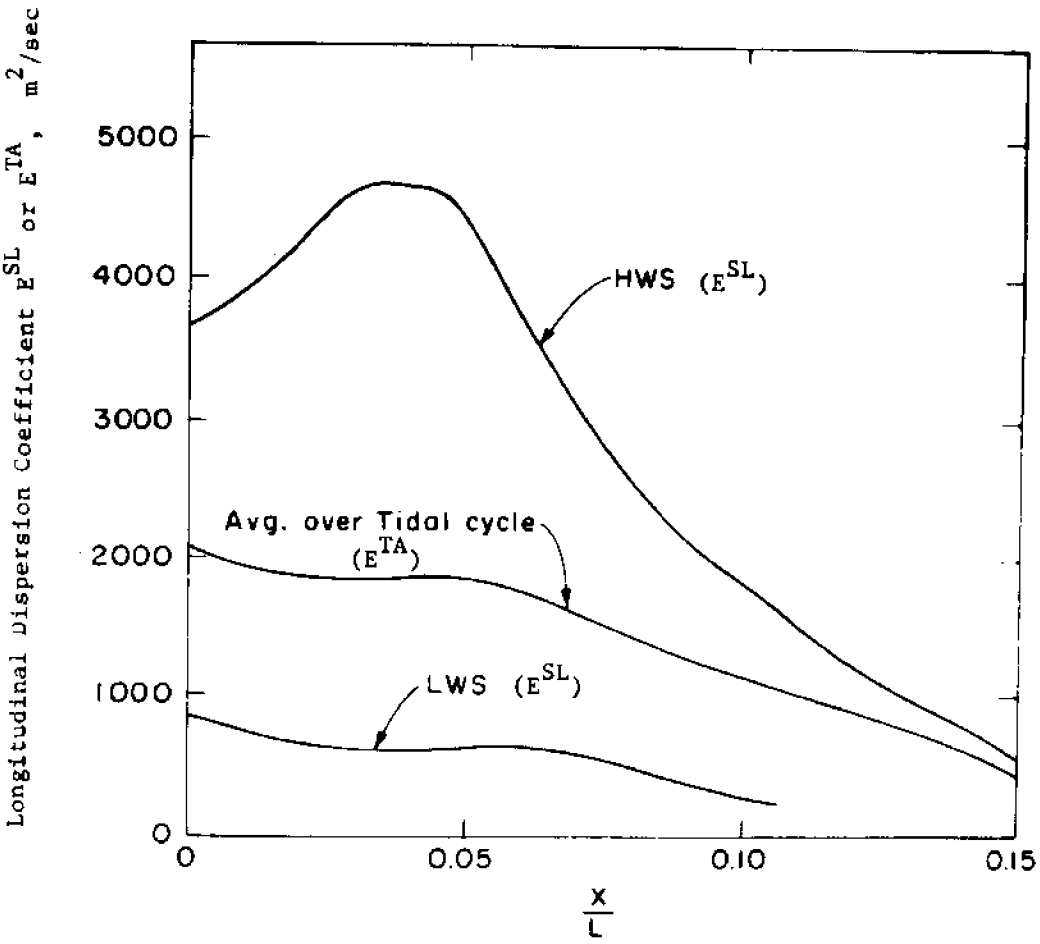

Comparison of Longitudinal Dispersion Coefficients for Assumptions of Time-Averaged Over a Tidal Cycle, High Water Slack and Low Water Slack
(Based on data from Stigter and Siemons, 1967)

Figure 1.3

mathematical model descriptive rather than predictive in nature. Under the slack tide approximation, the specification of salinity at the ocean boundary is still unresolved. In the low water slack case, one has no knowledge as to what the boundary salinity might be. In the high water slack case it is reasonable to assume it to be the ocean salinity, but then the problem becomes that of defining where the boundary salinity is located. Figure 1.4 illustrates the problem of specifying the salinity ocean boundary condition for the three cases: Low Water Slack (LWS), High Water Slack (HWS) and time-averaged-over-a-tidal-cycle (TA).

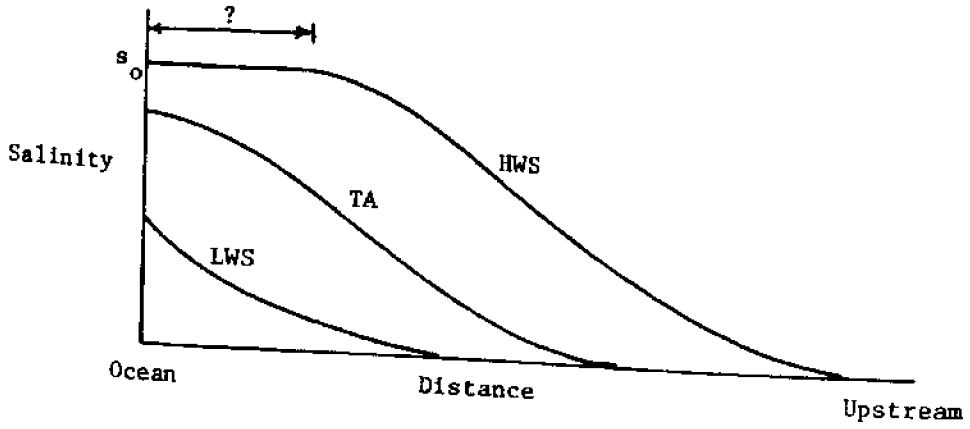

Typical Salinity Distributions
for Three Assumptions

Figure 1.4

An additional restriction on the use of the non-tidal time approaches is the inability to represent the effect of variations in the amplitude of the tide at the ocean entrance. Even changes in the mean sea-level elevation would require additional knowledge of the tidal hydraulics in order to incorporate the effects into the mathematical model. Thus studies of the transient behavior of the estuary which include the effect of the varying ocean elevation are not possible under these simplifications.

1.4 Objectives and Summary of This Study

The objective of this study is the development of a predictive, one-dimensional mathematical model for the transient salinity distribtuion. This is accomplished by means of simultaneous finite difference solutions to the tidal time salt balance Equation 1-6 and to the continuity and momentum equations which define the tidal motion. Coupling between the salt balance equation and the momentum equation is included by means of an equation of state relating salinity and density. The longitudinal dispersion coefficient is assumed to be proportional to the local longitudinal salinity gradient. The coefficient of proportionality is related to a stratification parameter involving the gross tidal and fresh water discharge properties of the estuary. It has been found that the boundary condition on salinity at the ocean entrance can be specified by using one condition during the flood tide and another condition during the ebb tide.

The resulting mathematical model, as solved by a finite-difference numerical technique, can be used in a predictive manner for

transient conditions of ocean surface elevation and time-varying fresh water discharges. Steady-state studies are also possible inasmuch as they represent cases of repeating ocean surface elevations and constant fresh water discharge. The results produced by the mathematical model are salinity, water surface elevation and discharge as functions of longitudinal distance and time. The salinity results can also be obtained in terms of high water slack, low water slack or time-averaged-over-the-tidal-cycle salinity distributions should they be desired.

II. Review of Previous Investigations

2.1 Tidal Prism Relationships

Ketchum (1951) has presented an approach to the steady state salinity intrusion problem based on dividing an estuary into segments whose lengths are equal to the average excursion of a particle of water during the flood tide. Complete mixing is assumed within each segment at high tide, and exchange coefficients are based on this assumption. As a result of the complete mixing assumption this method is limited to steady-state studies of estuaries where the well mixed condition is approached. Estuaries of this type are characterized by very large ratios of tidal prism to fresh water discharge and are a rather limited class as compared to the partially mixed estuary so common to the Atlantic coast of North America.

2.2 Steady State Investigations

Arons and Stommel (1951) used a time-averaged-over-a-tidal-cycle approach (Equation 1-7) for an estuary of rectangular cross-section and assumed that the longitudinal dispersion coefficient was proportional to the product of the tidal excursion length and the maximum tidal velocity at the entrance. The steady-state equation is

$$u_f \frac{\partial \bar{s}}{\partial x} = \frac{\partial}{\partial x} \left[E^{TA} \frac{\partial \bar{s}}{\partial x} \right] \qquad (2\text{-}1)$$

where $E^{TA} \sim L_{ex}\, u_o$, the tidal excursion times the maximum velocity at the entrance.

Integration of Equation 2-1 yielded a solution for the salinity

distribution as a function of two dimensionless parameters, x/L a distance parameter, and dimensionless parameter called the "Flushing number". As mentioned in Section 1.3, the ocean boundary salinity cannot be specified under these conditions except by having previous knowledge. The results are applicable only to steady-state studies of estuaries which can be approximated by a constant rectangular cross-section, but of special interest is the use of the flushing number which is a function of fresh water discharge, tidal amplitude, depth of the channel, tidal period and total estuary volume. This flushing number was proposed as a possible means of classifying estuaries.

Ippen and Harleman (1961) made an analytical study of salinity intrusion for the case of an estuary of rectangular cross section which took into account the tidal hydraulics inasmuch as the low water slack salinity distribution served for predicting the distribution at any other time during the tidal cycle. By analyzing twenty different salinity flume tests conducted at the Waterways Experiment Station (WES) they found that they could predict the salinity distributions when the dispersion coefficient in Equation 2-1 is expressed as an inverse function of x:

$$E^{LWS}_{(x)} = \frac{E^{LWS}_{o} B}{x + B} \qquad (2\text{-}2)$$

where x = 0 defines the ocean boundary. It is of interest to note that the distance parameter, B, is in reality a means of handling the problem of specifying the ocean boundary condition. B is the distance seaward from the boundary, x = 0, to a point where $s = s_o$ at low water

slack. (Note: The time-averaged equation is said to be applied for the low water slack salinity distribution, thus this is really a slack tide approximation.) Although this approach thus provides for the ocean boundary condition it now leaves the parameter B undetermined, but with the possibility of being correlated to stratification conditions.

One integration of Equation 2-1 yields

$$- u_f s = E^{LWS}_{(x)} \frac{\partial s}{\partial x} \tag{2-3}$$

A second integration with $E^{LWS}_{(x)}$ specified by 2-2 yields

$$\frac{s}{s_o} = \exp \left[- \frac{u_f}{2K^{LWS}_o} (x + B)^2 \right] \tag{2-4}$$

It was found that the parameters E^{LWS}_o and B could be correlated with a stratification number, G/J which is defined by the following ratio:

$$\frac{G}{J} = \frac{\text{rate of energy dissipation per unit mass of fluid}}{\text{rate of potential energy gain per unit mass of fluid}} \tag{2-5}$$

Ippen and Harleman have effectively made use of an analytical solution for the tidal hydraulics to provide a means of shifting the low water slack salinity distribution (Equation 2-4) so that distributions at other times throughout the tidal period can be found. The expression for the dispersion parameter $E^{LWS}_{(x)}$ as given by Equation 2-2 has reformulated the problem of ocean boundary condition and dispersion relationship in terms of the correlation of the two parameters B and E^{LWS}_o. The basis for this G/J relationship and the experimental work which leads

to its use as a stratification parameter are described by Ippen et. al (1960) and Harleman et. al (1961). Figures 2.1 and 2.2 show the correlation obtained by Ippen and Harleman in their study of the salinity flume tests.

Although the correlation of dispersion coefficient with the G/J parameter provided a means of predicting salinity distributions for a significant range of different fresh water flows and tidal amplitudes, the parameter itself is not a convenient one for real estuaries as the rate of energy dissipation is not simply obtained.

In addition, the method is limited to steady-state salinity distributions produced under conditions of constant fresh water inflow in estuaries of constant cross-section. Harleman and Abraham (1966) re-analyzed the W.E.S. data using the low water slack condition and the dispersion relationship of Equation 2-2 and found that a dimensionless parameter consisting of the tidal prism, Froude number (based on maximum tidal velocity at the ocean), fresh water discharge and tidal period was uniquely related to the stratification number G/J. This parameter, called estuary number is defined:

$$\mathbb{E} = \frac{P_T F_o^2}{Q_f T} \qquad (2\text{-}6)$$

where

P_t = tidal priam, defined as the volume of water entering the estuary on the flood tide

F_o = Froude number, $\frac{u_o}{\sqrt{gh}}$, u_o being the maximum flood

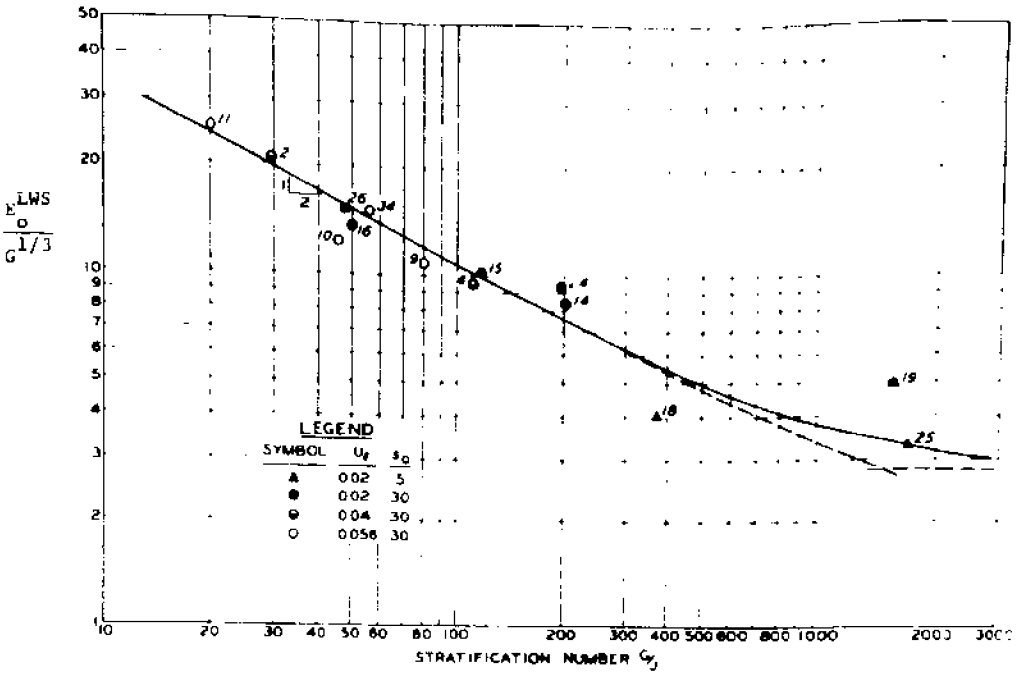

Correlation of Longitudinal Dispersion Coefficient K_o^{LWS}
with Stratification Number
(from Ippen and Harleman, 1961)

Figure 2.1

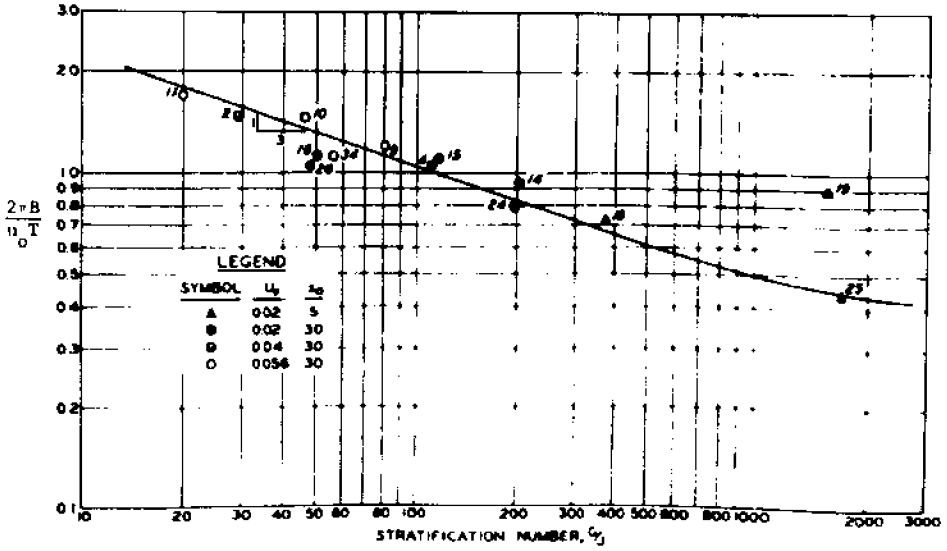

Correlation of Seaward Excursion Distance B
with Stratification Number
(From Ippen and Harleman, 1961)

Figure 2.2

velocity, h being the depth evaluated at the ocean

Q_f = fresh water discharge

T = tidal period.

Harleman and Abraham reformulated correlations of E_o^{LWS} B in terms of this new, more easily obtained estuary number; however an additional parameter $\frac{a}{h}$, (tidal amplitude/depth at the ocean) was required in the correlation of E_o^{LWS}. These correlations are:

$$\frac{E_o^{LWS}}{u_f B} = 0.055\left(\frac{h}{a}\right)^{2.7}\left[\frac{P_t F_o^2}{Q_f T}\right]^{1.2} \qquad (2\text{-}7)$$

$$\frac{2\pi B}{u_o T} = 0.70\left[\frac{P_t F_o^2}{Q_f T}\right]^{-0.2} \qquad (2\text{-}8)$$

An analysis of Rotterdam Waterway field data was successfully performed using this appraoch. These studies resulted in practical solutions for steady-state salinity intrusion for the case of constant geometry. It seemed reasonable that similar analytical techniques could be attempted for cases of variable area when this variation could be expressed in a simple form which permitted integration of the salt balance equation. However in studying an exponential area variation, Eronini (1968) found that different estuaries did not substantiate a general relationship sufficiently. For a particular variable area estuary, predictions of steady-state distributions based on information pertaining to one condition of stratification were developed (Harleman and Hoopes, 1963), but without any indications that the techniques

could be applied in a predictive manner to other estuaries.

In any case steady-state analyses impose definite limits with respect to prediction of salinity intrusion. Steady-state analyses are limited to conditions where an estuary is indeed in a quasi steady-state condition. This requires that both ocean tidal ranges and fresh water discharges remain relatively the same for a time period of the order of at least a month for most real estuaries. If salinity data is available at the end of such a period, steady-state analyses can be applied by back-calculating the dispersion coefficients using Equation 2-3. This dispersion relationship is valid for the conditions of fresh water discharge and average tidal range for which the data was taken, any extrapolation to other conditions is not justifiable without more data. Ward and Fischer (1971) have pointed out the limitations of the steady-state approach in their commentary on two papers by Paulson (1969, 1970) wherein they show that estuaries respond very slowly to changes in fresh water discharge, and that this response varies with location. Paulson appeared to have gathered salinity data corresponding to particular ranges of fresh water discharge in an effort to correlate longitudinal dispersion to fresh water discharge. The fact that the fresh water discharge was within a particular range does not imply anything as to whether or not a steady-state condition existed when that data was taken, consequently dispersion coefficients back-calculated on the basis of the steady-state assumption may be in error.

2.3 Mixing Parameter Approach

Preddy (1954) took a different approach in representing the

mixing which takes place in a tidal estuary. He assumed that at some point, x, along the estuary a unit amount of water would be distributed in the following manner during some time T. A proportion $P_1(x)$ is distributed uniformly seaward, a proportion $P_2(x)$ is distributed uniformly landward, and a proportion $1-P_1(x) - P_2(x)$ remains at location x. By applying the laws of conservation of salt and conservation of total mass Preddy derived the following integral equations.

$$\int_o^L s(x)\ A(x)\ P_2(x)\ \frac{L-x}{L}\ dx + \int_o^{-L} s(x)\ A(x)\ P_1(x)\ \frac{L+x}{L}\ dx = Q_f T s(x) + S \qquad (2\text{-}9)$$

$$\int_o^L A(x)\ P_2(x)\ \frac{L-x}{L}\ dx + \int_o^{-L} A(x)\ P_1(x)\ \frac{L+x}{L}\ dx = 0 \qquad (2\text{-}10)$$

where $s(x)$ is the average salt concentration during the period of time T, and S is the net change in salt upstream of the point of interest.

Preddy used long term average salinity and fresh water flow data for the Thames (1 January to 18 December) to permit the calculation of mixing parameters $P_1(x)$ and $P_2(x)$ by Equations 2-9 and 2-10. The L in this formulation is to be specified, a priori, as a length over which the mixing takes place, and is of the order of the excursion length. (Preddy took 9 miles in his Thames study.) Having derived the mixing parameters $P_1(x)$ and $P_2(x)$, he then shows that one can proceed to calculate new salinity distributions in time by a two step pro-

cess of: (1) displacing the water to allow for the natural flow and (2) calculating the new salinities at a number of points by numerical integration of the expression:

$$\frac{1}{A}\left[\int_{o}^{L} \frac{s(x)A(x)P_2(x)}{L} - dx + \int_{-L}^{o} \frac{s(x)A(x)P_1(x)}{L} dx \right.$$

$$\left. + s(x)\ A(x)\ (1-P_1(x) - P_2(x)\ )\right] \qquad (2\text{-}11)$$

The period of time, T, for this two step process is greater than a tidal cycle classifying the method as time varying, but averaged over a tidal cycle. By using a T of two tidal cycles Preddy predicted salinity distributions in the Thames Estuary at a time 14 days after a prescribed initial condition. Although the results were good for this particular case it is important to realize that the method is based on the assumption that mixing in an estuary is primarily a function of distance, and of some length L, and that this assumption ignores the effect of changing degrees of stratification which accompany changes in fresh water discharge. Furthermore the predictions for 14 days represents a short period of time in terms of an estuary's response to changes in fresh water flow and consequently, as compared to a period of about two months, the two-week prediction may show only that advection is the most important mechanism to be modeled. Finally it should be noted that a model of mixing which is <u>only</u> a function of location (x) is not a good representation of a process whose driving force is the salinity regime which itself is almost never stationary,

but on the contrary extremely mobile.

Di Toro (1969) has followed the basic philosophy advanced by Preddy but he has shown that the mixing process can be represented using an application of Markov chain theory. By employing a "maximum entropy" principle, Di Toro releases the method from Preddy's a priori L as a means of characterizing the mixing. The basic assumption that mixing is a function only of location has not been changed, however, so that even though the characterization of the mixing process has been placed on a more rational basis, it is none the less subject to the drawbacks of not reflecting changes in the stratification and in the location of the salinity region itself. It is also unfortunate that the boundary condition used by Di Toro in applying his method to the Delaware River Model Test Data was taken from the same distribution which he wished to derive. This was apparently due to absence of salinity data for the downstream regions, an unfortunate situation, but quite realistic, as interest in measuring salinity is rarely downstream near the ocean.

2.4 Unsteady Approach, But Time-Averaged Over a Tidal Cycle

Pritchard (1959) and later Boicourt (1969) have used an "averaged-over-a-tidal-cycle" approach of Equation 1-7 which written in a similar form is:

$$A \frac{\partial \bar{s}}{\partial t} + Q_f \frac{\partial \bar{s}}{\partial x} = \frac{\partial}{\partial x} \left[E^{TA} \bar{A} \frac{\partial \bar{s}}{\partial x} \right] \qquad (2\text{-}12)$$

As discussed in Section 1.3, the time average over a tidal cycle has produced the following changes: (1) it has changed the convection term

to one which contains the fresh water discharge, rather than the instantaneous discharge; (2) the area, $\bar{A}$, is no longer a function of time; and (3) the dispersion coefficient E^{TA} now includes the effect of the time averaging process. Also the effect of variations in the ocean tidal elevation cannot be accounted for as Equation 2-12 is uncoupled from the tidal dynamic equations.

Pritchard (1959) studied the longitudinal distribution of salinity in the Delaware Estuary as a function of time by using this time-averaged-over-a-tidal-cycle version of the one-dimensional convective-diffusion equation.

Using the Delaware River model data for steady-state conditions at flows of 16,475 cfs, 10,600 cfs and 5000 cfs he derived corresponding values of $E^{TA}\bar{A}$ from the steady-state Equation 2-3. Based on this information a correlation formula was derived to relate $E^{TA}\bar{A}$ to distance, x, and to fresh water flow, Q_f. The boundary conditions for a year's simulation were taken as fixed values of salinity at the ocean and at the upstream end. Using an implicit finite difference scheme, the response of the Delaware was simulated for different fresh water flow schemes on a weekly time spacing for 52 weeks.

This study was made primarily to compare the effects of different modifications of river inflow, and for this purpose has achieved its aim. However, the method does not present a complete solution to the prediction of longitudinal salinity for the following reasons.

1) It depends upon knowing, first of all, the manner in which the dispersion coefficients (time-averaged-over-

a-tidal-cycle) varies as a function of river flow. To know such a relationship implies having already available enough steady-state data so as to construct this correlation.

2) It requires a knowledge of the downstream, or ocean boundary, salinity which is really part of the solution. For Pritchard's study, assuming it to be constant, seems justified as he was making a comparison and also because he had data enabling him to schematize and predict $E^{TA}_{\bar{A}}$ all the way to the ocean. There are seasonal variations even in the ocean salinity, however, and these were not taken into account.

3) A complete study including the effect of tidal conditions is not possible due to the time-averaged over a tidal cycle assumption. Both the mean tide elevation and the high and low stages are important factors when studying transient salinity distributions as has been brought out by Cohen and McCarthy (1962) and Keighton (1966).

Boicourt (1969) has applied this same technique to a study of the salinity of Upper Chesapeake Bay. Instead of using steady-state salinity data to derive $E^{TA}_{\bar{A}}$ values he had an entire year's salinity records which he then interpolated to even intervals, integrated Equation 2-12 and obtained:

$$E^{TA}_{\bar{A}} = \frac{Q_f \bar{s}]_x + \int_o^x \bar{A} \frac{\partial \bar{s}}{\partial t} \, dx}{\left. \frac{\partial \bar{s}}{\partial x} \right|_x} \qquad (2\text{-}13)$$

wherein the $\bar{s}$ is an averaged-over-the-tidal-cycle salinity.

From the values of $E^{TA}_{\bar{A}}$ obtained for that year's data a correlation formula was developed, to express $E^{TA}_{\bar{A}}$ as a function of x and of fresh water discharge. As the seaward boundary condition was not at the ocean a separate model was developed which incorporated flow history into a statistical predictor model for the downstream boundary salinity.

Apart from the development of the $E^{TA}_{\bar{A}}$ correlation and the seaward boundary condition treatment Boicourt's method is essentially the same as Pritchard's. In this application the difficulties of obtaining applicable dispersion coefficients and appropriate boundary conditions are pointed out. In fact one might question the use of the boundary predictor model from the point of view that this procedure could just as well be used to predict salinity at <u>all</u> points in the Upper Chesapeake <u>without</u> using the convective-diffusion equation. What has in fact been done is that part of the solution has been predicted on a statistical basis and the rest of the solution [the interior points] developed using a mathematical model of the convective-diffusion equation.

2.5 Quasi Steady-state Studies

The term quasi steady-state is applied to a tidal time situation in which the tidal amplitudes and fresh water discharges repeat themselves from tidal cycle to tidal cycle, thus creating a time-varying salinity distribution which is repeating.

Stigter and Siemons (1967) used the salt balance equation and the tidal dynamics equations in coupled form to study the

salinity intrusion in a constant width representation of the Rotterdam Waterway. The solution of the equations was achieved through a finite-difference numerical model.

They showed that including the effect of density differences in the tidal calculations has a definite effect on the tidal elevations. This has later been shown for a one-dimensional, variable area study of the estuary of Maracaibro by Fisher et al (1970) who applied the tidal-time tidal dynamics equations.

Stigter and Siemons' ocean boundary condition on the salt balance equation was a complete specification of the salinity at this boundary for all points in time during the tidal cycle. Knowledge of this boundary condition is usually unavailable and consequently application of this model is limited to descriptive studies where the ocean boundary salinity is known.

The dispersion coefficient relationship for their study was taken as a function of x, the form being:

$$E = E_o (1 - x/L)^3 \qquad (2\text{-}14)$$

The E_o values were determined by fitting the available data.

Although this relationship of the dispersion coefficient was well adapted to their particular descriptive study, there is no reason to expect that it could be applied generally. Any relationship for the dispersion coefficient which is a function only of x is limited to a particular condition of fresh water discharge and tidal action. In real estuaries these conditions are always changing and

variable geometry will complicate these changes even further.

2.6 Unsteady Prediction of Pollutants in Well-mixed Estuaries

Harleman et al (1968) have used their numerical tidal model to provide the unsteady discharges and areas required for solution of the unsteady one dimensional mass balance equation for a non-conservative pollutant. They have shown that in the fresh water region of the estuary the dispersion coefficient can be expressed by a relationship in terms of the cross-sectional velocity u, Manning's 'n', and the hydraulic radius. This relationship was obtained from Taylor (1954) who experimentally verified the following expression for the longitudinal dispersion coefficient E_T for steady uniform flow in pipes:

$$E_T = 10.1\ a\ u^* \qquad (2\text{-}15)$$

where a is the pipe radius and u* is the friction velocity. Harleman (1966) has shown that the relationship of Equation 2-15 can be written in terms of the hydraulic radius, R_h, average velocity, u, and Manning's 'n' as

$$E_T = 77\ n\ u\ R_h^{5/6} \qquad (2\text{-}16)$$

The unsteady pollutant distribution was studied using a mathematical model of the mass balance equation. This work has been continued by Lee (1970), and has included the simulation of salinity intrusion by assuming a dispersion coefficient relationship as a function of x. Although such a technique can be useful in quasi steady-state studies where one has data available to make some dispersion coefficient

correlation possible, predictive studies for varying fresh water flows and tidal conditions are not possible using this model.

2.7 Other Studies

Shinohara et al (1969) developed a numerical technique for the prediction of quasi steady-state salinity distributions in well-mixed estuaries which employs a very innovative technique which allows him to simplify the advective term of the salt balance equation so that it contains, not the tidal velocity which varies from maximum ebb to maximum flood, but only the net seaward velocity during the tidal cycle. By fixing as an origin a point upstream which can be called the end of the estuary, the total volume of water from that origin to a section x is defined by:

$$\Psi = \int_0^x A(x,t)\, dx \tag{2-17}$$

The mean cross-sectional velocity u can be written in terms of Ψ by:

$$u = \frac{1}{A}\left(Q_f - \frac{\partial \Psi}{\partial t}\right) \tag{2-18}$$

Shinohara then transforms the independent variable x to Ψ and the resulting salt balance equation becomes:

$$\frac{\partial s}{\partial t} + Q_f \frac{\partial s}{\partial \Psi} = \frac{\partial}{\partial \Psi}\left(A^2 E_\Psi \frac{\partial s}{\partial \Psi}\right) \tag{2-19}$$

which is solved in finite difference form.

Thus by this transformation the salt balance equation is transformed to a form which contains a constant (or relatively constant) advection coefficient of $\frac{\partial s}{\partial \Psi}$ instead of the tidal discharge

u(x,t). The effects of changing elevations and velocities are incorporated in the transformed variable $\forall$ thus this method is still tied to the time-varying tidal hydraulics. Relationships are assigned to $A^2E_{\forall}$ for fully mixed estuaries assuming $E_{\forall}$ proportional to the product of mean tidal velocity and hydraulic radius as in Equation 2-16.

The seaward boundary condition is kept at a constant ocean salinity at the location x_o and whenever the $\forall_o$ becomes located seaward of this point all segments seaward of x_o are set to ocean salinity during the solution of the finite difference equation.

This method implies the knowledge of the quasi steady-state tidal elevations so as to evaluate $\forall(x,t)$ by Equation 2-17, consequently when this information is easily obtainable from tidal records or easily calculated due to simplified geometry, the method is readily applicable. The method could be extended to transient studies if the transient dispersion coefficient relationship could be determined and if a separate numerical model were used to provide the volumes $\forall(x,t)$. At this point, however, it would be simpler to set the entire problem in finite difference form without transforming variables, thus gaining the ability of coupling between the salt balance equation and momentum equation through the longitudinal density gradient.

Dornheim and Woolhiser (1968) recognized the need for a tidal-time mathematical model of estuarine water quality which included time-varying boundary conditions. After restricting the geometry of a typical estuary to that of a linearly expanding width and a uniform bed

slope, they formulated the equations of continuity and momentum, without the effects of the density gradient, in order to model separately the tidal hydraulics. These equations were then solved by a finite difference technique. The salt balance equation was formulated under the same conditions of geometry and with the assumption that the dispersion coefficient was a function only of distance, x. This equation was also solved in finite difference form.

The downstream boundary condition on salt was handled by extending the estuary into the ocean an arbitrary distance B, at which point the salinity was specified as the ocean salinity, s_o. The necessity of specifying the dispersion coefficient distribution E(x) categorizes the model as descriptive rather than predictive in nature. Unfortunately, in attempting to represent the Delaware Estuary the hydrodynamic model became unstable and they were not able to verify their model under approximate prototype conditions.

III. Definition of Problem and Approach to Solution

3.1 Introduction

Previous studies have not resulted in predictive models for salinity intrusion for several basic reasons. First, a prediction requires that the mathematical model be responsive to temporal variations in fresh water inflows and to changes in tidal amplitudes at the ocean. Secondly, the ocean boundary condition should be represented in some fashion which does not require physical data or statistical predictions of the variation in salinity during a tidal period. Finally, there must be some way of representing the longitudinal distribution of the dispersion coefficient which removes it from complete correlation to physical data for a particular estuary. Such a representation should be generally applicable to any estuary and should have governing parameters which can be evaluated from readily available information on stratification conditions.

Although some of the studies reported in the previous chapter have satisfied one or another of these requirements no one study has developed a predictive model. This study presents a predictive model of the salinity intrusion in a tidal estuary by developing a numerical solution to the one-dimensional salt balance equation and tidal dynamics equations. The equations are coupled through an equation of state relating salinity to density. As the tidal dynamics are included, the variations in ocean surface elevation are incorporated into the model as well as the variations in fresh water inflows. The tidal time approach permits a physically realis-

tic treatment of the ocean boundary salinity in two parts, depending on whether the flow is entering or leaving the estuary. Finally, it will be shown that by relating the local dispersion coefficient to the local salinity gradient, the time and spacially varying characteristics can be modeled with reference to a single parameter whose sensitivity to stratification conditions is expressed in terms of gross properties of the estuary.

Figure 3.1 illustrates how the numerical model functions in terms of input and output quantities and in terms of the coupling of the tidal dynamics and salt balance parts of the overall numerical model. The numerical techniques involved are those of finite differences as applied to the tidal dynamics equations of continuity and momentum and to the salt balance equation. Before treating these equations in detail certain definitions are presented with respect to the schematization of the estuary to one-dimensional quantities.

3.2 Definitions and Schematization

The reduction of the three-dimensional tidal estuary to one-dimension is accomplished by establishing a longitudinal axis and then dividing the estuary into segments of length, Δx. Then the complicated natural tidal and salinity characteristics must be represented in terms of simple geometric quantities. The following are definitions of these basic quantities (with reference to Figure 3.2).

1. V_{Total}: the total volume of the segment of length Δx.

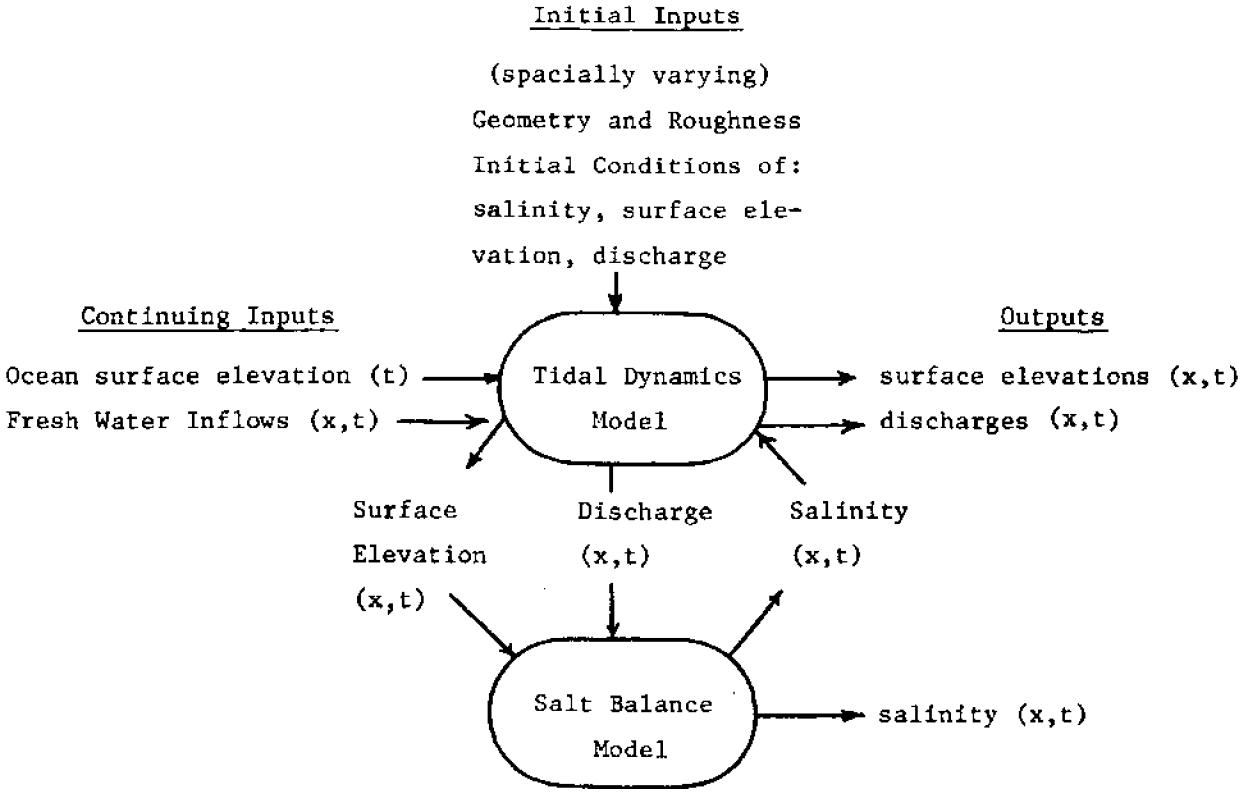

General Functioning of Numerical Model

Figure 3.1

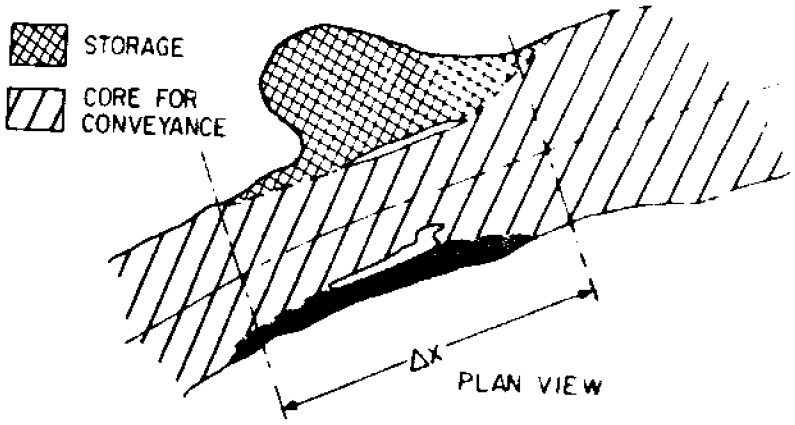

(a) Plan

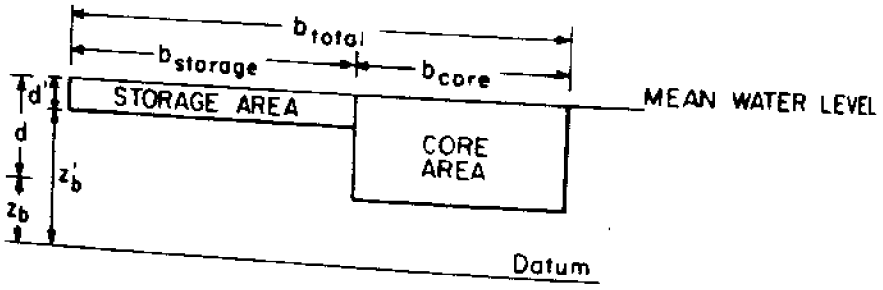

(b) Cross-sectional representation in terms of core and storage areas

(a) and (b) Schematization - Irregular Channels with embayments or storage areas

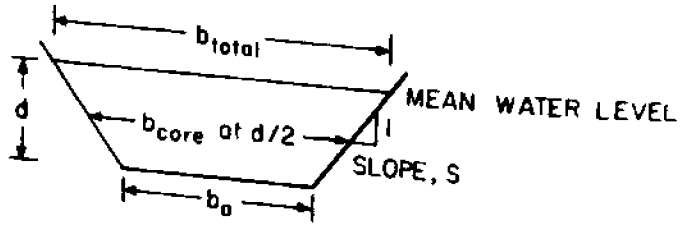

(c) Schematization - Trapezoidal Channel

Figure 3.2

2. A_{Total}: the representative area corresponding to the V_{Total} and equal to $\frac{V_{Total}}{\Delta x}$.

3. A_{core}: that area specified as being the conveyance area for the segment.

4. b_{core}: the width specified as that width corresponding to the conveyance or core area.

5. d: the core depth, equal to $\frac{A_{core}}{b_{core}}$.

6. $V_{storage}$: that volume of the segment specified to be non-participating in conveyance. It represents embayments or areas which are shoal or remote with respect to the main channel.

7. d': the average depth specified for the storage volume.

8. $b_{storage}$: the width corresponding to $V_{storage}$ and d' $\left(\frac{V_{storage}}{d'\Delta x}\right)$.

9. b_{Total}: the total width, equal to $b_{core} + b_{storage}$.

It is inevitable that subjectivity will influence the schematization process. The investigator must decide what portion of the reach Δx will be storage and what part will be core volume. Once these decisions are made, the segment is schematized to the cross-section shown in Figure 3.2b. The final quantities defining the schematized segment are b_{Total}, b_{core}, d', and d. Continuity is maintained by insuring that:

$$[b_{core}\, d + (b_{Total} - b_{core})\, d']\, \Delta x = V_{Total} \qquad (3\text{-}1)$$

This schematization is compatible with that of Harleman and Lee (1969) in as much as it represents an extension of their method. It is important to define d in terms of the core area flow, because the depth determined in this manner is representative of the depth over which the tidal wave propagates. If the entire volume of a segment (including embayment volumes) were divided by the corresponding width times Δx, the resulting depth may be much shallower and the propagation of the tidal wave would be a poor approximation of natural conditions.

When storage is not an important consideration, a trapezoidal schematization may be useful because of its ability to represent the change in water surface width with depth. This condition is encountered in broad shallow estuaries. This type of schematization (Figure 3-2c) is also provided for in this model. The rectangular channel is a special case of either of the two schematizations.

3.3 Tidal Dynamics Model

3.3.1 Continuity and Momentum Equations

The derivation of the unsteady continuity and momentum equations has been made by several investigators, for example Gilcrest (1949), Stoker (1957), Lai (1965) and Harleman and Lee (1969). The derivation will not be repeated in this study and the equations as derived by Harleman and Lee by the Material method will be used as the basis for mathematically describing the tidal motion. They are:

Continuity equation

$$b \frac{\partial h}{\partial t} + \frac{\partial Q}{\partial x} - q = 0 \qquad (3\text{-}2)$$

Momentum equation

$$\frac{\partial Q}{\partial t} + u \frac{\partial Q}{\partial x} + Q \frac{\partial u}{\partial x} + g \frac{\partial h}{\partial x} A + g \frac{Q|Q|}{AC^2 R_h} = 0 \qquad (3\text{-}3)$$

where:

b = total channel width (b_{Total})

h = depth from water surface to a horizontal datum

Q = cross-sectional discharge (= A_{core} x u)

q = lateral inflow per unit length

u = average cross-sectional longitudinal fluid velocity of conveyance area

g = acceleration of gravity

R_h = hydraulic radius = $\frac{A_{core}}{b_{core} + 2(d + \eta)}$

A = A_{core}, the cross-sectional area of primary flow

η = surface elevation relative to local mean water level

C = Chezy coefficient

3.3.2 Momentum Equation Including Density Effects

Equation 3-3 has been derived under the assumption that the effect of any density gradient is negligible. For this study it is desirable to include the effect of the density gradient, and consequently a modified derivation is presented, wherein the conveyance or core area is treated.

In the material method derivation of Harleman and Lee, Newton's Second Law is applied to a moving fluid element and the resulting equation is:

$$\rho\Delta x \left[\frac{\partial Q}{\partial t} + u \frac{\partial Q}{\partial x}\right] + \rho Q \frac{\partial u}{\partial x} \Delta x = \sum F_x \tag{3-4}$$

where ρ is the fluid density and where, $\sum F_x$, the sum of external forces, is in turn shown to be:

$$\sum F_x = - \frac{\partial P}{\partial x} \Delta x + (P_w)_x - (F_f)_x \tag{3-5}$$

where P is the resultant hydrostatic pressure force on the vertical cross section; $(P_w)_x$ is the x component of the horizontal pressure force due to convergent section boundaries; and $(F_f)_x$ is the frictional resisting force of the boundaries. At this point Harleman and Lee's derivation will be slightly modified to include the effect of a density gradient in the term

$$\frac{\partial P}{\partial x} \Delta x$$

Referring to Figure 3.3 for the two schematized forms:

$$P = \int_{z_b}^{h} \rho\, g(h - z)\, b' dz \tag{3-6}$$

where $\rho = \rho(x)$ and $b' = b'(x,z)$. Then, applying Leibnitz' Rule;

$$\frac{\partial P}{\partial x} = \rho g A \frac{\partial h}{\partial x} + \rho g \int_{z_b}^{h} (h - z) \frac{\partial b'}{\partial x} dz + g \int_{z_b}^{h} b'(h - z) \frac{\partial \rho}{\partial x} dz \tag{3-7}$$

The third term on the right hand side of equation 3-7 represents the effect of the density gradient which was not included in the corresponding equation 10 of Harleman and Lee. Expanding this term to

$$g \frac{\partial \rho}{\partial x} \left[h \int_{z_b}^{h} b' dz - \int_{z_b}^{h} z b' dz \right]$$

the term is seen to be

$$g \frac{\partial \rho}{\partial x} \; d_c \, A$$

where d_c is the distance from the surface to the centroid of the cross section. When this expanded form of $\frac{\partial P}{\partial x}$ is substituted into Equation 3-5 and combined with the expressions derived for the other terms one obtains:

$$\sum F_x = -\rho g \frac{\partial h}{\partial x} A \Delta x - g \frac{\partial \rho}{\partial x} \; d_c \, A \Delta x \; \frac{-\rho g Q |Q|}{A C^2 R_h} \qquad (3\text{-}8)$$

and the resulting version of the Momentum equation used in this study becomes:

$$\frac{\partial Q}{\partial t} + u \frac{\partial Q}{\partial x} + Q \frac{\partial u}{\partial x} + g \frac{\partial h}{\partial x} A + g \frac{A d_c}{\rho} \frac{\partial \rho}{\partial x} + \frac{g Q |Q|}{A C^2 R_h} = 0 \qquad (3\text{-}9)$$

The Chezy coefficient, C, is expressed in terms of Manning's roughness n by

$$C(x,t) = \frac{1.49}{n(x)} \; [R_h(x,t)]^{1/6} \qquad (3\text{-}10)$$

thus permitting the natural roughness of the channel to be specified as a function of x. The continuity equation, 3-2, and the momentum equation 3-9 are solved by an explicit finite difference scheme which is described in detail by Harleman and Lee (1969).

3.3.3 Boundary Conditions

The boundary conditions for the tidal dynamics equations do

not present any unusual difficulties. It is necessary to know the surface elevation as a function of time at the ocean end of the estuary. This is usually obtained from tidal observations or from tide tables. At the upstream end of the estuary the boundary condition depends upon the type of estuary. For an estuary of the closed end type, that is one in which the tidal motion is terminated by a dam or natural waterfall, the specification of zero velocity becomes the appropriate upstream boundary condition. The fresh water inflow at the end of the estuary is treated as a lateral inflow into the most upstream segment of the finite-difference model.

In the case of an open end estuary, the location of the upstream boundary should be above the region affected by tidal motion. The specification of the river velocity or discharge hydrograph becomes the appropriate boundary condition. These boundary conditions can be written as:

$\eta(0,t)$ specified

$Q(L,t)$ specified, for open end case

or $Q(L,t) = 0$ for closed end case.

3.3.4 Initial Conditions

Specification of the dependent variables η and Q at all locations at time $t = 0$ form the necessary initial conditions.

$\eta(x,0)$ specified

$Q(x,0)$ specified

At the start of the calculation $\eta(x,0)$ and $Q(x,0)$ can be set to arbitrary values, for example to zero, and five to eight tidal cycles

of calculation will provide convergence to the appropriate values in the quasi steady-state case. In the transient case this calculation will provide a convergent "lead-in".

3.4 Salt Balance Model

3.4.1 Conservation of Salt Equation

3.4.1a Three-dimensional Formulation

The following derivation is based on that of Holley and Harleman (1965).

By considering an elemental volume Δx by Δy by Δz as shown in Figure 3.4 one can formulate for the x direction:

$$\text{Flux in} = \left(\rho su - \rho D_m \frac{\partial s}{\partial x}\right) \Delta z \Delta y$$

$$\text{Flux out} = \left[\left(\rho su - \rho D_m \frac{\partial s}{\partial x}\right) + \frac{\partial}{\partial x}\left(\rho su - \rho D_m \frac{\partial s}{\partial x}\right)\Delta x\right] \Delta z \Delta y$$

$$\text{Net Flux} = \left[-\frac{\partial}{\partial x}(\rho su) + \frac{\partial}{\partial x}\left(\rho D_m \frac{\partial s}{\partial x}\right)\right] \Delta x \Delta y \Delta z$$

where,

u,v,w = instantaneous fluid velocity components in directions x, y and z

ρ = density of fluid

s = instantaneous concentration of salt

D_m = molecular diffusion coefficient.

By equating the rate of change of salt mass within the element to the net fluxes in the three coordinate directions, one obtains a conservation of salt mass equation of the form:

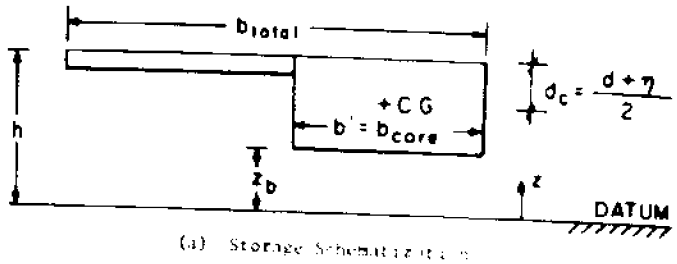

(a) Storage Schematization

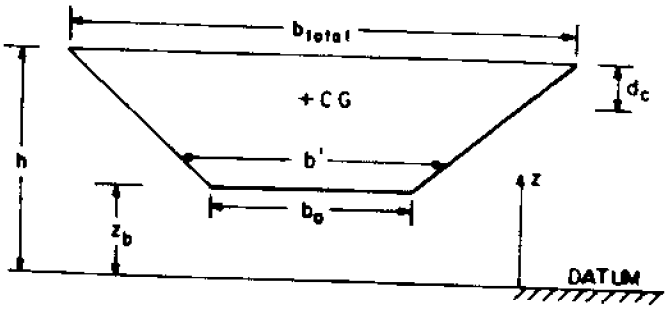

(b) Trapezoidal Schematization

Geometry for Deriving Momentum Equation

Figure 3.3

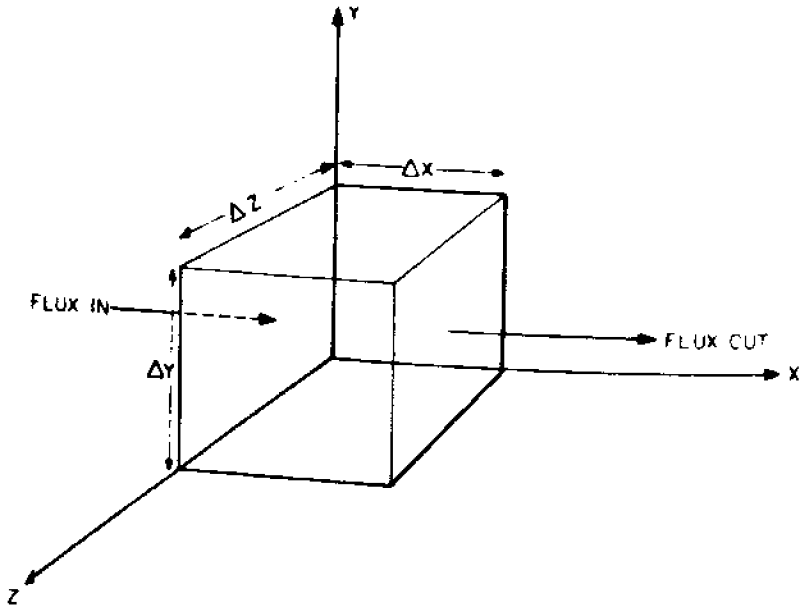

Three Dimensional Control Volume

Figure 3.4

$$\frac{\partial}{\partial t}(\rho s) + \frac{\partial}{\partial x}(\rho s u) + \frac{\partial}{\partial y}(\rho s v) + \frac{\partial}{\partial z}(\rho s w)$$

$$= \frac{\partial}{\partial x}\left(\rho D_m \frac{\partial s}{\partial x}\right) + \frac{\partial}{\partial y}\left(\rho D_m \frac{\partial s}{\partial y}\right) + \frac{\partial}{\partial z}\left(\rho D_m \frac{\partial s}{\partial z}\right) \qquad (3\text{-}11)$$

To adapt equation 3-11 to turbulent flow one defines instantaneous values of velocity and salinity concentration as equal to time averaged values plus deviations:

$$u = \bar{u} + u' \qquad v = \bar{v} + v' \qquad w = \bar{w} + w'$$

$$s = \bar{s} + s', \text{ and a time average} \qquad (3\text{-}12)$$

of a quantity as

$$\bar{q} = \frac{1}{\tau}\int_{t}^{t+\tau} q \, dt$$

Substituting these relationships into Equation 3-11 and averaging over a period of time which is large relative to the turbulence time scale, one obtains:

$$\frac{\partial(\rho\bar{s})}{\partial t} + \frac{\partial}{\partial x}(\rho\bar{u}\,\bar{s}) + \frac{\partial}{\partial y}(\rho\bar{v}\,\bar{s}) + \frac{\partial}{\partial z}(\rho\bar{w}\,\bar{s})$$

$$+ \frac{\partial}{\partial x}(\rho\overline{u's'}) + \frac{\partial}{\partial y}(\rho\overline{v's'}) + \frac{\partial}{\partial z}(\rho\overline{w's'}) =$$

$$\frac{\partial}{\partial x}\left(\rho D_m \frac{\partial\bar{s}}{\partial x}\right) + \frac{\partial}{\partial y}\left(\rho D_m \frac{\partial\bar{s}}{\partial y}\right) + \frac{\partial}{\partial z}\left(\rho D_m \frac{\partial\bar{s}}{\partial z}\right) \qquad (3\text{-}13)$$

wherein the bar implies a time average.

The transport due to turbulent fluctuations is modeled by a diffusive relationship analagous to Fick's first Law:

$$\rho\overline{u's'} = -\rho\, e_x \frac{\partial\bar{s}}{\partial x}$$

$$\rho\overline{v's'} = -\rho\, e_y \frac{\partial \bar{s}}{\partial y}$$

$$\rho\overline{w's'} = -\rho\, e_z \frac{\partial \bar{s}}{\partial z} \qquad (3\text{-}14)$$

where e_x, e_y, and e_z are turbulent diffusion coefficients. Substituting the relationships of 3-14 into equation 3-13 yields:

$$\frac{\partial \rho\bar{s}}{\partial t} + \frac{\partial}{\partial x}(\rho\bar{u}\,\bar{s}) + \frac{\partial}{\partial y}(\rho\bar{v}\,\bar{s}) + \frac{\partial}{\partial z}(\rho\bar{w}\,\bar{s}) =$$

$$\frac{\partial}{\partial x}\left[\rho(D_m + e_x)\frac{\partial \bar{s}}{\partial x}\right] + \frac{\partial}{\partial y}\left[\rho(D_m + e_y)\frac{\partial \bar{s}}{\partial y}\right] + \frac{\partial}{\partial z}\left[\rho(D_m + e_z)\frac{\partial \bar{s}}{\partial z}\right] \qquad (3\text{-}15)$$

As the turbulent diffusion coefficients are generally several orders of magnitude greater than the molecular diffusion coefficients, the latter are neglected. The density term ρ has very little variation even in estuary flow in as much as ocean salinity accounts for only about a 2% increase in density from that of fresh water. Consequently it can be eliminated and one is left with a three-dimensional convective-diffusion equation for turbulent flow.

$$\frac{\partial \bar{s}}{\partial t} + \frac{\partial}{\partial x}(\bar{u}\,\bar{s}) + \frac{\partial}{\partial y}(\bar{v}\,\bar{s}) + \frac{\partial}{\partial z}(\bar{w}\,\bar{s}) =$$

$$\frac{\partial}{\partial x}\left(e_x \frac{\partial \bar{s}}{\partial x}\right) + \frac{\partial}{\partial y}\left(e_y \frac{\partial \bar{s}}{\partial y}\right) + \frac{\partial}{\partial z}\left(e_z \frac{\partial \bar{s}}{\partial z}\right) \qquad (3\text{-}16)$$

3.4.1b Spatial Integration to One-dimensional Form

The derivation of the one-dimensional salt balance equation is obtained by spatially averaging the three-dimensional equation 3-16. Defining u and s as spatial averages and describing these

averages in terms of $\bar{u}$, $\bar{s}$ and spatial deviations u" and s", one formulates

$$\bar{u} = u + u'' \qquad \bar{s} = s + s''$$

$$\bar{v} = v'' \qquad \bar{w} = w'' \tag{3-17}$$

where

$$u = \frac{1}{A}\int_A \bar{u}dA \text{ and } s = \frac{1}{A}\int_A \bar{s}dA$$

The expressions in 3-17 are then substituted into the three-dimensional equation 3-16 and a spatial average taken. The details of this integration can be found in Okubo (1964) and Holley and Harleman (1965). The most general form resulting from such an integration is

$$\frac{\partial(As)}{\partial t} + \frac{\partial(Qs)}{\partial x} = \frac{\partial}{\partial x}\left[e_x A \frac{\partial s}{\partial x} - \int_A u''s''dA\right] \tag{3-18}$$

The work of Taylor (1954) and of Aris (1956) has shown that for steady uniform flow and for s" much less than s; the spatial average of u"s" is analagous to a dispersive process and can be represented by a longitudinal dispersion coefficient, E, in the equation

$$e_x A \frac{\partial s}{\partial x} - \int_A u''s''dA = EA \frac{\partial s}{\partial x} \tag{3-19}$$

As $E >> e_x$ the longitudinal dispersion coefficient E can now be given a meaningful interpretation in terms of the dispersive flux

$$EA \frac{\partial s}{\partial x} = \int_A u''s''dA \tag{3-20}$$

and the one-dimensional salt balance equation can be written

$$\frac{\partial(A_{Total}s)}{\partial t} + \frac{\partial(Qs)}{\partial x} = \frac{\partial}{\partial x}\left(EA_{Total}\frac{\partial s}{\partial x}\right) \qquad (3\text{-}21)$$

It is recognized that an argument could be made for using the conveyance or core area A_{core} for the dispersive flux term in equation 3-21. By using A_{Total} the dispersive flux through areas not included in the conveyance area has been provided for. Whether A_{Total} or A_{core} is the more appropriate choice is undoubtedly related to the particular estuary being schematized, and as advection is the primary means of transport in tidal time studies it is doubtful that the calculation would be very sensitive to the difference between the two assumptions. It is pointed out, however, that the first term $\frac{\partial(A_{Total}s)}{\partial t}$ is correct <u>only</u> when the total area, A_{Total}, is specified, in as much as the salt content of the entire volume is referred to in this term.

A simplified form of equation 3-21 is obtained under conditions of no lateral inflow. Under these conditions the continuity equation (3-2) becomes

$$b\frac{\partial h}{\partial t} + \frac{\partial Q}{\partial x} = 0 \qquad (3\text{-}22)$$

By expanding the first two terms of equation 3-21 one obtains

$$s\frac{\partial A_{Total}}{\partial t} + A_{Total}\frac{\partial s}{\partial t} + s\frac{\partial Q}{\partial x} + Q\frac{\partial s}{\partial x} = \frac{\partial}{\partial x}\left(EA_{Total}\frac{\partial s}{\partial x}\right) \qquad (3\text{-}23)$$

Referring to Figure 3.2b one can show where η is the instantaneous water surface elevation with respect to the reference water level,

$$A_{Total} = b_{core}\,(d + \eta) + (b - b_{core})(d' + \eta)$$

as $h = z_b + d + \eta$ or $h = z_b' + d' + \eta$

$$A_{Total} = b_{core}(h - z_b) + (b - b_{core})(h - z_b')$$

as z_b and z_b' are not functions of time;

$$\frac{\partial A_{Total}}{\partial t} = b_{core}\frac{\partial h}{\partial t} + (b - b_{core})\frac{\partial h}{\partial t} = b\frac{\partial h}{\partial t}$$

thus the first and third terms of 3-23 can be set equal to equation 3-22 because

$$\frac{1}{s}\left[\frac{\partial A_{Total}}{\partial t} + \frac{\partial Q}{\partial x}\right] = \frac{1}{s}\left[b\frac{\partial h}{\partial t} + \frac{\partial Q}{\partial x}\right] = 0$$

and equation 3-21 is written for the special case of no lateral inflow as

$$A_{Total}\frac{\partial s}{\partial t} + Q\frac{\partial s}{\partial x} = \frac{\partial}{\partial x}\left(EA_{Total}\frac{\partial s}{\partial x}\right) \qquad (3\text{-}24)$$

3.4.2 Dispersion Coefficient Calculation

In the saline region of a partially mixed estuary the dispersion coefficient is closely related to the density induced circulation which, due to the spatial averaging inherent in the one-dimensional approximation, is represented by longitudinal dispersion. It is reasonable to assume that this density induced circulation will be greatest in regions of strongest longitudinal salinity gradient, $\frac{\partial s}{\partial x}$, and consequently the dynamic relationship developed in this study for the dispersion coefficient is achieved by relating E(x,t) to the absolute value of the local salinity gradient.

This relationship is formulated as

$$E(x,t) = K \left| \frac{\partial \overset{\circ}{s}}{\partial \overset{\circ}{x}} \right| + E_T \qquad (3\text{-}25)$$

where $\overset{\circ}{s} = s/s_o$ and $\overset{\circ}{x} = x/L$, L being the length of the estuary. E_T is the dispersion coefficient applicable to a completely mixed region, (Eq. 3-25) where $\partial s/\partial x = 0$ or to the fresh water tidal region upstream of the limit of salinity intrusion. The term $K \frac{\partial \overset{\circ}{s}}{\partial \overset{\circ}{x}}$ accounts for the additional dispersion in the salinity intrusion region. The parameter K has the dimensions of a dispersion coefficient (L^2/t); it is assumed to be independent of x and t and to depend upon the degree of stratification which exists in the estuary. To demonstrate the basis for this assumption, the salinity distributions corresponding to three of the WES steady state salinity intrusion tests were studied. The longitudinal salinity distribution data was depth and time-averaged over a tidal period as shown in Figure 3.5. The analysis was performed by considering the steady-state, time-averaged equation

$$u_f \frac{ds}{dx} = \frac{d}{dx} \left(E^{TA} \frac{ds}{dx} \right) \qquad (3\text{-}26)$$

which can be integrated once and solved for E^{TA} to give

$$E^{TA} = u_f \frac{s}{\left(\frac{ds}{dx}\right)} \qquad (3\text{-}27)$$

Figures 3.6a, b and c show the distribution with distance, x/L, of the quantities $-\frac{\partial \overset{\circ}{s}}{\partial \overset{\circ}{x}}$, E^{TA} and K where by assuming $E^{TA} = K \left| \frac{\partial \overset{\circ}{s}}{\partial \overset{\circ}{x}} \right|$, K can be expressed in terms of Equations 3-27 and 3-25 as

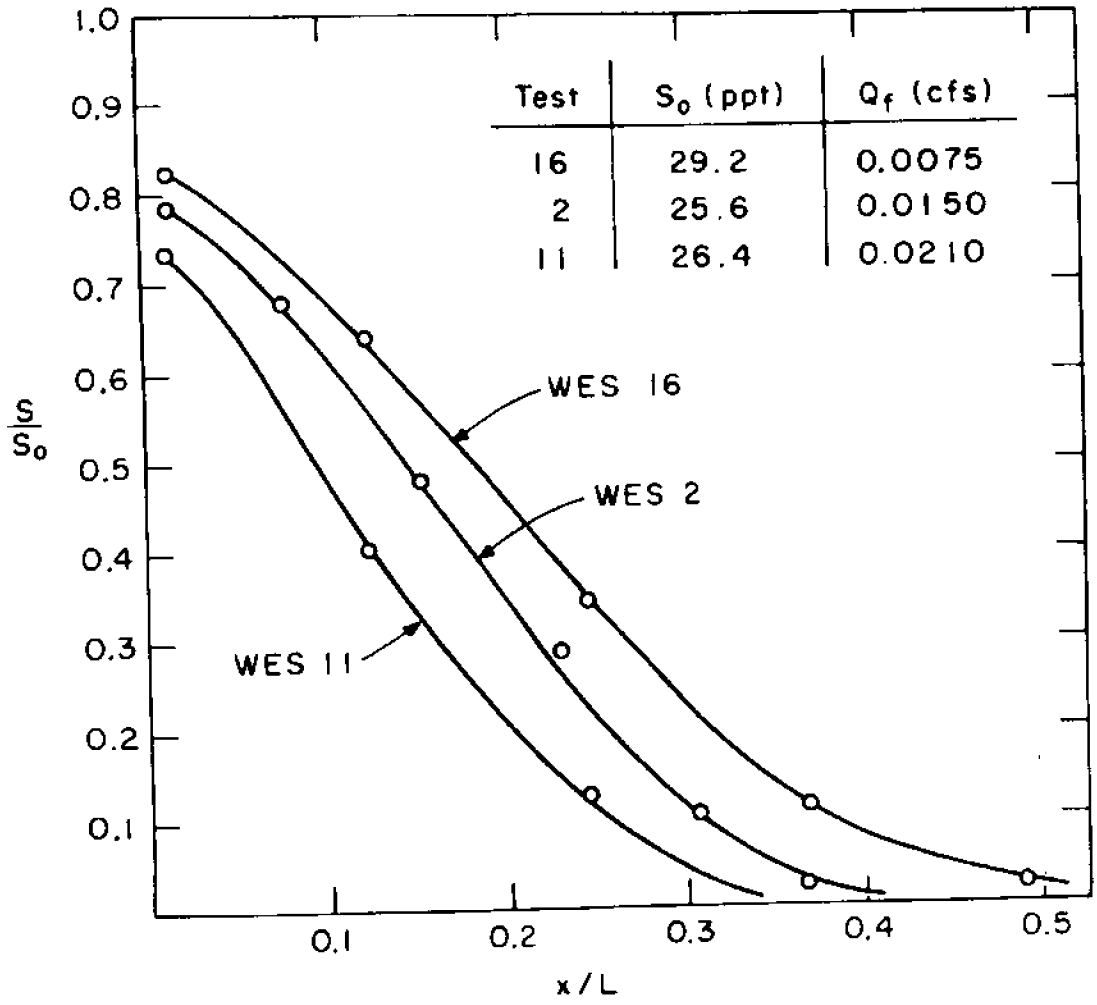

Steady-State, Longitudinal Salinity Distribution (Depth Averaged and Time-Averaged over a Tidal Period) for Three Fresh Water Flow Rates

Figure 3.5

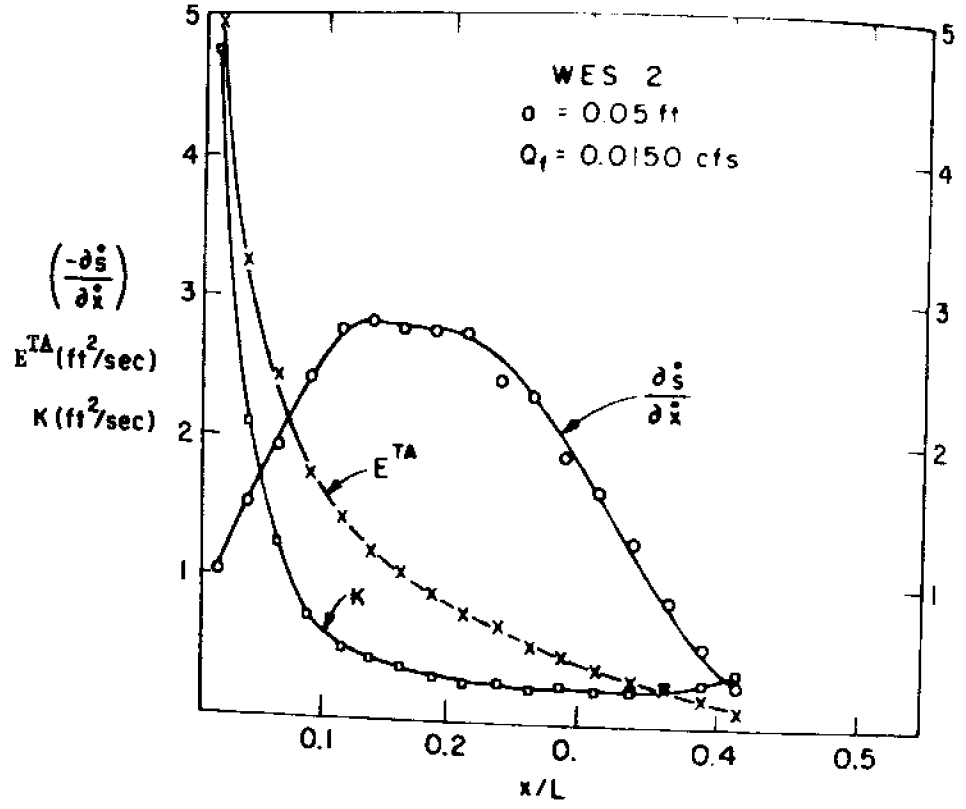

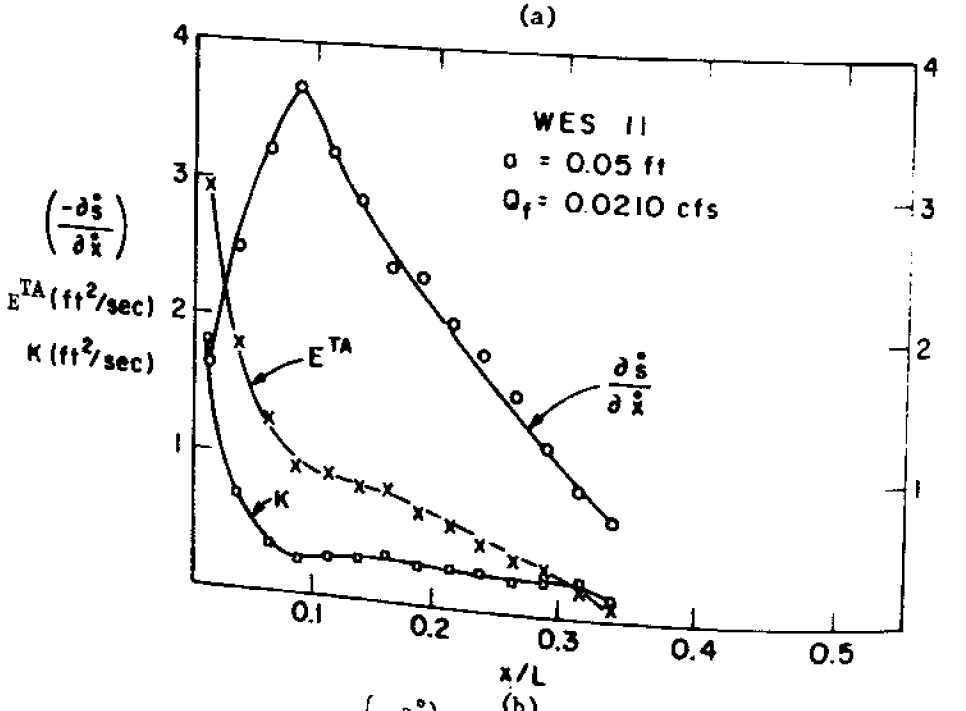

$\left(-\frac{\partial s^*}{\partial x^*}\right)$, E^{TA}, K vs x/L

Figure 3.6 (a and b)

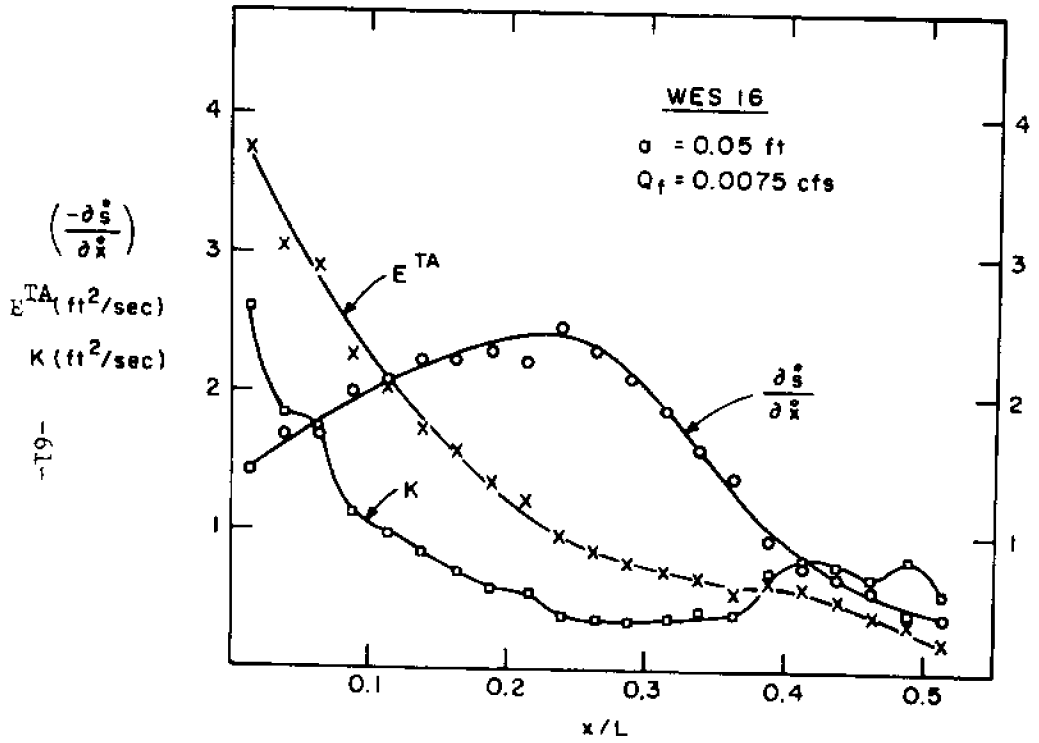

$-\left(\frac{\partial s^*}{\partial x^*}\right)$, E^{TA}, and K vs. x/L for W.E.S. 16

Figure 3.6c

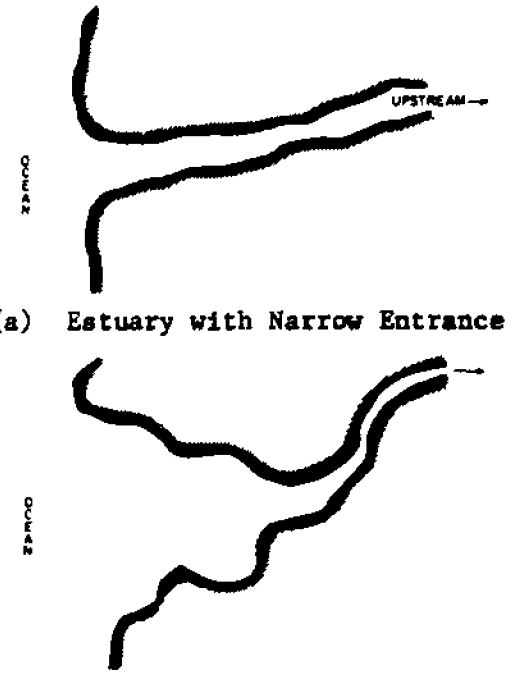

(a) Estuary with Narrow Entrance

(b) Estuary with Widening Entrance

Estuary Configurations at the Ocean Entrance

Figure 3.7

$$K = u_f L \frac{\overset{\circ}{s}}{\left(\frac{d\overset{\circ}{s}}{d\overset{\circ}{x}}\right)^2} \qquad (3\text{-}28)$$

Figure 3.6 shows that the assumption that the parameter K is a constant is well supported in the interior regions of the estuary-flume. The abrupt increase in both E^{TA} and K near the entrance is a consequence of the time-averaged, steady-state assumption of Equation 3-26 which requires that the dispersion coefficient increase so that the integrated form

$$u_f s = E^{TA} \frac{ds}{dx}$$

is satisfied as $\frac{ds}{dx} \to 0$ and $s \to s_o$ at the ocean. When one considers the tidal-time equations, the dispersion coefficient is not under this requirement and the formulation of Equation 3-25 will allow the dispersion coefficient to become less near the ocean which corresponds to the physical condition of a more mixed condition.

The final term of Equation 3-25, E_T, the dispersion coefficient applicable in completely mixed or fresh water regions of the estuary, can be described in terms of the section geometry and velocity written as Equation 2-16 by Harleman (1966). In this study Equation 2-16 is assumed to apply for the unsteady tidal flow situation and is

$$E_T(x,t) = 77\, n\, u\, R_h^{5/6} \qquad (3\text{-}29)$$

where $u(x,t)$ and $R_h(x,t)$ are the velocity and hydraulic radius at location x and time t.

The formulation of Equation 3-25 permits a dynamic calcula-

tion of E(x,t) which applies to the entire estuary, in both the partially and completely mixed regions.

3.4.3 Upstream Boundary Condition

There are two possible boundary conditions at the upstream end of the estuary. One could specify that the salinity be zero, (or near-zero) or one could specify that there be no flux of salt across the upstream boundary. Both are valid boundary conditions, however the specification of salt flux is the more general in as much as it permits the study of closed end estuaries where the salinity actually reaches the end of the estuary. However in many cases, including those studies in this investigation, the salinity intrusion is well downstream of the upstream end.

This boundary condition can also be viewed as a free boundary condition as the point of zero salt flux in the upstream direction is time-varying and is, in fact, part of the solution. Such boundary conditions can lead to complications in numerical models, however it was found that as long as the upstream boundary was specified far enough upstream so that is was out of the intrusion zone during the period of study, its exact location was not important. This finding becomes useful in saving computer time because one need not perform the calculations on that part of the estuary which is upstream of the saline region. In cases of doubt one should specify the upstream end of the estuary as the boundary location.

The upstream boundary condition can now be stated: At the upstream boundary there is no flux of salt across the boundary.

This boundary condition is developed by considering a discretized element of the estuary at the location of the boundary and making a mass balance using finite difference representations of the quantities involved. In this manner the constraint of no flux of salt across the boundary is incorporated into the mass balance and thereby into the finite difference equation resulting from the mass balance.

3.4.4 Ocean Boundary Treatment

3.4.4a Introduction

Ideally one would like to have a schematization which permitted a study of the estuary from its upstream end to a point so far at sea that the boundary salinity could be specified once and for all as the ocean salinity, s_o. Unfortunately such situations are not possible in a one-dimensional study as the ocean is not representable in one dimension.

When the ocean-estuary connection is that of a narrow entrance suddenly opening into the ocean as in Figure 3.7a it is clear that the ocean can not be part of the one-dimensionalized estuary. The schematization of points beyond the entrance itself would not be rigorously possible. In this case the physical boundary is readily definable, but this does not simplify the definition of the salinity boundary condition. On the ebb flow the salinity at the entrance will reflect the upstream conditions, and when the flow reverses the salinity will not immediately become ocean salinity but will reach

the ocean salinity in a manner depending upon the longshore currents. One can expect a significant variation in salinity over the tidal cycle at the ocean entrance in estuaries of this configuration.

In contrast to the estuary described in Figure 3.7a is the configuration shown in Figure 3.7b wherein the estuary gradually widens as it reaches the ocean. In such a case the definition of the ocean boundary location will result from practical considerations of schematization. The variations of salinity during the tidal cycle will depend not only upon the complicated currents but also upon the actual location which has been specified. If it is possible to carry out the schematization sufficiently far downstream, the variation in salinity throughout the tidal cycle will be small. The salinity at the ocean entrance can not be constant throughout the tidal period because the fresh water must leave the estuary during some portion of the tidal period and at this time the average salinity of the boundary cross-section will be decreased.

As this study treats the variation in salinity within the tidal cycle, the boundary treatment must apply for all times during the tidal cycle. An approach is taken which divides the tidal cycle in two parts according to the direction of flow at the ocean entrance and applies a different boundary treatment for each of the two parts. This division is made possible by the fact that the numerical model calculates the discharge at the ocean end of the estuary, thus providing the necessary criterion for applying either boundary condition.

3.4.4b Formulation During Flood Flow ($Q(o,t) \geq 0$

The salinity at the ocean boundary during flood flow is

approximated by specifying it equal to the ocean salinity, s_o. If the seasonal variation of ocean salinity is known, then the ocean salinity can be specified as a function of time $s_o(T)$, from tidal cycle to tidal cycle.

$$s(o,t) = s_o(T) \quad \text{for } Q(o,t) \geq 0$$

$$T = 1,2,3,\ldots$$

where T is the number of Tidal Cycles.

3.4.4c Formulation During Ebb Flow ($Q(o,t) < 0$)

Although it is possible to approximate the salinity at the ocean boundary by the ocean salinity during flood flow, during ebb flow a different means of continuing the solution must be employed. The approximation used is described in terms of the finite difference representation of the estuary, specifically in terms of making continuous mass balances at the most seaward element.

To perform these mass balances, the advective and dispersive flux must be evaluated during each time step at each boundary of the seaward element. With reference to Figure 3.8 one sees that during a particular time step the total flux on the upstream section (No. 2) of the element can be evaluated as

$$Q_2 \frac{(s_1+s_3)}{2} - E_2A_2 \frac{s_3-s_1}{2\Delta x} .$$

In order to write the total flux at the downstream section (No. 1) the advective flux can be written Q_1s_1, but the evaluation of the dispersive flux can not be expressed in terms of a difference representation of the salinity gradient centered on the section. In

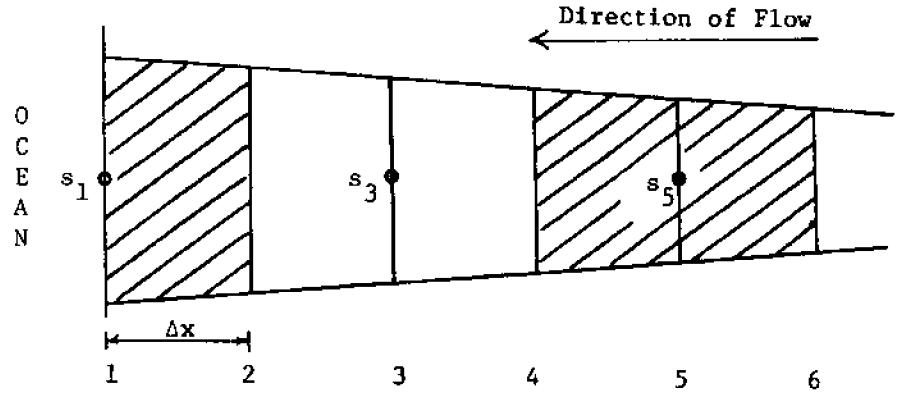

Flux at Section 1: $Q_1 s_1 - E_1 A_1 \left.\frac{\partial s}{\partial x}\right|_1$

Flux at Section 2: $Q_2 s_2 - E_2 A_2 \left.\frac{\partial s}{\partial x}\right|_2$

where $s_2 = \frac{1}{2}(s_1 + s_3)$

$$\left.\frac{\partial s}{\partial x}\right|_2 = \frac{s_3 - s_1}{2\Delta x}$$

and

$$\left.\frac{\partial s}{\partial x}\right|_1 \equiv \left.\frac{\partial s}{\partial x}\right|_2$$

Ocean Boundary Approximation
During Ebb Flow

Figure 3.8

order to continue the finite difference solution the dispersive flux at section number 1 is approximated by using the salinity gradient, $\frac{\partial s}{\partial x}$, evaluated at section number 2. The total flux at the downstream section (No. 1) is then approximated by

$$Q_1 s_1 - E_1 A_1 \frac{s_3 - s_1}{2\Delta x} \quad .$$

With the flux on each side of the element specified, a mass balance is made by setting the change in salt during each time step, $\frac{\partial (As)}{\partial t}$, equal to the net flux. As the mass balance is written in terms of the salinities at section 1 and 3 at the beginning and at the end of the time step, it provides the necessary boundary equation in terms of the unknown salinities at the end of each time step.

This approximation allows the solution of the implicit finite difference equations to continue during the period of ebb flow.

At the end of that portion of the tidal cycle corresponding to ebb flow, the salinity will be below that of the ocean salinity, s_o. Physically, it can not change to s_o instantaneously. To provide for this change, a linear interpolation in time is employed in order to bring the salinity from its value at the end of ebb flow to the ocean salinity value, s_o. This interpolation is applied over a transition period of one twentieth of a tidal cycle.

3.4.4d Description of Combined Ocean Boundary Treatment

As the calculation proceeds in time the discharge at the ocean entrance is continuously tested to see if it reverses direction.

In this manner the appropriate flood flow or ebb flow boundary treatment is applied. Figure 3.9 shows, in graphic form, the various aspects of this boundary treatment throughout a typical tidal cycle.

3.4.4e Special Provisions for Boundaries Taken Upstream of the Ocean

In some cases it may not be possible to treat the estuary by schematizing it all the way to the ocean. In such a case when the boundary location is specified upstream, the assumption of longshore currents sweeping away the diluted water is no longer applicable. Following low water slack there will be a more gradual increase of salinity to its maximum value at high water slack.

In order to provide for such a condition the procedure used to bring the salinity from its low water slack value to its maximum value is extended over a longer period of time depending upon the particular location of the boundary with respect to the ocean. For a location far from the ocean this might be as much as 2/5 of a tidal period. This would mean that the salinity from low water slack to low water slack plus 2/5T is specified by a linear interpolation between the low water slack and maximum salinity values.

3.4.5 Initial Conditions

It is required that an initial salinity distribution be specified at time t = 0. If the particular application is one wherein the ocean tidal amplitude and the fresh water discharge are fixed then a quasi steady state study is defined and the calculations will lead to a convergent solution for an arbitrary initial salinity

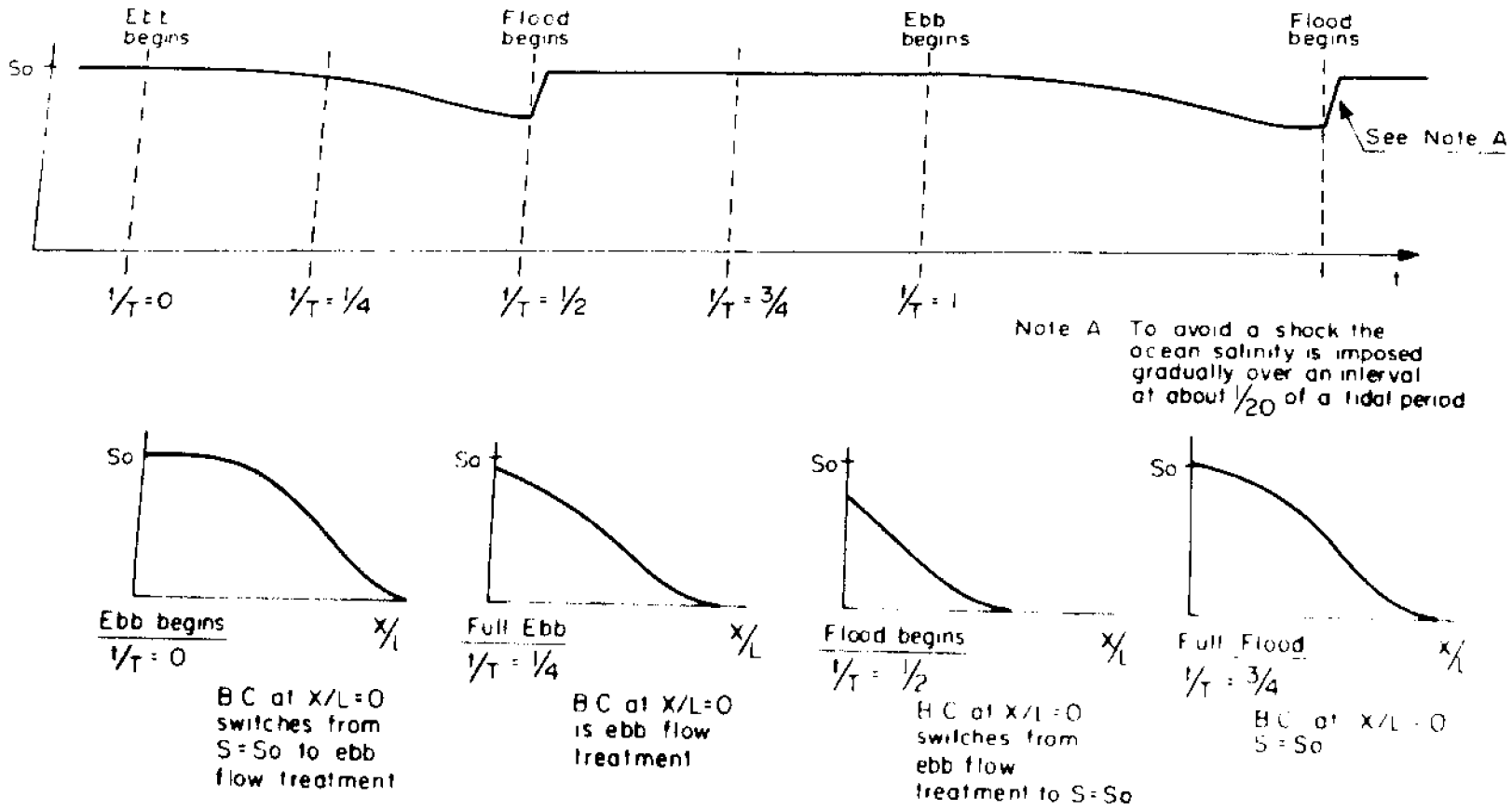

Description of Ocean Boundary Treatment

Figure 3.9

distribution. For such cases convergence may require as many as 50 to 200 tidal cycles, consequently it is worthwhile to make a reasonable estimate of the salinity distribution in order to reduce computing expense. Figure 3.10 shows possible initial distributions for quasi steady state studies.

A transient study is one in which the conditions of ocean tidal elevation and fresh water discharge vary over many tidal cycles throughout the period of study. It is assumed that for such a study the user will have a good approximation of the initial salinity distribution.

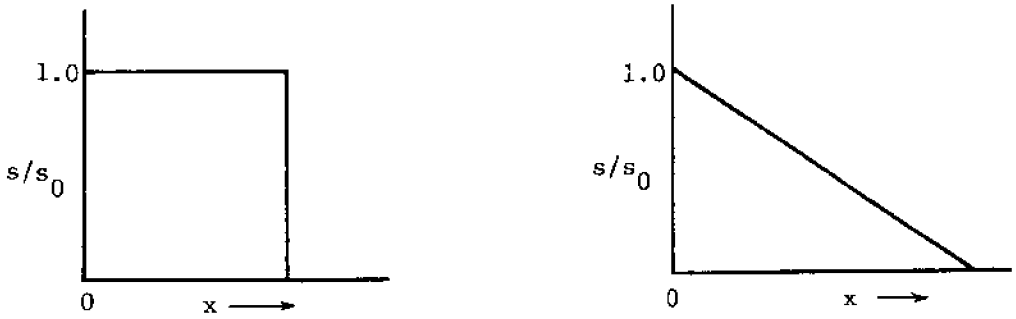

Possible Initial Salinity Distributions
for Quasi Steady-State Studies

Figure 3.10

3.5 The Equation of State Relating Density to Salinity

The relationship between density and salinity is a familiar relationship of physical oceanography. Knudsen (1901) developed tables relating density to salinity, temperature, and pressure. The empirically derived formulae are described in detail by Fofonoff (1962), however for the purpose of estuary studies a much simpler relationship can be used which is:

$$\rho = 0.75s + 1000 \tag{3-30}$$

where s is salinity in parts per thousand and ρ is in kg/m^3.

IV. The Relationship between Dispersion Coefficient and Stratification

4.1 Introduction

Previous studies such as those discussed in sections 2.4 and 2.5 have shown that the dispersion coefficient is related to the degree of stratification in the estuary. In this chapter the dispersion parameter K of Equation 3-25 is studied in terms of its relationship to the degree of stratification. The study consists of finding a convenient means of defining stratification in terms of gross estuary parameters. By applying the numerical model to cases for which quasi steady-state salinity distribution data exists, the relationship between the dispersion parameter K and the degree of stratification is developed.

4.2 Stratification

To compare the degree of vertical stratification corresponding to different conditions in an estuary one can plot the vertical salinity distribution for a specific location. Such plots were made by Ippen and Harleman (1961) for several W.E.S. salinity flume tests at station 40 ($x/L = 0.12$) corresponding to the conditions existing at approximately one quarter of a tidal cycle after time of high water in the ocean basin. Figure 4.1 shows these vertical salinity distributions for four different tests. The parameters varied during these tests were the fresh water discharge and the tidal amplitude as shown in the legend. It is of interest to note that Test 11 and Test 10 both have the highest fresh water discharge, yet in terms of stratification the increased tidal action of Test 10 has caused the

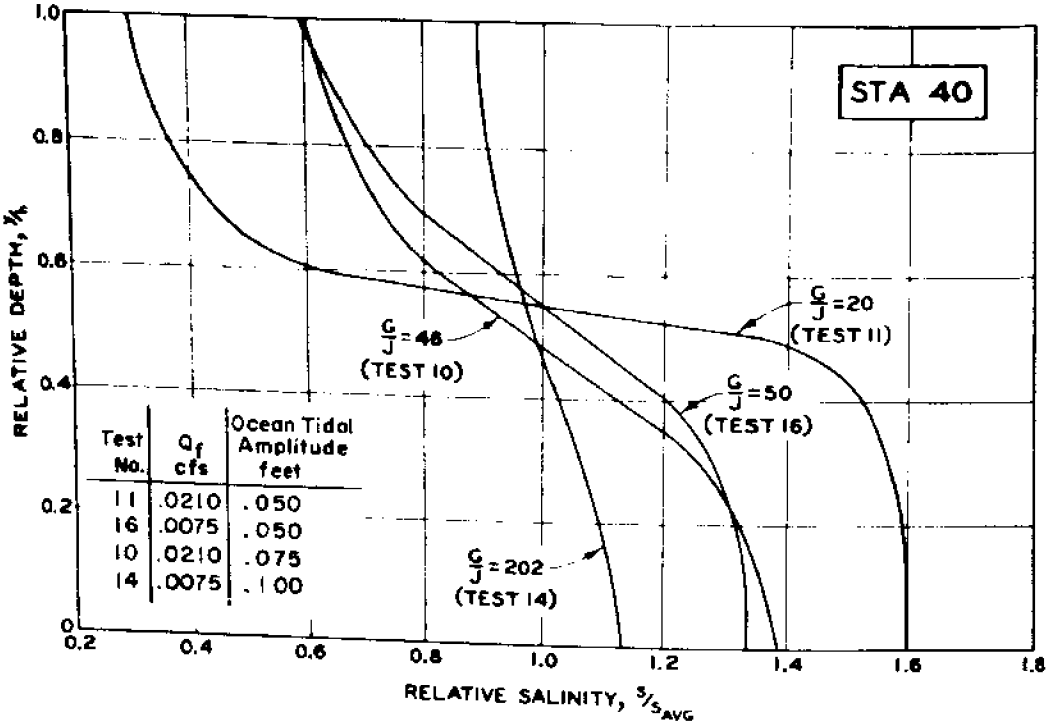

Vertical Salinity Profiles Showing
Different Degrees of Stratification
(from Ippen and Harleman, 1961)

Figure 4.1

vertical salinity structure to be almost the same as that of Test 16 which had the lowest fresh water discharge and the smallest tidal amplitude. The G/J values indicated for each profile correspond to a particular definition of stratification which will be discussed in the following paragraphs.

Two factors determine the degree of stratification. One is the tendency to stratify or form two distinct layers. This tendency increases as the density difference between the two fluids increases and also as their relative proportions become more equal. Acting against this is the turbulent mixing generated by the tidal motion which tends to reduce the density difference or stratification. Experiments made at M.I.T. in earlier studies were concerned with defining stratification in terms of gross estuary parameters. Salinity distribution data were obtained from a flume with fresh water entering at one end and a constant (ocean) salinity at the other end. Mixing was accomplished by means of oscillating screens. (Ippen et al, 1960.) The relationship of stratifying tendencies to destratifying mixing was described by a stratification number (G/J) and defined previously in Chapter 2 as:

$$\frac{G}{J} = \frac{\text{rate of energy dissipation per unit mass of fluid}}{\text{rate of potential energy gain per unit mass of fluid}} \qquad (2\text{-}5)$$

G was defined in terms of the energy input by the oscillating screens.

In defining J the following was used (Harleman et al, 1961):

$$J(x) = \frac{\gamma_x - \gamma_f}{\gamma_f} g\, u_f \frac{h}{L} \tag{4-1}$$

where γ is the specific weight of fluid.

It is important to note that this is not the rate of potential energy gain at location 'x', but is the total gain of potential energy from the fresh water end, seaward to location x, divided by the flume length, L. In other words the term $\frac{d\gamma}{dx}$ has been approximated by $\frac{\gamma_x - \gamma_f}{L}$, which is a reasonable approximation only as x approaches L. When applied to a particular estuary of fixed h and L, Equation 4-1 becomes simply a proportional relationship:

$$J_x \sim s u_f \tag{4-2}$$

After conducting steady state experiments with varying degrees of stratification, a correlation was found (Figure 4.2) between D'(x)/D(x) (the ratio of the local apparent diffusion coefficient to the constant density or turbulent diffusion coefficient) and the local stratification number, G/J(x).

Taking a more rigorous formulation of the rate of gain of potential energy per unit mass of fluid, J(x) can be defined by

$$J(x) = \frac{u_f}{\rho} \frac{d(\gamma h)}{dx} \tag{4-3}$$

For constant depth this expression can be written in terms of salinity by the proportional relationship:

$$J(x) \sim \frac{ds}{dx} u_f \tag{4-4}$$

This latter proportionality supports the assumption that the dispersion coefficient is proportional to the local salinity gradient as discussed in Chapter 3. A significant correlation between D'(x)/D(x)

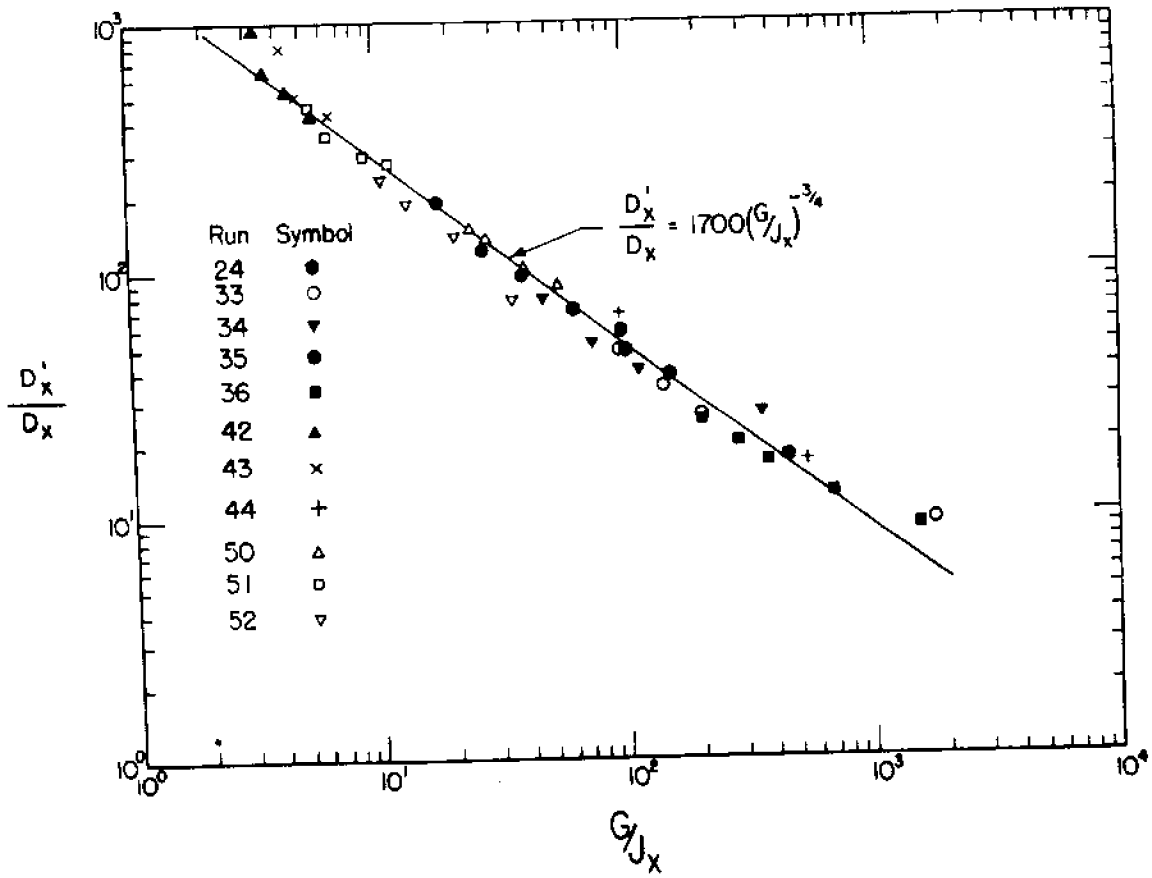

Ratio of Local Apparent Diffusion Coefficient to Turbulent Diffusion Coefficient Correlated with Local Stratification Parameter for $J_x \sim s\ u_f$ (from Harleman et al 1961)

Figure 4.2

and G/J(x) with J(x) defined by equation 4-3 is also evident as shown by Figure 4.3.

In applying this G/J ratio to cases of oscillating tidal motion, the G/J parameter has been used in a form applicable to the entire estuary. In this case J(x) becomes J_o, which when defined by equation 4-2, represents an average rate of energy gain for the entire estuary.

Ippen and Harleman (1961) used the G_o/J_o number as a means of correlating the results of the W.E.S. salinity flume tests with their dispersion parameters E_o^{LWS} and B. The correlation between E_o^{LWS}/E_T and G_o/J_o is shown in Figure 4.4. Although this correlation shows promise as a means of finding the value of a single parameter such as E_o^{LWS} in terms of gross estuary parameters, Figure 4.4 pertains to only <u>one</u> estuary and can not be extrapolated to others.

Despite the success in correlating E_o^{LWS}/E_T for the W.E.S. series of tests, the G_o/J_o number is not a convenient parameter due to the difficulty in evaluating the rate of energy dissipation, G_o. Recognizing this, Harleman and Abraham (1966) developed another parameter $\frac{P_T \mathbb{F}_o^2}{Q_f T}$ which they called estuary number $\mathbb{E}$ and which is easily evaluated in terms of available quantities; P_T being the tidal prism, $\mathbb{F}_o$ the Froude number at the ocean entrance, Q_f the fresh water discharge, and T the tidal period. They found (Figure 4.5) that this parameter correlated very well against J_o, a fact which is not surprising if one considers the following:

Let G_o be given by the expression (Harleman, Eq. 14.10, 1966)

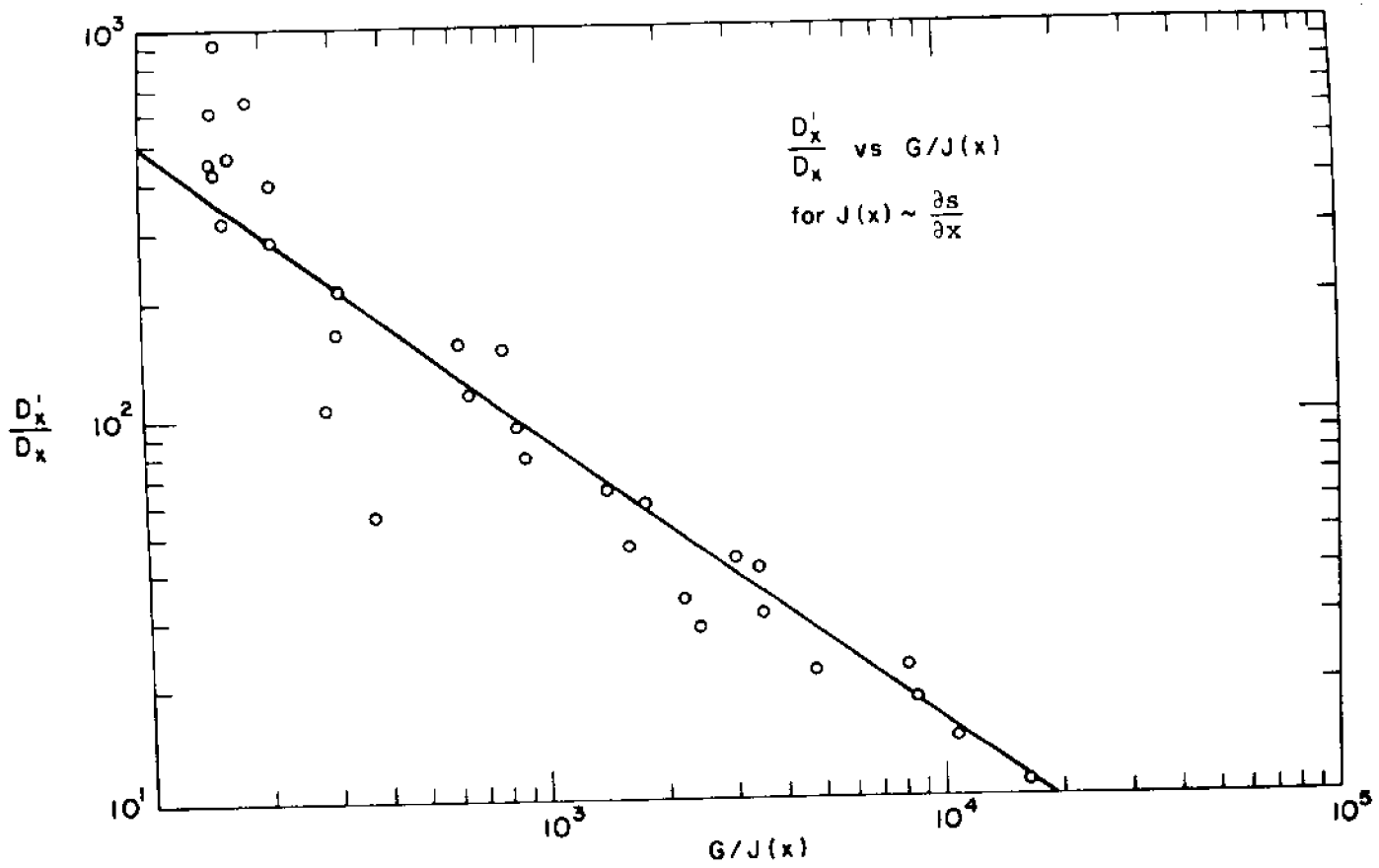

Ratio of Local Apparent Diffusion Coefficient to Turbulent Diffusion Coefficient Correlated with Local Stratification Parameter for $J_x \sim \frac{\partial s}{\partial x} u_f$

Figure 4.3

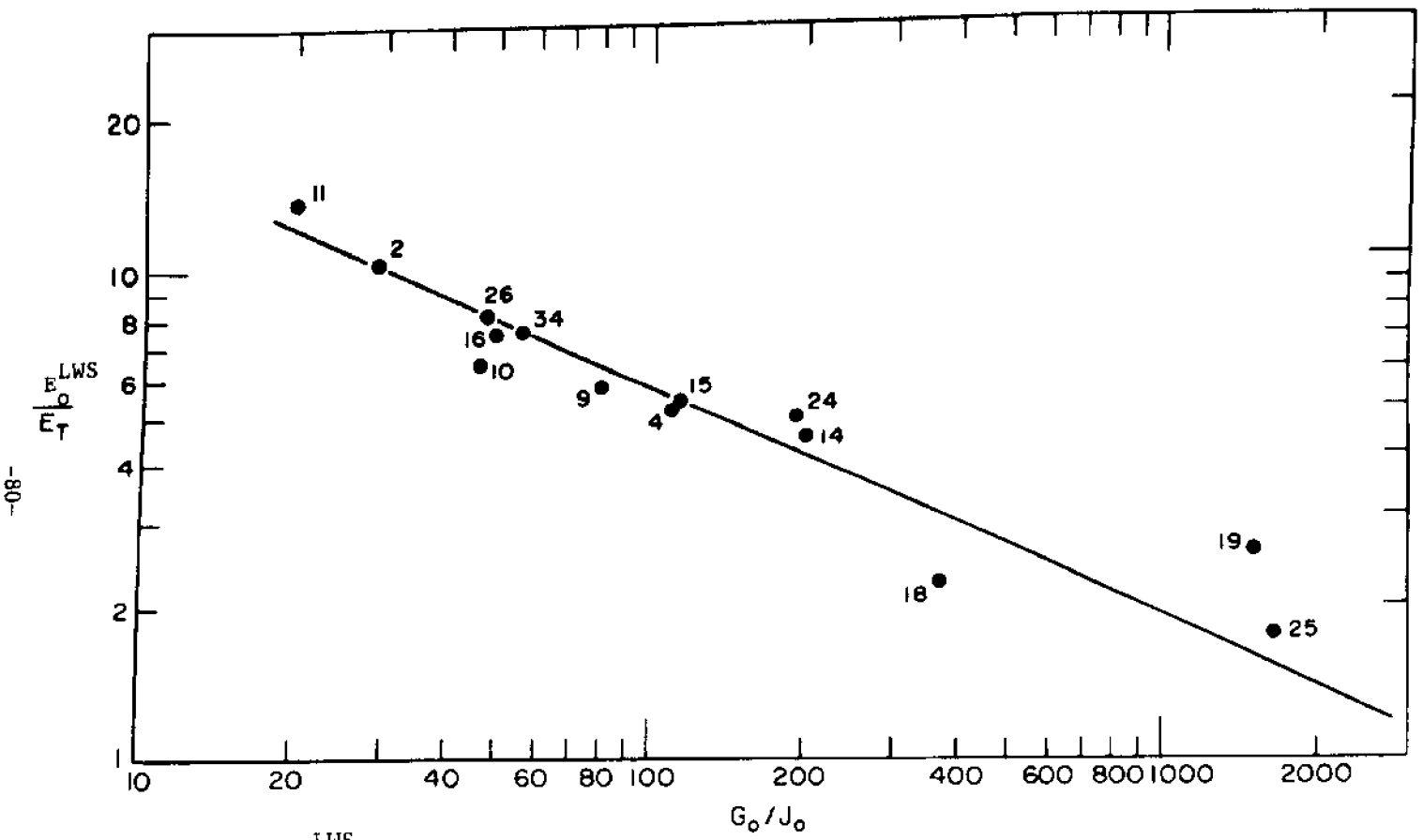

$\frac{E_o^{LWS}}{E_T}$ VS. G_o/J_o for WES Tests

Figure 4.4

$$G_o = \frac{g u_o^3}{C^2 h} \tag{4-5}$$

For J_o as defined by 4-1

$$\frac{G_o}{J_o} = \left(\frac{L}{C\ h^2\ \frac{\Delta\rho}{\rho}}\right)\left(\frac{u_o^3}{u_f}\right) \tag{4-6}$$

As

$$\frac{P_T}{T} = \frac{\int_{flood} Q dt}{T} = \overline{Q}_{flood}$$

where $\overline{Q}_{flood}$ is the average flood discharge, and

$$\mathbb{F}_o^2 = \frac{u_o^2}{gh},$$

where u_o is the maximum tidal velocity at the ocean entrance, then

$$\mathbb{E} = \frac{P_T \mathbb{F}_o^2}{Q_f T} = \left(\frac{1}{gh}\right)\left(\frac{\overline{u}_{flood}\ u_o^2}{u_f}\right) \tag{4-7}$$

As this correlation was made for the W.E.S. flume data with constant h, constant L, and almost the same $\frac{\Delta\rho}{\rho}$, and as $\overline{u}_{flood}$ is not very different from u_o, the maximum tidal velocity, it is seen that expressions 4-6 and 4-7 are both approximately proportional to $\frac{u_o^3}{u_f}$. Consequently the very good correlation of $\mathbb{E}$ vs. G/J shown in Figure 4.5 can be expected.

The Estuary Number including the density effects is used in this study as a measure of stratification based on the following two reasons:

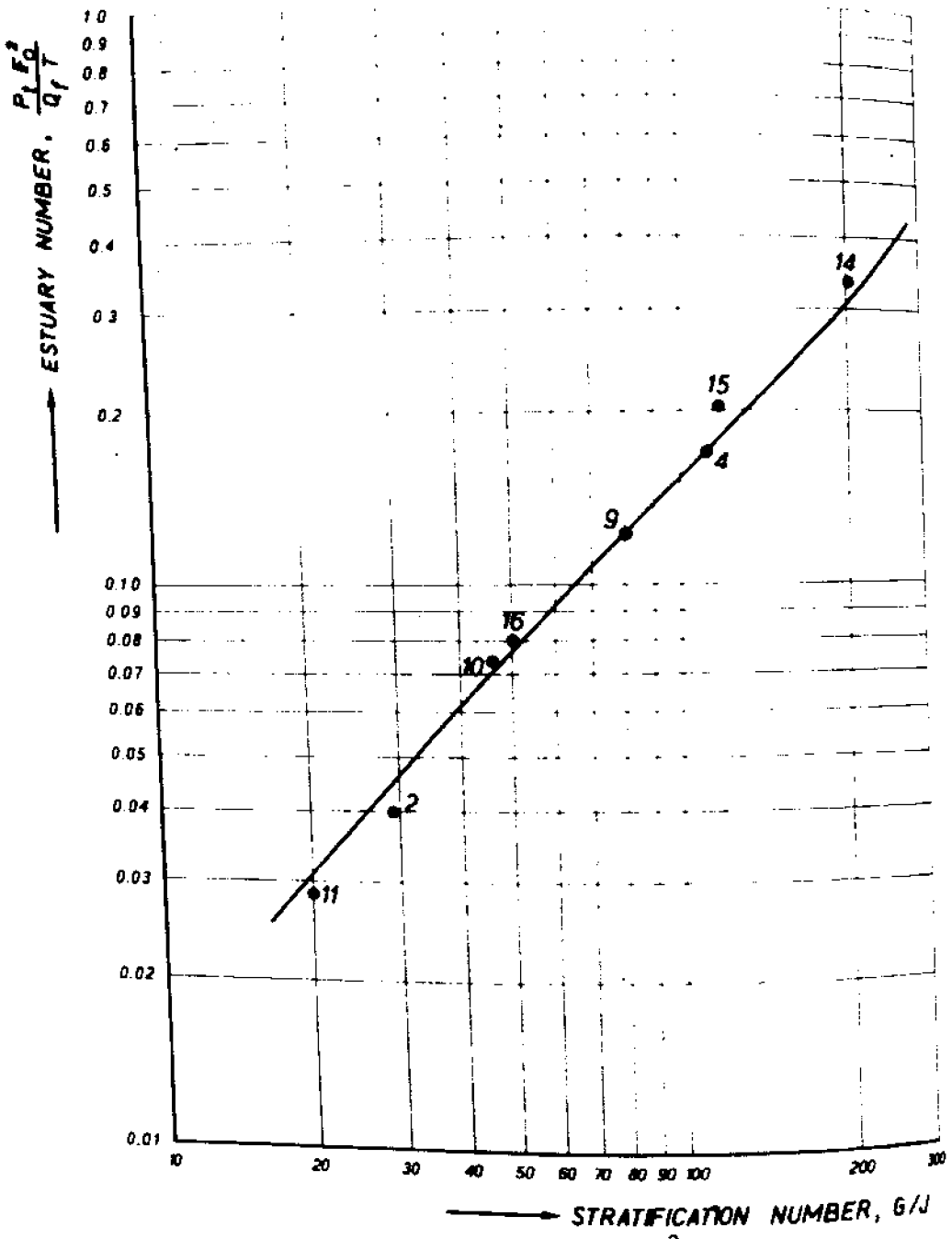

Correlation of Estuary Number $\frac{P_T F_o^2}{Q_f T}$, with Stratification Number, G/J

(from Harleman and Abraham, 1965)

Figure 4.5

1) It can be shown to be a measure of the ratio of stabilizing or stratifying effects to unstabilizing or mixing effects.

2) It is composed of available quantities which can be evaluated from the boundary conditions, the geometry and some knowledge of the tidal hydraulics.

This number is defined as:

$$\mathbb{E}_D = \frac{P_T \mathbb{F}_D^2}{Q_f T} \tag{4-8}$$

where P_T is the tidal prism defined as the volume of water entering on the flood tide.

$\mathbf{F}_D$ is the densimetric Froude number, $\frac{u_o}{\sqrt{gh\,\frac{\Delta\rho}{\rho}}}$, wherein u_o is the maximum flood velocity at the entrance and $\Delta\rho$ is the change in density over the entire length of the estuary.

4.3 Relation of Dispersion Parameter K to Stratification

4.3.1 Introduction

Previous studies have shown that the dispersion coefficient is dependent upon the degree of stratification. For example, in the W.E.S. series, Figure 4.4 shows a definite correlation between E_o^{LWS}/E_T and G_o/J_o. In this study the dispersion coefficient is expressed in terms of a parameter K times the absolute value of the local, non-dimensional, longitudinal salinity gradient.

$$E(x,t) = K \left| \frac{\partial \overset{\circ}{s}}{\partial \overset{\circ}{x}} \right| + E_T \tag{3-25}$$

Although the $\frac{\partial \overset{\circ}{s}}{\partial \overset{\circ}{x}}$ will reflect changes in stratification to

some extent, it is expected that it will also show a correlation to stratification.

In order to define a relationship between K and stratification, the numerical model was run for several quasi steady-state conditions for which data was available. The K values which best fit the salinity data were determined and the corresponding estuary numbers E_D were evaluated.

4.3.2 Analysis of Waterways Experiment Station Salinity Flume Data

A rectangular flume 327 feet long, 0.75 feet wide and with a mean depth of 0.5 feet was used for the W.E.S. salinity experiments. This study has considered five of the twenty tests reported by Ippen and Harleman (1961). These five tests all have the same roughness, but have different conditions of fresh water discharge and tidal amplitude. All tests were run until a quasi steady-state was obtained with a tidal period of 600 seconds. Table 4.1 presents the basic characteristics for these five tests. The procedure for determining K was as follows:

1) Using the quasi steady-state version of the numerical model developed in this study, the tidal hydraulics of the salinity flume were verified using a Manning's n equal to 0.020. This corresponds to the value determined in the original salinity flume

SUMMARY OF BASIC CHARACTERISTICS
W.E.S. TESTS

Tidal Period: 600 seconds

Manning's 'n' (Roughness): 0.020

Length 327 feet, Width 0.75 feet, Mean Depth 0.5 feet

Test No.	Ocean Salinity, S_o (ppt.)	Fresh Water Discharge, Q_f (cfs)	Tidal Amplitude, a(ft)
16	29.2	0.0075	0.05
2	25.6	0.0150	0.05
11	26.4	0.0210	0.05
10	26.8	0.0210	0.75
14	29.7	0.075	0.10

TABLE 4.1

study for those tests with side wall roughness. Figure 4.6 shows this verification in terms of surface elevations.

2) The best values of the dispersion parameter K were determined by computing the quasi steady-state salinity distribution corresponding to each of the K values selected. The quasi steady-state distribution is defined in terms of the numerical calculations as that distribution which, under conditions of constant fresh water discharge and repeating tidal amplitude, is the same as the distribution obtained in the previous tidal cycle, any small difference being less than a tolerable error. In this case the allowable error was specified as 0.02 ppt. The numerically determined salinity distributions (Figures 4.7a-e) were then compared with data obtained by integrating the two-dimensional salinity distribution data over the depth at specific times during the tidal cycle. The sum of the absolute values of the residual errors between the experimental, depth-averaged data and the corresponding numerical results were summed for each K value and the K value corresponding to the smallest sum of these residuals was chosen as the best K value for that particular test. Figure 4.8 illustrates the results of this procedure for the five tests studied.

4.3.3 Analysis of Rotterdam Waterway under Constant Area Approximation

Stigter and Siemons (1967), in making their numerical study

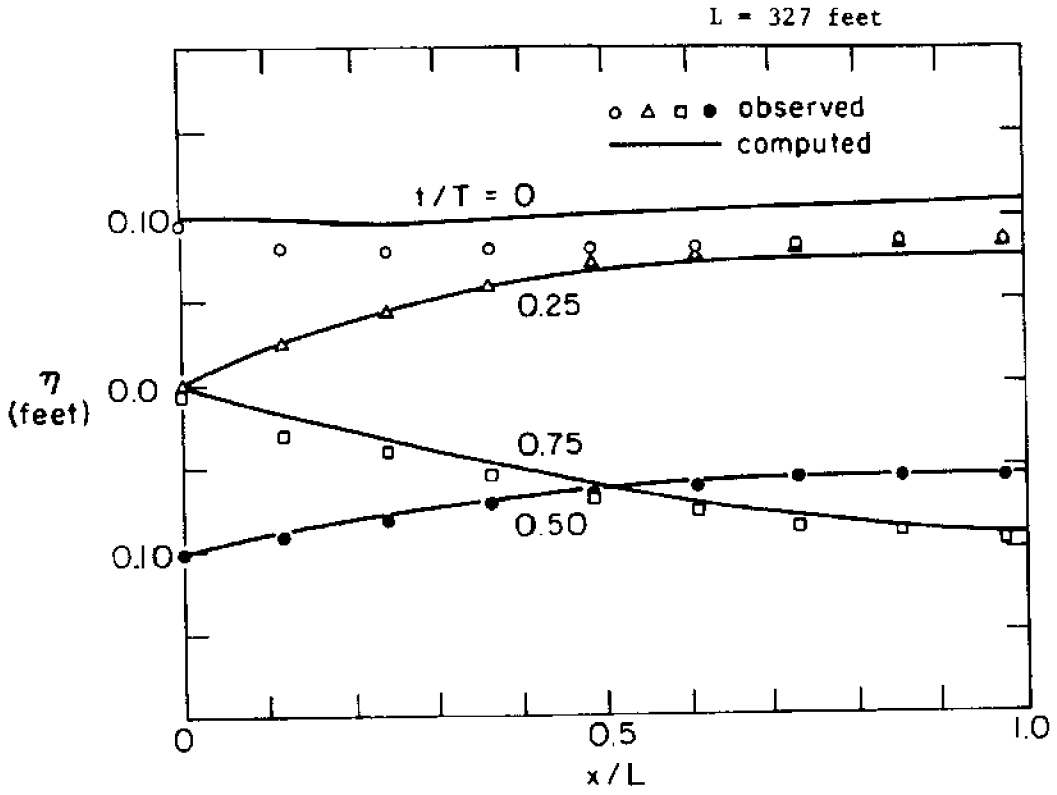

Example of Surface Elevation Verification (W.E.S. 14)

Figure 4.6

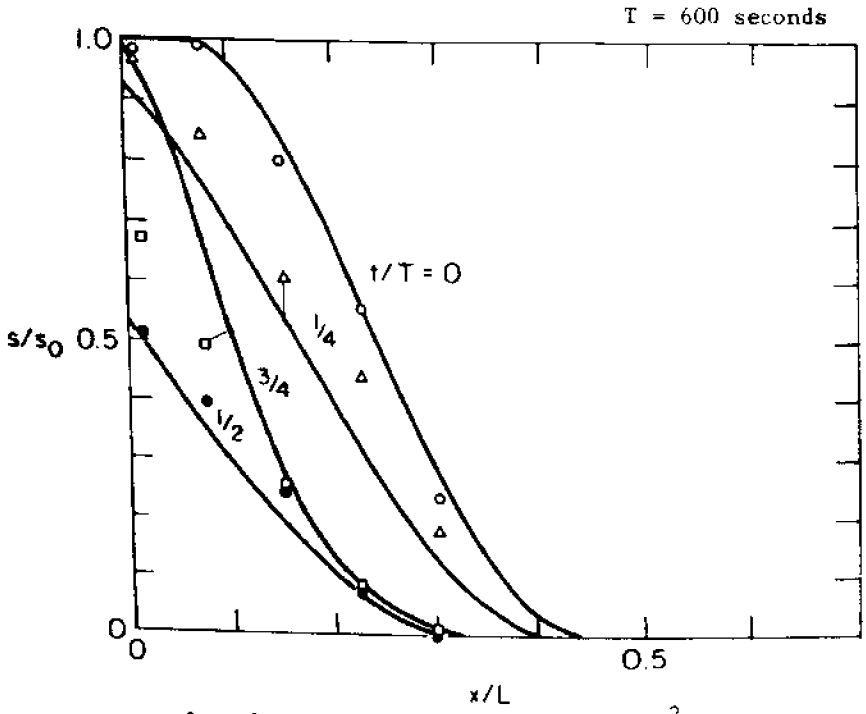

S_o = 25.6 ppt K = 0.35 ft^2/sec

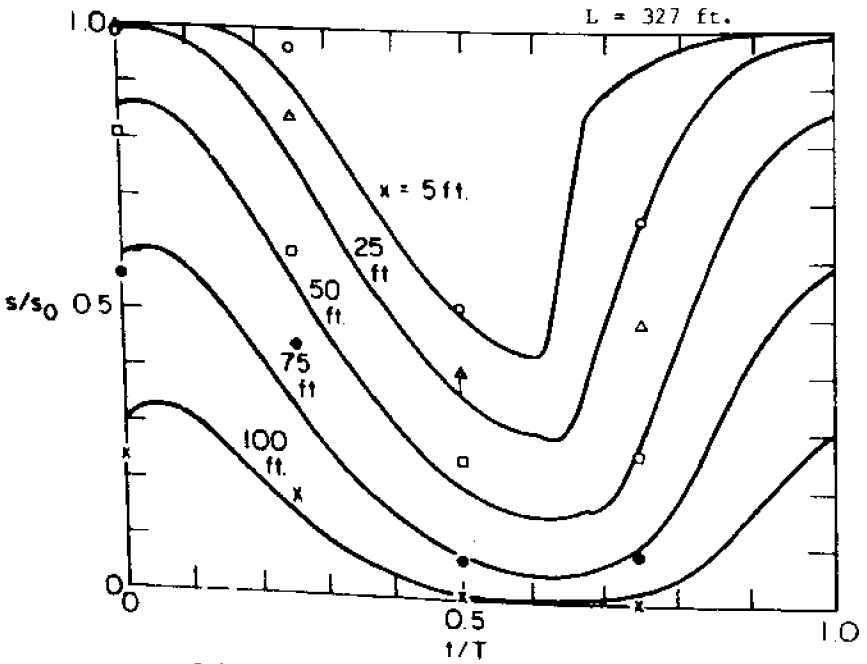

Salinity Verification for WES Test 2

Figure 4.7a

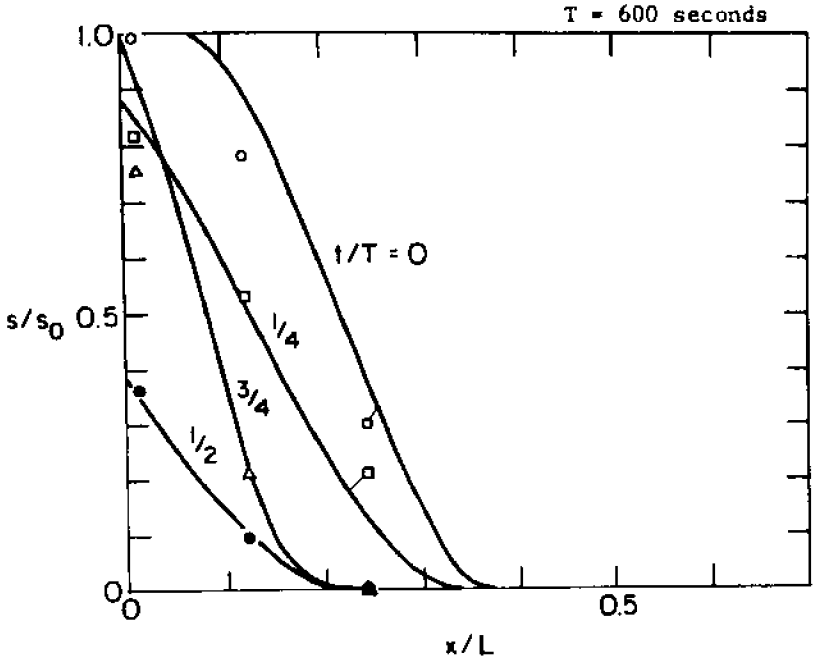

s_o = 26.4 ppt K = 0.25 ft^2/sec

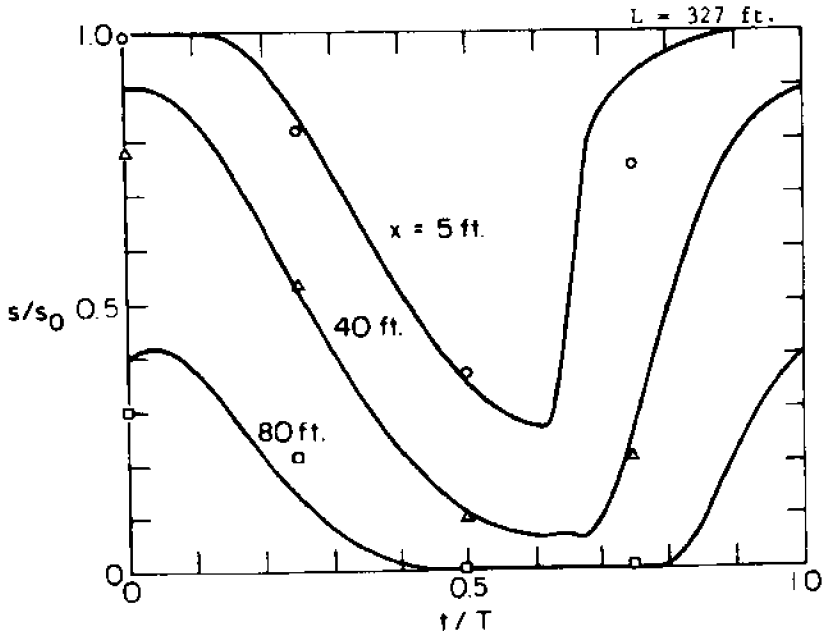

Salinity Verification for WES Test 11

Figure 4.7b

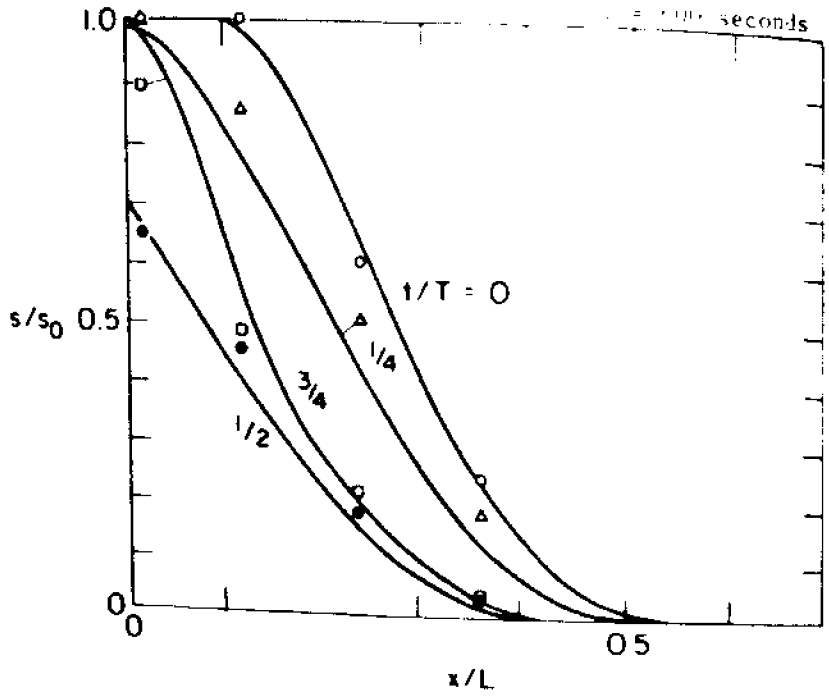

S_o = 29.2 ppt

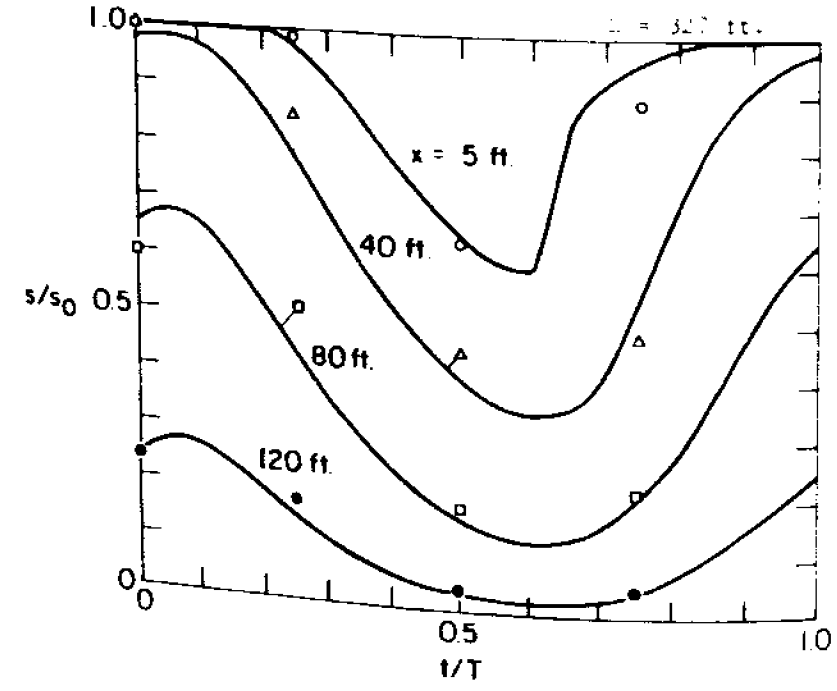

Salinity Verification for WES Test 16

Figure 4.7c

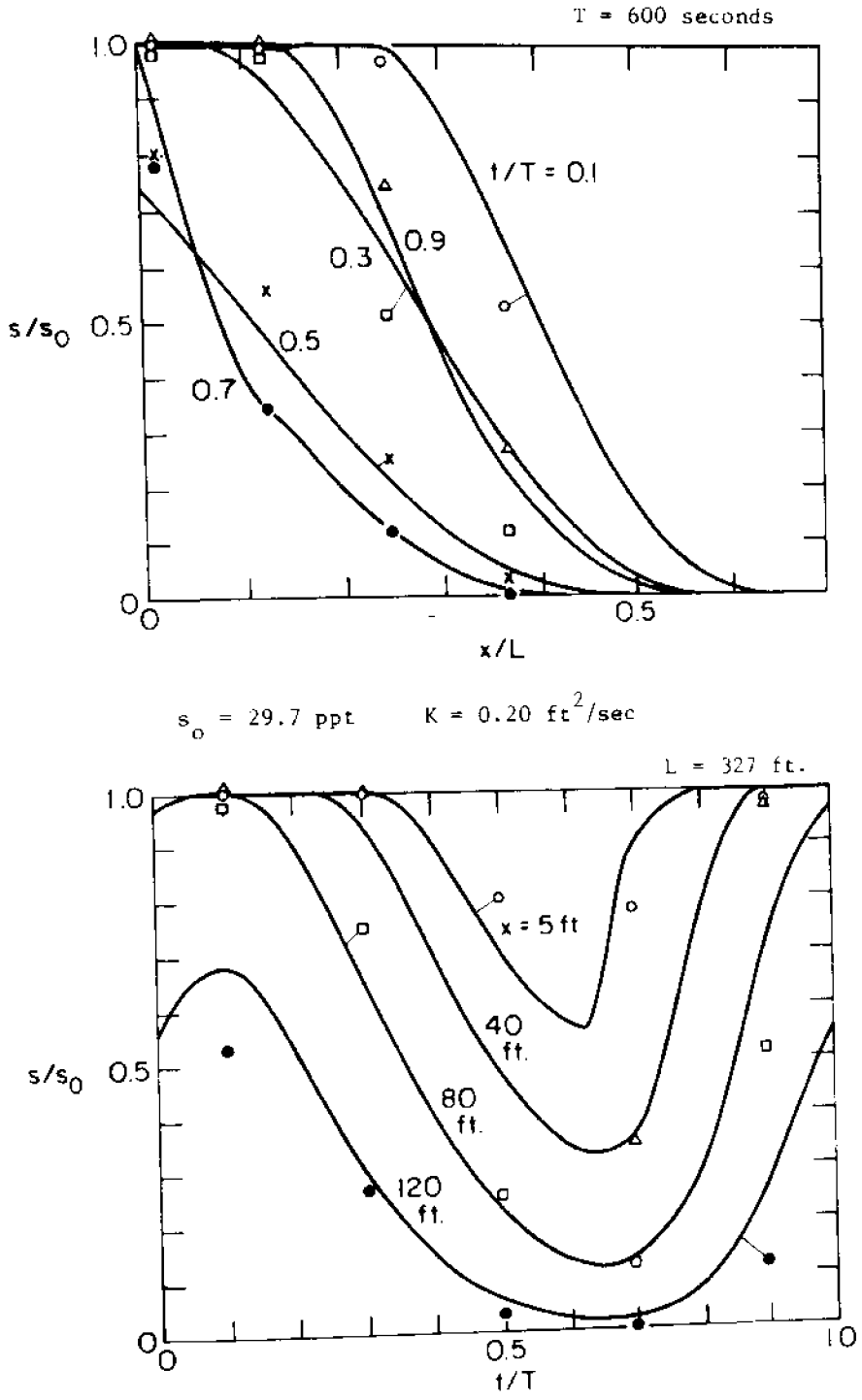

Salinity Verification for WES Test 14

Figure 4.7d

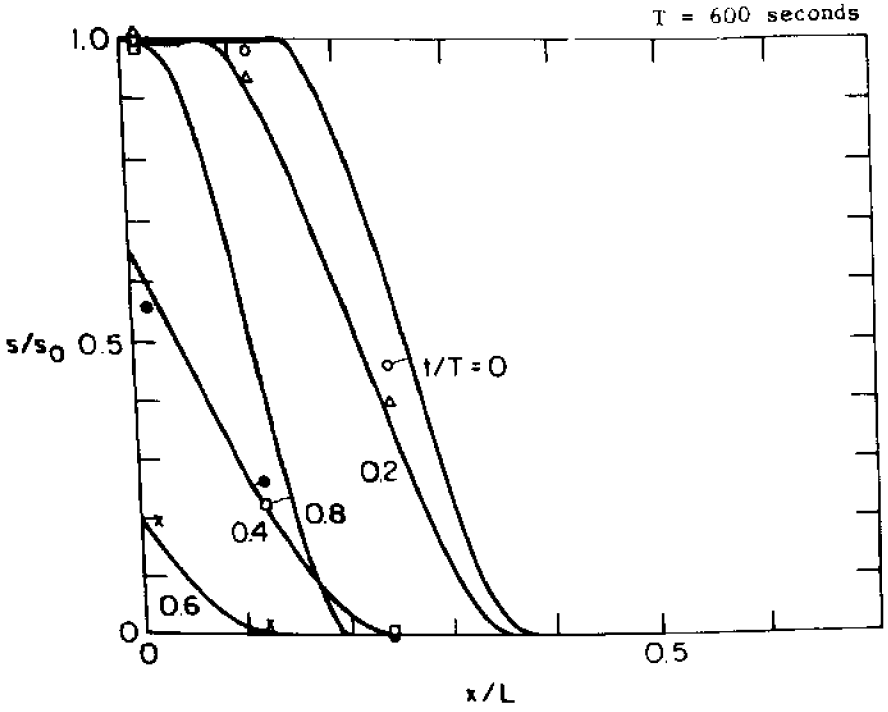

s_o = 26.8 ppt K = 0.1 ft^2/sec

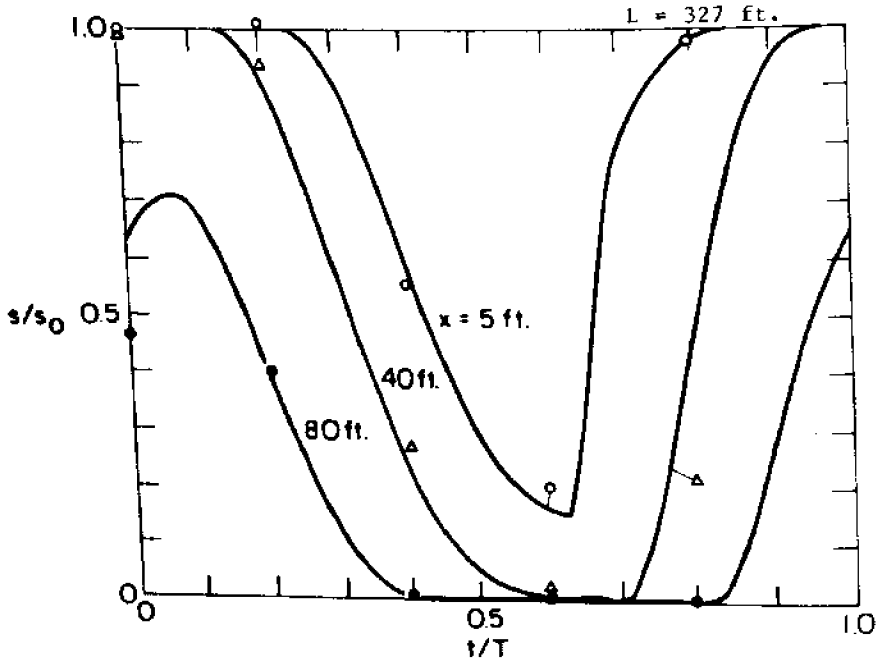

Salinity Verification for WES Test 10

Figure 4.7e

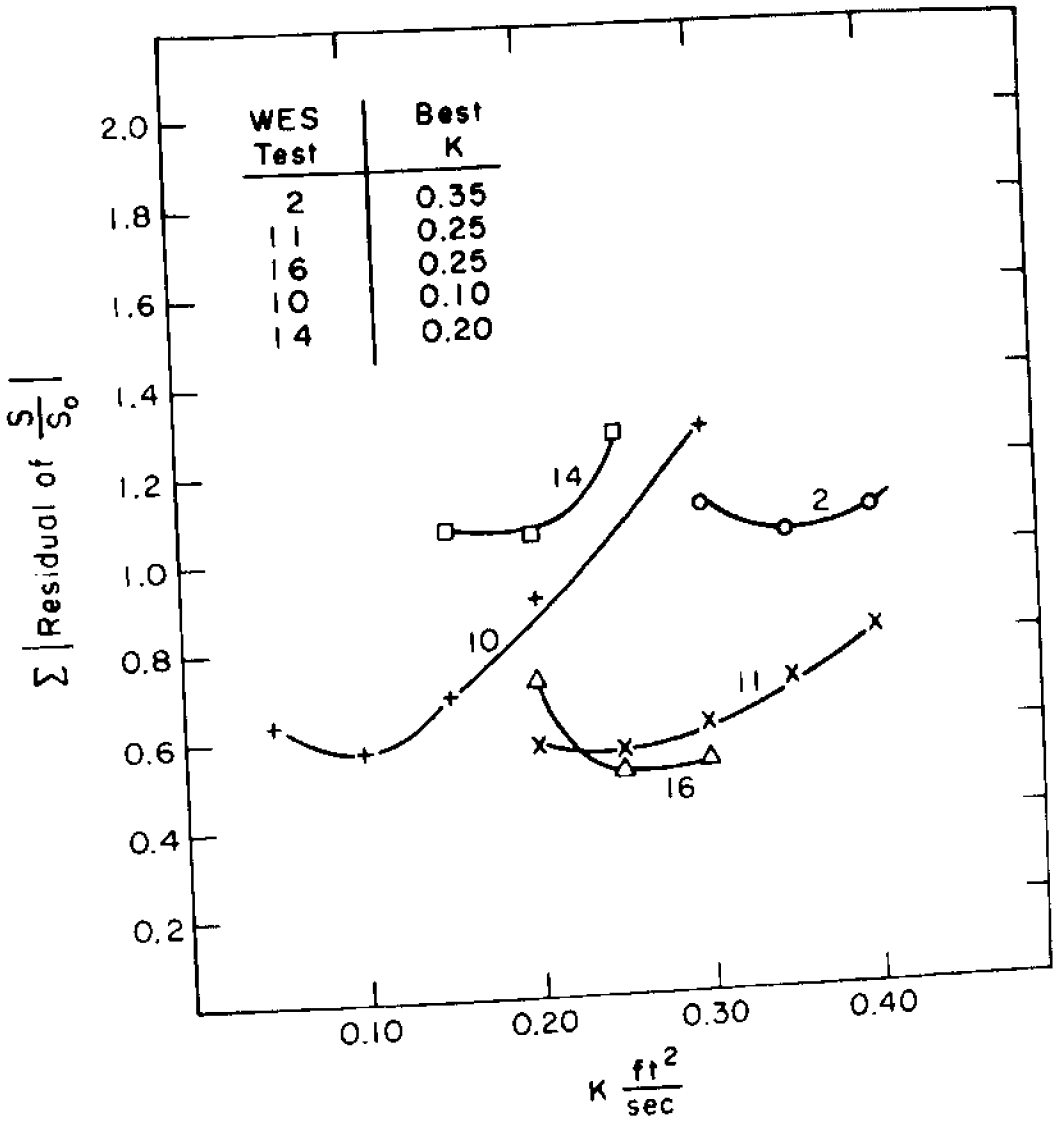

Determination of Best K Values
for WES Steady State Tests

Figure 4.8

(Section 2.5), have schematized the Rotterdam Waterway as a closed-end estuary of constant width and rectangular cross-section. The exact dimensions were chosen to yield a close representation of the prototype tidal conditions for the 24th of June, 1956. Although Stigter and Siemons worked with salinity data on the 24th of June, Harleman and Abraham have reported that data on the 26th of June would be more representative of a steady-state salinity condition for this period. In this study, it is assumed that the tidal data at the Hook of Holland on the 24th of June is approximately the same as that two days later, and that this data can be considered the ocean boundary condition at the end of the breakwater 2.7 km downstream. Figure 4.9 is a plan of the estuary, Figure 4.10 gives tidal elevations at the ocean as a function of time. The basic parameters of schematization are listed in Table 4.2. The resulting quasi steady-state High Water Slack and Low Water Slack salinity distributions are shown for values of K equal to 2000, 3000, and 4000 ft^2/sec in Figure 4.11. These distributions correspond to a convergence of successive distributions to within 0.02 ppt. The comparison of these curves to data given by Harleman and Abraham indicates that $K = 3000\ ft^2/sec$ is reasonable if one does not weigh the ocean values of Low Water Slack as much as the salinity values of the interior estuary region. The purpose of this analysis is to get an approximate value of K; it is recognized that the same precision obtainable with laboratory data can not be expected from field measurements.

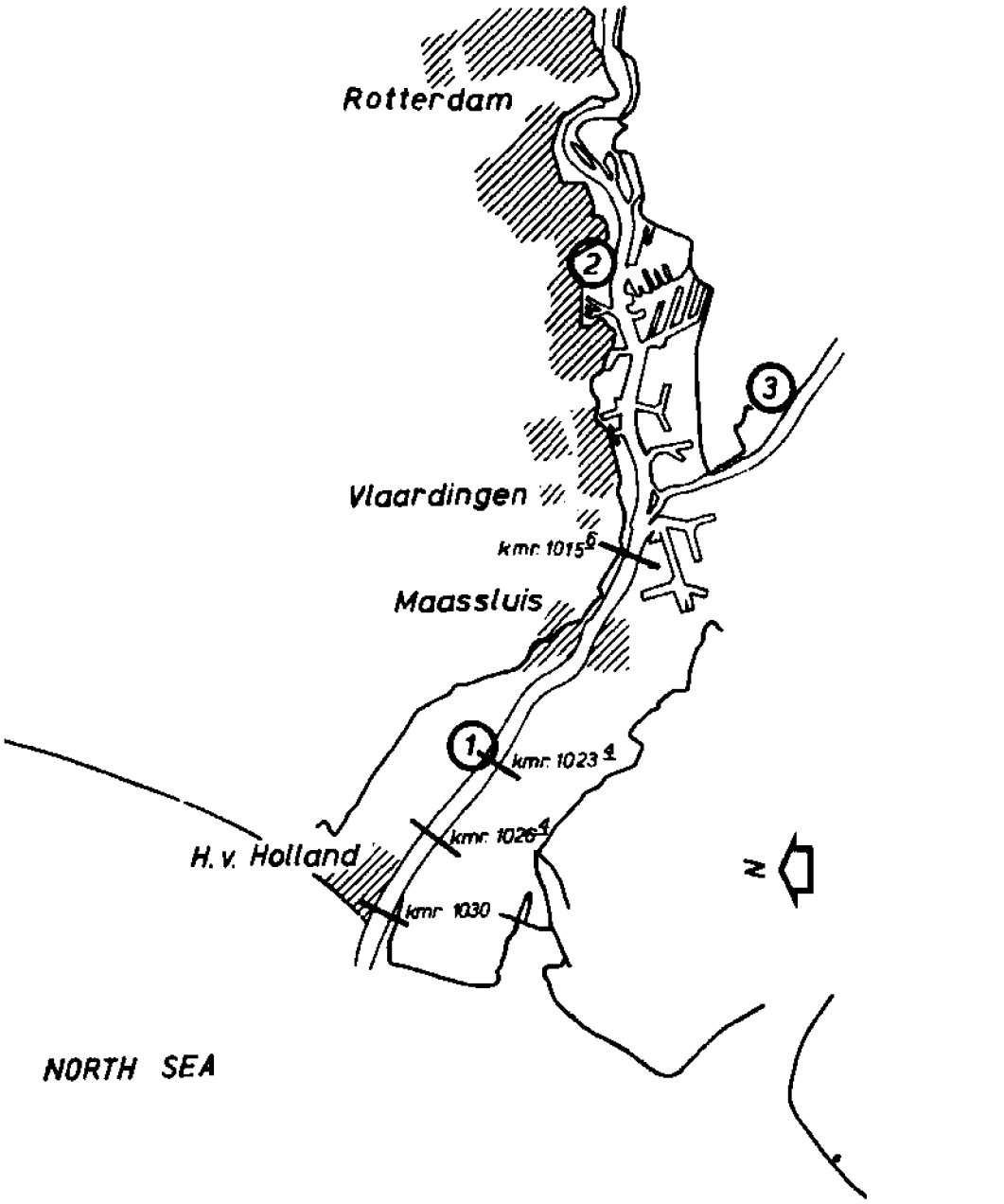

Plan of Rotterdam Waterway
(from Stigter and Siemons, 1967)

Figure 4.9

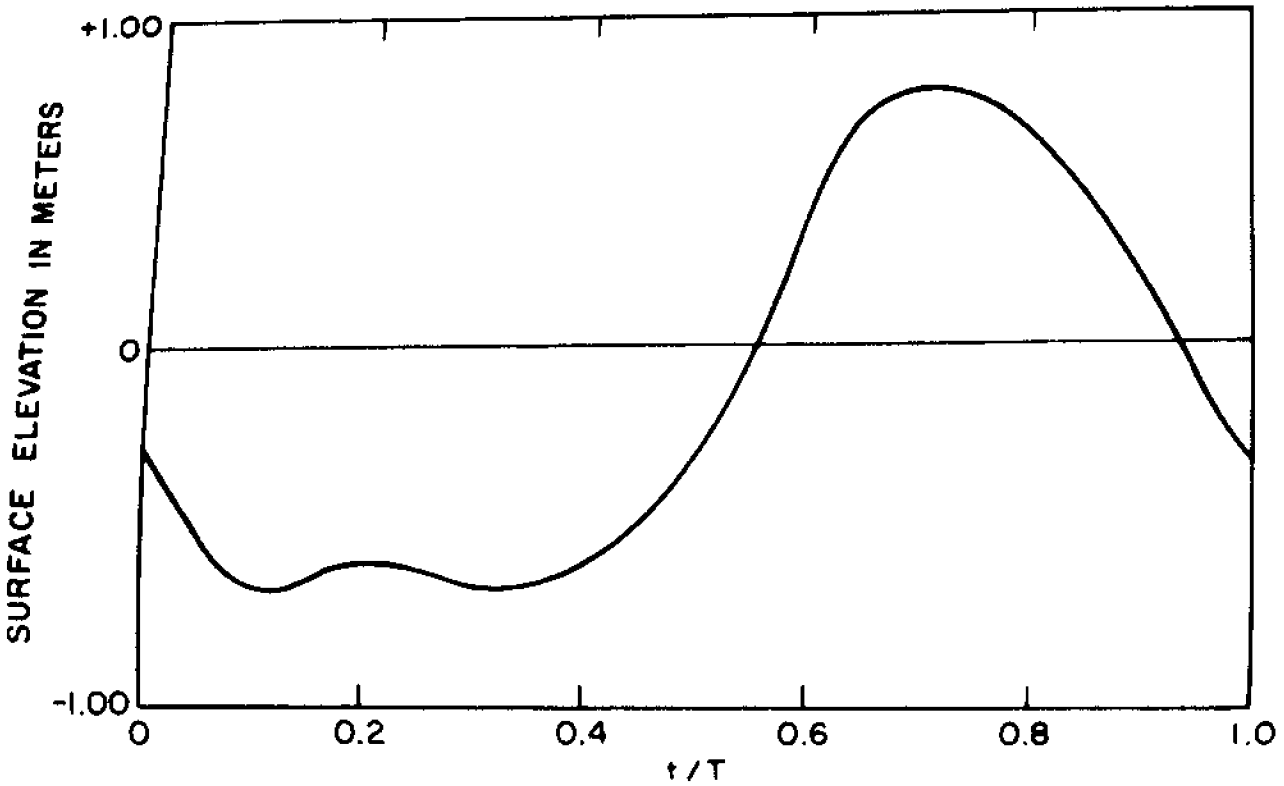

Water Surface Elevation, η(t) at Hook of Holland
(from Stigter and Siemons, 1967)

Figure 4.10

Table 4.2

Basic Parameters for
Rotterdam Waterway Study

Width	407.5 meters
Depth	13.0 meters
Fresh Water Discharge	960 m^3/sec

(From Harleman and Abraham, 1965. Profile II, 26th of June 1956 of their Table III.)

Length	98.64 km
Chezy coefficient	65 $m^{1/2}$/sec
Tidal period	44,700 seconds

(From Stigter and Siemons, 1967, their length was 95.94 km. 2.7 km have been added to carry the schematization from the Hook of Holland to the end of the breakwater.)

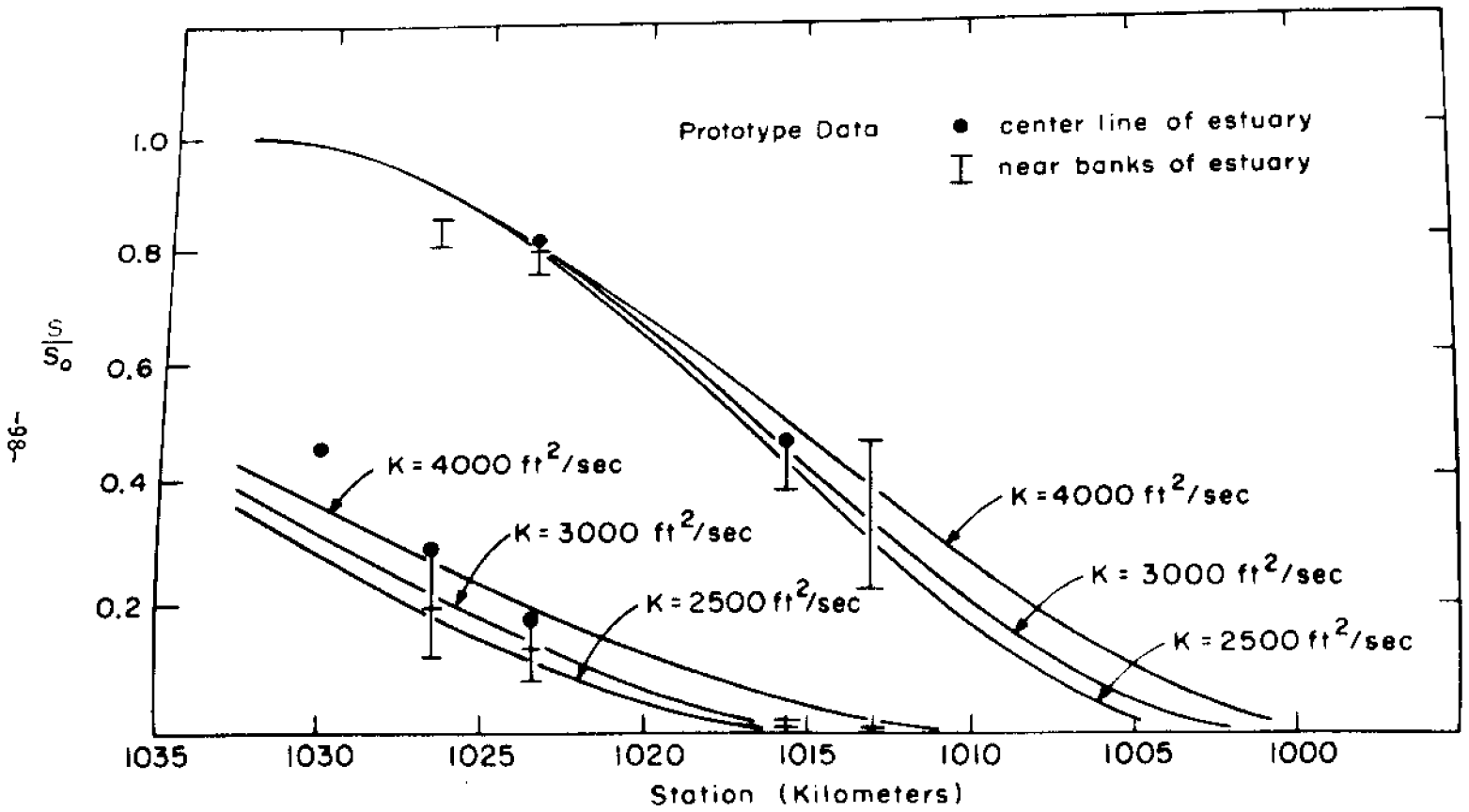

Rotterdam Waterway. Predicted High and Low Water
Slack Salinity Distributions for Different Values of K

Figure 4.11

4.4 Normalization of Dispersion Parameter and Relationship to Estuary Number

The objective in normalizing the Dispersion Parameter, K, and finding a relationship to Estuary Number is to find such a relationship which provides not only a good correlation for a particular estuary, but also a means of evaluating the dispersion parameter for estuaries without any recourse to field data for that estuary. It is desired to find a correlation which removes K as the only parameter needing experimental data for its determination.

It is important at this point to reemphasize the fact that K, the dispersion parameter in

$$E(x,t) = K \left| \frac{\partial \overset{\circ}{s}}{\partial \overset{\circ}{x}} \right| + E_T \qquad (3\text{-}25)$$

is not the dispersion coefficient itself. It becomes an approximation of the dispersion coefficient, E(x,t), only when multiplied by the non-dimensional salinity gradient. (Assuming E_T small with respect to E(x,t)). Consequently any change in salinity gradient due to a change in fresh water discharge or in tidal velocities is immediately incorporated into a change in the dispersion coefficient by the nature of expression 3-25. This fact has made it easier to find a correlation than for cases such as the study of Harleman and Abraham, in which the maximum dispersion coefficient E_o^{LWS} was being correlated.

To normalize the dispersion parameter K it was first attempted to divide it by the well-mixed dispersion coefficient,

E_T as calculated using u_o the maximum flood velocity. This type of normalization has been used in Figure 4.4 for the W.E.S. tests and in Figure 4.12 by Ippen (1966). He shows that when both flume-sized estuaries and real estuaries are plotted together a distinct scale effect is evidenced. This has also resulted in this study as shown by Figure 4.13 where the five W.E.S. tests and the Rotterdam Waterway values of K/E_T have been plotted against densimetric estuary number $\mathbb{E}_D$.

This lack of correlation for estuaries of model and prototype dimensions can be explained by considering the fact that the width to depth ratio of model estuaries is distorted with respect to real estuaries so that the dispersion coefficient without considering salinity effects is proportionally much greater in the distorted model than in the prototype. Harleman (1971) has demonstrated this on a dimensional basis.

Defining dispersion coefficient as in Equation 3-20,

$$EA \frac{\partial s}{\partial x} = \int_A u''s'' \, dA \qquad (3\text{-}20)$$

one can see that in a distorted model (narrow cross-section) the velocity anomalities u'' will be much greater than for an undistorted model (very wide cross-section). Because of this dimensional sensitivity, the well-mixed dispersion coefficient, E_T, is not suitable as a normalizing parameter for relating estuaries of different dimensions.

A more obvious means of non-dimensionalizing K is shown by

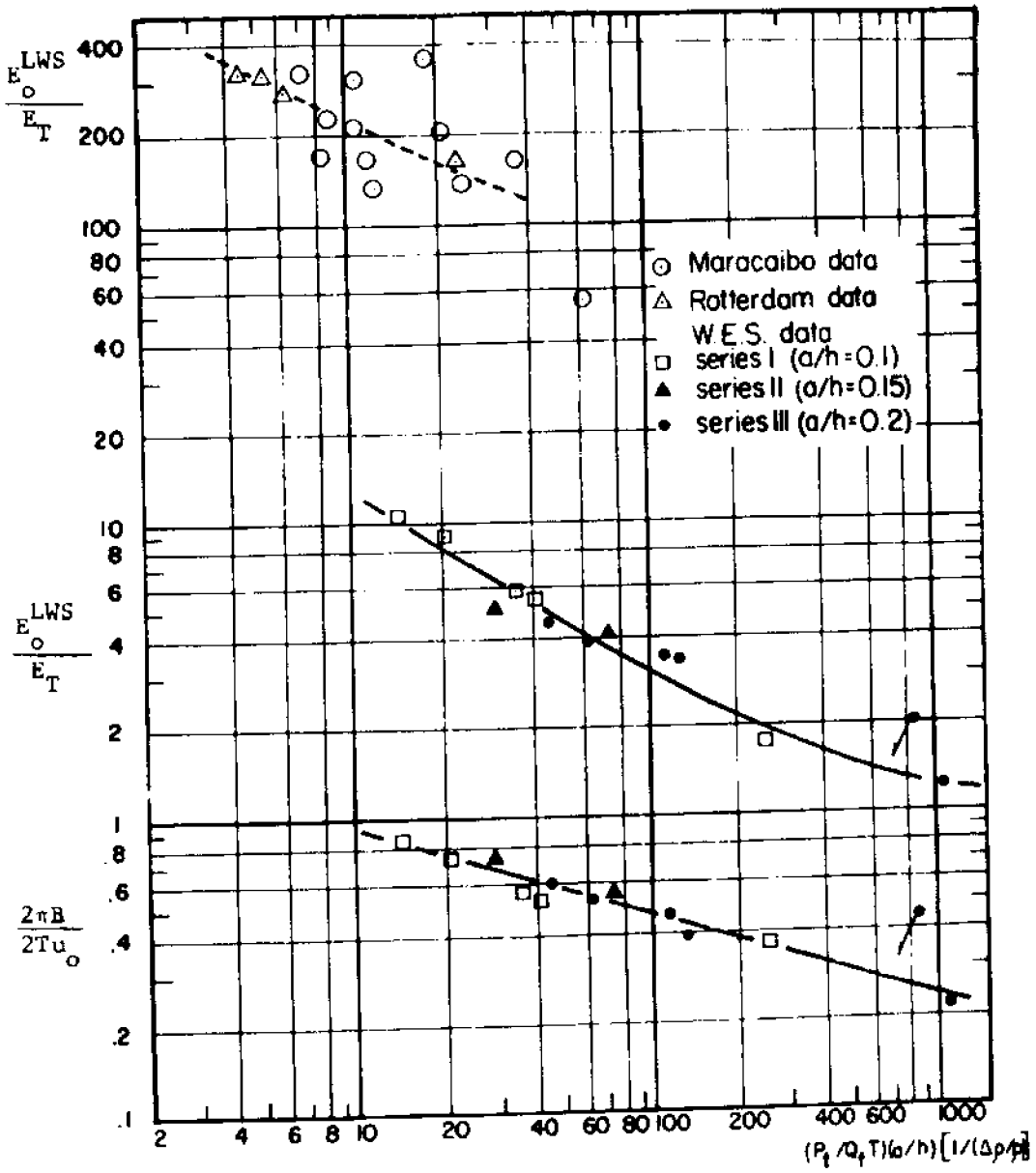

$\frac{E_o^{LWS}}{E_T}$ vs $\frac{P_T}{Q_f T}\left(\frac{a}{h}\right)\frac{1}{\Delta\rho/\rho}$ for Different Estuaries

(from Ippen, 1966)

Figure 4.12

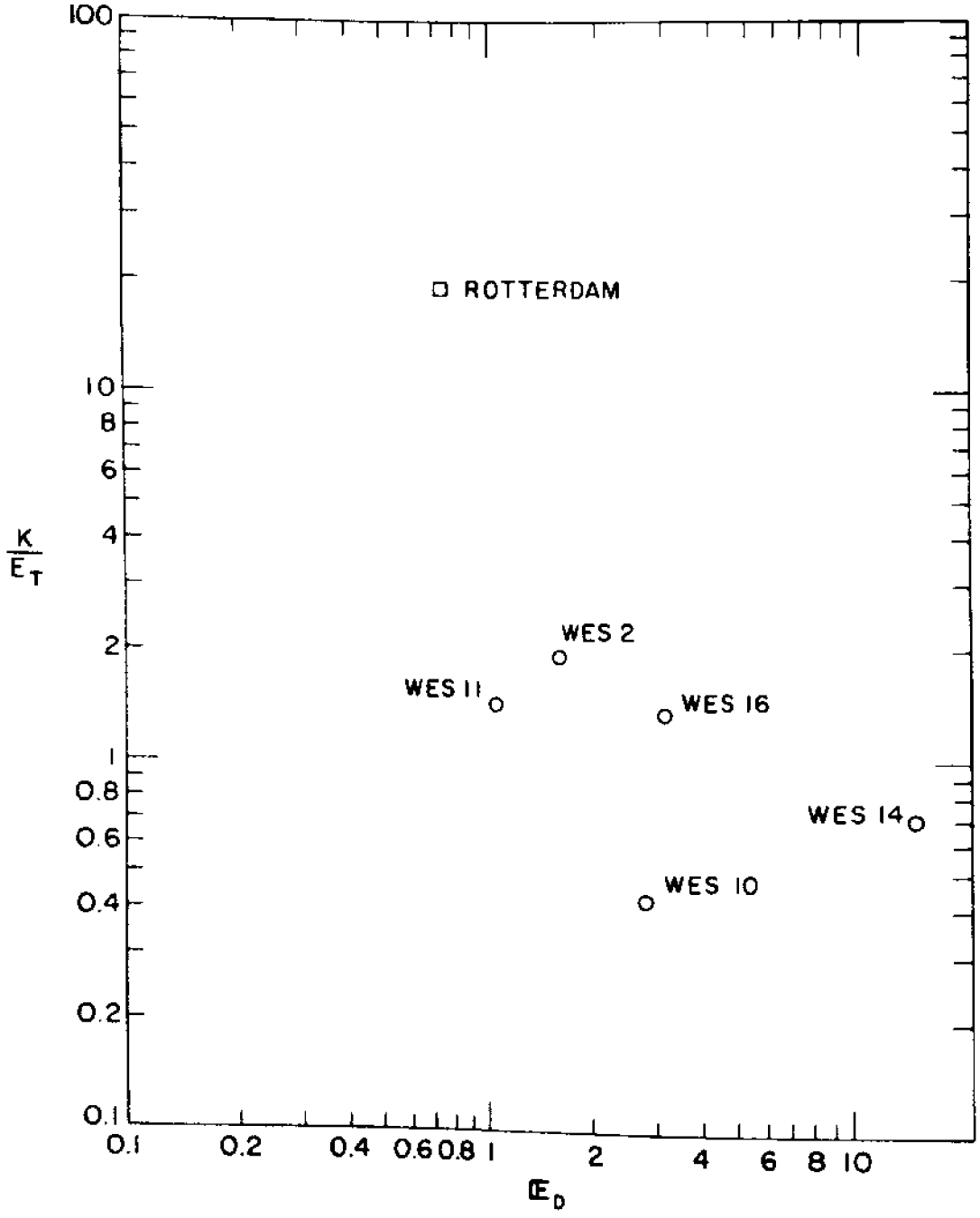

K/E_T vs E_D for WES and Rotterdam Waterway

Figure 4.13

considering the expression for K derived in Chapter 3 for the time-averaged, steady-state condition. For a constant area or variable area estuary this is

$$K = u_f L \frac{\overset{\circ}{s}}{\left(\frac{\partial \overset{\circ}{s}}{\partial \overset{\circ}{x}}\right)^2} \qquad (3\text{-}28)$$

where

$$u_f = \frac{Q_f}{A}$$

Therefore

$$\frac{K}{u_f L} = \frac{\overset{\circ}{s}}{\left(\frac{\partial \overset{\circ}{s}}{\partial \overset{\circ}{x}}\right)^2}$$

appears as a non-dimensional representation of K in terms of the ratio of two non-dimensional quantities which pertain only to the salinity distribution itself. The similar form in tidal time would be $\frac{K}{u_o L}$ where u_o is the maximum flood velocity at the entrance to the estuary. This form of non-dimensional dispersion parameter can also be shown to result from a non-dimensionalizing of the governing salt balance equation.

A plot of $\frac{K}{u_o L}$ vs. $\mathbb{E}_D$, where L is the estuary length and u_o is the maximum flood velocity, is presented in Figure 4.14 for the results of the five W.E.S. studies and for the Rotterdam Waterway study of this investigation. Although this plot is for constant-width estuaries it shows a correlation between estuaries whose lengths differ by a factor of 1000 and over considerable variation

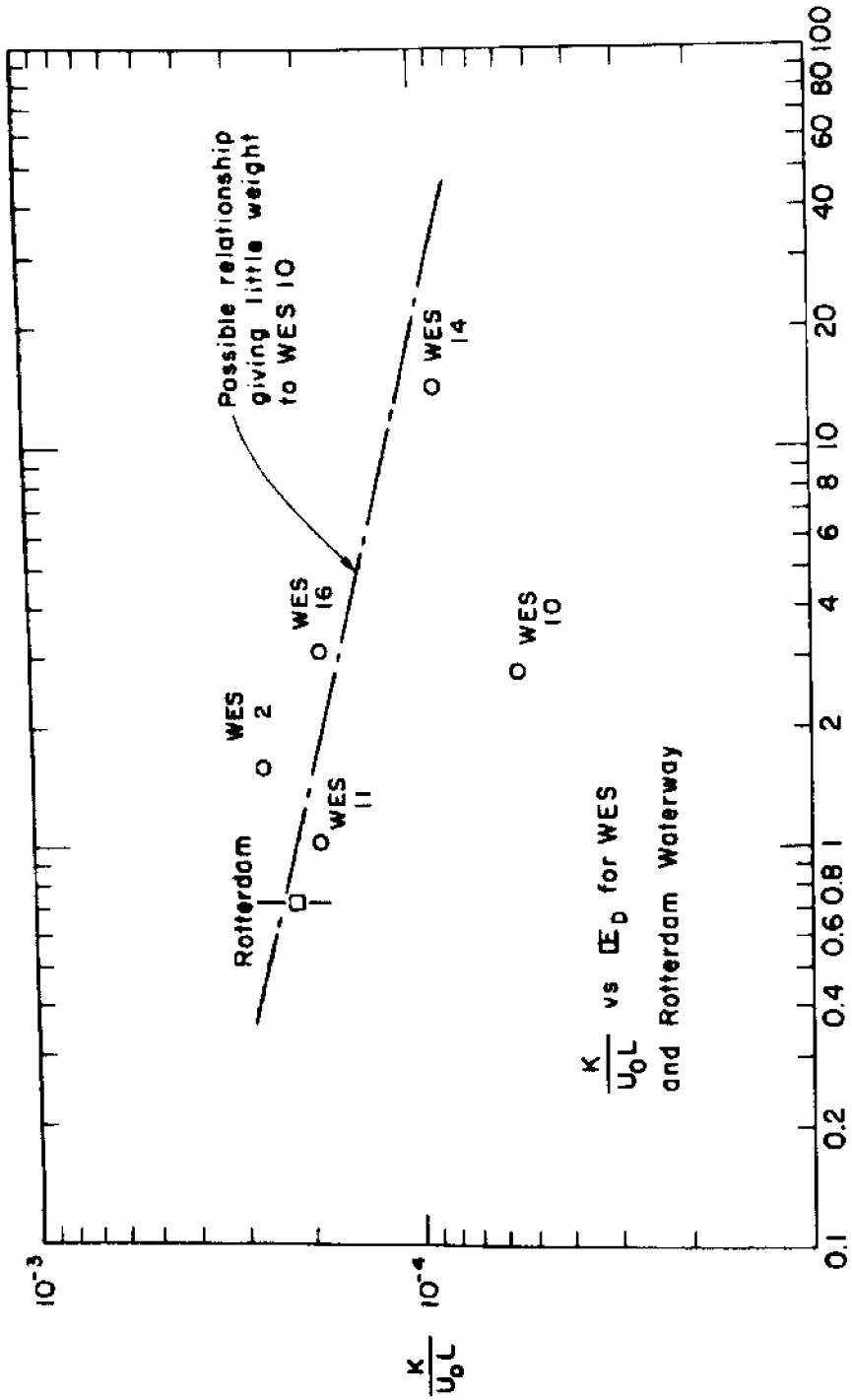
Possible relationship giving little weight to WES 10
WES 14
WES 16
WES 10
WES 11
WES 2
Rotterdam
$\frac{K}{U_0 L}$ vs $\mathcal{E}_D$ for WES and Rotterdam Waterway
$\frac{K}{U_0 L}$
10^{-3}
10^{-4}
0.1
0.2
0.4
0.6
0.8
1
2
4
6
8
10
20
40
60
80
100
$\mathcal{E}_D$

Figure 4.14

within the W.E.S. tests themselves. Based on these results, $\frac{K}{u_o L}$ was taken as the normalized dispersion parameter and further studies of variable-area estuaries were conducted both on a quasi steady-state and transient basis. The quasi steady-state studies have added other points to the curve which now extends over two full orders of magnitude in terms of the abscissa. This final correlation is presented in Chapter VI as Figure 6.28.

V. The Finite Difference Scheme

5.1 Introduction

The governing partial differential equations defining the unsteady salinity intrusion for variable area estuaries as set forth in Chapter 3 are not generally solvable by analytic methods. A solution, in terms of a finite difference representation of the equations, is developed. Such a solution is approximate by nature and is subject to possible errors which, if not detected and understood, could render the solution useless. The solution of the finite difference model is executed by digital computer and it is important to select a finite difference scheme which permits an efficient solution in terms of computer time.

The major part of this chapter will be devoted to the development of an accurate finite difference scheme for the solution of the salt balance equation. First, the finite difference representation of the tidal hydraulics will be presented essentially in the form of Harleman and Lee (1969), but with the addition of a term in the momentum equation representing the effect of the longitudinal density gradient.

5.2 Finite Difference Tidal Hydraulics Equations

The continuity equation

$$b \frac{\partial h}{\partial t} + \frac{\partial Q}{\partial x} - q = 0 \qquad (3\text{-}2)$$

is represented in finite differences in the manner of Harleman and Lee (1969).

The instantaneous water surface elevation above the reference datum. h, can be written as

$$h = z_o + d + \eta \tag{5-1}$$

where η is the instantaneous surface elevation with respect to the reference water level, $z_o + d$; therefore,

$$\frac{\partial h}{\partial t} = \frac{\partial \eta}{\partial t} \tag{5-2}$$

This permits Equation 3-2 to be written in terms of η as

$$b \frac{\partial \eta}{\partial t} + \frac{\partial Q}{\partial x} - q = 0 \tag{5-3}$$

The modification of the momentum equation including the effect of the density gradient is

$$\frac{\partial Q}{\partial t} + u \frac{\partial Q}{\partial x} + Q \frac{\partial u}{\partial x} + g \frac{\partial h}{\partial x} A + g \frac{Ad_c}{\rho} \frac{\partial \rho}{\partial x} + g \frac{Q|Q|}{AC^2 R_h} = 0 \tag{3-9}$$

This equation will also be written in terms of the two dependent variables η and Q by employing the relationship of Equation 5-1 and by replacing u by $\frac{Q}{A}$. ($A = A_{core}$). Expanding $\frac{\partial (Q/A)}{\partial x}$ one obtains

$$\frac{\partial Q}{\partial t} + \frac{2Q}{A} \frac{\partial Q}{\partial x} - \left(\frac{Q}{A}\right)^2 \frac{\partial A}{\partial x} + gA\left[\frac{\partial z_o}{\partial x} + \frac{\partial d}{\partial x} + \frac{\partial \eta}{\partial x}\right] + g \frac{Ad_c}{\rho} \frac{\partial \rho}{\partial x} + g \frac{Q|Q|}{AC^2 R_h} = 0 \tag{5-4}$$

Eliminating $\frac{\partial Q}{\partial x}$ by means of the continuity equation 5-3 and dividing by A,

$$\frac{1}{A} \frac{\partial Q}{\partial t} + \frac{2Q}{A^2} q - \frac{2bQ}{A^2} \frac{\partial \eta}{\partial t} - \frac{Q^2}{A^3} \frac{\partial A}{\partial x} + g\left[\frac{\partial z_o}{\partial x} + \frac{\partial d}{\partial x} + \frac{\partial \eta}{\partial x}\right] + g \frac{d_c}{\rho} \frac{\partial \rho}{\partial x} + \frac{gQ|Q|}{A^2 C^2 R_h} = 0 \tag{5-5}$$

Harleman and Lee show that the $\frac{Q^2}{A^3}\frac{\partial A}{\partial x}$ term can be neglected leaving the form of the momentum equation as

$$\frac{1}{A}\frac{\partial Q}{\partial t} + \frac{2Q}{A^2}q - \frac{2bQ}{A^2}\frac{\partial \eta}{\partial t} + g\left[\frac{\partial z_o}{\partial x} + \frac{\partial d}{\partial x} + \frac{\partial \eta}{\partial x}\right] + g\frac{d_c}{c}\frac{\partial c}{\partial x} + g\frac{Q|Q|}{A^2C^2R_h} = 0 \tag{5-6}$$

The finite difference equations are defined on a staggered grid as shown in Figure 5.1a. The continuity equation is explicitly solved first from time step n to time step n+2 using values of Q at time step n+1. This yields values of η at time step n+2. The momentum equation is then solved explicitly from time step n+1 to time step n+3 using the values of η at time step n+2. In this manner a solution is advanced in time.

By letting time step n represent the middle of the time interval for both the continuity equation 5-3 and the momentum equation 5-6 the finite difference equations are written:

Continuity Equation (with reference to Figure 5.1c)

$$\frac{b_j^n\left[\eta_j^{n+1} - \eta_j^{n-1}\right]}{2\Delta t} + \frac{Q_{j+1}^n - Q_{j-1}^n}{2\Delta x} - \frac{[Q_{trib}]_x}{2\Delta x} = 0 \tag{5-7}$$

where $[Q_{trib}]x$ = lateral inflow between sections j+1 and j-1.

Momentum Equation (with reference to Figure 5.1b)

$$\frac{1}{A_j^n}\left[\frac{Q_j^{n+1} - Q_j^{n-1}}{2\Delta t}\right] + \frac{2Q_j^{n-1}[Q_{trib}]_x}{\left(A_j^n\right)^2 2\Delta x} -$$

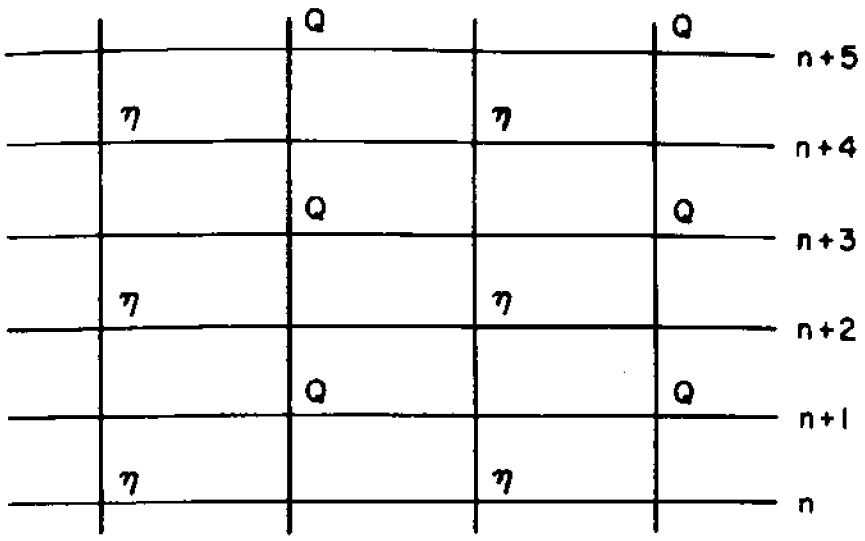

5.1a Staggered Mesh in Space and Time

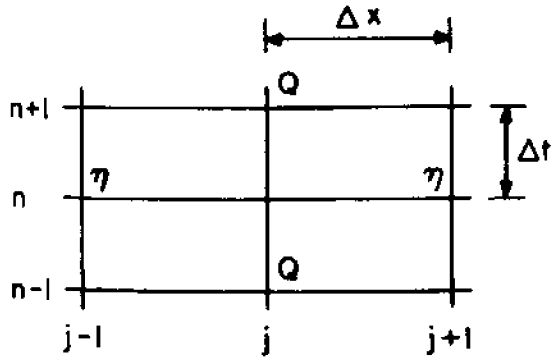

5.1b Staggered Explicit Molecule for Q

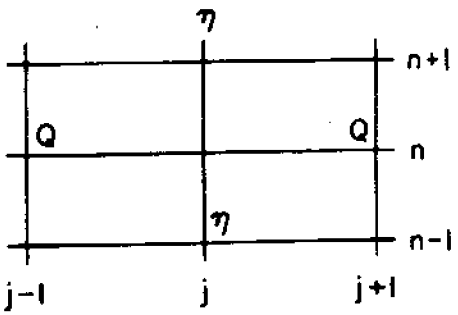

5.1c Staggered Explicit Molecule for η

Definition of Staggered Mesh

Figure 5.1

$$\frac{2b_j^n Q_j^{n-1}}{\left(A_j^n\right)^2} \cdot \frac{1}{2}\left[\frac{\eta_{j-1}^n - \eta_{j-1}^{n-2}}{2\Delta t} + \frac{\eta_{j+1}^n - \eta_{j+1}^{n-2}}{2\Delta t}\right] +$$

$$g\,\frac{([z_o]_{j+1} - [z_o]_{j-1})}{2\Delta x} + g\,\frac{(d_{j+1} - d_{j-1})}{2\Delta x} +$$

$$g\,\frac{(\eta_{j+1}^n - \eta_{j-1}^n)}{2\Delta t} + g\,\frac{(d_c)_j^n}{\rho_j^n}\,\frac{[\rho_{j+1}^n - \rho_{j-1}^n]}{2\Delta x} +$$

$$\frac{g|Q_j^{n-1}|}{\left(C_j^n\right)^2\left(A_j^n\right)^2 [R_h]_j^n} \cdot \frac{1}{2}\left(Q_j^{n+1} + Q_j^{n-1}\right) - W_j^n = 0 \qquad (5\text{-}8)$$

The Chezy coefficient is written in terms of the Manning's roughness n_j

$$C_j^n = \frac{1.49}{n_j}\left[(R_h)_j^n\right]^{1/6} \qquad (5\text{-}9)$$

The wind stress term introduced at the end of Equation 5-8 is

$$W_j^n = \frac{\beta_w \rho_a \mid V_j \cos\psi_j \mid V_j \cos\psi_j}{\rho [R_h]_j^n} \qquad (5\text{-}10)$$

where,

β_w = wind shear stress coefficient = 0.0026

ρ_a = air density

ρ = water density

V_j = absolute wind speed at section j

ψ_j = angle of wind to longitudinal axis of estuary at section j

For storage schematization (Figure 3.2b):

$$A_j^n = [b_{core}]_j \left[d_j + \frac{1}{2}\left(\eta_{j+1}^n + \eta_{j-1}^n\right)\right]$$

$$b_j^n = b_j$$

$$[R_h]_j^n = \frac{A_j^n}{[b_{core}]_j + 2d_j + \eta_{j+1}^n + \eta_{j-1}^n}$$

$$[d_c]_j^n = \frac{1}{2}\left[d_j + \frac{1}{2}\left(\eta_{j+1}^n + \eta_{j-1}^n\right)\right] \qquad (5\text{-}11)$$

For a trapezoidal schematization (Figure 3.2c):

$$b_j^n = [b_o]_j + 2S_j\left[d_j + \frac{1}{2}\left(\eta_{j+1}^n + \eta_{j-1}^n\right)\right]$$

$$A_j^n = \frac{1}{2}\left[b_j^n + [b_o]_j\right]\left[d_j + \frac{1}{2}\left(\eta_{j+1}^n + \eta_{j-1}^n\right)\right]$$

$$[R_h]_j^n = \frac{A_j^n}{[b_o]_j + 2\sqrt{1 + [S_j]^2}\left[d_j + \frac{1}{2}\left(\eta_{j+1}^n + \eta_{j-1}^n\right)\right]}$$

$$[d_c]_j^n = \frac{d_j + 1/2\left(\eta_{j+1}^n + \eta_{j-1}^n\right)}{6}\,\frac{(2\,b_{core} + b_{total})}{b_{core}} \qquad (5\text{-}12)$$

where

$b_{core} = \frac{1}{2}(b_o + b_{total})$, and S is the slope.

5.3 Finite Difference Salt Balance Equation

5.3.1 Simplified Form of Salt Balance Equation

The application of numerical methods to the partial differential equation 3-21 (salt balance equation) including its variable

coefficients and non-linear representation of the dispersion coefficient is far too complicated to yield results in terms of criteria of consistency, stability and convergence. It is common practice to consider a simplified version of the governing equation in order to apply techniques which permit an evaluation of the finite-difference scheme. The simplified form of the salt balance equation is obtained by considering a constant area, constant velocity and constant dispersion coefficient representation of equation 3-21 which reduces it to the linear convective-diffusion equation written with c(x,t) as the dependent variable.

$$\frac{\partial c}{\partial t} + V \frac{\partial c}{\partial x} = D \frac{\partial^2 c}{\partial x^2} \qquad (5\text{-}13)$$

where V is the velocity and D the diffusion (or dispersion) coefficient, and c(x,t) is the concentration of the substance being studied.

5.3.2 Stone and Brian's Method for a Minimum-Error Finite-Difference Scheme

Stone and Brian (1963) have considered an arbitrary six point scheme constructed by means of weighting factors and applicable to the $\frac{\partial c}{\partial t}$ and $\frac{\partial c}{\partial x}$ terms of Equation 5-13. Figure 5.2 shows how the weighting coefficients are assigned. The weighting coefficients a, $\frac{\epsilon}{2}$, b, d, $\frac{\theta}{2}$, g, and m are subject to the conditions

$$a + \frac{\epsilon}{2} + b + d = 1$$

$$g + \frac{\theta}{2} + m = 1 \qquad (5\text{-}14)$$

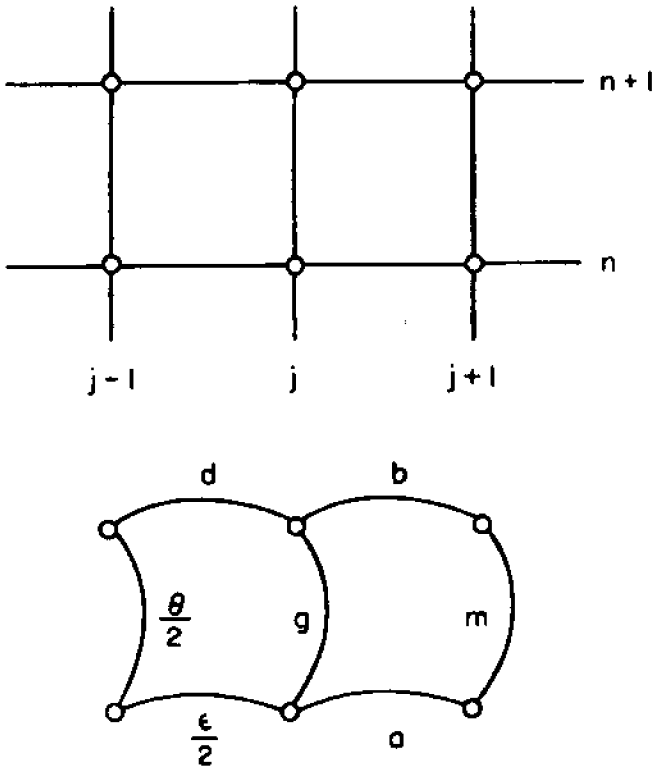

Arbitrarily Weighted
Six-point Computational Molecule

Figure 5.2

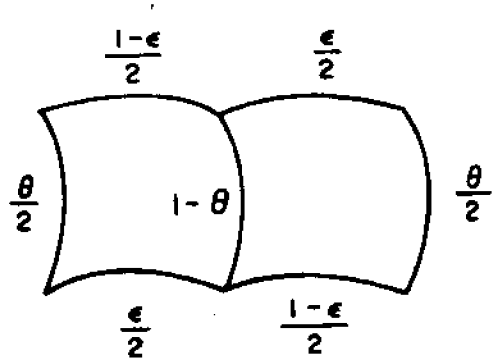

Six-point Computational Molecule
with Two Degrees of Freedom

Figure 5.3

An arbitrary form of the convective transport equation in difference form can then be written

$$\frac{1}{\Delta t}\left[\frac{\theta}{2}\left(c_{j-1}^{n+1}-c_{j-1}^{n}\right)+g\left(c_{j}^{n+1}-c_{j}^{n}\right)+m\left(c_{j+1}^{n+1}-c_{j+1}^{n}\right)\right]+$$

$$\frac{V}{\Delta x}\left[\frac{\epsilon}{2}\left(c_{j}^{n}-c_{j-1}^{n}\right)+d\left(c_{j}^{n+1}-c_{j-1}^{n+1}\right)+a\left(c_{j+1}^{n}-c_{j}^{n}\right)+b\left(c_{j+1}^{n+1}-c_{j}^{n}\right)\right]-$$

$$D\left[\frac{1}{2}\,\frac{\left(c_{j-1}^{n}-2c_{j}^{n}+c_{j+1}^{n}\right)}{(\Delta x)^{2}}+\frac{1}{2}\,\frac{\left(c_{j-1}^{n+1}-2c_{j}^{n+1}+c_{j+1}^{n+1}\right)}{(\Delta x)^{2}}\right]=0 \tag{5-15}$$

where the Crank-Nicholson (1947) representation of the $\frac{\partial^2 c}{\partial x^2}$ term is employed.

For appropriate boundary conditions the solution to the convective-diffusion equation (5-13) can be written in terms of a Fourier series by

$$u(x,t)=\sum_{w=1}^{\infty}A_{w}\,e^{-w^{2}\pi^{2}Dt}\sin w\pi\,(x-Vt) \tag{5-16}$$

The solution to the finite-difference analog of Equation 5-13 can also be written in terms of a Fourier series as

$$u_{j}^{n}=\sum_{w=1}^{J-1}A_{w}\,\rho^{n}\sin w\pi\,(j\Delta x-V\phi n\Delta t) \tag{5-17}$$

Stone and Brian have found the expressions for the decay factor ρ and velocity factor ϕ which correspond to the generalized six point difference Equation 5-15. The determination of the optimum combina-

tion of weighting coefficients is the next step in their analysis. The criterion that $\rho \to 1$ as $D \to 0$ requires that $c = \frac{\epsilon}{2}$, $a = d$, and $m = \frac{\theta}{2}$ which leave the remaining degrees of freedom ϵ , and θ. The computational molecule becomes that shown in Figure 5.3. At this point the velocity factor ϕ and decay factor ρ are considered as functions of the wave angle $w\pi\Delta x$ for different values of $\beta = \frac{V\Delta t}{\Delta x}$. Figure 5.4 shows some of the results which have permitted Stone and Brian to discriminate between combinations of ϵ and θ. The two curves for $\theta = \frac{1}{3}$ showing the velocity factor as a function of wave angle indicates a good representation in the lower frequency range, whereas the curve for $\theta = 0$ indicates a poor representation. The

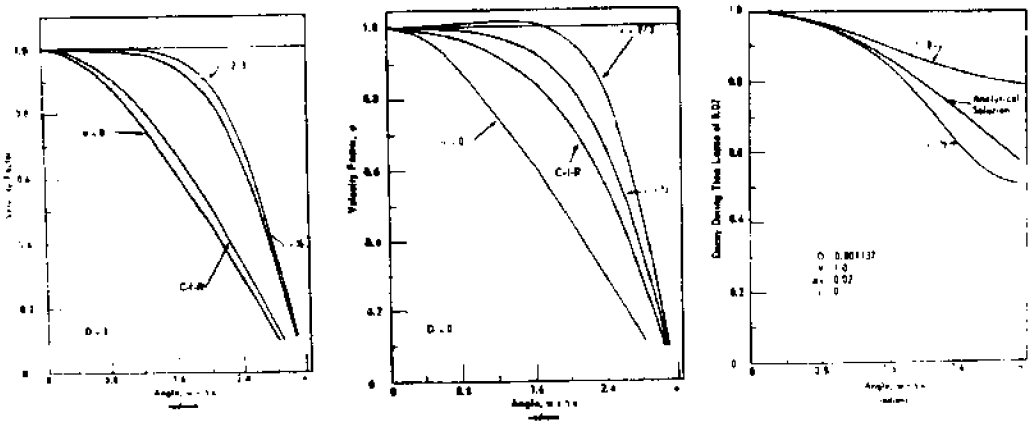

a) Velocity factors for $\beta = 0.1$

b) Velocity factors for $\beta = 0.3$

c) Harmonic decay for = 1/2 and $\theta = 0$

Curves for $\epsilon = 2/3$ and $1/2$ correspond to $\theta = 1/3$.
The curve for $\theta = 0$ corresponds to $\epsilon = 1/2$.
$\beta = \frac{V\Delta t}{\Delta x}$

Velocity and Decay Factors
(from Stone and Brian, 1963)

Figure 5.4

comparison of different schemes in terms of their velocity and decay factor provides a rational basis for the selection of the best scheme. This comparison is, in fact, a measure of the convergence of the scheme.

Further investigation into the nature of a finite difference scheme, can be achieved by evaluating its truncation error, ε_T. This truncation error is defined as in Richtmeyer and Morton (1967) as the difference between the partial differential equation and the finite difference equation. It is evaluated by taking a solution to the partial differential equation and expanding it in a Taylor series and then substituting into the difference equation. By expanding a solution, c, of 5-13 about the point n, j of the difference scheme where the time levels are given as $n + \frac{1}{2}$ and $n - \frac{1}{2}$, the truncation error is (for $\epsilon = \frac{1}{2}$)

$$\varepsilon_T = -(\Delta t)^2 \left[\frac{D}{8}\left(\frac{\partial^4 c}{\partial t^2 \partial x^2}\right) + \frac{1}{24}\left(\frac{\partial^3 c}{\partial t^3}\right) + \frac{V}{8}\left(\frac{\partial^3 c}{\partial t^2 \partial x}\right)\right] +$$

$$(\Delta x)^2 \left[\frac{\theta}{2}\left(\frac{\partial^3 c}{\partial t \partial x^2}\right) + \frac{V}{6}\left(\frac{\partial^3 c}{\partial x^3}\right) - \frac{D}{12}\left(\frac{\partial^4 c}{\partial x^4}\right)\right] +$$

$$\text{Higher Order Terms} \qquad (5\text{-}18)$$

The truncation error of 5-18 shows that the scheme is consistent because as Δx and Δt go to zero, ε_T goes to zero. It also points out that the Stone and Brian scheme is a second order scheme as its terms are proportional to $(\Delta x)^2$ and $(\Delta t)^2$. Finally, it is noted that

there is no numerical dispersion term or term proportional to $\frac{\partial^2 c}{\partial x^2}$. Some previous investigations have used first order schemes which contained numerical dispersion. Such numerical dispersion is easily evaluated by finding the truncation error, ε_T. The truncation error is expressed in terms of $\frac{\partial^2 c}{\partial x^2}$ and other terms, the coefficient of the $\frac{\partial^2 c}{\partial x^2}$ being the numerical dispersion coefficient.

In applying the finite difference scheme values of $\epsilon = \frac{1}{2}$ and $\theta = \frac{1}{3}$ were used as recommended by Stone and Brian.

5.3.3 Construction of the Finite Difference Equation

Two approaches are possible in the construction of the finite difference equation. One approach is to take each term in the P.D.E. and to write the partial derivatives according to the scheme decided upon. Then the variable coefficients of these derivatives and the other terms must be written. At this point there are usually alternative ways in which each coefficient or non-derivative quantity can be written, and the best way of writing these quantities is not always obvious. In the case of a mass balance equation, (e.g. the salt balance equation 3-21) another approach is that of considering a mass balance on an elemental volume of the schematized system being studied. Thus, as the original partial differential equation should be obtained as Δx and Δt go to zero, it becomes a valid representation. The advantage is that in evaluating the change in flux and in storage, the variable coefficients [A, E, Q] are represented in a rational manner.

Although the first approach was followed in deriving the

finite difference equations for the tidal hydraulics, the second approach is taken for the finite difference equation for the salt balance.

Following the indications of Stone and Brian, the weighting coefficients corresponding to the six point computational molecule are:

$$a = \frac{\epsilon}{2} = b = d = \frac{1}{4}$$

The time derivative weighting coefficients are taken as

$$g + \theta = 1$$

thus allowing the user of the model to vary the value of θ. (In this study $\theta = \frac{1}{3}$ and $g = \frac{2}{3}$ were used.)

The finite difference equation is derived by performing a mass balance over an elemental volume (defined by the distance locations 2m-1 and 2m+1) and considering conditions at time 2n as defined by the average of conditions at time 2n+1 and 2n-1 if necessary. The alternating grid and schematic control volume are shown in Figure 5-5. The origin of the longitudinal axis, x, is taken at the ocean with the positive sense upstream.

$$\begin{array}{l}\text{Increase in salt} \\ \text{during time } 2\Delta t\end{array} = \begin{array}{l}\text{Net salt advected} \\ \text{into the volume} \\ \text{during time } 2\Delta t\end{array} + \begin{array}{l}\text{Net salt dispersed} \\ \text{into the volume} \\ \text{during time } 2\Delta t\end{array} \qquad (5\text{-}19)$$

The increase in salt mass during time $2\Delta t$ can be expressed as that present at time 2n+1 less that present at time 2n-1:

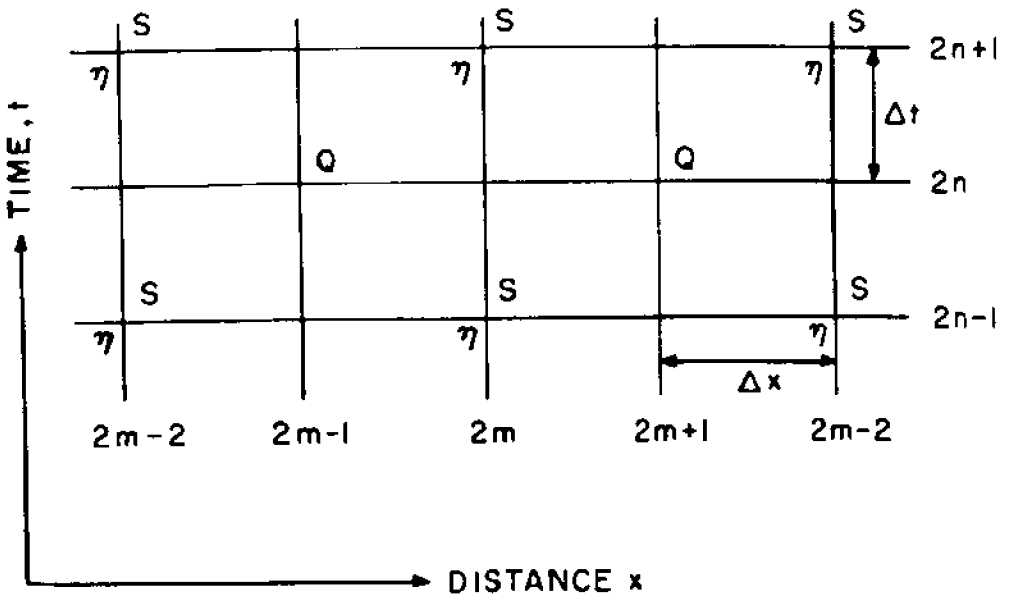

a) Alternating Grid

x = 0 at ocean, increasing towards upstream end

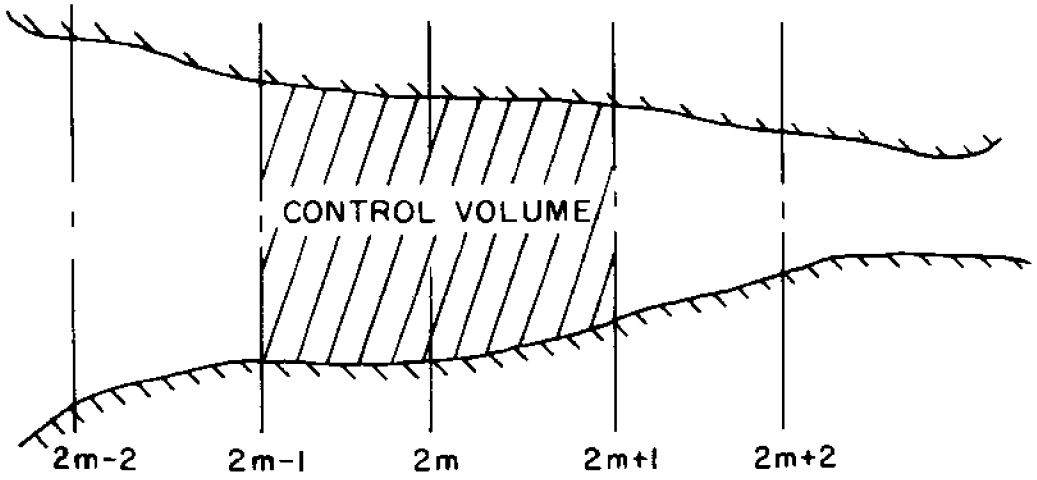

b) Plan View Showing Control Volume

Sketch for Difference Formulation of the Salt Balance Equation

Figure 5.5

$$\text{Increase in salt during time } 2\Delta t = \left[\frac{\theta}{2}(As)_{2m-2}^{2n+1} + g(As)_{2m}^{2n+1} + \frac{\theta}{2}(As)_{2m+2}^{2n+1}\right] 2\Delta x - \left[\frac{\theta}{2}(As)_{2m-2}^{2n-1} + g(As)_{2m}^{2n-1} + \frac{\theta}{2}(As)_{2m+2}^{2n-1}\right] 2\Delta x \tag{5-20}$$

The net salt advected into the elemental volume during time $2\Delta t$ is given by that advected in across boundary 2m-1 less that advected out across boundary 2m+1.

$$\text{Net salt advected into the volume during time } 2\Delta t = \left[Q_{2m-1}^{2n}\frac{\left(s_{2m-2}^{2n+1} + s_{2m}^{2n+1} + s_{2m-2}^{2n-1} + s_{2m}^{2n-1}\right)}{4} - Q_{2m+1}^{2n}\frac{\left(s_{2m+2}^{2n+1} + s_{2m}^{2n+1} + s_{2m+2}^{2n-1} + s_{2m}^{2n-1}\right)}{4}\right] 2\Delta t \tag{5-21}$$

The net salt dispersed into the control volume during time $2\Delta t$ is similarly expressed as that dispersed in across boundary 2m-1 less that dispersed out across boundary 2m+1.

$$\text{Net salt dispersed into the volume during time } 2\Delta t = \left[-\frac{(EA)_{2m-1}^{2n}}{2}\left[\frac{s_{2m}^{2n+1} - s_{2m-2}^{2n+1} + s_{2m}^{2n-1} - s_{2m-2}^{2n-1}}{2\Delta x}\right] + (EA)_{2m+1}^{2n}\left[\frac{s_{2m+2}^{2n+1} - s_{2m}^{2n+1} + s_{2m+2}^{2n-1} - s_{2m}^{2n-1}}{2\Delta x}\right]\right] 2\Delta t \tag{5-22}$$

Substituting the expressions 5-20, 5-21, and 5-22 into Equation 5-19, then solving for the salinities at time 2n+1 in terms of those at time 2n-1 and multiplying by $\frac{2}{\Delta t}$, one obtains:

$$
\begin{aligned}
& s_{2m-2}^{2n+1}\left[2\theta\,\frac{\Delta x}{\Delta t}\,A_{2m-2}^{2n+1}-Q_{2m-1}^{2n}-\frac{(EA)_{2m-1}^{2n}}{\Delta x}\right]+ \\
& s_{2m}^{2n+1}\left[4g\,\frac{\Delta x}{\Delta t}\,A_{2m}^{2n+1}-Q_{2m-1}^{2n}+Q_{2m+1}^{2n}+\frac{(EA)_{2m-1}^{2n}}{\Delta x}+\frac{(EA)_{2m+1}^{2n}}{\Delta x}\right]+ \\
& s_{2m+2}^{2n+1}\left[2\theta\,\frac{\Delta x}{\Delta t}\,A_{2m+2}^{2n+1}+Q_{2m+1}^{2n}-\frac{(EA)_{2m+1}^{2n}}{\Delta x}\right]= \\
& s_{2m-2}^{2n-1}\left[2\theta\,\frac{\Delta x}{\Delta t}\,A_{2m-2}^{2n-1}+Q_{2m-1}^{2n}+\frac{(EA)_{2m-1}^{2n}}{\Delta x}\right]+ \\
& s_{2m}^{2n-1}\left[4g\,\frac{\Delta x}{\Delta t}\,A_{2m}^{2n-1}+Q_{2m-1}^{2n}-Q_{2m+1}^{2n}-\frac{(EA)_{2m-1}^{2n}}{\Delta x}-\frac{(EA)_{2m+1}^{2n}}{\Delta x}\right]+ \\
& s_{2m+2}^{2n-1}\left[2\theta\,\frac{\Delta x}{\Delta t}\,A_{2m+2}^{2n-1}-Q_{2m+1}^{2n}+\frac{(EA)_{2m+1}^{2n}}{\Delta x}\right]
\end{aligned}
\qquad (5\text{-}23)
$$

Equation 5-23, when applied to all control volumes centered about interior salinity points, establishes the interior set of simultaneous equations which when combined with the boundary equations will permit a solution to proceed in increments of $2\Delta t$.

5.3.4 Boundary Equations

5.3.4a Compatability

In the previous section the finite difference equation for

an interior elemental volume was developed in terms of a mass balance on that volume. The discretization of the estuary is a series of these elemental volumes and for each interior elemental volume there is an equation of the form 5-23. The compatibility condition is that the flux across the boundary of each interior elemental volume be identical to the flux across the corresponding boundary of the adjoining volume. Violation of this compatibility condition would create or destroy mass. Inspection of the expressions 5-21 and 5-22 show that for the interior elements this compatibility condition is satisfied. This condition will be used in order to correctly formulate the boundary equations as shown in the next sections.

5.3.4b Upstream Boundary

Figure 5.6 shows the representation of the estuary near the section at which the boundary condition of zero flux of salt is established. An elemental volume, one-half the length of the interior volumes, is considered and a mass balance performed. The advective flux across section 2m-1 into the final volume can be written:

$$Q_{2m-1}^{2n} \frac{\left(s_{2m-2}^{2n+1} + s_{2m}^{2n+1} + s_{2m-2}^{2n-1} + s_{2m}^{2n-1}\right)}{4}$$

With reference to Equation 5-21, it is seen that this is the same advective flux formulated across 2m-1 in terms of the volume centered at 2m-2. The dispersive flux into the final volume is also compatible

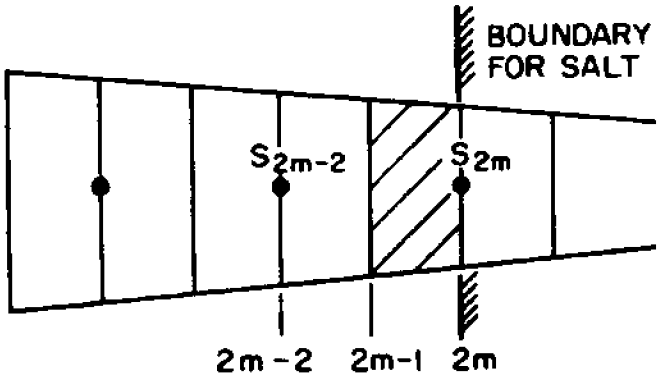

Schematic Representation of the
Upstream Boundary

Figure 5.6

with the adjoining element when written:

$$-\frac{(EA)^{2n}_{2m-1}}{2}\left[\frac{s^{2n+1}_{2m}-s^{2n+1}_{2m-2}}{2\Delta x}+\frac{s^{2n-1}_{2m}-s^{2n-1}_{2m-2}}{2\Delta x}\right]$$

To express the change in salt by storage, an evaluation similar to that of Equation 5-20 must be made. The quantity, As, applicable to the final volume will be evaluated at sections 2m and 2m-2 and the weighting factors will be chosen as $(1-\frac{\theta}{2})$ and $\frac{\theta}{2}$ so as to compliment the coefficients coming from the equations of the adjoining volumes.

$$\text{Increase in salt during time } 2\Delta t = \left[\frac{\theta}{2}(As)^{2n+1}_{2m-2}+(1-\frac{\theta}{2})(As)^{2n+1}_{2m}\right]\Delta x - \left[\frac{\theta}{2}(As)^{2n-1}_{2m-2}+(1-\frac{\theta}{2})(As)^{2n-1}_{2m}\right]\Delta x \qquad (5\text{-}24)$$

Equating the increase in salt to the flux across section 2m-1 and multiplying by $\frac{2}{\Delta t}$ yields the boundary equation.

$$s^{2n+1}_{2m-2}\left[\theta\frac{\Delta x}{\Delta t}A^{2n+1}_{2m-2}-Q^{2n}_{2m-1}-\frac{(EA)^{2n}_{2m-1}}{\Delta x}\right]+$$

$$s^{2n+1}_{2m}\left[(2-\theta)\frac{\Delta x}{\Delta t}A^{2n+1}_{2m}-Q^{2n}_{2m-1}+\frac{(EA)^{2n}_{2m-1}}{\Delta x}\right]=$$

$$s^{2n-1}_{2m-2}\left[\theta\frac{\Delta x}{\Delta t}A^{2n-1}_{2m-2}+Q^{2n}_{2m-1}+(EA)^{2n}_{2m-1}\right]+$$

$$s_{2m}^{2n-1}\left[(2-\theta)\frac{\Delta x}{\Delta t}A_{2m}^{2n-1}+Q_{2m-1}^{2n}-\frac{(EA)_{2m-1}^{2n}}{\Delta x}\right] \tag{5-25}$$

5,3.4c Ocean Boundary

As described in section 3.4.4, treatment of the ocean boundary is divided into two parts depending upon the direction of flow. In the case of flood flow, the ocean salinity is specified at the boundary and this specification can be incorporated into the set of simultaneous equations as an additional equation of the form

$$s_1^{2n+1} = s_o \tag{5-26}$$

The last interior elemental volume centered at section 3 (Figure 5.7) can be treated in the normal fashion as the specification of the boundary salinity is all that is necessary for evaluation of its corresponding difference equation.

In treating the case of ebb flow a computational half element is considered as shown in Figure 5.8. By an argument similar to that for the upstream boundary condition, the weighting factors $(1-\frac{\theta}{2})$ and $\frac{\theta}{2}$ are used at stations 1 and 3 respectively in evaluating the time rate of change of As. Then

$$\begin{aligned}\text{Increase in salt during time } 2\Delta t = &\left[(1-\tfrac{\theta}{2})(As)_1^{2n+1}+\tfrac{\theta}{2}(As)_3^{2n+1}\right]\Delta x\\ &-\left[(1-\tfrac{\theta}{2})(As)_1^{2n-1}+\tfrac{\theta}{2}(As)_3^{2n-1}\right]\Delta x\end{aligned} \tag{5-27}$$

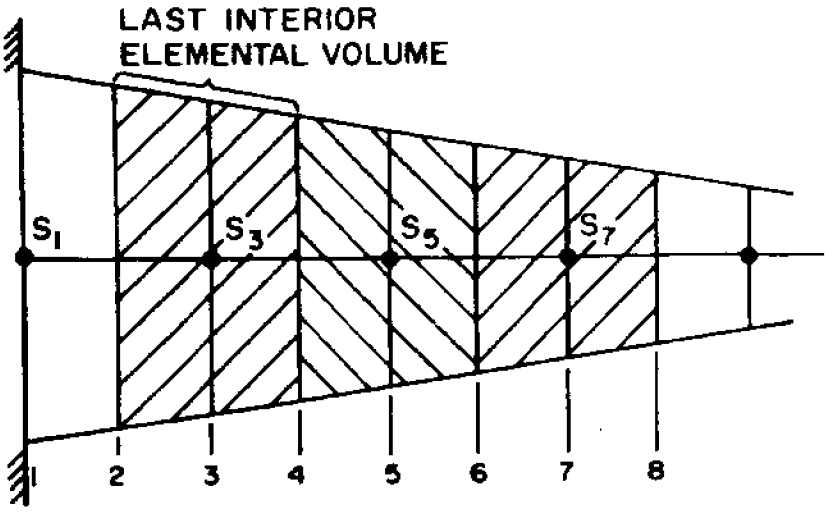

Schematic Representation of Ocean Boundary
Flood Flow

Figure 5.7

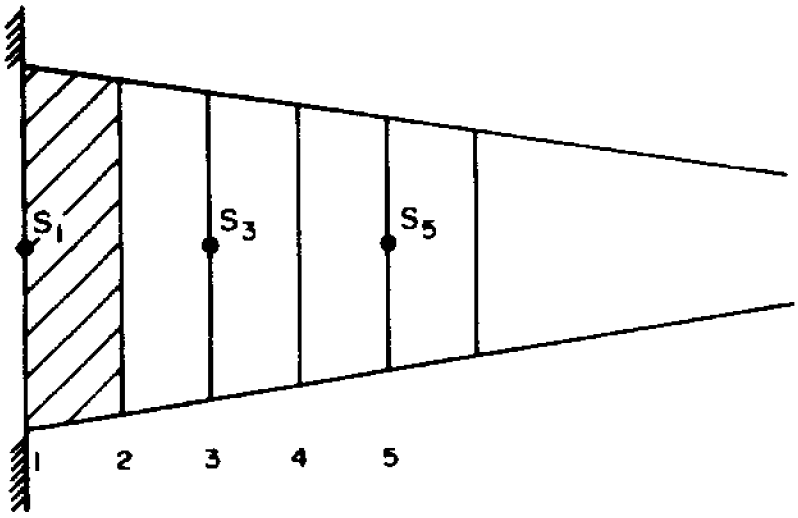

Schematic Representation of Ocean Boundary
Ebb Flow

Figure 5.8

The advective flux across section 1 is written

$$\text{Advective Flux in} = Q_1^{2n} \left(\frac{s_1^{2n+1} + s_1^{2n-1}}{2} \right) \tag{5-28}$$

where Q_1^{2n} can be obtained by continuity as

$$Q_1^{2n} = Q_2^{2n} + \frac{\Delta x}{4\Delta t} \left[b_{\text{core}_1} \left(\eta_1^{2n+1} - \eta_1^{2n-1} \right) + b_{\text{core}_2} \left(\eta_2^{2n+1} - \eta_2^{2n-1} \right) \right]$$

$$\text{and } \eta_2 = \frac{1}{2} (\eta_1 + \eta_3) \tag{5-29}$$

The advective flux across section 2 is

$$\text{Advective Flux out} = Q_2^{2n} \frac{\left(s_1^{2n+1} + s_3^{2n+1} + s_1^{2n-1} + s_3^{2n-1} \right)}{4} \tag{5-30}$$

The dispersive flux across section 1 is approximated by

$$\text{Dispersive Flux in} = \frac{(EA)_1^{2n}}{2} \left(\frac{s_3^{2n+1} - s_1^{2n+1}}{2\Delta x} + \frac{s_3^{2n-1} - s_1^{2n-1}}{2\Delta x} \right) \tag{5-31}$$

and the dispersive flux across section 2 is

$$\text{Dispersive Flux out} = \frac{(EA)_2^{2n}}{2} \left(\frac{s_3^{2n+1} - s_1^{2n+1}}{2\Delta x} + \frac{s_3^{2n-1} - s_1^{2n-1}}{2\Delta x} \right) \tag{5-32}$$

Combining these relations in the form of a mass balance results in the ocean boundary equation for downstream flow.

$$s_1^{2n+1}\left[(2-\theta)\frac{\Delta x}{\Delta t}A_1^{2n+1} - 2Q_1^{2n} + Q_2^{2n} - \frac{(EA)_1^{2n} - (EA)_2^{2n}}{\Delta x}\right] +$$

$$s_3^{2n+1}\left[\theta\frac{\Delta x}{\Delta t}A_3^{2n+1} + Q_2^{2n} + \frac{(EA)_1^{2n} - (EA)_2^{2n}}{\Delta x}\right] =$$

$$s_1^{2n-1}\left[(2-\theta)\frac{\Delta x}{\Delta t}A_1^{2n-1} + 2Q_1^{2n} - Q_2^{2n} + \frac{(EA)_1^{2n} - (EA)_2^{2n}}{\Delta x}\right] +$$

$$s_3^{2n-1}\left[\theta\frac{\Delta x}{\Delta t}A_3^{2n-1} - Q_2^{2n} - \frac{(EA)_1^{2n} - (EA)_2^{2n}}{\Delta x}\right] \qquad (5\text{-}33)$$

5.3.5 Representation of the Dispersion Coefficient

$$E(x,t) = K\left|\frac{\partial \overset{\circ}{s}}{\partial \overset{\circ}{x}}\right| + E_T \qquad (3\text{-}25)$$

$$E_T(x,t) = 77\ n\ u\ R_h^{5/6} \qquad (3\text{-}29)$$

The above two equations serve to define the dispersion coefficient for the salt balance equation. The $\frac{\partial \overset{\circ}{s}}{\partial \overset{\circ}{x}}$ term introduces a non-linearity if introduced directly and consequently it is evaluated at the previous time step. The "u" of Equation 3-26 is defined by $Q(x,t)/A_{core}(x,t)$ and the hydraulic radius R_h is calculated by Equation 5-11 or 5-12 depending on the type of schematization.

5.3.6 Solution of Simultaneous Linear Equations

The simultaneous, linear equations resulting from the application of the implicit finite difference molecules form a tri-diagonal set of equations. The solution of such equations is commonplace in the field of numerical methods. Usually the solution is performed as an

adaptation of the Gauss elimination procedure consisting of a forward pass which reduces the tri-diagonal matrix to a matrix with unity on the diagonal and single upper diagonal. Back substitution is then performed. The bookkeeping is reduced to enable rapid solution by digital computer and only the three diagonals are treated during the process. Further details can be found in many texts and publications, for example: Carnahan, Luther and Wilkes, 1969; Richtmeyer and Morton, 1967, and Ames, 1969.

5.4 Choice of Δx and Δt

The requirements imposed on possible values of Δx and Δt are most severe in the case of the solution of the continuity equation and the conservation of momentum equation.

This criteria is

$$\Delta t \leq \frac{\Delta x}{u + c} \tag{5-34}$$

where u is the average cross-sectional velocity and c is the wave speed, $\sqrt{gh}$, at the same location. This is the Courant criteria for stability of explicit schemes and is an approximate measure as the non-linear aspect of the equations is not accounted for in Equation 5-34.

The choice of Δx should be based upon the necessity of detail for a particular application in the case of real estuaries. The definition of the toe of the salinity distribution is a useful aid in determining a Δx which is not too large. This is a trial and error procedure wherein one examines the degree to which the salinity

oscillates about the asymptote (usually s = 0). A smaller Δx will reduce the oscillation, a larger Δx will allow it to be greater. Once Δx is chosen Equation 5-34 will give an approximate criteria for Δt.

VI. Schematization of Real Estuaries, Verification of Tidal Hydraulics and Determination of Dispersion Parameter under Steady State Conditions

6.1 Introduction

A longitudinal dispersion relationship of the form

$$E(x,t) = K \left| \frac{\partial \overset{\circ}{s}}{\partial \overset{\circ}{x}} \right| + E_T \qquad (6\text{-}1)$$

was developed in Chapter III, experimental salinity distribution data from laboratory tidal channels was used in Chapter IV to verify this relationship and to show that the dimensionless dispersion parameter $K/u_o L$ was a function of the degree of stratification as measured by the estuary number (Figure 4.14). The objectives of this chapter are to show that this dispersion relationship is valid in real estuaries and to provide additional information on the correlation of the dimensionless dispersion parameter and the estuary number under the condition of quasi steady salinity intrusion. The validity of the numerical model as a predictive tool under transient conditions will be demonstrated in Chapter VII.

Three east coast estuaries, the Delaware, Potomac and Hudson were chosen for this phase of the study. These estuaries were chosen because of the availability of salinity distribution data which might reasonably be assumed to be representative of steady-state conditions. In addition, the treatment of the downstream boundary condition, which is appreciably different in these three estuaries, is representative of the range of boundary effects found

in the majority of estuarine problems.

6.2 Steady-State Concepts for Real Estuaries

A truly quasi-steady-state salinity distribution probably never exists in an actual estuary. The assumption of such a steady-state condition implies that the tidal range at the ocean end is constant from one tidal period to the next and that the rate and distribution of all fresh water inflows to the estuary is also constant. It must also be assumed that the period of time during which tides and inflows are constant is long enough to allow the salinity distribution to stabilize to a quasi-steady condition from an antecedent transient condition.

Historically, steady-state mathematical models were among the first tools available for studying estuaries. Consequently there was a need to find or approximate a steady-state in nature in order to apply these tools to real situations. In this study the quasi steady-state condition permits a determination of the dispersion parameter K for a corresponding condition of stratification as measured by the estuary number, E_D. The validity of the K values determined will depend upon the degree of approximation inherent in the steady-state assumption for a given estuary.

6.3 The Delaware Estuary

6.3.1 Geometry and Schematization

The general shape of the Delaware Estuary is shown in Figure 6.1. The region being studied is defined by the head of tide (a closed end) at Trenton and by the natural ocean entrance at the

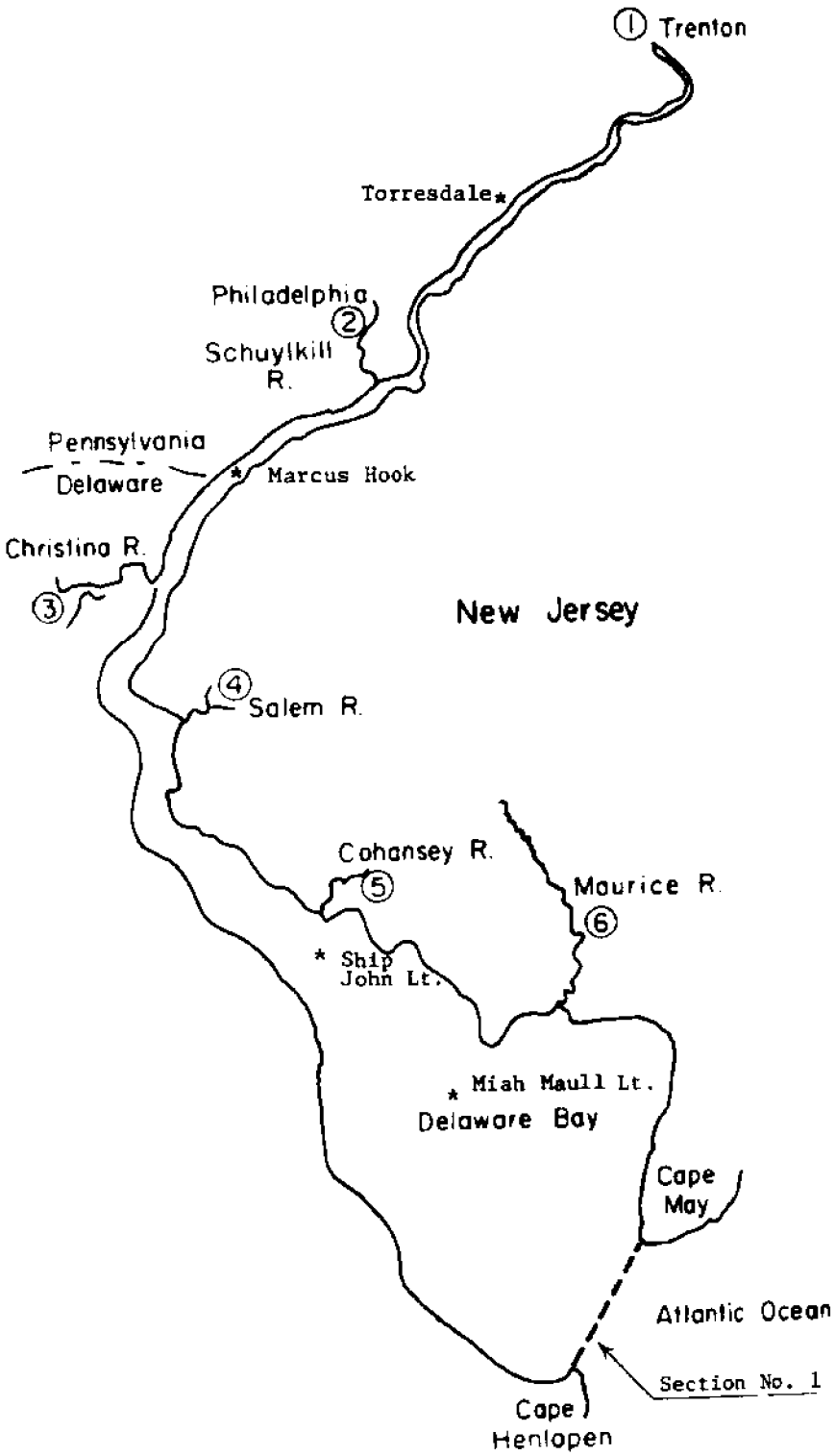

Plan of Delaware Estuary
Figure 6.1

two capes, Cape May to the north and Cape Henlopen to the south. The ocean boundary is well defined in this case. A schematization has been performed based on the "Table of the Accumulated Mid-tide Volumes", U.S. Army Corps of Engineers (1951), Data Source Reference 1. Storage is not included in this schematization and the resulting schematized cross-sections are of the form shown in Figure 3.2b with $b_{total} = b_{core}$. Figure 6.2 (a,b,c) show the variations in width, b_{core}, and depth, d as well as a comparison of the resulting cross-sectional areas used in the computer program to the data source.

The schematization has been extended to 70 sections as shown in Table 6.1. The first section is at the ocean boundary where $x = 0$. The length of the estuary is 693,475 feet (131.34 statute miles) from the first section at the ocean to the last section at the head of tide. An interval of discretization of about 1.9 miles or $\Delta x = 10{,}050$ feet was established. Some of the cross-sections were interpolated from intervals of 3.4 miles, therefore the accuracy in terms of the geometric detail is only good to this larger interval.

The choice of Δt is based on considerations of stability as defined by Equation 5-34. Applying this relationship for an assumed cross-sectional velocity of 2 ft/sec and a wave velocity, $c = \sqrt{gh}$ for $h = 41$ feet, gives $\Delta t < 262$ seconds. This value was considered an upper bound and a smaller value of $\Delta t = 178.85$ seconds was taken corresponding to a division of the tidal period of 44,712 seconds into 250 increments.

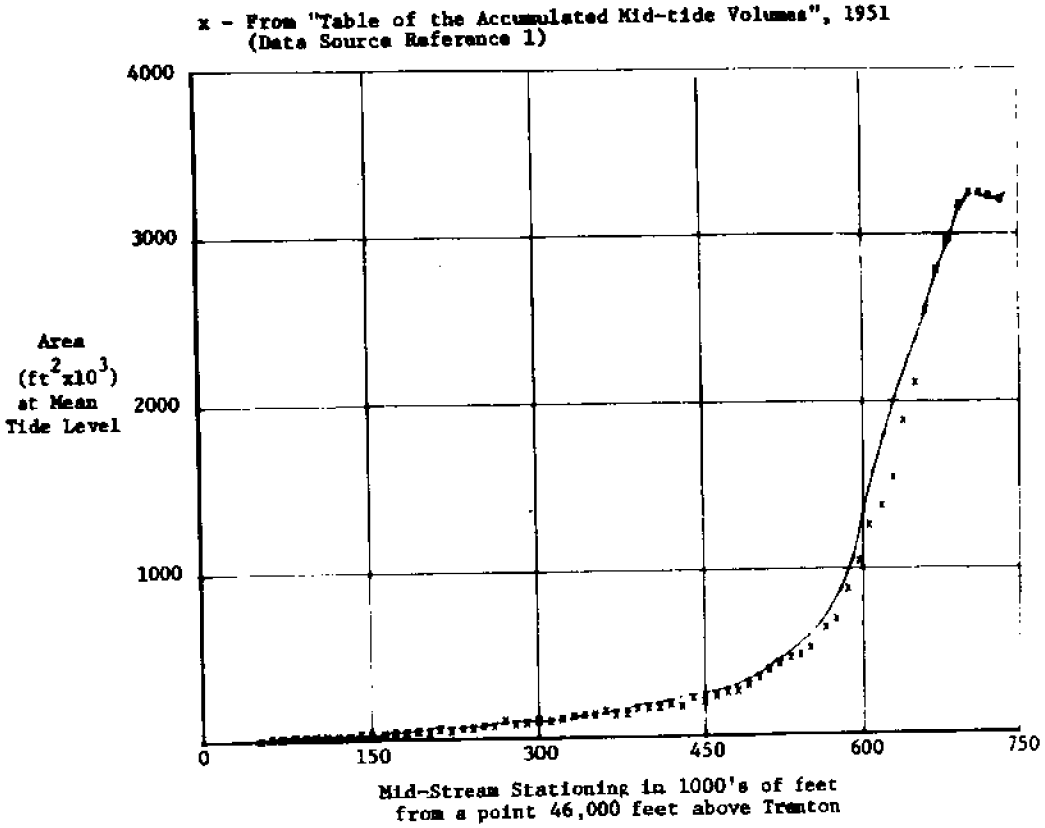

Areas Used in Delaware Study

Figure 6.2(a)

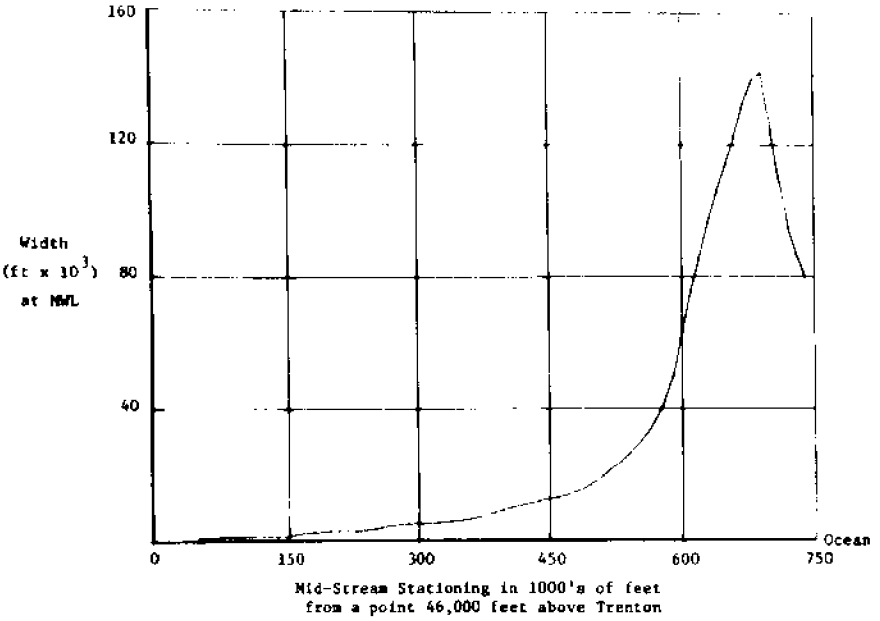

Widths ($b_{total} = b_{core}$) Used in Delaware Study

Figure 6.2(b)

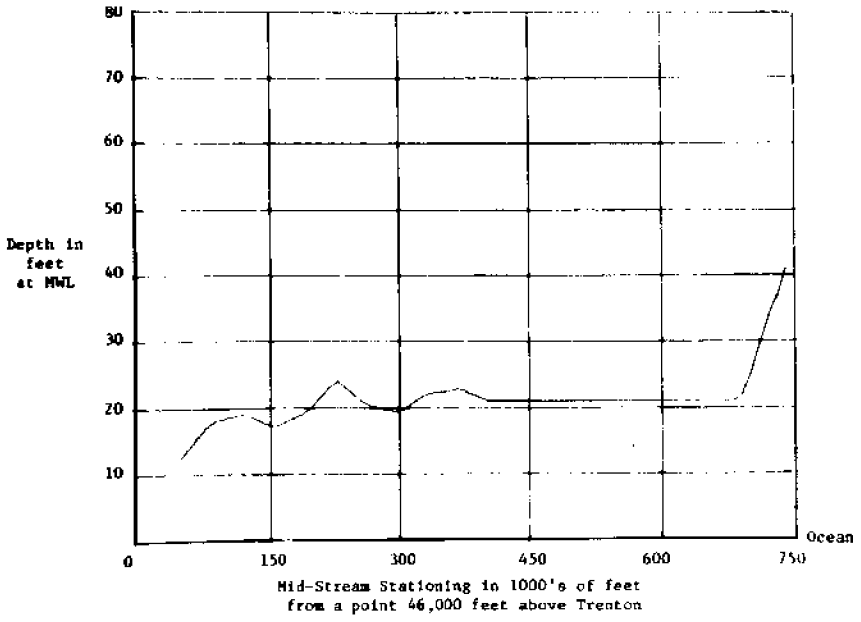

Depths Used in Delaware Study

Figure 6.2(c)

Section No.	Depth (ft)	z_o (ft)	Width (ft)	Section No.	Depth (ft)	z_o (ft)	Width (ft)
1	41.00	-20.00	79500.	36	41.00	-20.00	79500.
2	37.00	-16.00	86800.	37	37.00	-16.00	86800.
3	34.00	-13.00	95000.	38	34.00	-13.00	95000.
4	30.00	-9.00	108000.	39	30.00	-9.00	108000.
5	26.00	-5.00	124600.	40	26.00	-5.00	124600.
6	22.00	-1.00	142000.	41	22.00	-1.00	142000.
7	21.00	0.00	140000.	42	21.00	0.00	140000.
8	21.00	0.00	132500.	43	21.00	0.00	132500.
9	21.00	0.00	122800.	44	21.00	0.00	122800.
10	21.00	0.00	114200.	45	21.00	0.00	114200.
11	21.00	0.00	106000.	46	21.00	0.00	106000.
12	21.00	0.00	96254.	47	21.00	0.00	96254.
13	21.00	0.00	85982.	48	21.00	0.00	85982.
14	21.00	0.00	75247.	49	21.00	0.00	75247.
15	21.00	0.00	63357.	50	21.00	0.00	63357.
16	21.00	0.00	50246.	51	21.00	0.00	50246.
17	21.00	0.00	41499.	52	21.00	0.00	41499.
18	21.00	0.00	36230.	53	21.00	0.00	36230.
19	21.00	0.00	32009.	54	21.00	0.00	32009.
20	21.00	0.00	28816.	55	21.00	0.00	28816.
21	21.00	0.00	26189.	56	21.00	0.00	26189.
22	21.00	0.00	23869.	57	21.00	0.00	23869.
23	21.00	0.00	21677.	58	21.00	0.00	21677.
24	21.00	0.00	19590.	59	21.00	0.00	19590.
25	21.00	0.00	17618.	60	21.00	0.00	17619.
26	21.00	0.00	16084.	61	21.00	0.00	16084.
27	21.00	0.00	14900.	62	21.00	0.00	14900.
28	21.00	0.00	13912.	63	21.00	0.00	13912.
29	21.00	0.00	13111.	64	21.00	0.00	13111.
30	21.00	0.00	12481.	65	21.00	0.00	12481.
31	21.00	0.00	11910.	66	21.00	0.00	11910.
32	21.00	0.00	11366.	67	21.00	0.00	11366.
33	20.97	0.03	10759.	68	20.97	0.03	10759.
34	20.95	0.05	10080.	69	20.95	0.05	10080.
35	21.32	-0.32	9265.	70	21.32	-0.32	9265.

Schematization of Delaware Estuary at M&L
(Section No. 1: Cape May - Cape Henlopen, shown in Figure 6.1)

Table 6.1

The mean water level increases about $1\frac{1}{3}$ feet from the capes to Trenton, however this change was not included in the schematization as a change in datum. The approximation implied by this procedure is a deepening of the cross-section equal to the difference between local mean water level and mean water level at the ocean entrance. As the water depth is considerably more than this difference, no significant error is involved.

6.3.2 Verification of the Tidal Hydraulics

Although a detailed verification of a similar schematization was given by Harleman and Lee (1969) it is necessary to repeat the verification because the schematization for this study is carried to the ocean entrance and because the effect of the density gradient is included in the momentum equation. The resistance coefficient, Manning's n, becomes the controlling variable for achieving verification as has been shown by Harleman and Lee. The values of Manning's n used in this study are shown in Figure 6.3.

The U.S. Army Corps of Engineers' Mean Tide Curves (1948), Data Source Reference 2, provide verification of surface elevation data throughout the tidal period for several stations and includes the phase relation between stations. Figure 6.5 shows the verification obtained using the Manning's n relation of Figure 6.3 and the salinity distribution shown in Figure 6.4. Comparison with the Mean Tide Curves is made at Ship John, Marcus Hook, and at Torresdale. Figure 6.5(a) shows the tidal elevation at the ocean entrance which serves as the boundary condition, $\eta(0,t)$ for the quasi steady-state

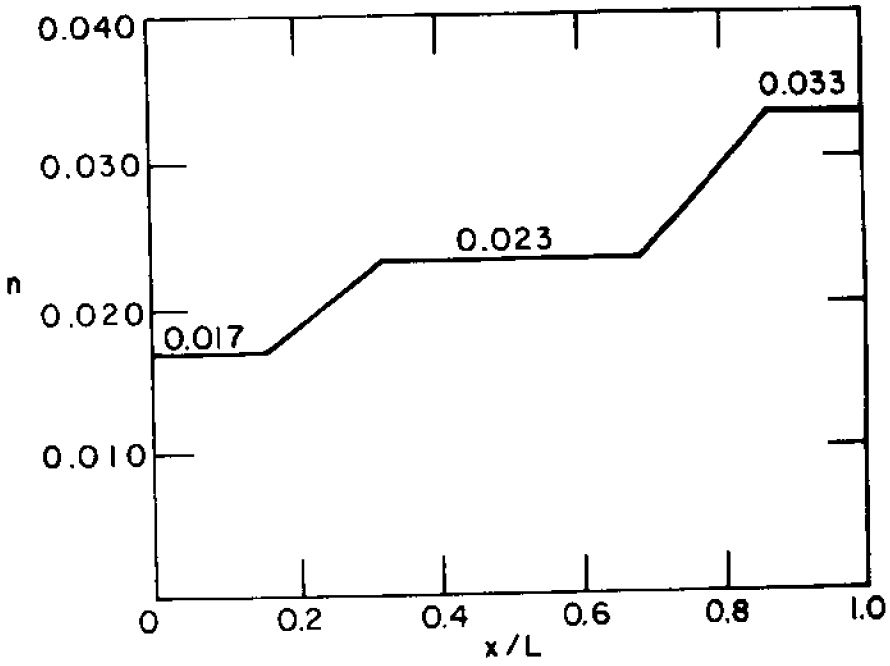

Manning's n variation for Delaware Study

Figure 6.3

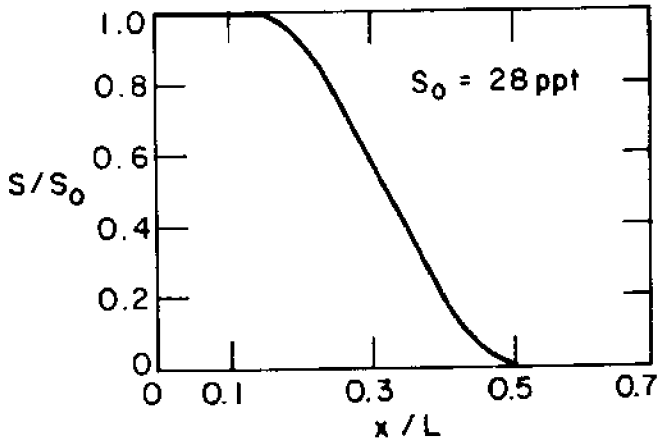

Salinity Distribution in Delaware
used for Verification of Tidal Hydraulics

Figure 6.4

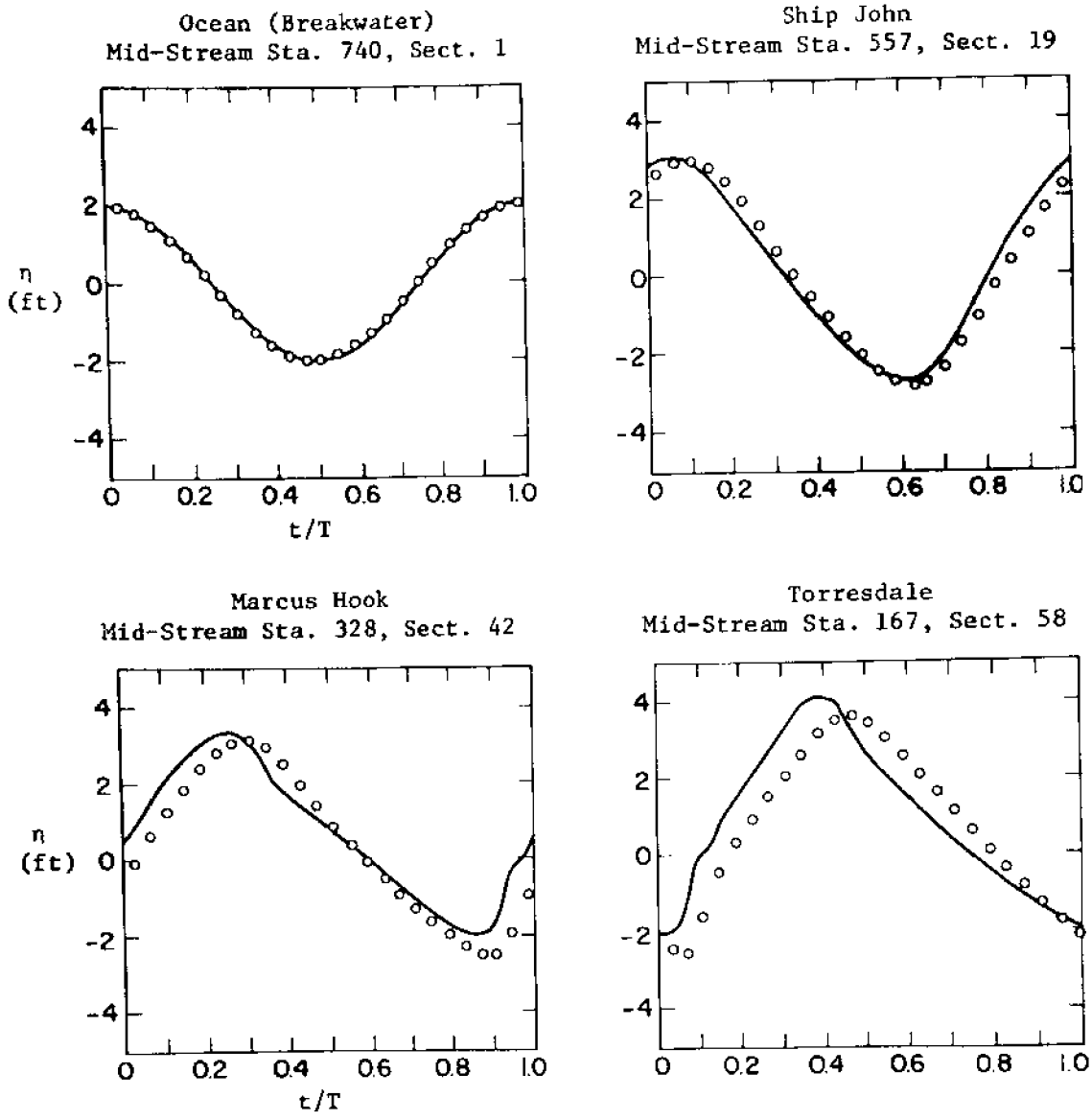

Comparison of Predicted Water Surface Elevations
at Three Stations Given the Ocean Tidal Variation at the Capes

Figure 6.5

verification of the tidal hydraulics. For the upstream stations the predicted elevations lag those from the Mean Tide Curves by .02 to .05 of a tidal period at Ship John and at Marcus Hook, increasing to .05 to .07 of a tidal period at Torresdale, the lag near high water being the larger of the two. The computed tidal range at the three stations is in excellent agreement at Ship John and Torresdale and differs by about 5% at Marcus Hook. The predicted water surface elevations are generally higher than the verification data. In terms of mean water level, the predicted values are about 2 inches high at Ship John, 4 inches high at Marcus Hook and 6 inches high at Torresdale. In general the verification is satisfactory.

No attempt has been made to compare discharge or velocity measurements because of the difficulty in obtaining data which corresponds to the cross-sectional average velocity.

6.3.3 Quasi Steady-State Salinity Distribution Studies

Slack Water salinity distribution data is presented in the Delaware River Model Study No. 2 (1954), Data Source Reference 3, for several different steady conditions of fresh water inflow. This data is actual steady-state data, inasmuch as it was obtained by a repeating ocean tidal amplitude and constant fresh water inflows in the model. This study has used the data corresponding to three different fresh water discharges; 5000 cfs, 10,600 cfs and 16,475 cfs. These fresh water discharges correspond to inflows downstream as far as and including the Schuylkill river. Other discharges further

downstream were included in the steady-state study. These were 1,100 cfs at the Christina River, 450 cfs at the Salem River, 725 cfs at the Cohansey River and 1,450 cfs at the Maurice River. These downstream tributaries were considered secondary in their effect on the salinity profile and were held at these values during the steady-state calculations.

The numerical model can easily furnish slack water salinity values because it produces discharges and salinities throughout the tidal period. In this study the high water slack salinities have been chosen for verification purposes. The high water slack salinities are obtained during the numerical computation as follows: at the end of each tidal period the discharge at each station is reviewed to determine the time increment corresponding to the change from flood flow to ebb flow. The salinity at this time in the tidal period is selected as the high water slack salinity.

By comparing the high water slack salinities calculated by the numerical model with those measured in the Delaware model it is possible to find the value of the dispersion parameter K corresponding to each condition of fresh water discharge. Two procedures were used to find the K values.

The first procedure was to assume a value of K and a good approximation for an initial salinity distribution. The numerical model was run until the salinity distributions in two successive tidal cycles were within a tolerable error. Although this procedure was satisfactory in studying the constant width estuaries of the

W.E.S. flume and the Rotterdam Waterway, it was found in the Delaware Study that a convergence to about 0.04 ppt was not a good indication of a steady state because the convergence was very slow. In the W.E.S. studies a tolerance of 0.02 ppt could be reached with only two to three tidal periods of calculation after a 0.04 ppt was reached. For the Delaware such a convergence would require thirty to forty tidal cycles. During these additional tidal cycles of computation the salinity distribution would change significantly.

In an effort to find a more sensitive means of determining the quasi steady condition a second procedure was developed which resulted in a substantial saving in computer time.

This procedure starts the quasi steady state calculations with the final desired salinity distribution as the initial condition. Then, for a particular value of the dispersion parameter, K, the calculation is made for about ten tidal periods. The movement of the toe of the high water slack salinity distribution is determined using the last five tidal cycles. This is done for several values of K and the movement of the toe is plotted for each K. Such a plot will determine the value of the dispersion parameter K which holds the toe of the high water slack salinity distribution steady, thus defining the K for that steady-state condition. The reason for choosing the toe of the distribution is that salinity data near the mouth of the estuary was not available.

Figure 6.6 shows the determination of the best K values for the three conditions of fresh water discharge. To show that

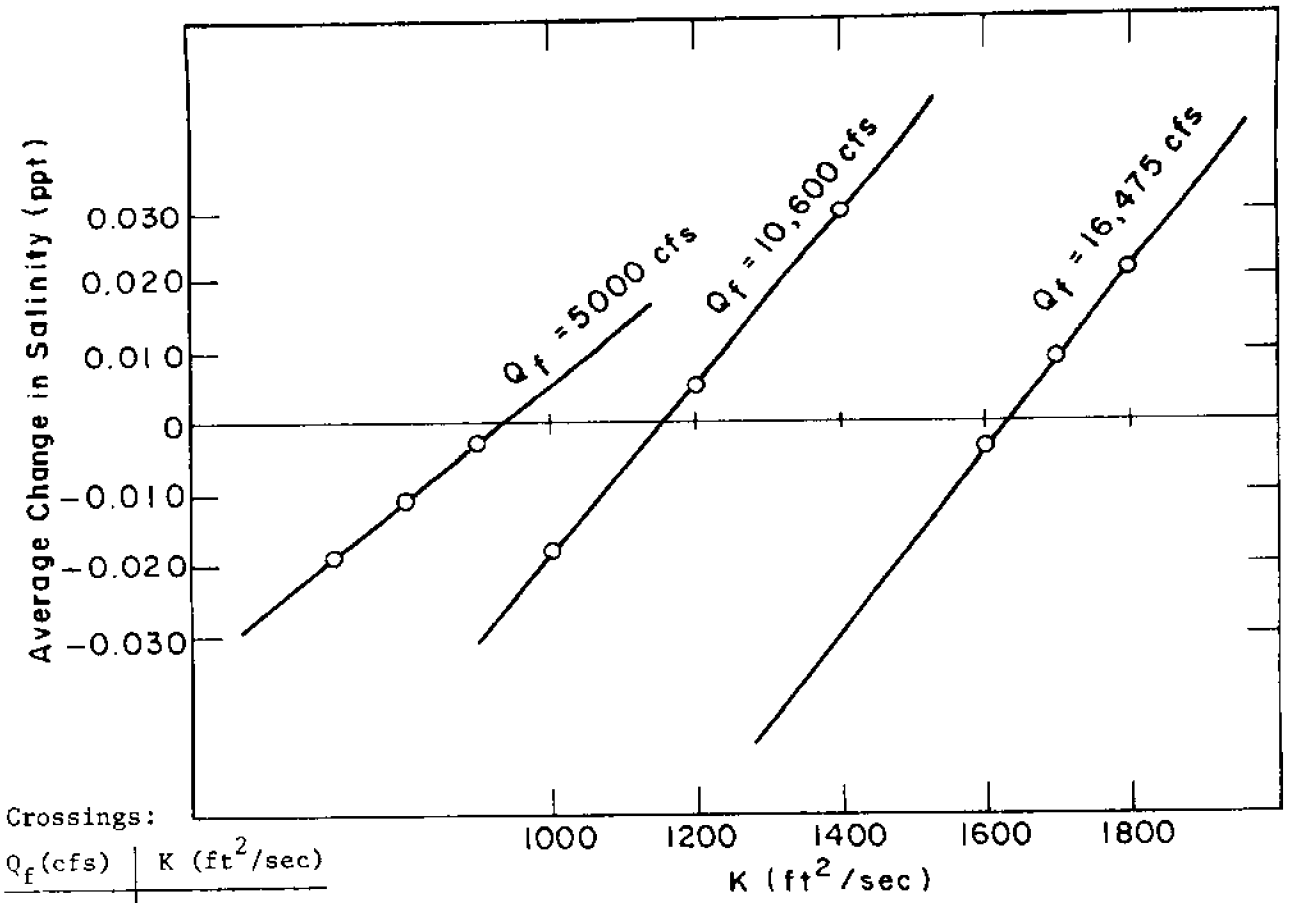

Crossings:

Q_f(cfs)	K (ft^2/sec)
5000	938
10,600	1158
16,475	1632

Average Change in Salinity of Toe
During One Tidal Cycle Vs. K

Figure 6.6

convergence is the result of a sufficient number of tidal cycles a run of 60 tidal cycles was made starting from an initial condition which was a linear salinity distribution. Figure 6.7 shows the resulting convergence.

The high water slack salinity distribution after 30 cycles of calculation has a tolerance of 0.07 ppt which means that the previous cycle's (29th cycle's) salinity values differed from this cycle's values by a maximum of 0.07 ppt. Thirty more tidal cycles of calculation produce a significant change in the high water slack distribution as evidenced by the curve for 60 cycles. The maximum difference in salinity between successive cycles, is now reduced to 0.02 ppt which shows that convergence is taking place.

It should be noted that in the studies of real estuaries, the dispersion coefficient relationship was assumed to be

$$E(x,t) = K \left| \frac{\partial s}{\partial x} \right| + 3\, E_T \qquad (6\text{-}2)$$

The multiplication of E_T by a factor of three results in an increase in E(x,t) which is significant only in the fresh water region. The justification for this modification is based on the range of possible values for the dispersion coefficient in the fresh water region suggested by Holley, et al (1970) and also by the demonstration by Lee (1970) that the factor of three will have a relatively insignificant effect. The additional dispersion is of some benefit numerically due to increased damping.

The calculation of the estuary number, $E_D = \frac{P_T E_D^2}{Q_f T}$ is part

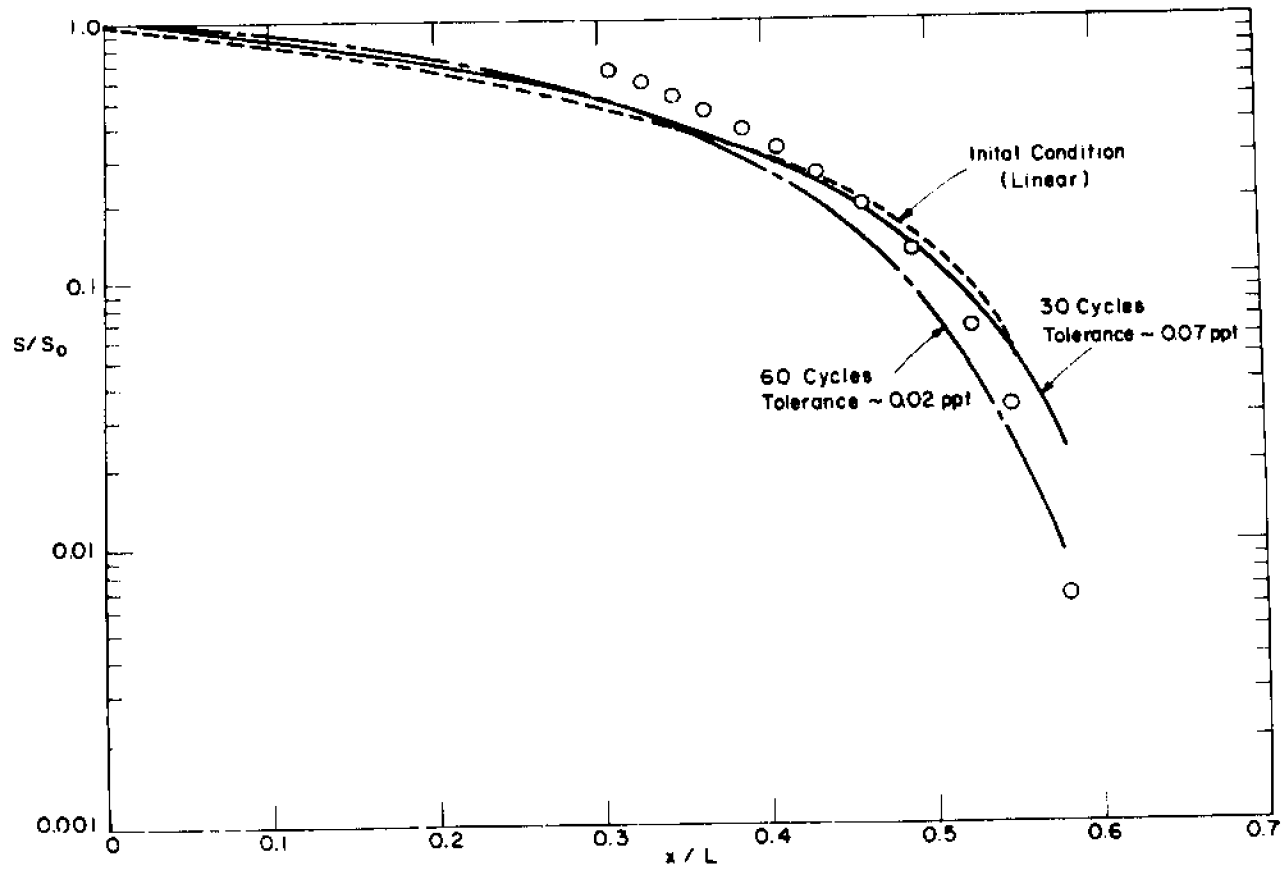

Demonstration of Slow Convergence to Steady-State for Delaware

Figure 6.7

Legend

o Delaware River Model Data

-------- Initial Condition (Linear)

– — – — Distribution after 60 Cycles

———— Distribution after 30 Cycles

of the numerical calculations and proceeds as follows.

1) P_T, the tidal prism is defined as the total volume of water entering the estuary on the flood tide. It is calculated by numerical integration of the discharge at the entrance.

2) $\mathbb{F}_D = \frac{u_o}{\sqrt{gh\frac{\Delta\rho}{\rho}}}$ is defined by the maximum velocity at the entrance, the depth at the entrance and the maximum change in density from the fresh water end to the ocean or downstream end of the estuary. As the discharge, Q, of the staggered finite-difference scheme is defined at the second station from the ocean or seaward end of the estuary the area and depth at that same location are used in the calculation.

3) Q_f is the fresh water discharge and is taken to be the sum of all fresh water discharges upstream of the salinity intrusion region. In the case of the Delaware it is the sum of the inflow at Trenton and the discharge of the Schuylkill River.

4) T is the duration of the tidal period in seconds, and is taken to be 44,712 seconds for the Delaware study.

For the three conditions of fresh water discharge, Q_f, the parameters defining the estuary number $\mathbb{E}_D$ are

Q_f cfs	P_T cu.ft.	u_o ft/sec	h ft.	$\frac{\Delta\rho}{\rho}$	$\mathbb{F}_D$	$\mathbb{E}_D$
5,000	9.03×10^{10}	2.04	37	0.021	.409	67.4
10,600	9.02×10^{10}	2.04	37	0.021	.409	31.7
16,475	9.00×10^{10}	2.04	37	0.021	.408	20.4

The dimensionless dispersion parameters K/u_oL which correspond to the K values shown in Figure 6.6 are based on the above u_o values and the total length L = 693,475 feet.

Q_f in ft^3/sec	K in ft^2/sec	K/u_oL
5,000	938	6.63×10^{-4}
10,600	1158	8.18×10^{-4}
16,475	1632	1.15×10^{-3}

The values of the dimensionless dispersion parameter K/u_oL and the corresponding estuary numbers E_D are plotted in Figure 6.28. They are in good agreement with the previous results from the W.E.S. and Rotterdam studies.

6.4 The Potomac Estuary

6.4.1 Geometry and Schematization

Figure 6.8 shows the general plan of the Potomac from the head of tide at Chain Bridge, a few miles above Washington, D.C., downstream to its confluence with Chesapeake Bay - a distance of about 114 statute miles. The irregular form of the Potomac is further complicated by embayments which represent a considerable volume of storage, about 10% of the entire accumulated volume from Chain Bridge to the Chesapeake.

Jaworski and Clark have compiled data on the geometry of the Potomac in a form which is especially adaptable to mathematical modeling (Data Source Reference 4). Table 6.2 and 6.3, taken from the data developed by Jaworski and Clark, form the basis for the

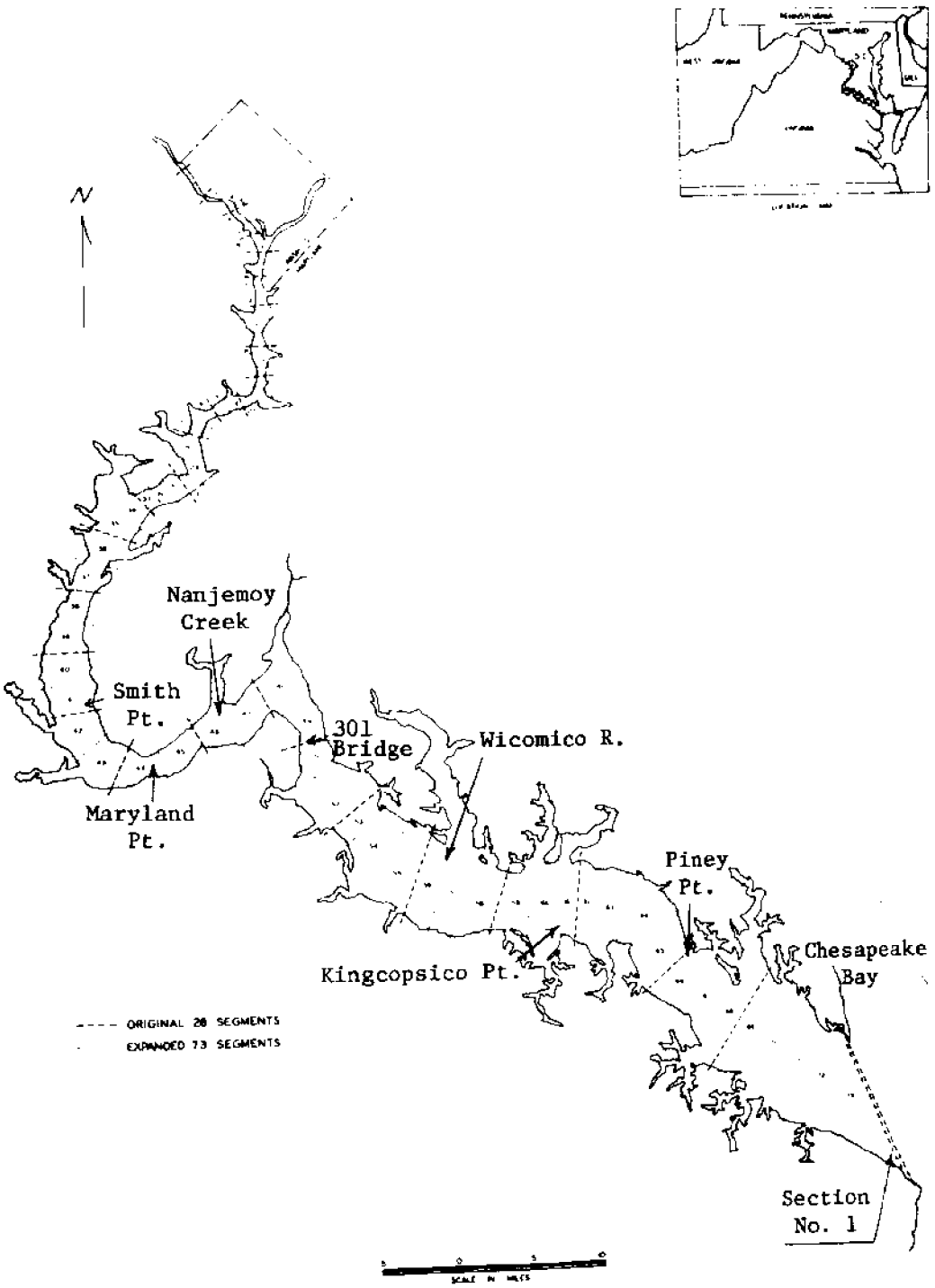

POTOMAC ESTUARY

(from Data Source Reference 4)

Figure 6.8

Segment Geometry of Potomac Estuary
Excluding Embayments (Mean Water Data)
(from Jaworski and Clark, Data Source Reference 4)

Segment Number	Length in ft (from Chain Bridge)	Average Width in ft	Average Depth in ft
1	14,890	559	24.7
2	10,665	1,302	20.0
3	9,187	2,092	10.8
4	9,504	2,677	10.5
5	8,396	2,911	13.2
6	11,404	2,708	13.2
7	13,992	3,739	12.2
8	11,300	4,227	13.2
9	13,516	3,386	20.0
10	10,085	5,695	13.2
11	13,570	4,118	18.5
12	24,129	6,086	17.0
13	15,312	8,053	15.5
14	14,732	12,368	12.1
15	22,387	8,732	20.5
16	21,859	10,799	17.9
17	22,123	16,950	13.7
18	25,291	15,475	14.2
19	28,354	8,856	20.3
20	24,816	13,186	15.3
21	27,614	10,371	22.3
22	32,103	17,406	20.7
23	33,739	24,757	18.8
24	31,152	30,397	20.2
25	28,934	20,830	18.35
26	42,135	27,043	25.0
27	31,416	26,846	33.0
28	51,163	44,342	27.4

Table 6.2

Embayment Data for Potomac Estuary (Mean Water Data)
(from Jaworski and Clark, Data Source Reference 4)

Name	Average Depth ft	Volume $ft^3 \times 10^8$	Location (Miles below Chain Bridge)
Columbia Island Channel	6.40	0.16	4.65 - 5.76
Tidal Basin	10.40	0.46	5.81
Washington Channel	24.45	1.98	7.60 - 8.20
Anacostia River	15.45	5.56	7.60 - 8.20
Four Mile (Hunter Pt.)	12.45	0.79	8.79 - 9.70
Oxon Creek (Upper)	9.40	1.28	10.55 - 12.13
Oxon Creek (Lower)	9.35	1.71	12.13 - 13.57
Hunting Creek	3.35	0.71	12.13 - 13.50
Broad Creek	4.30	0.70	14.90 - 15.92
Piscataway Creek	4.20	1.53	18.11 - 18.63
Little Hunting Creek	3.10	0.14	19.90 - 20.33
Dogue Creek	4.05	0.72	21.85 - 22.80
Gunston Creek	5.00	3.27	24.02 - 25.42
Pomonkey Creek	3.95	0.35	26.73 - 27.10
Belmont Bay	4.80	3.33	31.45 - 34.09
Occoquan Bay	5.80	8.63	31.45 - 34.09
Powells Creek	2.80	0.54	34.79 - 35.92
Mattawoman Creek	8.80	6.56	34.13 - 35.60
Quantico Creek	2.70	0.79	38.10 - 38.55
Chicamuxen Creek	3.70	0.84	36.91 - 37.75
Chopawamsic Creek	2.67	0.36	40.75
Mallows Bay	4.65	0.21	41.64 - 42.44
Aquia Creek	4.60	4.65	46.89 - 48.40
Potomac Creek	3.58	2.76	49.20 - 49.70
Nanjemoy Creek	3.55	4.44	58.18 - 59.20
Port Tobacco River	6.75	11.06	62.00 - 63.80

Table 6.3
(to be continued)

Name	Average Depth ft	Volume $ft^3 \times 10^8$	Location (Miles below Chain Bridge)
Upper Machodoc Creek	5.80	4.16	69.45 - 71.32
Rosier Creek	3.80	0.55	72.60 - 73.27
Cuckold Creek	2.80	0.47	72.00 - 72.21
Monroe Creek	3.80	0.70	75.90
Mattox Creek	5.80	3.60	75.98 - 77.32
Popes Creek	1.85	0.23	79.15
Wicomico River	9.92	38.62	80.52 - 82.85
St. Clement Bay	9.90	15.25	86.05 - 88.35
Breton Bay	9.90	13.40	89.36 - 90.20
Nomini Bay	6.80	8.57	87.26 - 89.48
Lower Machodoc Creek	7.85	7.27	91.15 - 93.38
Herring Creek	4.80	0.88	96.10
St. Georges Creek	5.75	4.45	102.96 - 104.35
St. Mary's River	11.75	33.51	102.96 - 104.35
Yeocomico River	6.63	9.39	103.80 - 104.65
Smith Creek	7.75	3.77	105.15 - 106.65
Coan River	6.60	6.63	107.20 - 109.00
Hull Creek	6.60	1.34	113.00

Table 6.3
(continued)

schematization of the Potomac. The first table defines the estuary geometry, excluding embayments, for 28 segments of unequal length (Table 6.2). This table defines the core width and the depth. However, the data must be interpolated to equal intervals and it is necessary to provide a definition of the cross-section at the two ends of the estuary. This definition was made by using the local U.S.C. & G.S. charts (101-SC) for the schematization of the cross-sections at the end locations. A continuous parabolic interpolation was performed yielding 40 cross-sections at equal intervals of 15481 feet.

At this point the conveyance area or core area of the schematization is defined. It is now necessary to include the embayments which provide storage. With reference to Figure 3.2b it is seen that the embayment volume can be schematized into an equivalent box of length Δx, depth d' and width $b_{total} - b_{core}$. As the length of the equivalent storage volume is given, definition of the depth, d', is sufficient to determine the equivalent width. Fortunately the data of Jaworski and Clark includes both embayment volumes and their average depths. Table 6.3 gives the name, average depth, volume and location of the significant embayments. The schematization was extended to include this data by assigning embayment volumes to those of the 40 segments whose reaches corresponded to the embayment locations. The longitudinal distance over which some embayments extend corresponds to portions of one or more segments. In such cases the volume assigned is proportional to that part of the longitudinal distance corresponding to each segment. The resulting schema-

tized cross-sections are described numerically in Table 6.4 and graphically in terms of b_{core}, b_{total}, d and d' in Figures 6.9 and 6.10.

The Δx for this schematization in 15481.2 feet which corresponds to a total length of 603,768 feet (114.35 miles) from the first section (x = 0) at the entrance to the last section at Chain Bridge. The required Δt to insure stability of the finite difference scheme for the tidal hydraulics equations was found to be Δt = 372 seconds for a tidal period T = 44640 seconds (12.4 hours).

6.4.2 Verification of the Tidal Hydraulics

In the absence of data defining the tidal elevations throughout the tidal cycle for various stations, data from the Tide Tables (National Ocean Survey, formerly Coast and Geodetic Survey) was used. This data defines high and low water elevations and times of high and low water for mean conditions. One of the chief difficulties in using this source of data is in establishing the datums for the high and low water data. The tide tables refer to the local datum for the particular station, but do not give any information on these local datums.

In the study of the Potomac Estuary the variation in mean water level was neglected as in the case of the Delaware. In using Tide Table data for verification, it was decided to use only the range (HW - LW) and the Time Lags in as much as the verification of High and Low Water planes requires knowledge of the local datums.

	Section no.	d feet	z_0 feet	b_{total} feet	b_{core} feet	d' feet
Chesapeake Bay	1	30.00	10.00	59811.	57500.	6.60
	2	27.87	12.13	49325.	49325.	0.00
	3	27.65	12.35	48184.	41695.	6.60
	4	30.46	9.54	46673.	34032.	8.72
	5	32.97	7.03	48740.	28043.	10.63
	6	31.57	8.43	26016.	26016.	0.00
	7	27.63	12.37	28213.	27029.	4.80
	8	23.99	16.01	29123.	26386.	7.85
	9	20.49	19.50	33838.	22519.	8.37
	10	18.34	21.66	36988.	20944.	8.71
	11	19.10	20.90	27865.	25918.	9.90
	12	20.21	19.79	54428.	30468.	9.52
	13	19.49	20.51	30108.	28637.	9.02
	14	18.90	21.20	29914.	24840.	5.47
	15	19.45	20.55	23500.	21527.	3.34
	16	20.56	19.44	22586.	17053.	5.80
	17	21.96	18.04	13752.	13752.	0.00
	18	22.43	17.57	14927.	10458.	6.75
	19	18.15	21.35	18008.	11893.	6.75
	20	15.43	24.57	20975.	12896.	3.56
	21	19.31	20.69	9519.	9519.	0.00
	22	19.15	20.85	10146.	10146.	0.00
	23	14.79	25.21	19852.	14793.	3.60
	24	13.33	26.67	23450.	17007.	4.60
	25	14.19	25.82	16272.	16272.	0.00
	26	17.42	22.58	12503.	11410.	3.49
	27	20.45	19.55	12179.	8905.	3.22
	28	17.95	22.05	17187.	9924.	7.80
	29	12.23	27.77	23908.	11878.	5.52
	30	15.97	24.03	7456.	7456.	0.00
	31	16.94	23.06	9221.	6140.	4.76
	32	18.99	21.01	7849.	4183.	4.79
	33	13.19	26.81	6155.	5702.	3.51
	34	19.12	20.88	5751.	3398.	4.20
	35	12.20	27.80	5535.	4103.	5.92
	36	12.94	27.06	5311.	2909.	8.30
	37	12.71	27.29	6001.	2892.	17.30
	38	10.47	29.53	2577.	2150.	9.37
	39	23.03	16.97	1005.	1005.	0.00
Chain Bridge	40	20.00	20.00	110.	110.	0.00

Potomac Estuary
Schematized Geometry after Including Embayments

Table 6.4

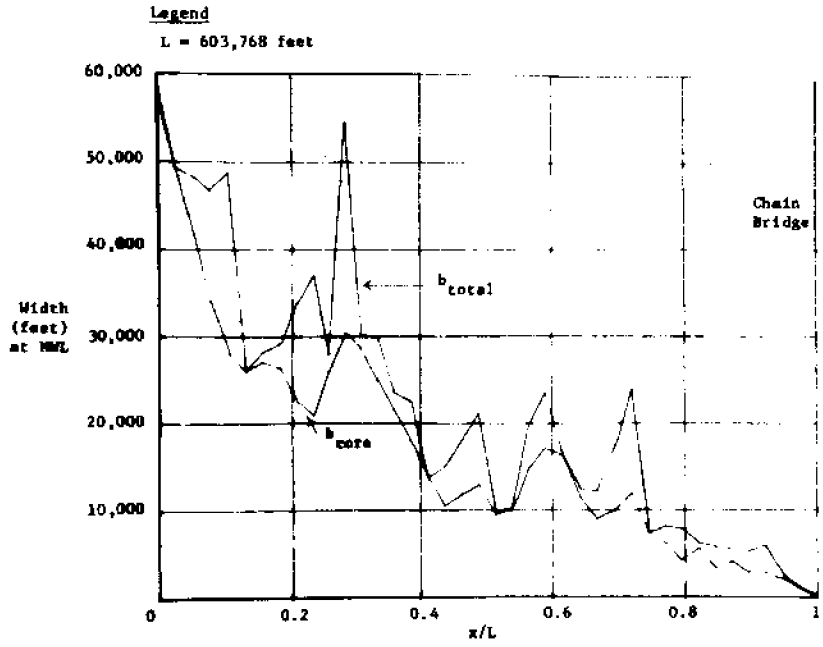

Schematized Widths for Potomac Estuary

Figure 6.9

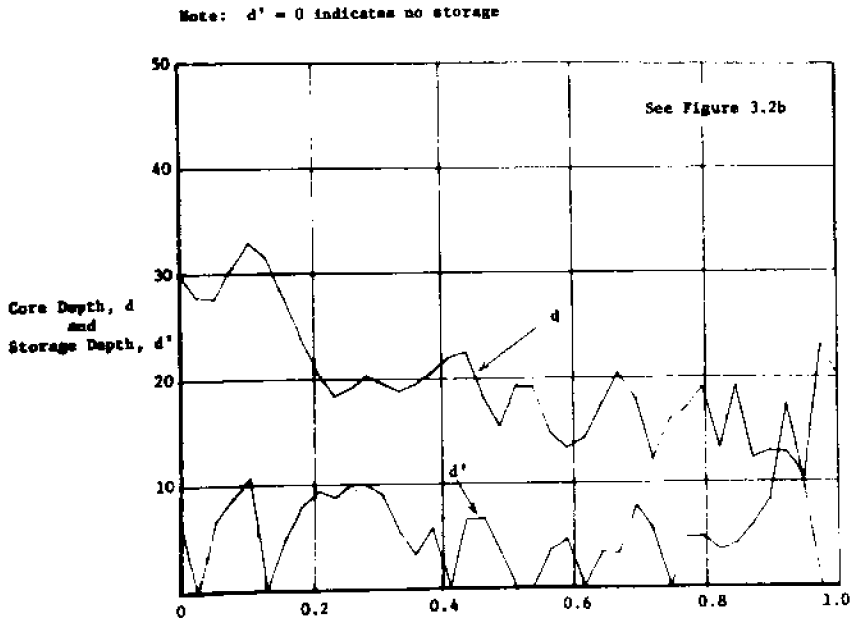

Schematized Depths for Potomac Estuary

Figure 6.10

The 1969 Tide Tables were used, the pertinent reference station being Washington, D.C.

To verify tidal range a mean tide condition was taken with the range at the entrance 1.4 feet and the range at Washington, D.C. 2.9 feet. The tidal data based on this condition is shown in Table 6.5. The numerical model was run with an average fresh water discharge of 3400 cfs at Chain Bridge and with a the salinity distribution as shown in Figure 6.11. The tidal hydraulics are relatively insensitive to changes in the salinity distribution.

Quasi steady-state studies of the discharge and water surface elevations were made using different values and distributions of Manning's n. The best verification found corresponds to a Manning's n of 0.018. This verification in terms of tidal range and High and Low Water phase lags is presented in Figures 6.12 and 6.13 respectively. The asterisks in these figures represent the verification data of Table 6.4. The tidal period was taken as 12.4 hours and the time increment, Δt, was 372 seconds. As the lags are given at intervals of $2\Delta t$ the seeming lack of continuity in Figure 6.13 can be attributed to the discretization.

6.4.3 Quasi Steady-State Salinity Distribution Study

To verify the numerical model under quasi steady state salinity distribution conditions it is desirable to have salinity data for various stations along the length of the estuary at frequent intervals of observation. The two sources of data available consisted of a collection of thirteen surveys made by the

REFERENCE STATION - WASHINGTON, D.C. WASH. CHANNEL.

DATUM= 1.50 HW= 2.90 LW= 0.00
TOTAL LENGTH= 114.35 STATUTE MILES
DISTANCE, CHAIN BRIDGE TO HEAD = 0.00
DISTANCE, CHESAPEAKE BAY LINE TO FOOT = 0.00

STA.	NAME	S.MILES BELOW CHAIN B.	S.MILES FROM OCEAN	K/L FROM OCEAN	TIME (HR.,MIN) HW	TIME (HR.,MIN) LW	HEIGHT RELATIVE HW	HEIGHT RELATIVE LW	HEIGHT LOCAL HW	HEIGHT LOCAL LW
2255	CHAIN BRIDGE	0.00	114.35	1.00000	0 29	0 10	-0.10	0.00	2.80	0.00
2251	KEY BRIDGE	3.35	111.00	0.97070	0 10	0 0	-0.10	0.00	2.80	0.00
2245	WASHINGTON,D.C. CHANNEL ENT.	7.60	106.75	0.93354	0 0	0 0	0.00	0.00	2.90	0.00
2243	WASHINGTON NATIONAL AIRPORT	8.10	106.25	0.92914	0 1	0 -8	0.00	0.00	2.90	0.00
2241	BELLEVUE	9.20	105.15	0.91955	0 1	0-10	-0.10	0.00	2.80	0.00
2239	ALEXANDRIA	11.70	102.65	0.89769	0 -7	0-23	-0.10	0.00	2.80	0.00
2237	RIVERVIEW	17.00	97.35	0.85133	0-22	0-38	-0.40	0.00	2.50	0.00
2235	FORT WASHINGTON	17.95	96.40	0.84303	0-22	0-38	-0.50	0.00	2.40	0.00
2233	MOUNT VERNON	20.90	93.45	0.81723	0-32	0-48	-0.70	0.00	2.20	0.00
2231	MARSHALL HALL	23.05	91.30	0.79843	0-33	0-57	-0.80	0.00	2.10	0.00
2229	GUNSTON COVE	24.60	89.75	0.78487	0-43	-1 0	-0.90	0.00	2.00	0.00
2227	GLYMONT	28.30	86.05	0.75251	-1 2	-1 19	* 0.62	* 0.62	1.53	0.00
2225	INDIAN HEAD	30.60	83.75	0.73240	-1 12	-1 29	* 0.59	* 0.59	1.71	0.00
2223	HIGH POINT	31.30	83.05	0.72628	-1 17	-1 34	* 0.55	* 0.55	1.60	0.00
2221	DEEP POINT	34.00	80.35	0.70267	-1 27	-1 44	* 0.55	* 0.55	1.59	0.00
2219	QUANTICO CREEK	38.20	76.15	0.66594	-1 52	-2 9	* 0.49	* 0.49	1.35	0.00
2217	LIVERPOOL POINT	42.80	71.55	0.62571	-2 22	-2 39	* 0.45	* 0.45	1.30	0.00
2215	CLIFTON BEACH	46.80	67.55	0.59073	-2 15	-2 46	* 0.38	* 0.38	1.10	0.00
2213	AQUIA CREEK	49.00	65.35	0.57149	-2 47	-3 4	* 0.41	* 0.41	1.19	0.00
2211	MARYLAND POINT LIGHT	53.30	61.05	0.53389	-3 27	-3 44	* 0.39	* 0.39	1.13	0.00
2209	RIVERSIDE	56.80	57.55	0.50329	-3 52	-4 17	* 0.34	* 0.34	0.98	0.00
2207	UPPER CEDAR POINT LIGHT	60.10	54.25	0.47442	-4 23	-4 53	* 0.41	* 0.41	1.19	0.00
2203	MATHIAS POINT	62.70	51.65	0.45169	-4 32	-4 56	* 0.41	* 0.41	1.19	0.00
2201	LOWER CEDAR POINT LIGHT	68.80	45.55	0.39834	-5 20	-5 56	* 0.52	* 0.52	1.51	0.00
2197	COLONIAL BEACH	74.90	39.45	0.34499	-5 38	-6 8	* 0.55	* 0.55	1.59	0.00
2191	COBB POINT BAR LIGHT	81.50	32.85	0.28729	-5 56	-6 29	-1.00	0.00	1.90	0.00
2189	ST. CLEMENTS ISLAND	86.70	27.65	0.24180	-6 5	-6 39	-1.00	0.00	1.90	0.00
2183	COLES POINT	94.10	20.25	0.17709	-6 10	-6 55	* 0.62	* 0.62	1.80	0.00
2181	PINEY POINT	99.20	15.15	0.13249	-6 27	-7 16	* 0.48	* 0.48	1.39	0.00
2173	LYNCH POINT	103.00	11.35	0.09926	-6 24	-6 58	* 0.45	* 0.45	1.30	0.00
2177	KITTS POINT	105.20	9.15	0.08007	-6 51	-7 23	* 0.52	* 0.52	1.51	0.00
2171	TRAVIS POINT	107.20	7.15	0.06253	-6 33	-7 5	* 0.41	* 0.41	1.19	0.00

Tidal Data for Verification Purposes - Potomac Estuary
(based on U.S.C. & G.S. Tide Tables, 1969)
Table 6.5

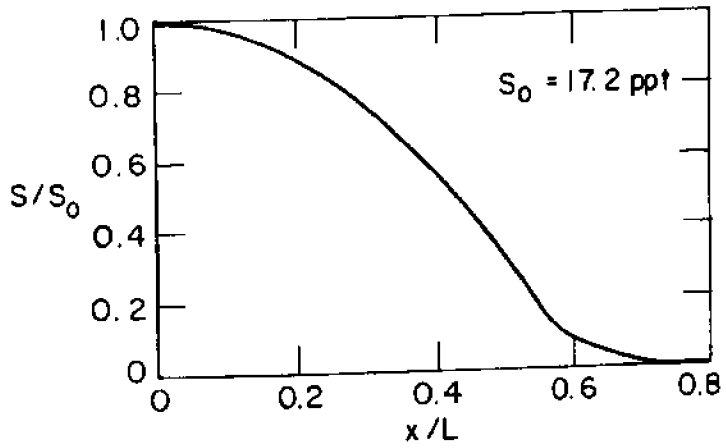

Salinity Distribution in Potomac
used for Verification of Tidal Hydraulics

Figure 6.11

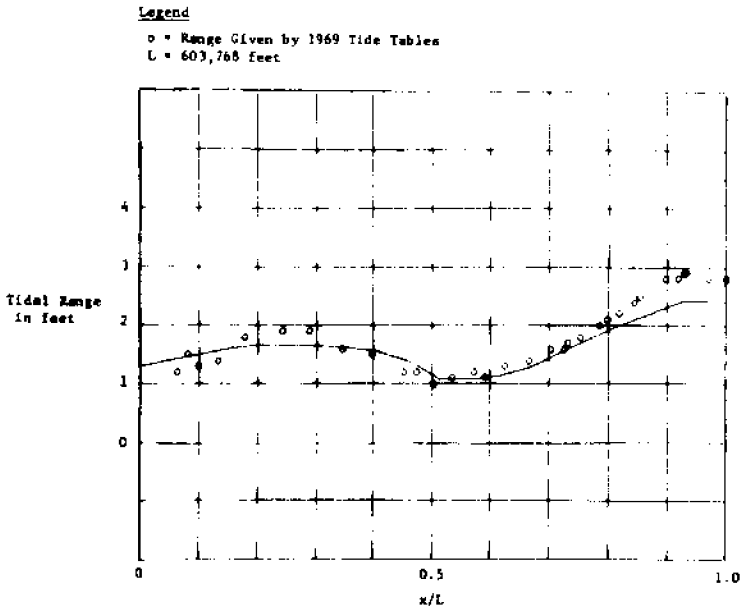

Potomac Estuary Tidal Range Verification

Figure 6.12

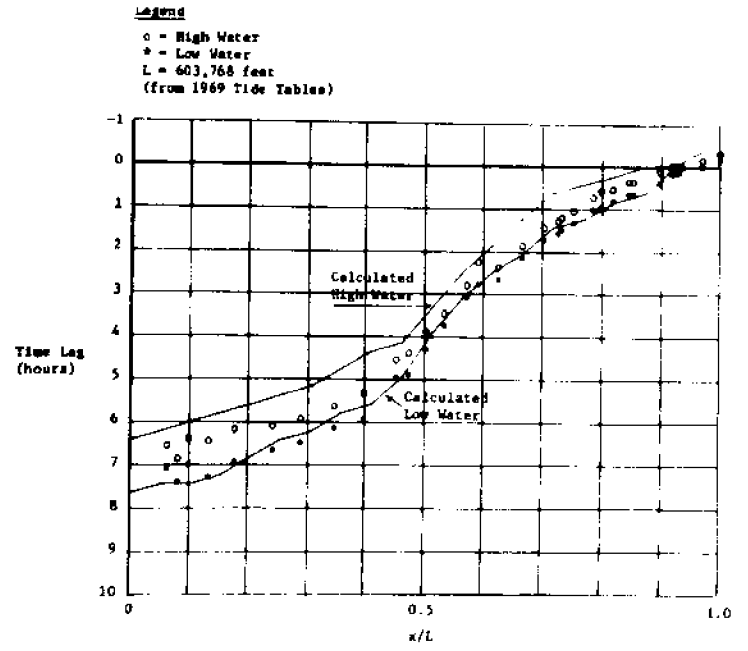

Potomac Estuary
Verification of Time Lags for High and Low Water

Figure 6.13

Chesapeake Bay Institute during 1965 and 1966 (Data Source Reference 5) and the Nutrient Transport Study data furnished by the FWPCA covering the period February 1969 to March 1970 (Data Source Reference 6).

The Chesapeake Bay Institute data is in the form of salinity measurements at different depths for eleven stations covering the estuary from its confluence with the Chesapeake to the Arlington Bridge at Washington. Unfortunately the data was taken at monthly intervals which is far too large an interval to define a steady-state condition.

The Nutrient Transport Study data consists of surface chloride data only, however it was taken at weekly intervals. After reviewing the Nutrient Transport Study data, it was decided to take the period May 5 - May 27, 1969 as an approximation of a steady-state period. The hydrograph and salinities for this period are shown in Figures 6.14 and 6.16. An average fresh water discharge of 3960 cfs was calculated as the quasi steady-state fresh water input at Chain Bridge. (Figure 6.15 shows the determination of an average salinity at the most downstream station, Piney Point.)

The boundary salinity relationship at the entrance to the Potomac Estuary is distinct from that of the Delaware in that the entrance is not at the ocean, but at the confluence of the Potomac with the Chesapeake Bay - another estuary. The Chesapeake is decidedly larger and the principal source of fresh water is the Susquehanna River which has a median discharge at Harrisburg, Pennsylvania of from 7,000 cfs to 75,000 cfs as compared with the

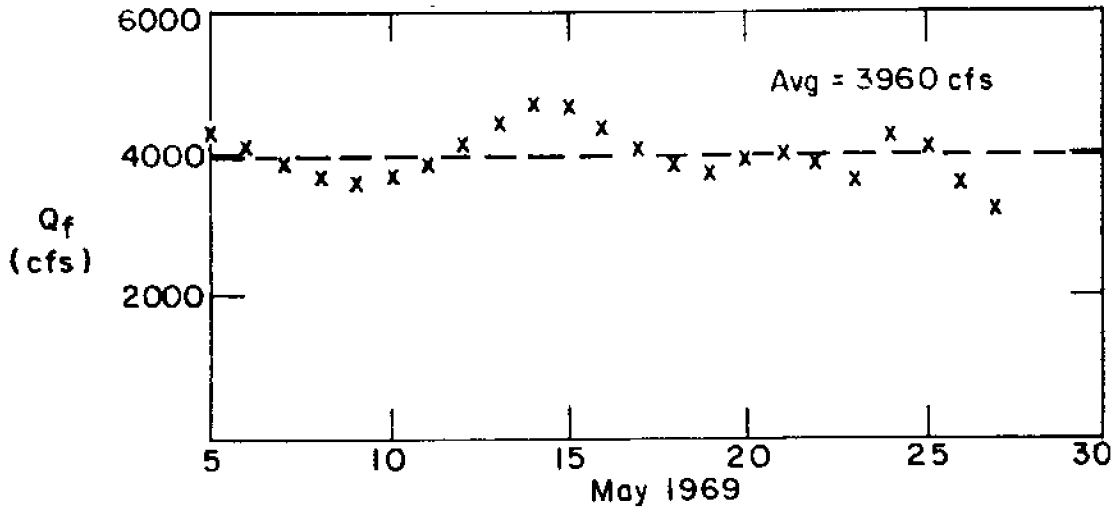

Discharge Near Washington for Assumed Steady State Period
(from Data Source Reference 7)

Figure 6.14

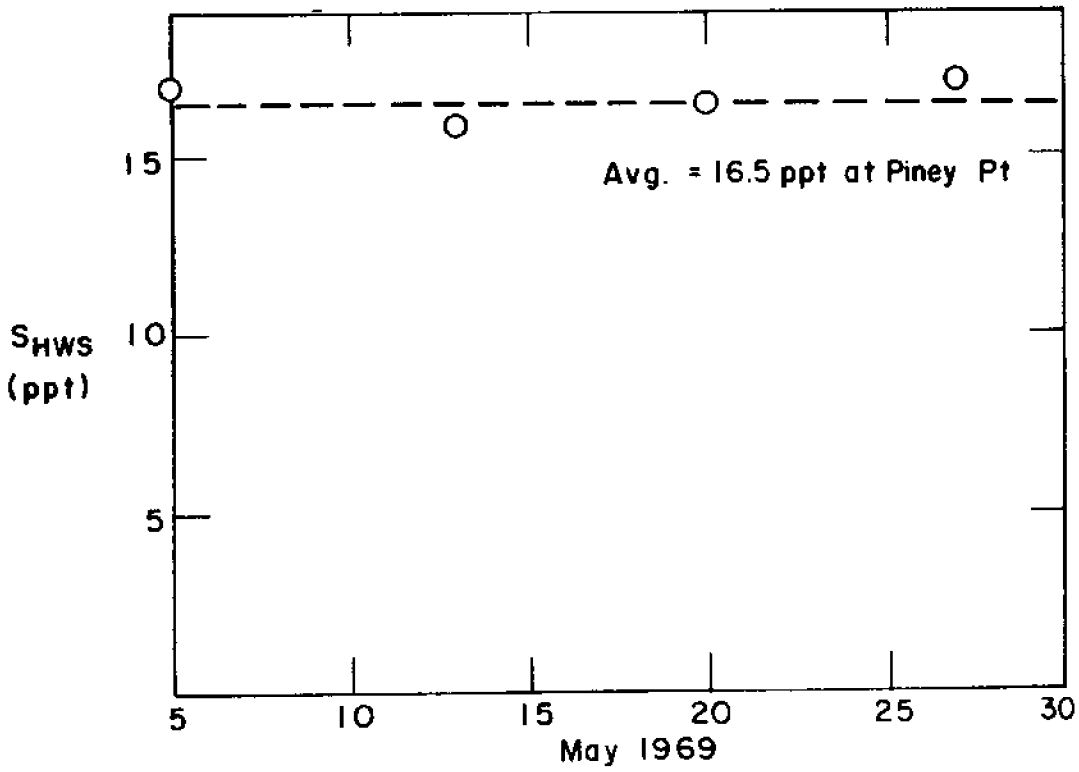

High Water Slack Salinities at Piney Point, Maryland
During Assumed Steady State Period
(from Data Source Reference 6)

Figure 6.15

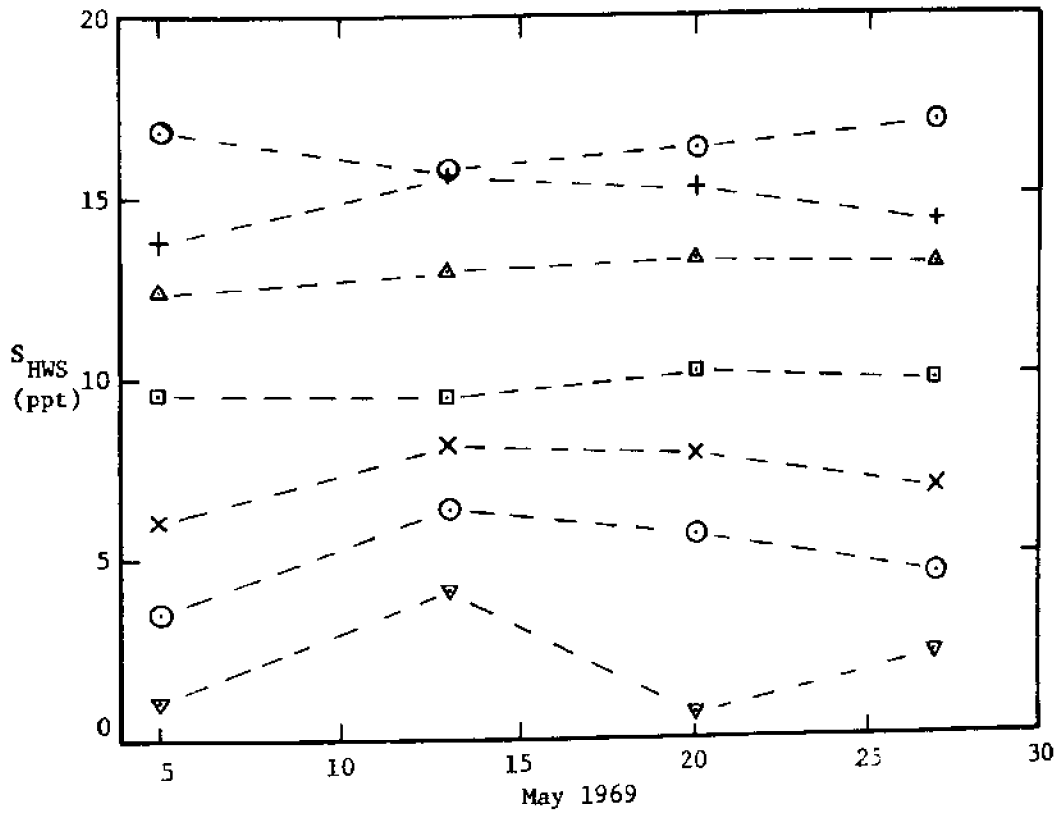

Stations in order of decreasing salinity: Piney Pt., Kingcopsico Pt., Wicomico R., 301 Bridge, Nanjemoy Cr., Maryland Pt., Smith Pt.

High Water Slack Salinities
During Assumed Steady State Period
(from Data Source Reference 6)

Figure 6.16

Potomac River near Washington, D.C. which has a median discharge varying from 3,000 cfs to 20,000 cfs. Figure 6.17 gives an idea of the relative sizes of the two estuaries.

The case of a smaller estuary emptying into a larger estuary is analogous in several respects to an ocean boundary on the smaller estuary. The flow in the larger estuary will act in a similar fashion to the longshore currents which were the basis for the development of the ocean boundary condition. Consequently if the salinity of the larger estuary is known in the vicinity of the entrance to the smaller, then this salinity can be taken as the maximum salinity, s_o, during flood flow. This assumes that the salinity in the larger estuary does not vary appreciably over the tidal cycle.

By taking the excursion in the Chesapeake during flood flow as about 8 miles (maximum velocity of about 9/10 kts.) and referring to the salinity contours of Figure 6.17, one can estimate that a total variation in salinity of 1 ppt. can be expected during the flood flow. As this variation is not extreme, the ocean boundary treatment can be employed as a reasonable approximation as long as the salinity, s_o, is specified for the flood flow.

In this study data on the salinity in the Chesapeake was not available for the period of time corresponding to the Potomac salinity survey. In order to use the data which was available for the Potomac it was necessary to extrapolate the salinity at Piney Point to the physical boundary of the Potomac Estuary. The maximum

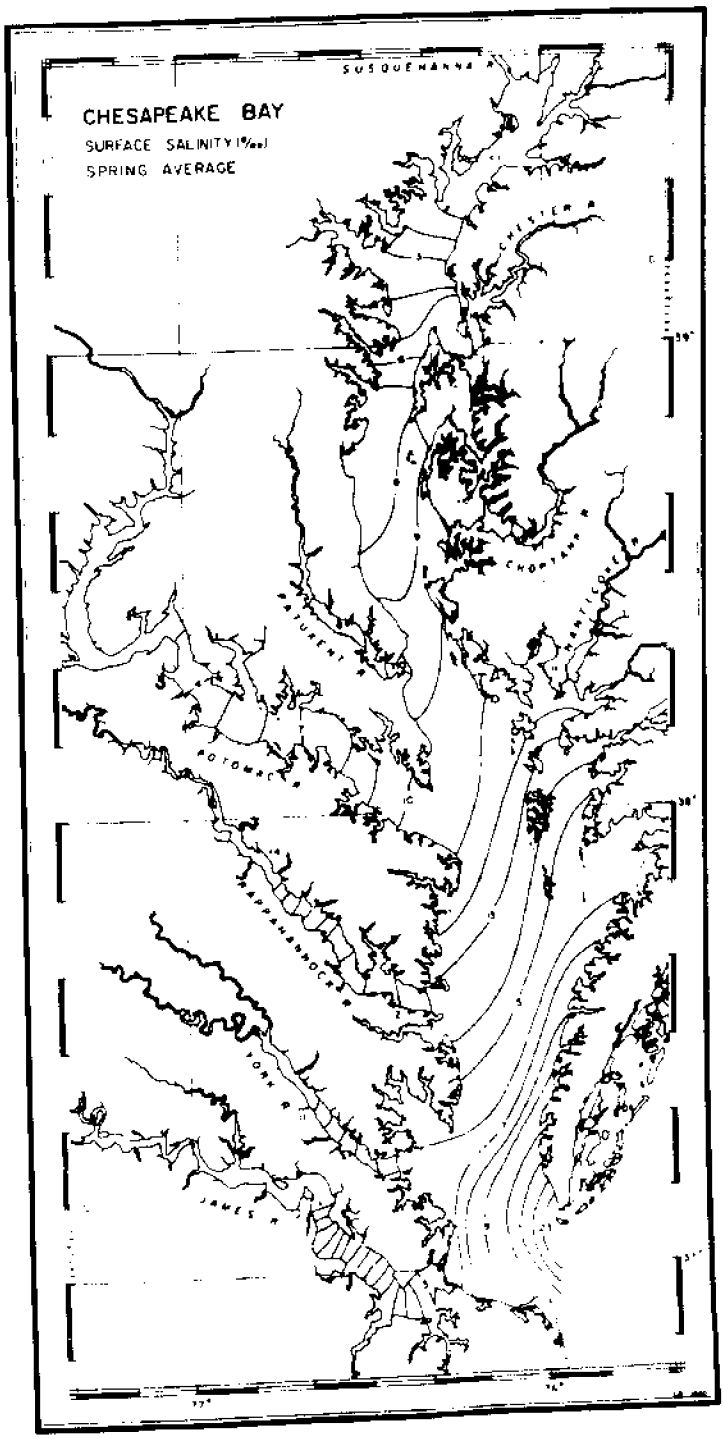

Plan of Chesapeake Bay
(from Stroup and Lynn, 1963)

Figure 6.17

salinity at the entrance was specified as 17.2 ppt. (9.5 ppt. Chlorides) which is 0.7 ppt. greater than the salinity shown at Piney Point in Figure 6.15.

Using the technique described in section 6.3.3 for the Delaware, a best K value of 600 ft^2/sec was determined. The maximum entrance velocity, u_o, was calculated to be 0.54 ft/sec and the length of the estuary from its entrance (x = 0) to Chain Bridge is 603,768 feet. This determines the dimensionless dispersion coefficient, K/u_oL, as 1.84×10^{-3}. The tidal prism, P_T, was $9.77 \times 10^9 ft^3$, the fresh water discharge, Q_f, was 3960 cfs as shown in Figure 6.14, and the tidal period was taken as 12.4 hours (44640 seconds). $\Delta\rho/\rho$ is 0.0129 and the entrance depth is 27.9 feet thus determining F_D as 0.16 and giving a corresponding estuary number E_D of 1.4. The point defined by these K/u_oL and E_D values is plotted in Figure 6.28, it is in good agreement with the previous correlation. Because of the smaller tidal range in the Potomac, in comparison with the Delaware, the estuary number is an order of magnitude smaller. This is indicative of a more highly stratified condition in the Potomac.

6.5 The Hudson Estuary

6.5.1 Geometry and Schematization

The Hudson Estuary is characterized as being a narrow, sometimes deep estuary over much of its length, however it is complicated and difficult to represent by a one-dimensional schematization at its lower end. Immediately below the Battery, the East River joins the Hudson at the northern end of Upper Bay

(Figure 6.18) and there are connections to the Raritan River. The Lower Bay, as defined by a line between Sandy Hook and Coney Island, appears as the ocean end of the estuary.

The Upper and Lower Bays are difficult to schematize to one-dimensional cross-sections. This problem plus the fact that the Battery is a Reference Station for tidal elevation data make the Battery a logical location for the entrance to the estuary as studied by this one-dimensional technique. Another factor which led to the establishment of the Battery as the downstream boundary is the fact that there is a lack of salinity data seaward of this location.

The schematization from the Battery to the head of tide at Troy is based on cross-sections taken from local charts N.O.S. numbers 369, 746, 282, 283 and 284. Cross-sections were taken at one mile intervals, thus permitting intervals of discretization of one mile or larger. For this study a two mile interval (Δx) was used and the assignment of embayment volumes to the corresponding segments was made on this basis.

A further refinement was incorporated in the schematization technique. With reference to Figure 6.19 it is seen that the shoal area of some cross-sections extend far from the main channel. In such cases it is difficult to decide which part of the shoal area participates in the conveyance area and which part acts as storage. Shoal areas and widths have been treated separately from the channel area in this schematization, thereby permitting the user of the numerical model to assign them as participating in the conveyance

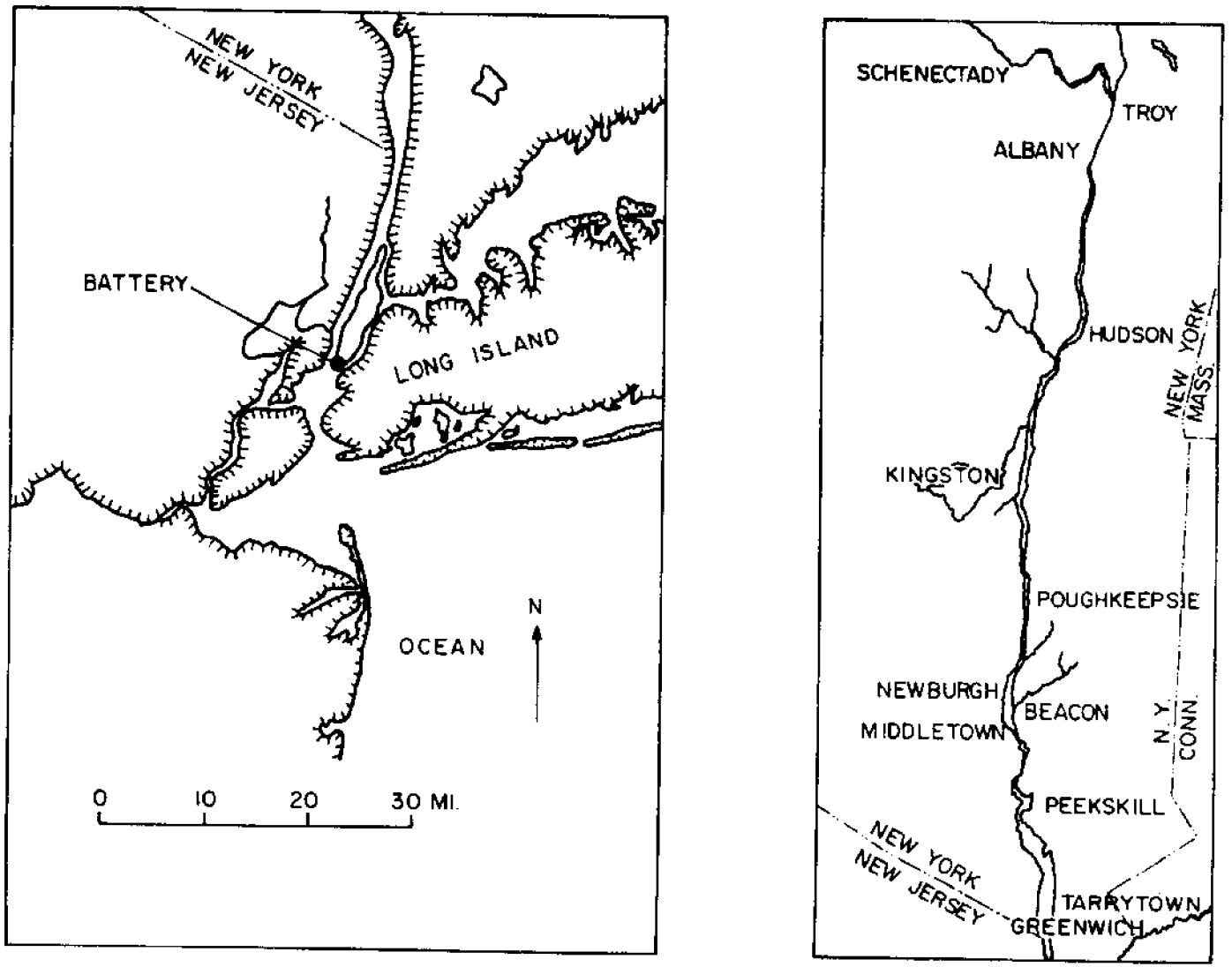

Plan of Hudson Estuary

Figure 6.18

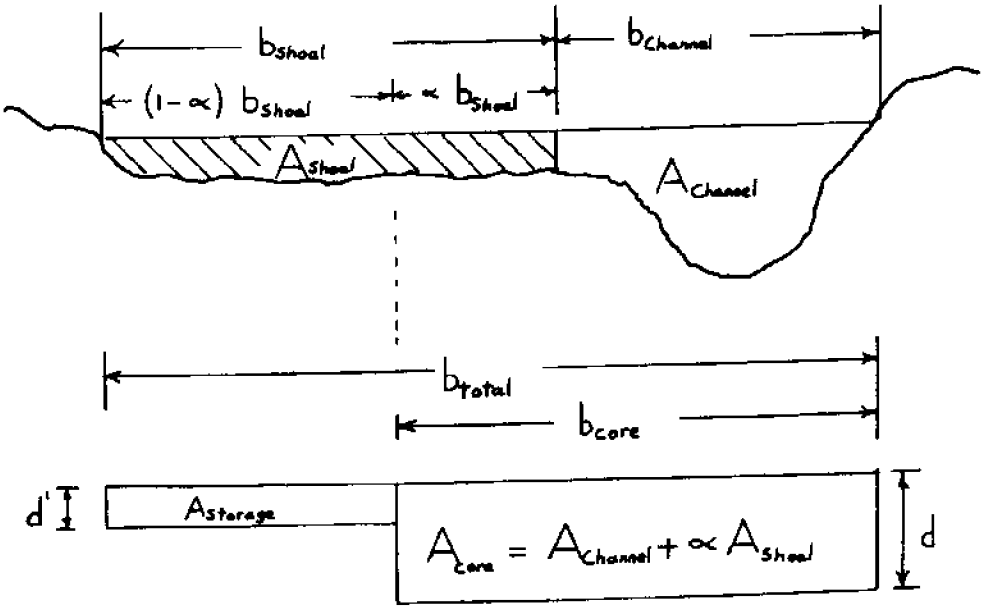

Sketch Showing Method of
Handling Shoal Areas in Schematization

Figure 6.19

area or as storage in terms of a factor of proportionality, α. This feature does not make the decisions regarding the shoal areas less subjective, however it does make it possible to evaluate the sensitivity of the numerical model to changes in α. In this study it was found that the tidal hydraulics were not very sensitive to α and therefore a value of 0.5 was assigned.

The datum corresponding to the soundings on the various charts has been established for this case and is shown in Figure 6.20. This figure also serves to define the high and low water planes which will be used for verification purposes. By establishing a reference datum at 200 feet below mean water level at the Battery the change of datum is incorporated into the schematization through the variable z_o as follows. Figure 3.2 shows that the distance from the reference datum to the local mean water level is $z_o + d$. Figure 6.20 shows the local mean water level (MWL) for all locations and permits the designation of z' as the difference between local MWL and MWL at the Battery. It is now possible to define z_o as

$$z_o = z' + 200 - d \qquad (6\text{-}3)$$

The numerical definition of the schematization is given in Table 6.6 and the graphical representation of b_{core}, b_{total}, d and d' are given by Figures 6.21 and 6.22. The final Δx used was 10715 feet which was obtained by interpolating the cross-section data to 76 sections the first being at the Battery and the last at Troy. The total distance is 152.2 miles (803,616 feet). The tidal period was taken as 44640 seconds, and the Δt based on stability

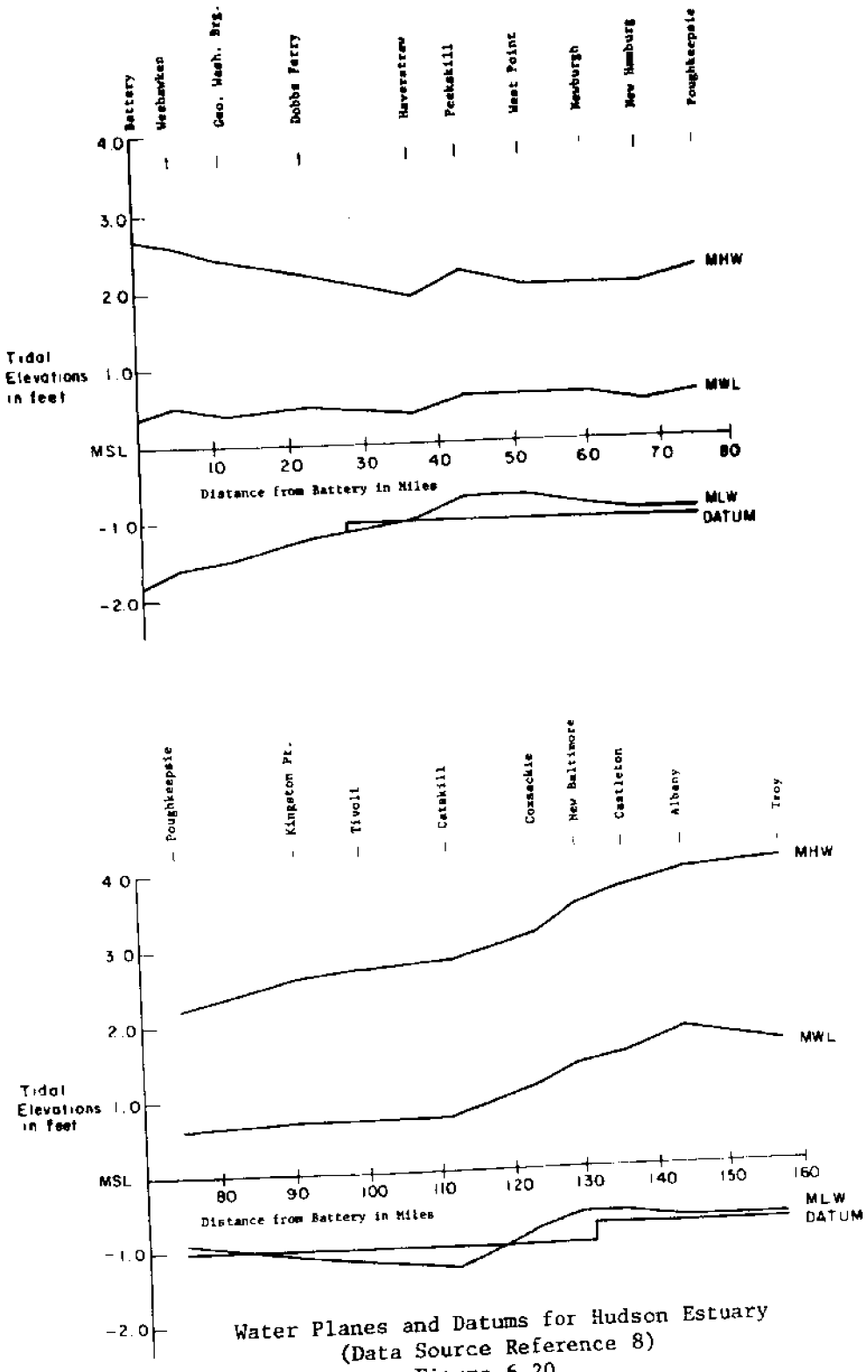

Water Planes and Datums for Hudson Estuary
(Data Source Reference 8)
Figure 6.20

	Station No.	d	z_0	b_{total}	b_{core}	d'
Battery	1	41.34	150.06	4820.	3875.	12.20
	2	45.25	155.10	4116.	2862.	12.20
	3	43.39	157.00	4175.	2650.	12.10
	4	36.32	164.14	4040.	3088.	9.50
	5	40.60	159.82	4039.	3489.	11.35
	6	26.06	171.33	4665.	4413.	5.17
	7	26.42	174.11	4550.	4550.	0.00
	8	25.53	174.34	5175.	5175.	0.00
	9	23.31	170.61	4775.	4775.	0.00
	10	29.33	171.23	4613.	4613.	0.00
	11	27.06	172.56	5163.	5050.	2.70
	12	25.44	175.06	6100.	5550.	2.97
	13	20.38	180.12	10376.	7625.	4.53
	14	16.03	184.54	13125.	11475.	5.54
	15	14.23	183.82	12281.	12150.	5.39
	16	17.61	182.30	11181.	11125.	4.50
	17	20.52	179.86	13750.	9175.	5.62
	18	18.18	181.25	11040.	9450.	3.34
	19	15.37	185.03	15937.	13353.	3.36
	20	22.93	177.64	10096.	8013.	5.07
	21	44.04	156.53	4111.	3550.	5.80
	22	43.32	157.35	5281.	3950.	5.76
	23	48.33	152.37	3080.	2275.	2.94
	24	70.35	131.33	2174.	1763.	2.70
	25	75.85	124.75	1944.	1875.	2.60
	26	71.59	129.01	2114.	2056.	2.60
	27	68.39	132.21	3122.	1894.	5.03
	28	68.53	132.07	3203.	2850.	3.35
	29	67.66	132.94	6517.	5733.	3.75
	30	64.75	135.95	7206.	6519.	4.51
	31	70.55	130.05	5758.	5021.	4.50
	32	70.63	129.80	5350.	4981.	3.07
	33	76.85	123.65	4072.	3913.	2.91
	34	79.91	120.59	3705.	3081.	7.17
	35	79.79	120.71	3619.	3313.	3.50
	36	86.42	114.14	2552.	2463.	3.60
	37	87.79	112.81	2550.	2475.	3.33
	38	85.01	115.59	2438.	2438.	0.00
	39	83.76	116.84	2625.	2625.	0.00
	40	80.73	119.87	2029.	1963.	3.60
	41	84.35	116.25	2625.	2625.	0.00

Hudson Estuary
Schematized Geometry Including Embayments and Local Datum

Table 6.6
(to be continued)

Station No.	d	z_0	b_{total}	b_{core}	d'
42	34.42	166.20	3262.	3013.	3.05
43	36.33	164.37	3253.	3075.	6.28
44	27.89	172.91	5452.	4138.	4.53
45	31.60	169.10	4102.	3633.	6.30
46	25.80	174.90	5999.	4038.	15.20
47	22.41	178.29	4622.	4475.	4.02
48	23.17	177.53	4044.	3739.	3.70
49	25.61	175.09	4254.	3225.	3.70
50	19.91	180.79	3831.	3388.	3.09
51	24.44	175.96	3867.	2575.	4.00
52	19.24	181.46	3969.	3104.	2.70
53	17.12	183.59	3522.	2844.	2.67
54	20.02	180.68	4045.	2513.	2.96
55	16.58	184.12	4364.	2800.	3.17
56	17.47	183.23	2715.	1944.	7.40
57	15.79	184.93	2768.	2244.	4.22
58	13.88	186.95	3250.	2606.	2.81
59	16.24	184.66	3543.	2656.	4.15
60	16.32	184.60	3760.	2238.	2.97
61	17.10	183.84	3297.	1240.	8.85
62	18.37	182.73	1996.	1606.	3.20
63	18.05	183.13	2218.	1450.	3.25
64	19.17	182.10	1887.	1663.	3.45
65	20.60	180.77	3611.	1256.	12.23
66	20.94	180.72	1328.	1206.	3.49
67	19.12	182.41	1450.	1250.	8.82
68	21.99	179.46	1175.	1094.	5.35
69	22.75	178.73	1624.	1110.	7.05
70	22.99	178.69	1119.	975.	4.00
71	24.25	176.70	1034.	938.	11.21
72	19.25	182.49	1009.	939.	23.64
73	12.30	189.43	763.	763.	0.00
74	13.34	188.31	828.	763.	7.40
75	12.41	189.21	675.	675.	0.00
Troy 76	6.45	192.10	1146.	700.	5.15

Table 6.6
(continued)

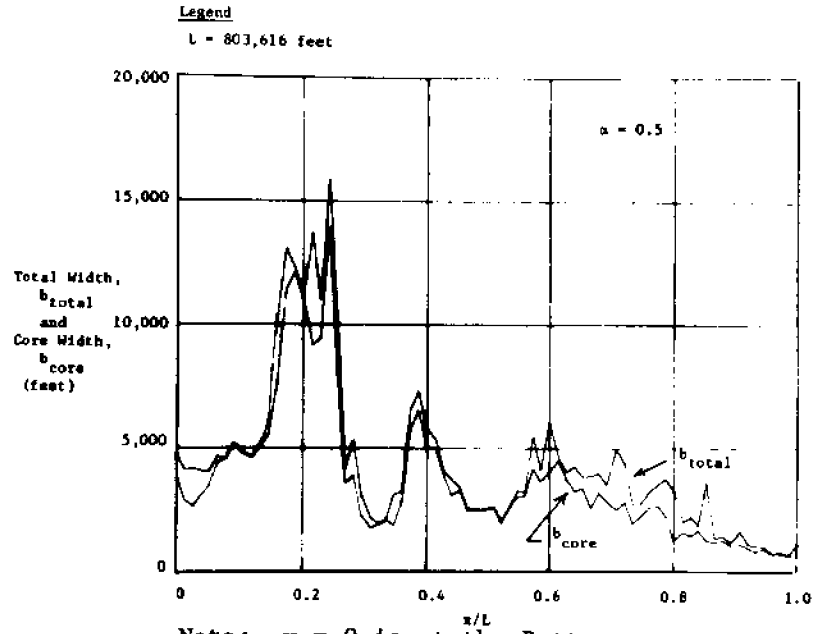

Note: x = 0 is at the Battery

Schematized Total and Core Widths
for Hudson Estuary

Figure 6.21

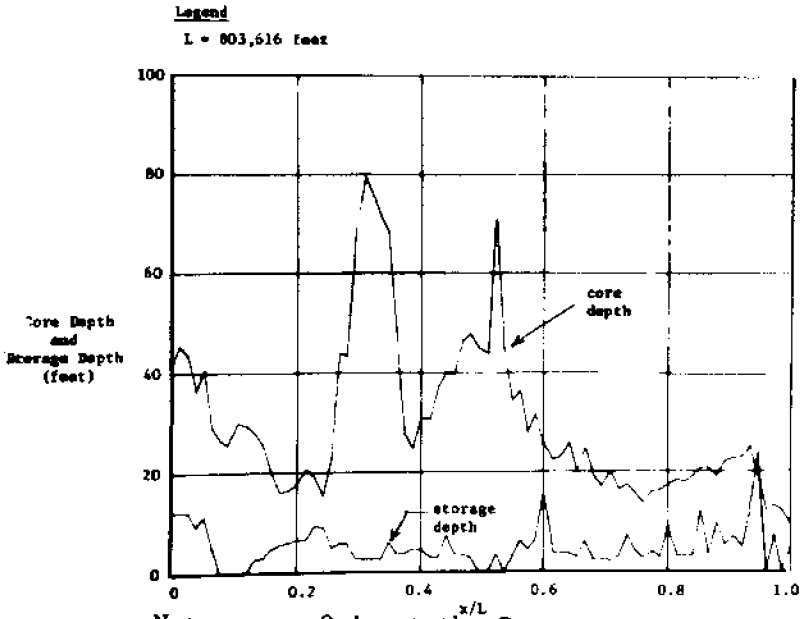

Note: x = 0 is at the Battery

Schematized Core Depth and Storage Depth
for Hudson Estuary

Figure 6.22

considerations was taken so as to divide the tidal period into 200 intervals of $\Delta t = 223.2$ seconds.

6.5.2 Verification of the Tidal Hydraulics

A freshwater discharge of 3500 cfs and a salinity distribution as shown in Figure 6.23 was assumed for the study of the tidal hydraulics. Various distributions of Manning's n were tried and the resultant high and low water planes were compared to those shown in Figure 6.20. The tidal amplitude corresponding to the conditions at the Battery was 2.25 feet. The best fit to the given high and low water planes was achieved using a Manning's n of 0.015 for the entire estuary. The comparison of calculated water planes to those given in Figure 6.20 is shown in Figure 6.24. The calculated phase lags are compared with those given by the Tide Tables (1969) and this comparison is shown in Figure 6.25.

6.5.3 Quasi Steady State Study

The summer and fall of 1964 was a period of extended low flow for the Hudson River. Data corresponding to the end of this period has been made available from the 1964 KYMA Survey (Data Source Reference 9). This period of the KYMA Survey, 10 - 25 November 1964, has been assumed to be a steady state period. Figure 6.26 shows the fresh water hydrograph at Green Island (just above Troy) which illustrates the extended period of low flow. The average tidal range during the KYMA Survey was 5.6 feet at the Battery and mean water level at the Battery was 0.4 feet above mean sea level. The average fresh water discharge for this period was calculated to be 3500 cfs (Data Source Reference 10). The salinity distribution of Figure 6.23 defines the high water slack salinities

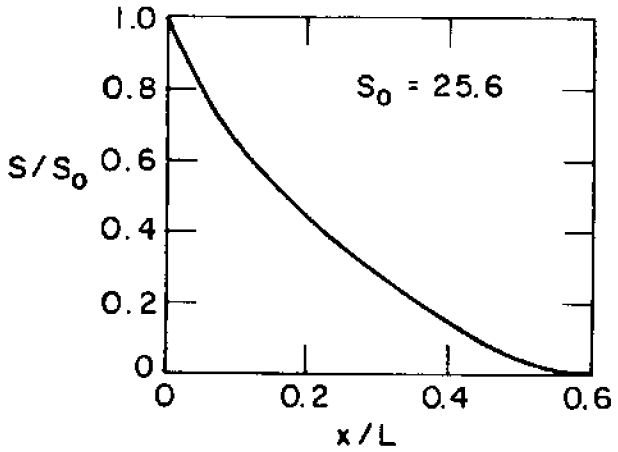

Salinity Distribution in the Hudson
used for Verification of Tidal Hydraulics

Figure 6.23

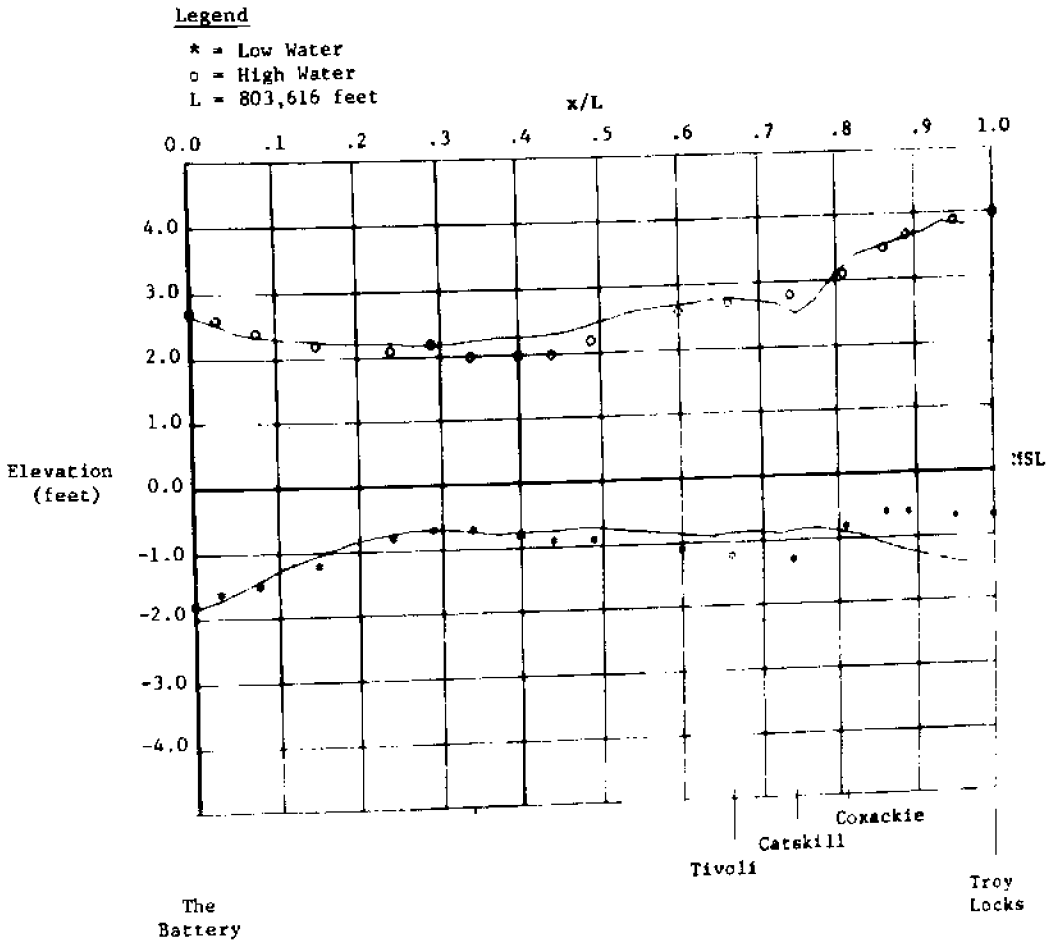

Hudson Estuary
Verification of High and Low Water Planes

Figure 6.24

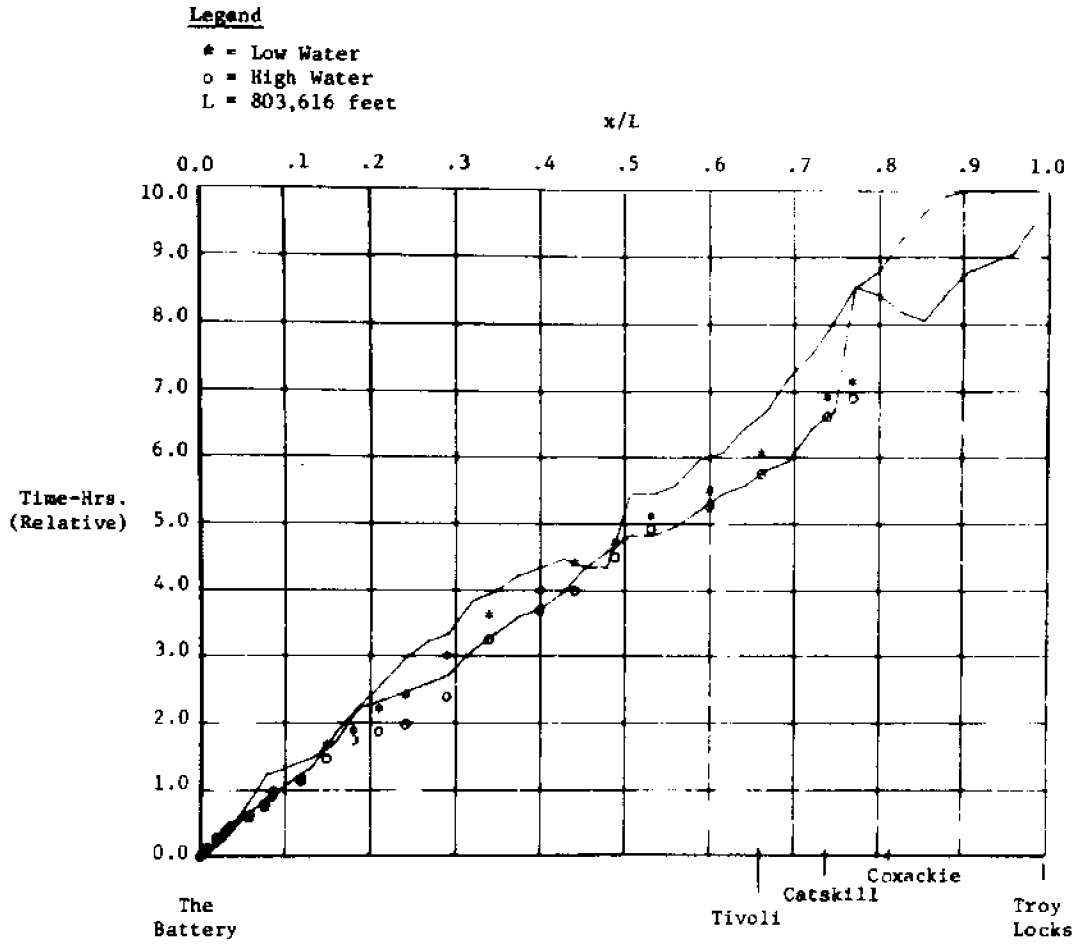

Hudson Estuary
Verification of Lags of High and Low Water Relative to the Battery

Figure 6.25

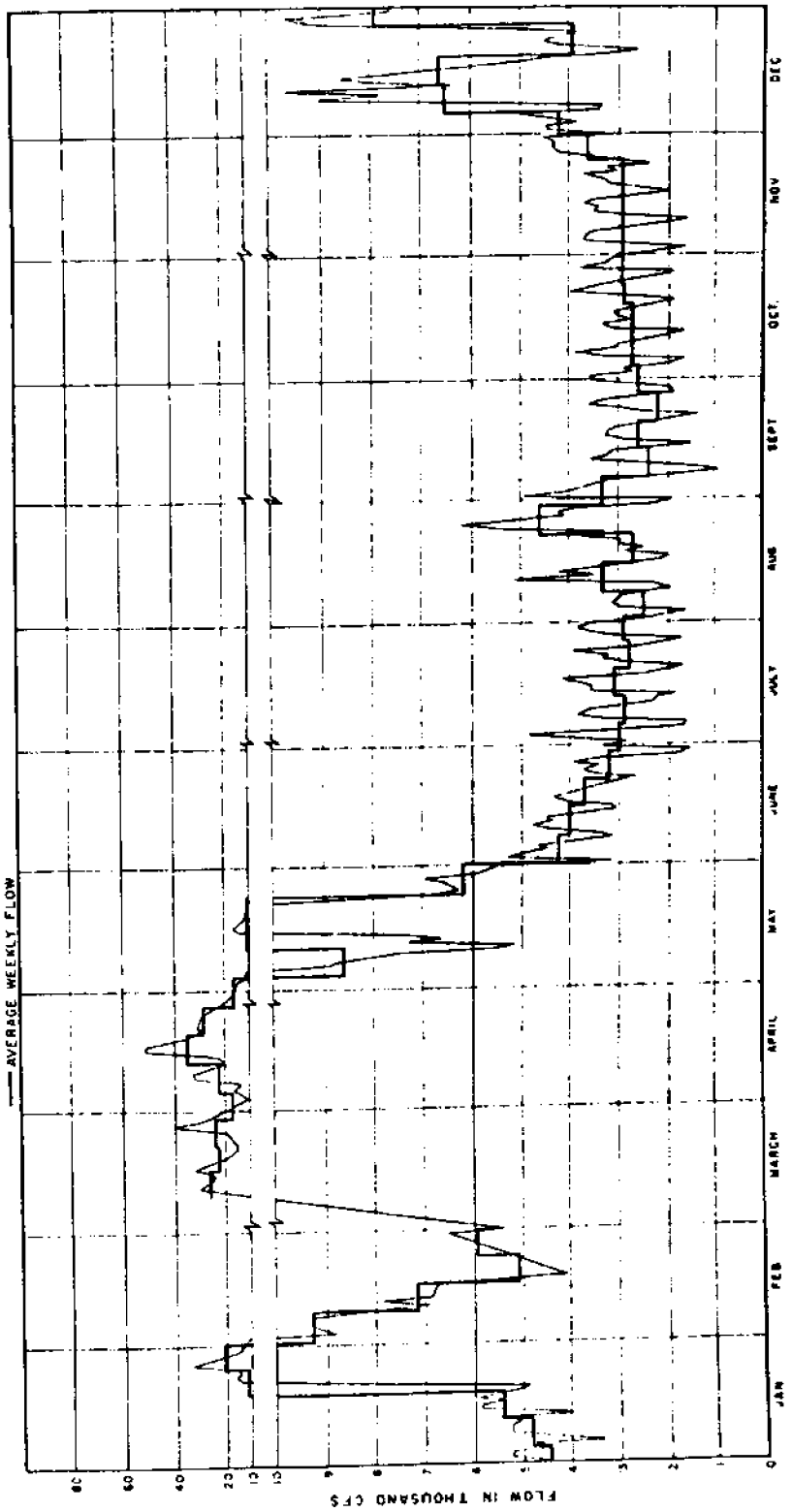

Hudson Inflow at Green Island
(Data Source Reference 9)

Figure 6.26

resulting from the KYMA study and is taken to be the steady-state distribution to be verified.

The Hudson Estuary represents a third and different type of estuary in terms of salinity boundary conditions. With reference to the plan of Figure 6.18 it is evident that below the tip of Manhattan (just above the Upper Bay) the estuary is not one-dimensional. The East River connection to Long Island Sound, the Raritan River, and the geometric configuration of the Lower Bay make the situation highly two-dimensional.

The location of the downstream boundary at the Battery assures a good representation of the tidal hydraulics, but requires that the downstream boundary condition on salinity be handled in a manner which takes into account the fact that the salinity at the entrance increases gradually during the flood flow. This is the case discussed in section 3.4.4e wherein longshore currents are absent from the boundary. The boundary salinity during flood flow at the Battery is prescribed by a ramp function interpolating the salinity from time of low water slack to time of low water slack plus 2/5 of a tidal period. The maximum salinity is the high water slack salinity in this case. Figure 6.27 illustrates this boundary treatment by comparing the ramp function specification of $\frac{2}{5}T$ with that of $\frac{1}{20}T$ which was used in the case of an ocean boundary. The salinity variation being represented was assumed to be sinusoidal for the purpose of this illustration. This assumption is roughly justified for the Battery based on data averaged over an entire year.

The dispersion parameter, K, was determined using the same

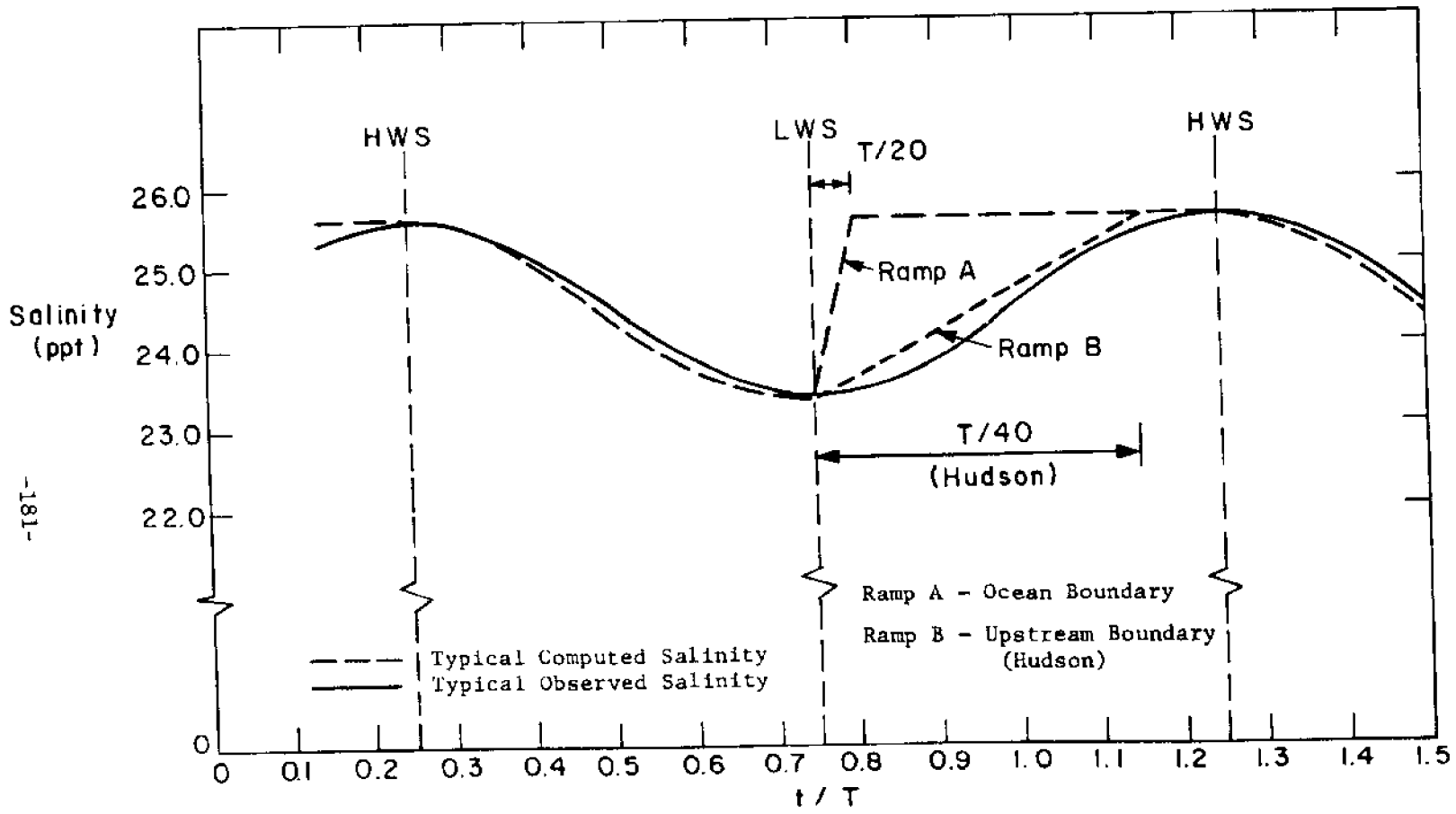

Representation of Entrance Boundary Condition
on Salinity for Hudson Estuary

Figure 6.27

technique described in section 6.3.3 for the Delaware. The resulting value was K = 1685 ft^2/sec. The maximum entrance velocity was 2.44 ft/sec which determines the dimensionless dispersion parameter, K/u_oL, as 8.59×10^{-4}. Other parameters corresponding to this value were the tidal prism, $P_T = 5.93 \times 10^9$ ft^3; the fresh water discharge, $Q_f = 3500$ ft^3/sec, the tidal period, T = 44640 sec, the entrance depth, h = 45.3 feet, and $\frac{\Delta\rho}{\rho} = .0192$. These values determine the densimetric Froude number, $\mathbb{F}_D = .461$, and the estuary number is $\mathbb{E}_D = 8.1$. The point on Figure 6.28 which corresponds to this steady-state study falls somewhat below the line indicated by the other studies. This difference may be related to the fact that the seaward boundary was chosen at the Battery and that the salinity on the flood tide is not constant at this section. There are no continuous measurements of salinity at the Battery with which to verify the assumption represented in Figure 6-27.

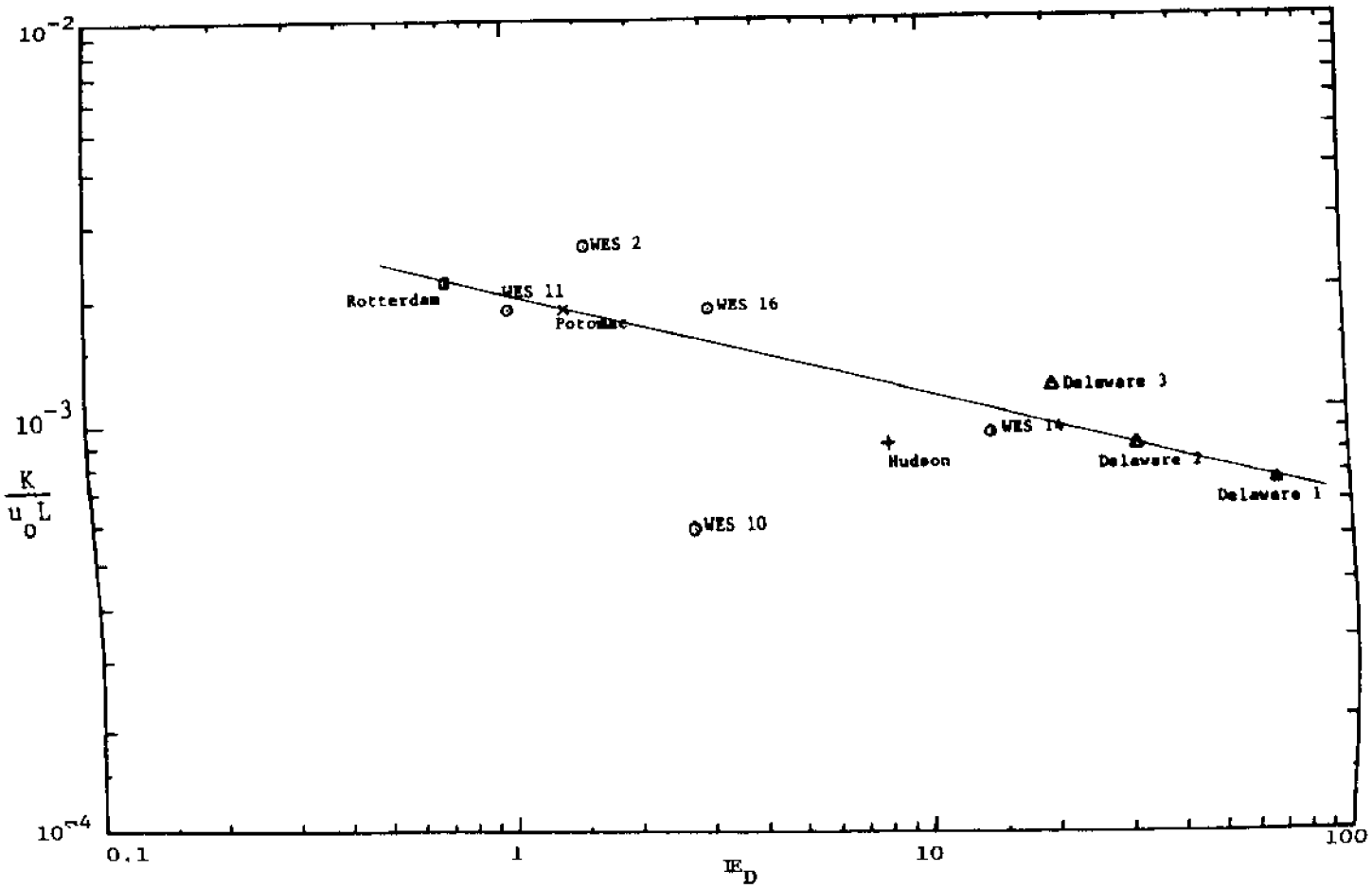

Correlation of Dispersion Parameter to Degree of Stratification

Figure 6.28

VII. Application of the Numerical Model to the Prediction of Longitudinal Salinity Distributions Under Transient Conditions

7.1 Introduction

The objective of this chapter is to demonstrate the application and validity of the numerical model to the prediction of longitudinal salinity distributions under transient conditions. In a given estuary transient conditions are usually the result of daily and seasonal variations in tidal amplitude and fresh water inflow from tributaries. Thus, the normal condition of an estuary is almost always the transient state in which the salinity distribution is continually responding to temporal changes.

One of the difficulties of demonstrating the validity of the predictive model is the lack of reliable field data. For example, salinities frequently are measured only at high water slack at various locations on a daily, weekly or even a monthly basis. It is not uncommon to find "daily" high water slack salinities recorded without reference to which of the two possible times of high water slack the observations were made. Since most tides have some diurnal inequality, there can be a significant variation in the salinity between successive high water slacks at a fixed station. The estuaries chosen for the transient salinity intrusion studies are the Delaware, Potomac and Hudson. These were chosen on the basis of the availability of salinity distribution data extending over a reasonable number of tidal cycles and because the geometric schematizations and verifications of the tidal characteristics had already been carried out in connection with the quasi steady-

state studies presented in Chapter VI.

7.2 The Delaware Estuary

The period 10 - 11 August to 4 - 5 October 1932 was selected as the period of interest for a transient study. The Delaware River Model Study No. 1 (Data Source Reference 11) shows initial and final high water slack salinity profiles for the surface salinities of the prototype estuary corresponding to this period. Unfortunately the salinities are given only as far downstream as Miah Maull Light. Wicker (1955) shows the ocean salinity at 32 ppt; this value is used for the boundary salinity for the incoming flow from the ocean.

The fresh water inputs during this period were made available through the U.S. Army Corps of Engineers, Waterways Experiment Station (Data Source Reference 12). Fresh water inflow data as a function of time is given for three locations:

1) at Trenton

2) at the junction of the Schuylkill river, and

3) at the junction of the Christina river.

The daily discharge values were interpolated to values at each of 107 tidal cycles covering the period of interest. The three hydrographs are shown in Figure 7.1. Three other tributaries were assigned constant flow rates of 82 cfs for the Salem river, 132 cfs for the Cohansey river and 265 cfs for the Maurice river. These inflows are proportioned with respect to a representative flow of 3000 cfs just below the Schuylkill river.

The ocean boundary condition on tidal elevations was taken from the predicted values shown in the U.S. Coast and Geodetic Survey Tide

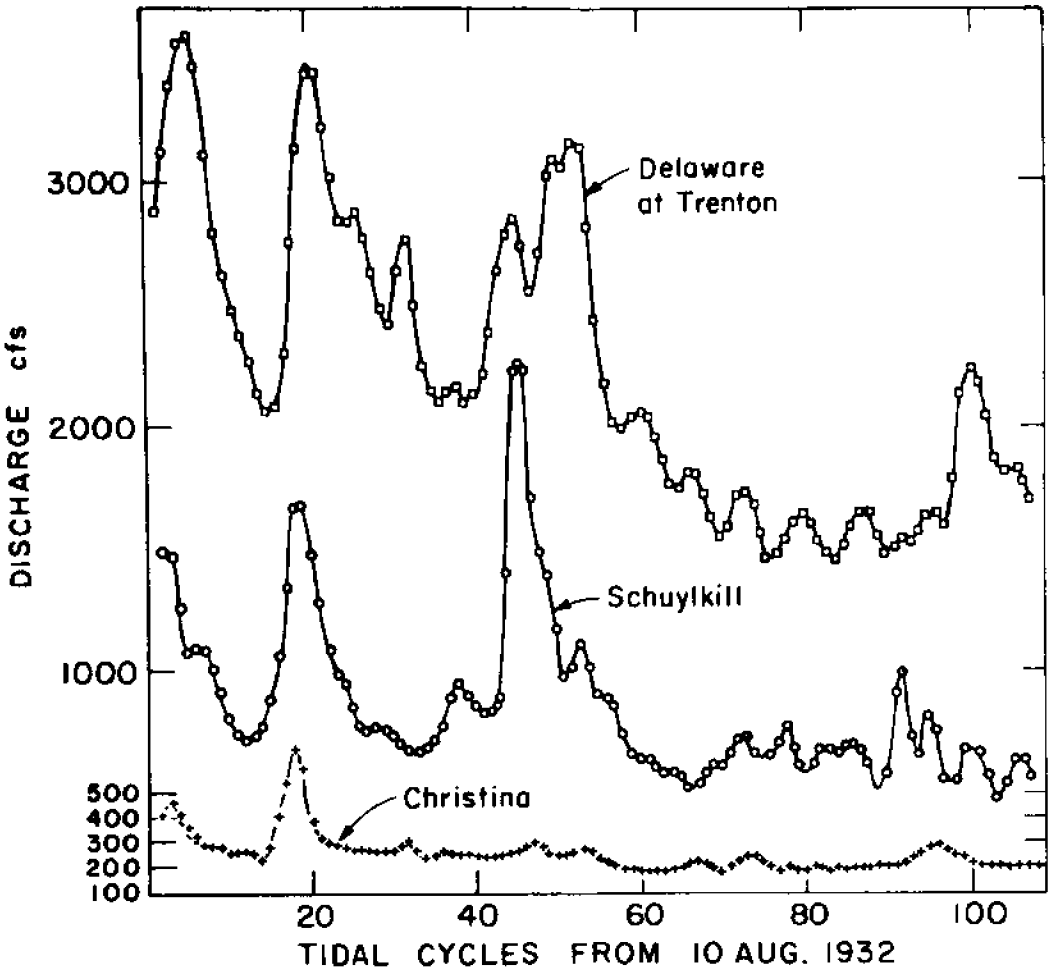

Inflow Hydrograph for Delaware Transient Study

Figure 7.1

Tables (1932). The ocean surface elevation throughout each tidal period of 44712 seconds was obtained by fitting a cosine curve to the high and low water values (Figure 7.2).

For verification of the numerically predicted salinities, this study employed Drawing C-47, "Salinity Movements, Year 1932" of the Sanitary Water Board, Commonwealth of Pennsylvania (Data Source Reference 13). This source of data gives high water slack isochlors for the surface chlorinity throughout the entire year 1932. The initial salinity distribution was taken as that corresponding to the first high water slack chlorinity distribution for the period of interest.

Having thus specified the initial condition for salinity, a 10 cycle lead-in run was made prior to 10 - 11 August in order to provide initial conditions of water surface elevation $\eta(x,0)$ and discharge $Q(x,0)$. The numerical calculation was performed using the correlation line shown in Figure 6.28 in order to continually provide a dispersion parameter which is related to the degree of stratification. At the end of each tidal period of calculation the estuary number, $\mathbb{E}_D$ is computed and the dispersion parameter, K, for the next tidal period is obtained from the correlation of Figure 6.28 as

$$K = 0.002\, u_o\, L\, (\mathbb{E}_D)^{-\frac{1}{4}} \qquad (7\text{-}1)$$

The results of the transient salinity calculation are presented in Figure 7.3. The salinity as a function of time is shown for several stations as oscillating curves describing the salinity variation throughout each tidal cycle. The non-oscillating curve represents the high water slack field data as defined by the isochlors of Drawing D-37

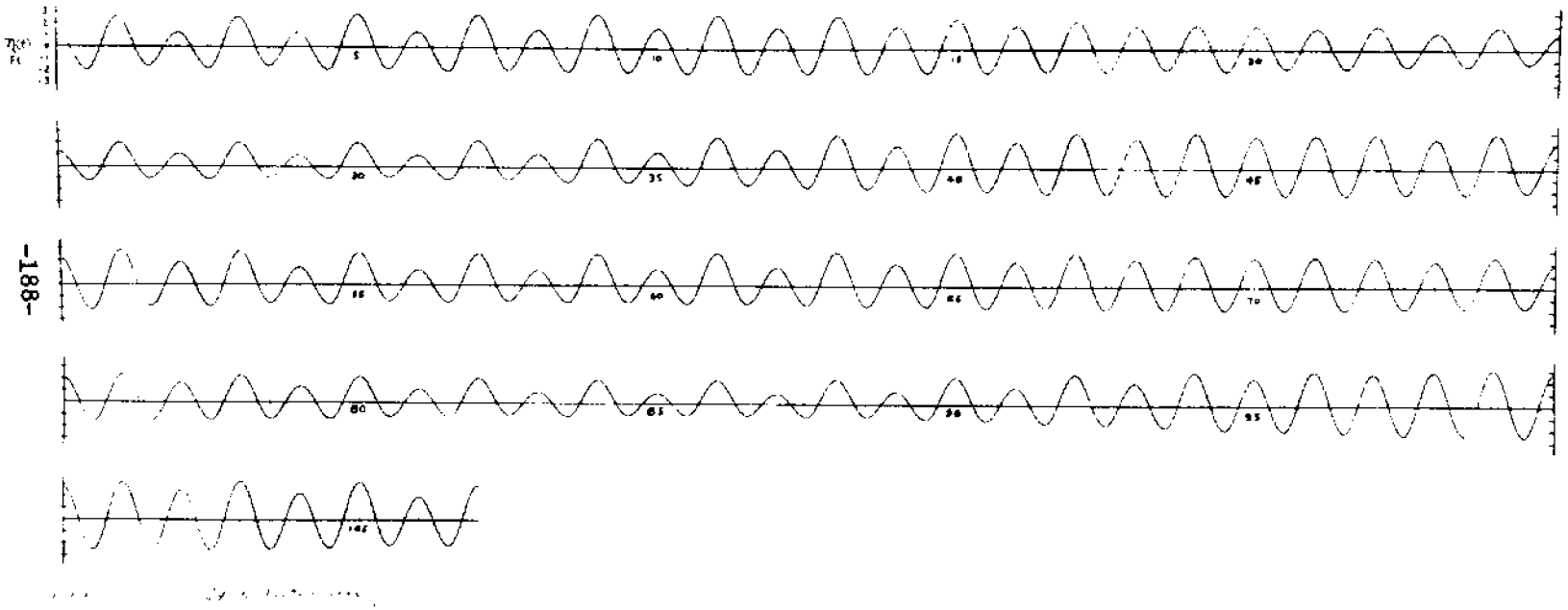

Time Series of Ocean Tidal Elevations
from U.S.C. & G.S. Tide Tables 1932, 10 August - 5 October

Figure 7.2

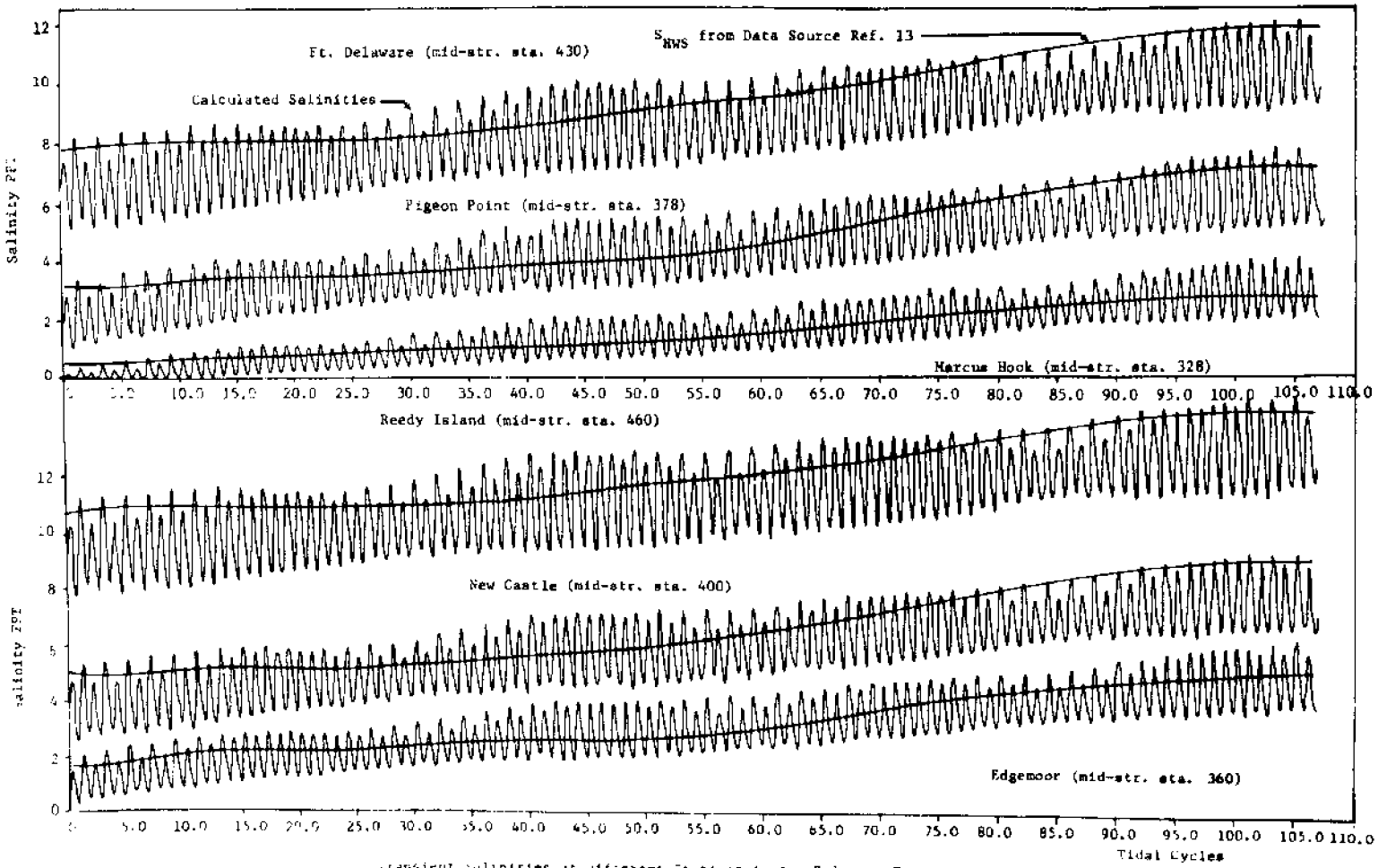

Transient Salinities at Different Stations in the Delaware Estuary
11 August through 5 October, 1932

of the Sanitary Water Board. Verification is good for all stations throughout the entire 107 cycle span.

The field data in this case refer to surface salinities, consequently the numerical model is taking these to be representative of average salinities over the entire cross-section. Wicker (1955) has described the salinity regime of the Delaware and points out that the density structure is fairly homogeneous with similar variations in the salinity-depth relationships for different conditions of fresh water discharge. Under these conditions it is expected that the use of surface salinities should not introduce any appreciable errors in the verification process.

The result shown in Figure 7.3 is an example of the use of the numerical model in a completely predictive manner. No adjustable parameters have been used, the only field data is that necessary to define an initial salinity distribution and the value of the ocean salinity of 32 ppt.

7.3 The Potomac Estuary

The period 24 - 25 July through 21 August 1969 (54 tidal cycles) was chosen for the purpose of a transient verification. The fresh water hydrograph at Chain Bridge shown in Figure 7.4 indicates a period of strong changes in fresh water input preceded by a period of low flow. Figure 7.5 shows the salinity data from the Nutrient Transport Study (Data Source Reference 6) corresponding to this period. It is difficult to explain nearly equal values of salinity at the Wicomico River and Kingcopsico Point on the 1st of August and the salinity at Kingcopsico

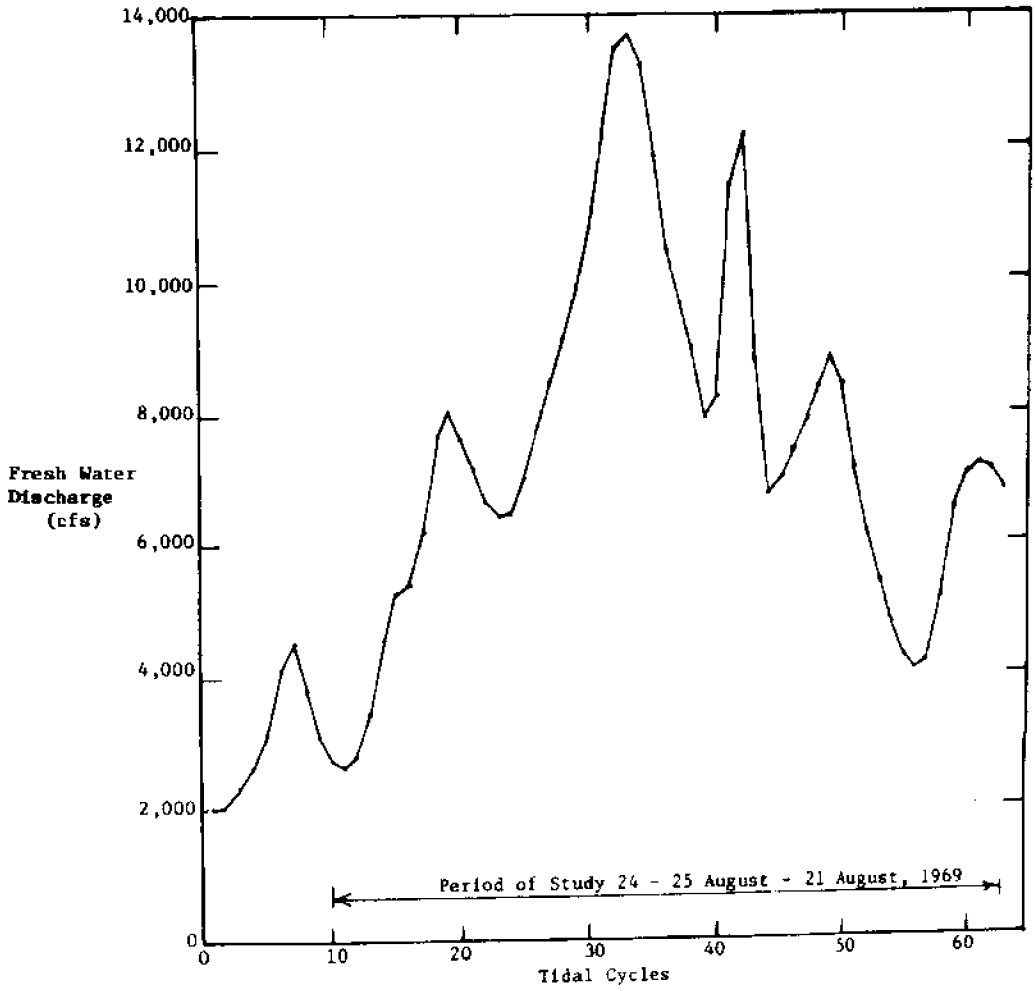

Hydrograph of Fresh Water Inflow at Chain Bridge
Potomac Estuary
(From Data Source Reference 7)

Figure 7.4

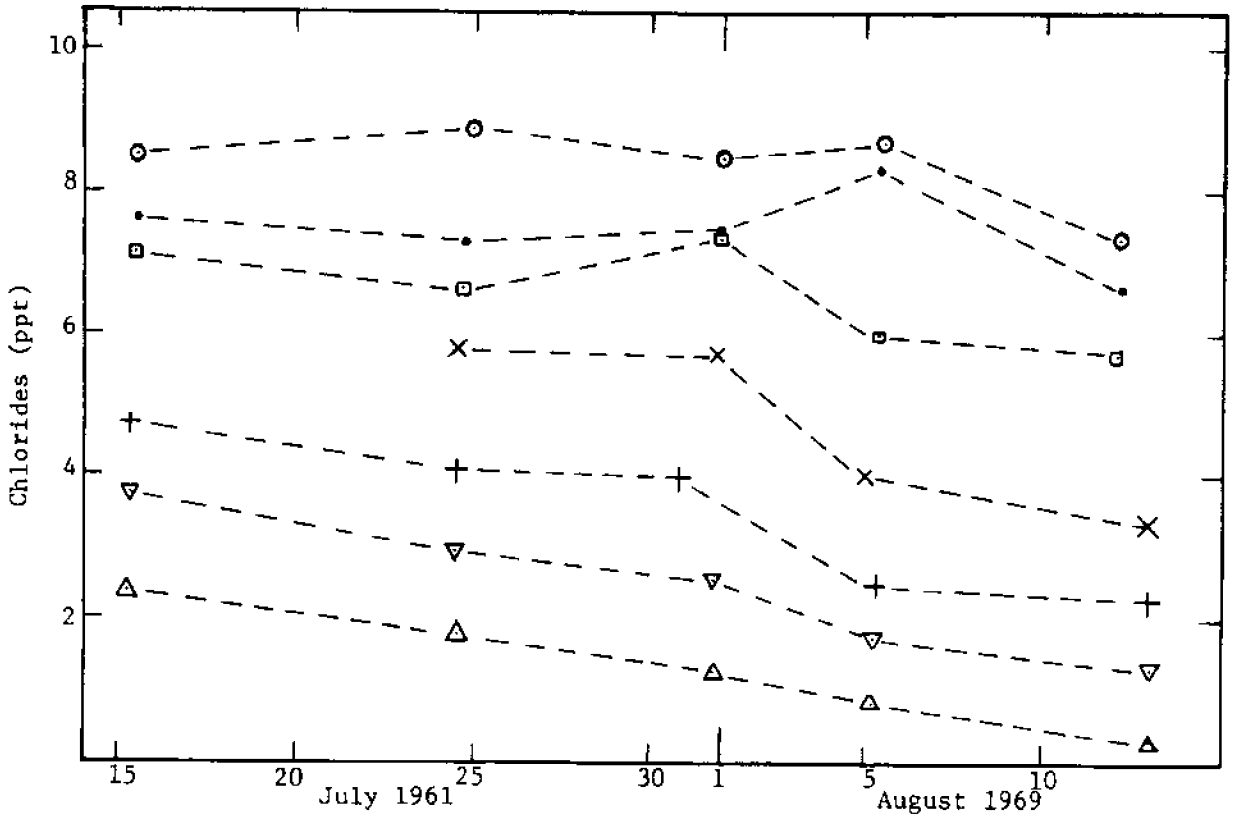

Potomac River Estuary - Transient Chlorinity (24-25 July through 21 August, 1969)

Figure 7.5

Point on the 5th of August, consequently some doubt exists as to the accuracy of the field data at these times and stations.

In order to apply the numerical model to this transient situation it was assumed that the fresh water hydrograph at Chain Bridge was the principal source of fresh water and that the salinity data from Data Source Reference 6 is surface salinity data. Due to these assumptions it is expected that the verification of this data will not be as precise as in the case of the Delaware study. The variation of salinity from surface to bottom is also more pronounced than for the Delaware which makes the use of surface salinities less accurate in terms of verification of the numerical model which computes cross-sectional average salinities.

As discussed in section 6.4.3, the Potomac is a tributary estuary of Chesapeake Bay. This requires that the salinity in the Chesapeake near the entrance of the Potomac be specified in a manner analogous to the specification of the ocean salinity in the case of an estuary terminating at the ocean.

As Chesapeake Bay data was not available for this period of study, the maximum salinity at the entrance of the Potomac was specified in terms of the salinity data at Piney Point. In using this data as a basis for estimating the entrance salinity it is assumed that it is high water slack data. In order to estimate the corresponding salinity at the entrance, which is about 15 miles downstream, data from another source was used. This was data from the Chesapeake Bay Institute Cruise (Data Source Reference 5) which gave a monthly report on salinity

at several stations including stations at the confluence of the Potomac and Chesapeake. In using this data, which is depth averaged, the difference in salinity between that measured at the Chesapeake and that measured at Piney Point was plotted against fresh water discharge in the Potomac in order to show that this difference is not a function of the Potomac discharge. Figure 7.6 illustrates this lack of correlation. The average difference of 0.53 ppt was then added to the Piney Point values and the result interpolated to each tidal cycle of the period of study.

An initial condition on the salinity is derived from the salinity data on or about the 25th of July, and the relationship between dispersion coefficient K and the Estuary Number is that given by Figure 6.28.

The definition of the tidal elevations at the Chesapeake boundary was taken from the Tide Tables (1969) for this period in terms of the variation at Washington back-calculated to the Chesapeake boundary as follows.

As the relationship of the datum from Washington to the Chesapeake was not known, the following assumption was made in order to relate the high and low water values given at Washington with maximum and minimum elevations about the mean water level at the entrance to the Potomac. The Tide Tables show that the relative heights of high and low water for stations near the Chesapeake can be obtained by multiplying the reference station values by 0.45. This multiplication will give the high and low water elevations relative to the local datum.

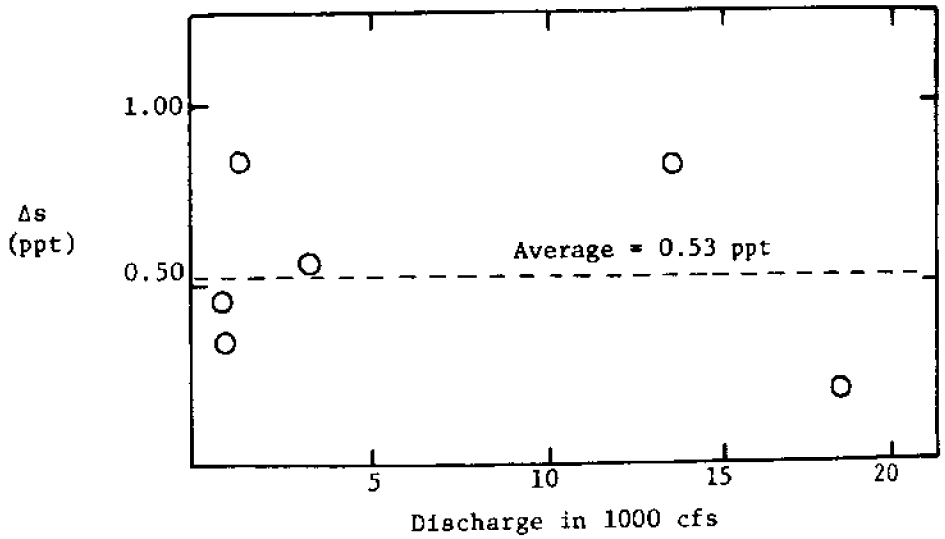

Difference in Depth-averaged Salinity vs. Fresh Water Discharge for Potomac Entrance and Piney Point (C.B.I. Cruise, 1966, Data Source Reference 5)

Figure 7.6

It is noted that the datum at Washington is 1.5 feet below Mean River Level. The mean range at Washington is 3.0 feet which forms the basis for the assumption that the datum is 1/2 the mean range below Mean River Level for the estuary. A typical range at the entrance for the period of interest is 1.7 feet, which gives rise to an approximate formula for obtaining the maximum and minimum water surface elevations, η_{min} and η_{max} at the entrance in terms of the high and low water values at Washington.

$$\eta_{max}\Big|_{entrance} = HW\Big|_{Washington} \times 0.45 - 0.65$$

$$\eta_{min}\Big|_{entrance} = LW\Big|_{Washington} \times 0.45 - 0.65 \qquad (7\text{-}2)$$

The tidal variations in elevation at the entrance to the estuary as calculated by 7-2 are shown in Table 7.1.

Having thus defined the initial condition on salinity, the time-varying boundary conditions on entrance salinity, entrance tidal elevations and fresh water discharge, the numerical model is used to calculate the transient salinity distribution. The resulting salinity variations are shown in Figure 7.7 together with the verification data of Figure 7.5. The numerical predictions are a fair representation of the verification data, the largest deviations occurring at the Kingcopsico Point and Wicomico River. The data for these locations show inconsistency for the 1st and 5th of August (14th and 23rd of the cycle) as mentioned previously. The agreement upstream is good, which indicates that the assumptions concerning the maximum salinity at the

Maximum and Minimum Tidal Elevations
at the Entrance to the Potomac
(Relative to MWL at the Entrance)

Table 7.1

Tidal Period	LW	HW
0		0.52
1	-0.47	0.89
2	-0.52	0.52
3	-0.52	0.88
4	-0.56	0.56
5	-0.56	0.92
6	-0.65	0.61
7	-0.60	0.92
8	-0.69	0.70
9	-0.65	0.97
10	-0.74	0.79
11	-0.69	0.92
12	-0.78	0.83
13	-0.69	0.92
14	-0.78	0.88
15	-0.69	0.88
16	-0.74	0.88
17	-0.65	0.79
18	-0.69	0.88
19	-0.60	0.70
20	-0.65	0.83
21	-0.56	0.61
22	-0.60	0.83
23	-0.52	0.56
24	-0.52	0.79
25	-0.52	0.52
26	-0.47	0.74
27	-0.47	0.47
28	-0.47	0.74
29	-0.52	0.47
30	-0.43	0.74
31	-0.52	0.47
32	-0.43	0.74
33	-0.56	0.52
34	-0.47	0.79
35	-0.56	0.56
36	-0.47	0.79
37	-0.60	0.61
38	-0.47	0.79
39	-0.60	0.65
40	-0.47	0.79
41	-0.56	0.70
42	-0.47	0.79
43	-0.56	0.79
44	-0.47	0.74
45	-0.56	0.83
46	-0.47	0.74
47	-0.52	0.88
48	-0.47	0.70
49	-0.52	0.88
50	-0.43	0.65
51	-0.52	0.88
52	-0.43	0.61
53	-0.47	0.88
54	-0.43	0.56

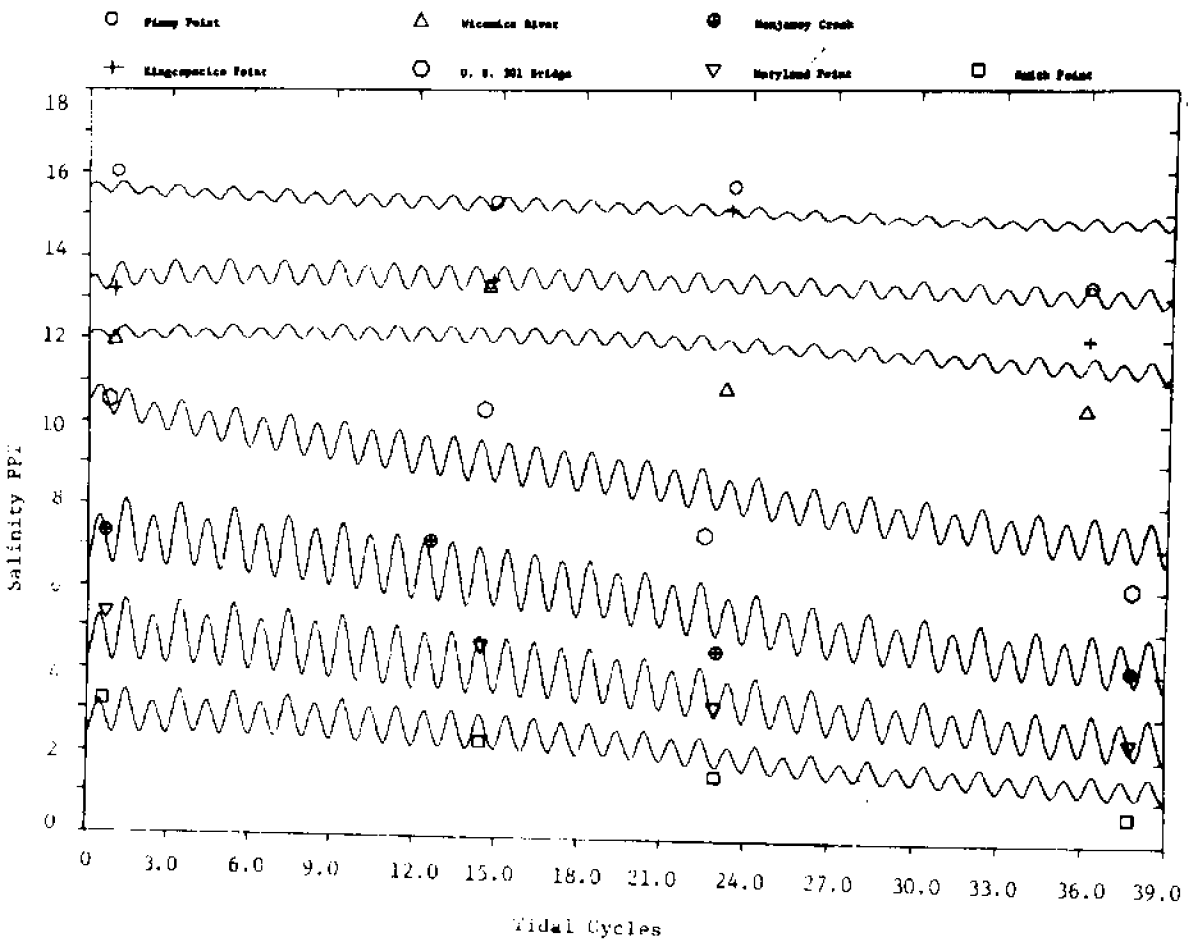

Transient Salinities at Different Stations in the Potomac Estuary
(24-25 July through 21 August, 1969. for station distances, see Figure 7.5)

Figure 7.7

downstream boundary have not affected upstream conditions to any great extent.

7.4 The Hudson Estuary

Data Source Reference 14 contains high water slack salinity data (Figure 7.8) which permits the study of transient conditions for the period 16 - 30 May, 1966. The fresh water hydrograph corresponding to this period was constructed from data of the U.S. Geological Survey (Data Source Reference 15) and is shown in Figure 7.9. Tidal elevations at the Battery as measured by the U.S.C. & G.S. were available and are shown in Table 7.2. These elevations have been adjusted in accordance with Figure 6.25 so as to correspond to a seaward boundary at 59th Street, Manhattan. The seaward boundary was shifted to this location in order to coincide with a salinity measurement station established there.

The salinity measurements at 59th Street, interpolated to each tidal cycle of the study period, serve to define the maximum entrance salinity for the salinity boundary condition. As discussed in section 6.5.3, the entrance boundary condition on salinity is treated in a different manner in this case due to the upstream location of the entrance. This treatment is illustrated in Figure 6.27.

Although the steady-state study of the Hudson resulted in a K value which fell below the correlation of Figure 6.28, this original correlation was used for determining the value of K during the 16 - 30 May 1966 study.

The resulting salinity variations at three stations upstream of 59th Street is shown in Figure 7.10 for the period of study. The

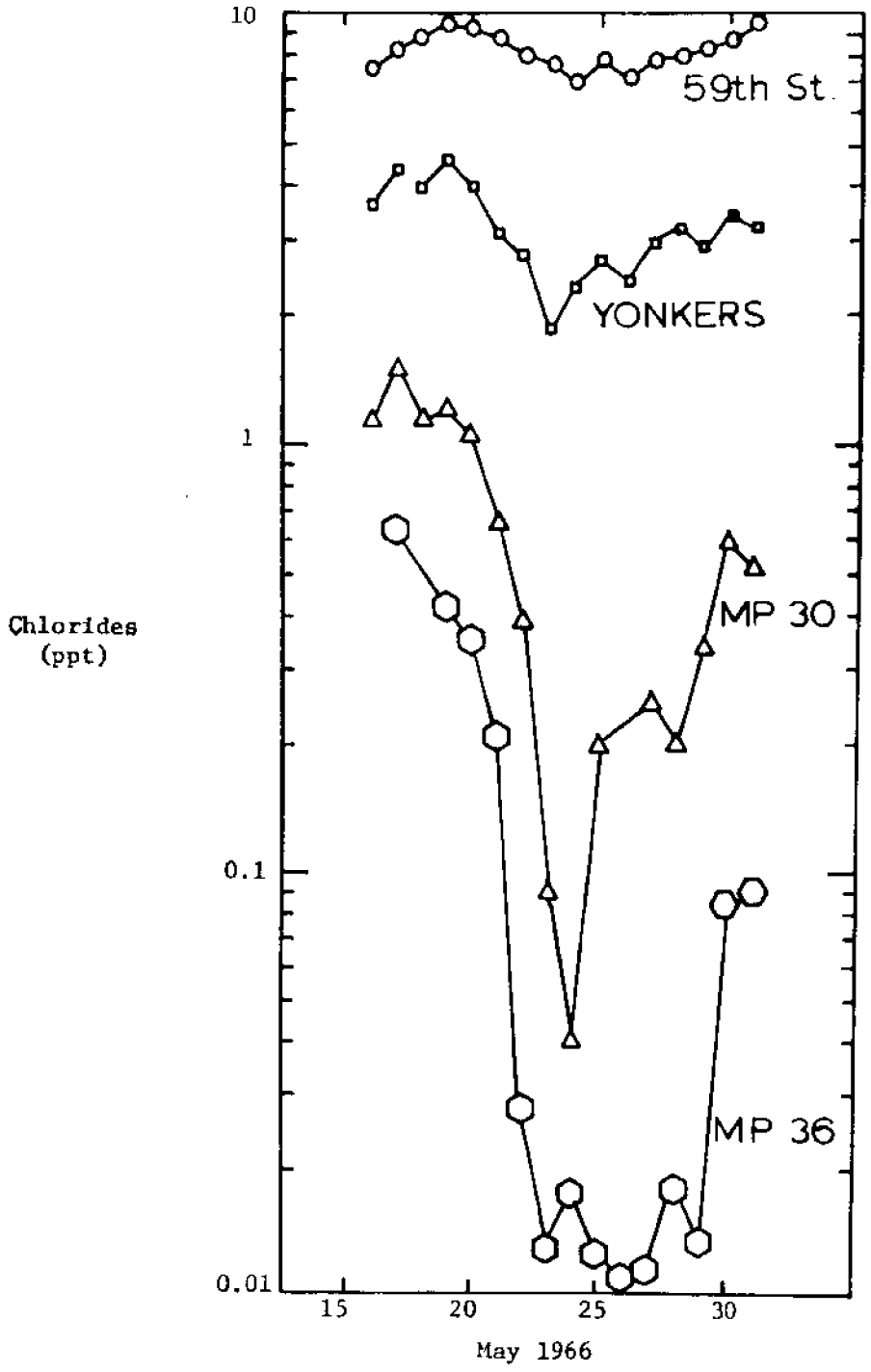

High Water Slack Chloride Profiles, Hudson Estuary
(From Data Source Reference 14)

Figure 7.8

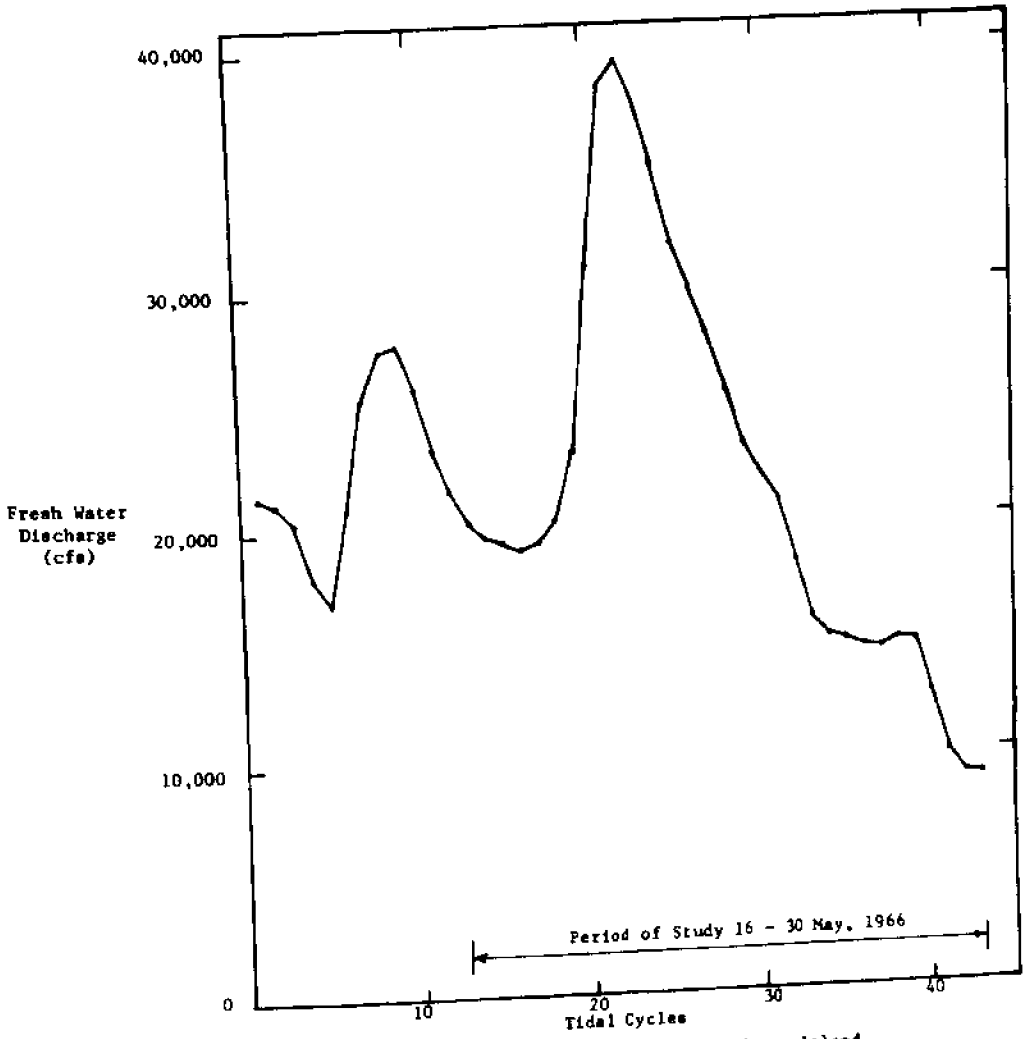

Hydrograph of Transient Inflow at Green Island
Hudson Estuary
(Data Source Reference 15)

Figure 7.9

Maximum and Minimum Tidal Elevations
at 59th Street in the Hudson
(Relative to MWL at 59th Street)

Table 7.2

Tidal Period	LW	HW	Tidal Period	LW	HW
0		2.20	16	-2.00	2.80
1	-1.30	1.80	17	-2.60	1.90
2	-1.40	2.60	18	-1.80	2.60
3	-1.20	2.10	19	-2.30	2.00
4	-1.70	2.70	20	-1.70	2.60
5	-1.70	2.10	21	-2.20	2.10
6	-1.70	3.00	22	-1.50	2.60
7	-1.80	2.50	23	-2.20	2.30
8	-1.80	3.00	24	-1.60	2.50
9	-2.20	2.10	25	-2.10	2.50
10	-2.20	3.10	26	-1.80	2.30
11	-2.40	2.00	27	-2.40	2.70
12	-2.20	3.20	28	-2.20	2.10
13	-2.50	2.20	29	-2.50	3.00
14	-2.00	3.20	30	-2.20	2.30
15	-2.50	2.00	31	-2.60	3.10

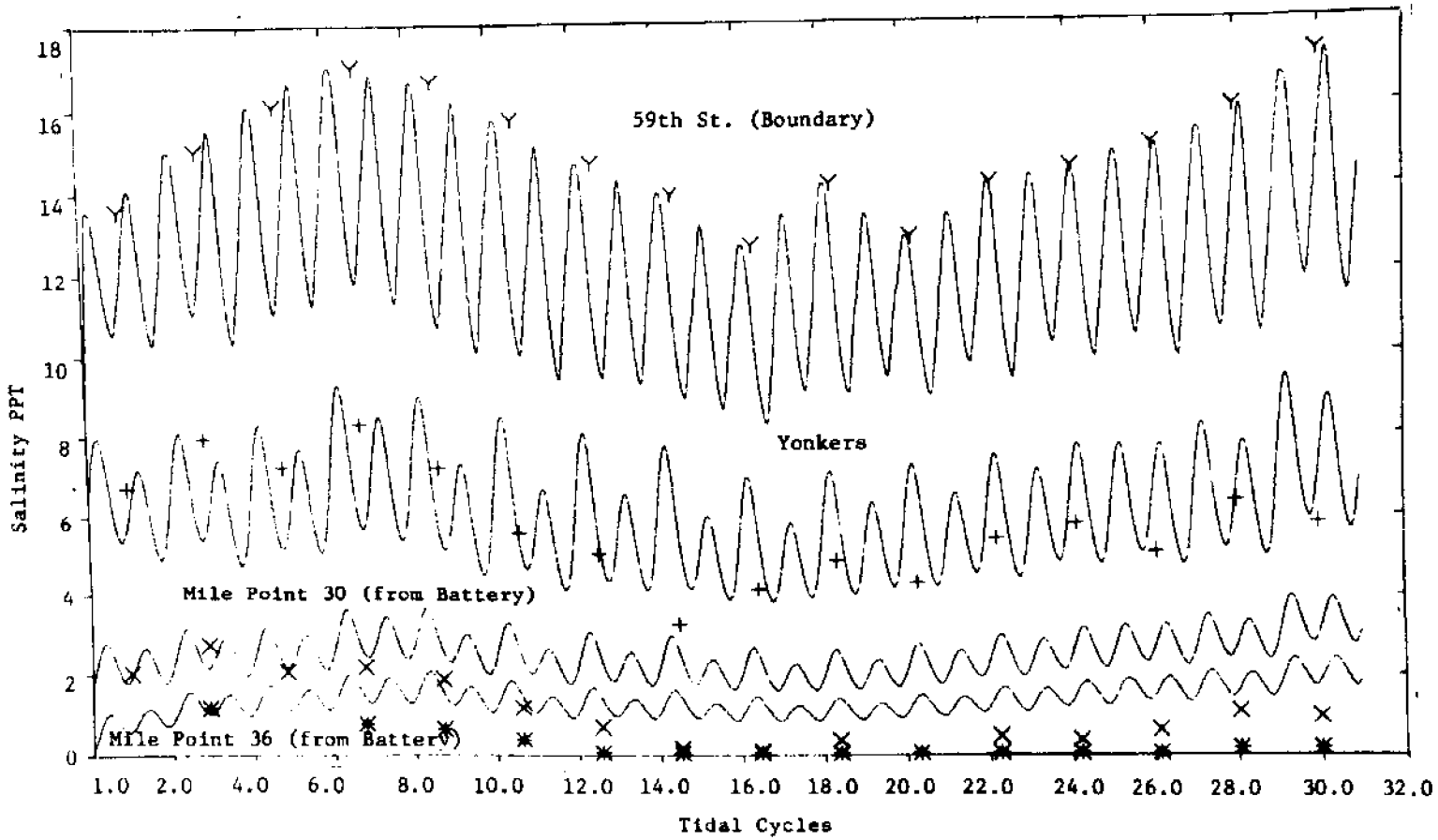

Transient Salinities at Different Stations in the Hudson Estuary
(16 May - 30 May, 1966)

Figure 7.10

variation at 59th Street is also shown. Comparison to the verification data of Figure 7.8 is indicated. It is noted that the verification data is in the form of daily high water slack salinities and consequently it is not possible to determine which of the high water slack times corresponds to this data. Consequently the location of these data points in Figure 7.10 is approximate within about two tidal periods. The comparison shows the predicted salinities to be somewhat higher than the field data.

For this numerical salinity prediction a tidal period of 12.4 hours was taken, the time increment was 223.2 seconds and the corresponding discretization interval was 10719.1 feet (about 2 miles).

7.5 Sensitivity of the Predicted Salinity Distribution to the $K/u_o L$ vs. $\mathbb{E}_D$ Correlation

To test the sensitivity of the predicted transient salinity distribution to the correlation of $K/u_o L$ vs. $\mathbb{E}_D$, a second run was made using the lower correlation line of Figure 7.11. This line expresses the relationship as

$$\frac{K}{u_o L} = 0.0015\ \mathbb{E}_D^{-\frac{1}{4}} \qquad (7\text{-}3)$$

The resulting salinity variations at the stations of interest are shown in Figure 7.12 which when compared with Figure 7.10 show better agreement with the verification data. The difference between the two predictions in terms of the high water slack salinity distribution at the end of the transient period is illustrated in Figure 7.13. In 31 tidal periods the maximum difference is 1.21 ppt or 7% of s_o.

Although the change in resultant salinity distributions favors

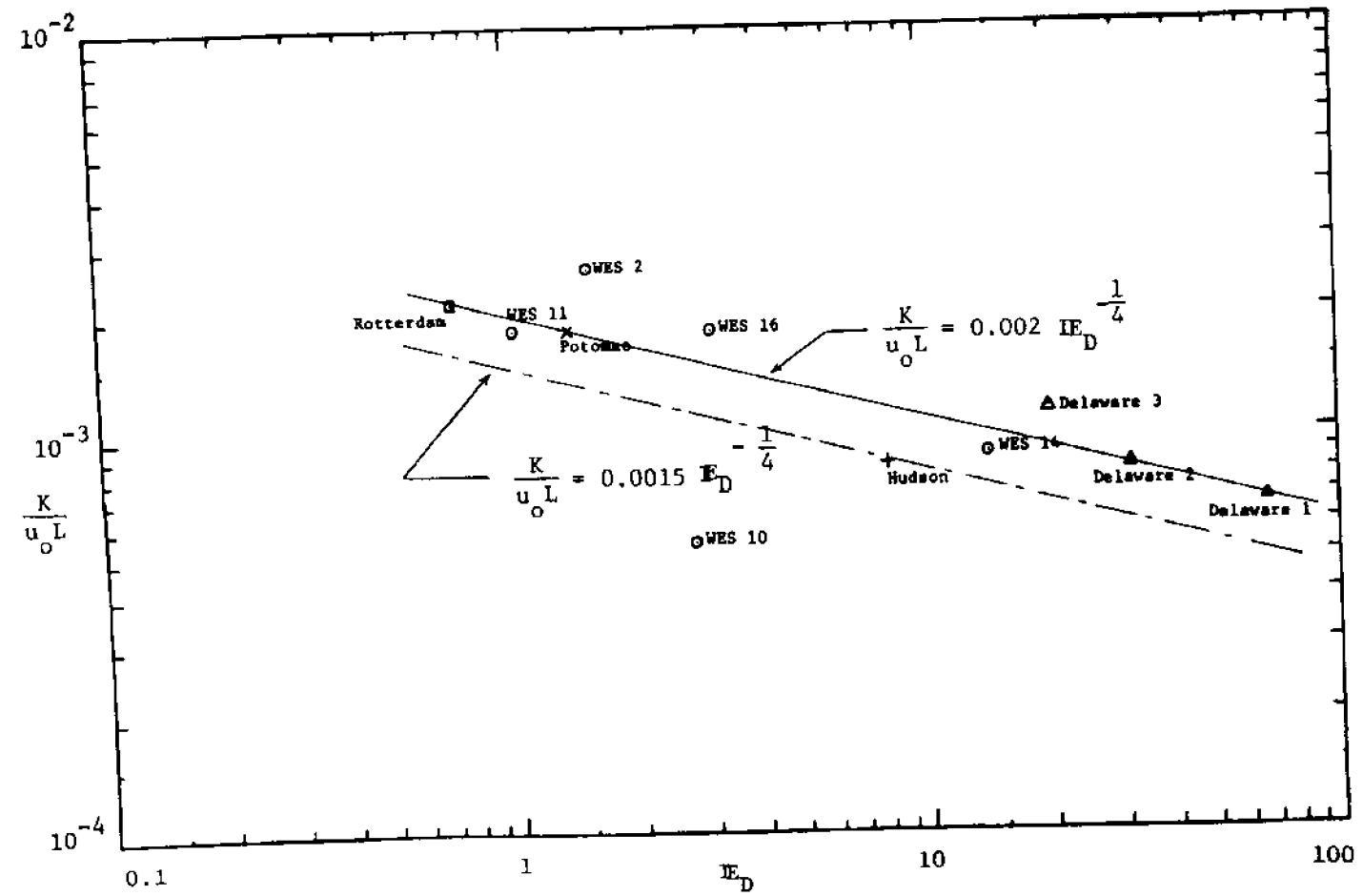

Comparison of Correlations used in Hudson Sensitivity Study

Figure 7.11

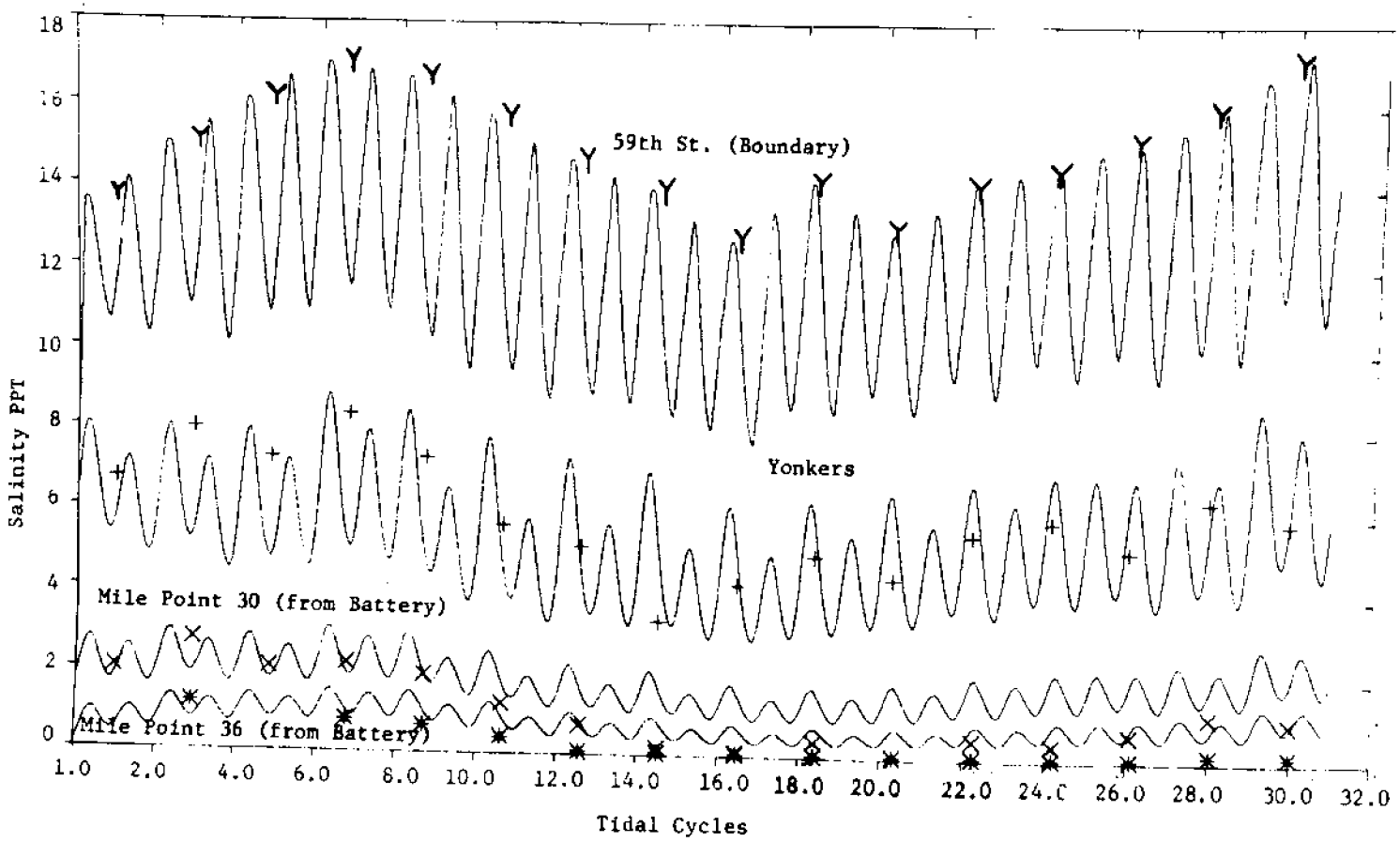

Transient Salinities Calculated Using $\frac{K}{u_o L} = 0.0015\ E_D^{-\frac{1}{4}}$ for Hudson Estuary

(16 May - 30 May, 1966)

Figure 7.12

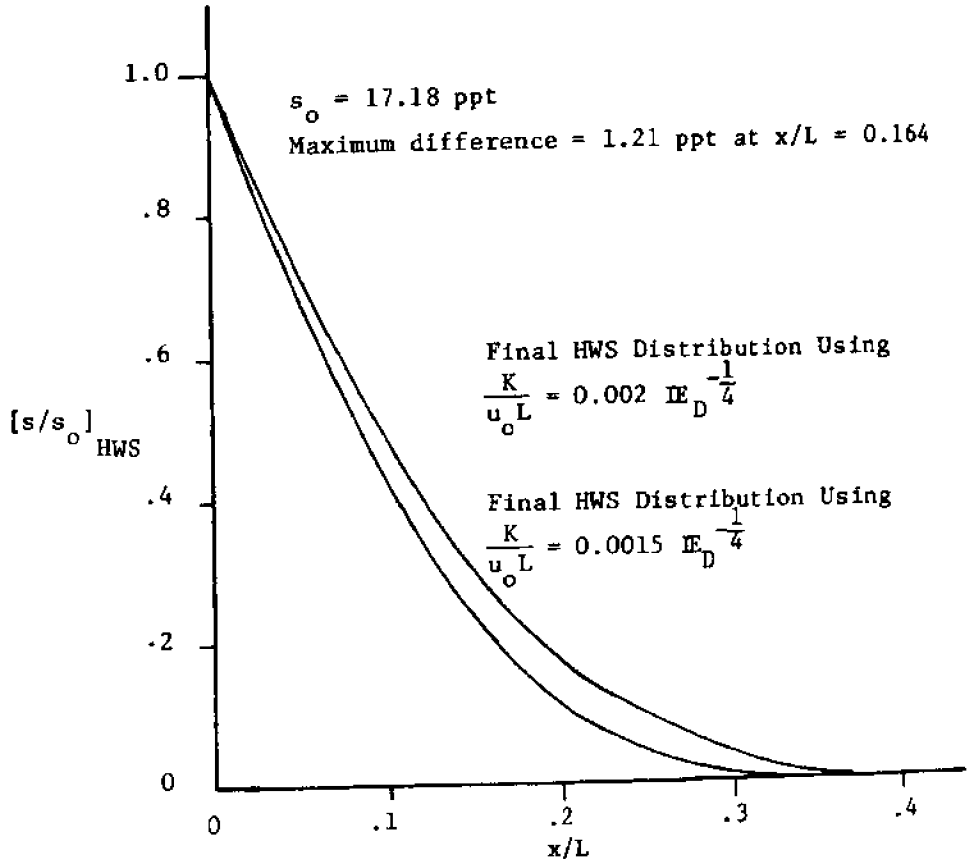

Sensitivity to Dispersion Parameter Correlation
after 31 Tidal Periods for Hudson Transient Study

Figure 7.13

the use of the modified correlation, the use of the original distribution represents the salinity response adequately. The improvement gained through the modification is worthwhile in terms of this particular study, but it is not large enough to put the use of the original correlation line in doubt.

VIII. Summary and Conclusions

8.1 Objective

The primary objective of this study is the prediction of the one-dimensional longitudinal salinity distribution in real estuaries during transient conditions of fresh water inflow and tidal elevations. The time scale for the prediction of the longitudinal salinity distribution is small compared to a tidal period, but greater than that which defines turbulent fluctuation. Therefore, the salinity distribution is defined at intervals within each tidal period and throughout successive tidal periods of a transient study. The prediction of the instantaneous salinity distribution at discrete intervals throughout each tidal period requires a knowledge of the tidal hydraulics; therefore, instantaneous water surface elevations and tidal discharges are predicted concurrently with the salinity.

8.2 Summary

8.2.1 Governing Equations

The governing equations which describe the one-dimensional longitudinal salinity distribution for an estuary of variable area are:

a) the continuity equation for the fluid,

b) the conservation of momentum equation,

c) the conservation of salt equation (salt balance equation), and

d) the equation of state relating salinity and density.

8.2.2 Boundary Conditions

The boundary conditions required to solve the governing equations are

a) specification of tidal elevations at the ocean entrance

as a function of time,

b) specification of fresh water inflow at the upstream boundary, and tributary inflows as functions of time,

c) specification of zero salt flux across the upstream boundary, and

d) specification of conditions on the salinity at the downstream entrance of the estuary.

Of the four boundary conditions, the first three are straight forward and the fourth requires special attention.

The boundary condition on salinity at the ocean entrance has been treated in two parts according to the direction of flow in the estuary. During the flood flow this boundary condition is formulated as $s(0,t) = s_o$, where s_o is the ocean salinity. During the ebb flow the salinity at the downstream boundary is determined by a mass balance, in finite difference terms, at the downstream segment. The Delaware represents this type of ocean boundary.

For an estuary which is a tributary of a larger estuarine system, the magnitude of the salinity s_o entering the tributary estuary on the flood tide is governed by the salinity distribution in the main estuary. The Potomac above its confluence with Chesapeake Bay and the Hudson above the Battery are examples of this case.

8.2.3 Longitudinal Dispersion Relationship

Solution of the conservation of salt equation requires the specification of the longitudinal dispersion coefficient, $E(x,t)$. This dispersion coefficient is shown to be related to the local non-dimensional salinity gradient, $\frac{\partial \overset{\circ}{s}}{\partial \overset{\circ}{x}}$, in the salinity intrusion region. A formulation

which includes a term applicable to the fresh water region of the estuary has been adopted.

$$E(x,t) = K \left|\frac{\partial \bar{s}}{\partial \bar{x}}\right| + 77\, n\, u\, R_h^{5/6} \qquad (8\text{-}1)$$

The constant of proportionality, K, has been related to the degree of stratification as measured by gross estuarine parameters. A correlation has been found between $K/u_o L$ and $\frac{P_T F_D^2}{Q_f T}$ which permits the definition of the dispersion parameter K for each period of a transient study. This correlation has been developed using steady-state data for both model studies and real estuaries, covering a wide range of stratification conditions.

8.2.4 Numerical Model

A finite-difference numerical model consisting of two components provides the solution to the given equations. The first component consists of an explicit, staggered finite-difference scheme for solution of the tidal hydraulics. This scheme was developed in a previous study. The second component of the numerical model consists of an implicit finite-difference scheme for the solution of the salt balance equation. The latter is a second order scheme resulting from a minimum error investigation and does not contain a numerical dispersion term in its truncation error. The boundary conditions are formulated in appropriate finite difference form and the two components are coupled through the salinity-density relationship.

8.2.5 Test Cases

Three real estuaries have been studied using the numerical model. They are the Delaware, the Potomac, and the Hudson. In each case a study has been made wherein the prediction of the transient salinity distribution

has been compared with available prototype data. This comparison was especially good in the case of a 107 tidal cycle study of the Delaware for which daily salinity data was available.

8.3 Conclusions

8.3.1 Ability to Predict Salinity Intrusion

The numerical model described in this study is capable of predicting the longitudinal salinity intrusion for real estuaries as demonstrated by the successful prediction of 107 tidal cycles for the Delaware Estuary. For such a classical estuary, defined from its head of tide to the ocean, it is only necessary to specify an initial conditon of salinity and the value of ocean salinity in order to calculate the response to changes in fresh water discharges and in tidal amplitudes. The method of calculation is flexible and can be extended to estuaries of different geometric configurations and downstream boundaries as evidenced by the studies on the Hudson and the Potomac. For these cases, which did not have a true ocean boundary, additional information on salinity at the downstream boundary was necessary for the solution.

8.3.2 Considerations of Cost

The calculation is feasible in terms of computer time and memory requirements. The cost of computation depends upon the number of sections chosen to represent the estuary and upon the corresponding number of time increments per tidal period. For the Delaware study the space-time grid was 70 x 250 and the cost of computation was about 45¢ per tidal cycle on an IBM 360/65 computer. This implies that a transient salinity study for an entire year would cost about $300 in computer time. When a coarser space-time grid is used considerable reduction in cost results. The

Potomac study was made using a 40 x 120 grid and the cost was about 14¢ per tidal cycle or about $100 for a year's run. The memory requirement for a grid of 200 x 900 is only 110K-bytes.

8.3.3 Comparison with Previous Methods

The prediction of salinity as a function of distance and time by this method represents a definite advance with respect to previous methods such as those utilizing the concept of time-averaging over a tidal cycle. This advance is based on the following considerations.

a.) Previous studies using the time-average approach (such as Pritchard, 1959) are limited to the particular estuary for which salinity distribution data has been available in order to back-calculate the time-average longitudinal dispersion coefficient, E^{TA}. Such correlations are valid only for the range of fresh water inflows covered by the field data.

In this study the longitudinal dispersion coefficient is assumed to be proportional (by a factor K) to the local, dimensionless value of the longitudinal salinity gradient, plus an additional term which represents the longitudinal dispersion coefficient in the fresh water region. A dimensionless form of the factor of proportionality, $\frac{K}{u_o L}$, has been shown to be related to a dimensionless estuary number, $\frac{P_T F_D^2}{Q_f T}$ which expresses the degree of stratification in an estuary. This correlation is generally applicable to different estuaries covering a wide range of geometric and hydraulic conditions. For the laboratory and field cases studies the estuary number varies by two orders of magnitude. Within this range, the parameter $\frac{K}{u_o L}$ varies only by a factor of 5.

Not only does this justify the use of this method over a wide variation of stratification conditions for a particular estuary (such as

those produced by variations in fresh water inflow), but it makes the method applicable to studies involving changes in the geometry of an estuary such as those produced by dredging or other major works. This method also makes it possible to study estuaries for which no previous salinity distribution data exists.

b.) The effect of the variation in ocean tidal elevations and range is incorporated into this method, whereas they are omitted in the time-average-over-a-tidal-cycle method. The changes in tidal amplitude affect the degree of stratification and therefore the dispersion parameter. The incorporation of these hydraulic factors into the time varying salinity prediction is essential if the effects on salinity distribution of the ocean tidal amplitudes are to be represented on either a short term or a long term basis.

c.) The calculation of the salinity throughout the tidal cycle makes it possible to present resulting distributions in a variety of ways according to the need of a particular study. The salinity can be presented in terms of an instantaneous longitudinal distribution for a particular time, a time-averaged over a tidal cycle salinity, a high water slack salinity, or a low water slack salinity.

8.4 Recommendations for Future Work

The numerical model described can be readily combined with numerical models of mass transport of other substances in tidal estuaries. In this manner, the dispersion coefficient in the salinity region can be incorporated into the mass transport study. The concepts used in developing this numerical model can also be extended to the study of one-dimensional estuary networks and to two-dimensional studies in which the

salinity is averaged over the depth.

There is a great need for data on the time-varying behavior of real estuaries. In particular, data is needed which defines the two-dimensional (vertical and longitudinal) circulation and salinity distribution. With such data it is hoped that two-dimensional studies will provide a more rational basis for a formulation of the one-dimensional dispersion coefficient which incorporates the effects of changing stratification conditions without recourse to correlation.

BIBLIOGRAPHY AND REFERENCES

Ames, W.F. (1969), Numerical Methods for Partial Differential Equations, Barnes and Noble, New York.

Aris, R. (1956), "On the Dispersion of a Solute in Fluid Flowing Through a Tube", Proceedings, Royal Society of London, Series A, Vol. 235, No. 1200, April 10, 1956, pp. 67-77.

Arons, A.B. and Stommel, H. (1951), "A Mixing-Length Theory of Tidal Flushing", Transactions, American Geophysical Union, Vol. 32, No. 3, June 1951.

Boicourt, W. (1969), "A Numerical Model of the Salinity Distribution in Upper Chesapeake Bay", Technical Report 54, Chesapeake Bay Institute, The Johns Hopkins University, May 1969.

Carnahan, B., Luther, H.A., and Wilkes, J.O. (1969), Applied Numerical Methods, John Wiley & Sons, New York.

Cohen, B. and McCarthy, L.T., Jr. (1962), "Salinity of the Delaware Estuary", U.S. Geological Survey Water-Supply Paper 1586-B.

Crank, J. and Nicholson, P. (1947), Proc. Cambridge Phil. Soc., 43, 50.

Di Toro, D.M. (1969), "Maximum Entropy Mixing in Estuaries", Journal of the Hydraulics Division, ASCE, Vol. 95, No. HY4, Proc. Paper 6685, pp. 1247-1271, July 1969.

Dornhelm, R.B. and Woolhiser, D.A. (1968), "Digital Simulation of Estuarine Water Quality", Water Resources Research, Vol. 4, No. 6, December 1968.

Eronini, L.O. (1968), "Salinity Intrusion in Variable Area Estuaries", M.S. Thesis, Department of Civil Engineering, M.I.T., February 1968.

Fisher, J.S., Nava, R.E., and Cross, R.H. (1971), "Mathematical Model of the Maracaibo Estuary", Technical Report No. 136, Ralph M. Parsons Laboratory, Department of Civil Engineering, M.I.T., February 1971.

Fofonoff, N.P. (1962), The Sea, Vol. 1, Edited by M.N. Hill, Interscience, New York-London.

Gilcrest, B.R. (1958), Chapter X, Engineering Hydraulics, Edited by H. Rouse, John Wiley & Sons, New York.

Harleman, D.R.F. (1966), Chapter 12, Estuary and Coastline Hydrodynamics, A.T. Ippen, Editor, McGraw-Hill, New York.

Harleman, D.R.F. (1966), Chapter 14, Estuary and Coastline Hydrodynamics, A.T. Ippen, Editor, McGraw-Hill, New York.

Harleman, D.R.F. (1971), Chapter V, "Estuarine Modeling: An Assessment", Water Pollution Control Research Report, Environmental Protection Agency, Washington, D.C., February 1971.

Harleman, D.R.F., McDougall, D.W., Galvin, C.J., and Hoopes, J.A. (1961), "An Analysis of One-Dimensional Convective Diffusion Phenomena in an Idealized Estuary", Technical Report No. 42, Hydrodynamics Laboratory, Department of Civil Engineering, M.I.T., January 1961.

Harleman, D.R.F. and Hoopes, J.A. (1963), "The Prediction of Salinity Intrusion Changes in Partially Mixed Estuaries", Proceedings, 10th Congress, IAHR.

Harleman, D.R.F. and Abraham, G. (1966), "One-Dimensional Analysis of Salinity Intrusion in the Rotterdam Waterway", Publication No. 44, Delft Hydraulics Laboratory, October 1966.

Harleman, D.R.F., Lee, C.H., and Hall, L.C. (1968), "Numerical Studies of Unsteady Dispersion in Estuaries", Journal of the Sanitary Engineering Division, ASCE, Vol. 94, No. SA5, Proc. Paper 6160, October 1968, pp. 897-911.

Harleman, D.R.F., and Lee, C.H. (1969), "The Computation of Tides and Currents in Estuaries and Canals", Technical Bulletin No. 16, Committee on Tidal Hydraulics, U.S. Army Corps of Engineers, September 1969.

Holley, Jr., E.R., and Harleman, D.R.F. (1965), "Dispersion of Pollutants in Estuary Type Flows", Report No. 74, Hydrodynamics Laboratory, Department of Civil Engineering, M.I.T., January 1965.

Holley, E.R., Harleman, D.R.F., and Fischer, H.B. (1970), "Dispersion in Homogeneous Estuary Flow", Journal of the Hydraulics Division, ASCE, Vol. 96, No. HY8, Proc. Paper 7488, pp. 1691-1709, August 1970.

Ippen, A.T., Harleman, D.R.F., and Lin, J.D. (1960), "Turbulent Diffusion and Gravitational Convection in an Idealized Estuary", Technical Report No. 38, Hydrodynamics Laboratory, Department of Civil Engineering, M.I.T., March 1960.

Ippen, A.T. and Harleman, D.R.F. (1961), "One-Dimensional Analysis of Salinity Intrusion in Estuaries", T.B. No. 5, Committee on Tidal Hydraulics, U.S. Army Corps of Engineers, June 1961.

Ippen, A.T. (1966), "Salt-Water Fresh-Water Relationships in Tidal Canals", Proceedings of the 2nd Annual American Water Resources Conference, Chicago, Illinois, November 1966.

Keighton, W.B. (1966), "Fresh-Water Discharge-Salinity Relations in the Tidal Delaware River", U.S. Geological Survey, Water-Supply Paper 1586-G.

Ketchum, B.H. (1951), "The Exchanges of Fresh and Salt Waters in Tidal Estuaries", Journal of Marine Research, Vol. X, No. 1.

Knudsen, M. (1901), Hydrographical Tables, Bianco Luno, Second ed., 1931.

Lai, Chintu (1965), "Flows of Homogeneous Density in Tidal Reaches, Solution by Implicit Method", Open File Report, U.S. Geological Survey, Washington, D.C.

Lee, C.H. (1970), One-Dimensional, Real-Time Model for Estuarine Water Quality Prediction, Ph.D. thesis, Department of Civil Engineering, M.I.T.

Okubo, A. (1964), "Equations describing the diffusion of an introduced pollutant in a one-dimensional estuary", Studies in Oceanography, pp. 216-226, University of Tokyo Press.

Paulson, R.W. (1969), "The Longitudinal Diffusion Coefficient in the Delaware River Estuary as Determined from a Steady-State Model", Water Resources Research, Vol. 5, No. 1, February 1969.

Paulson, R.W. (1970), Variation of the Longitudinal Dispersion Coefficient in the Delaware River Estuary as a Function of Fresh Water Inflow, Water Resources Research, Vol. 6, No. 2.

Preddy, W.S. (1954), "The Mixing and Movement of Water in the Estuary of the Thames", Journal of Marine Biological Association, U.K., Vol. 33, pp. 645-662.

Pritchard, D.W. (1955), "Estuarine Circulation Patterns", Proceedings, ASCE, Sep. No. 717, Vol. 81, June 1955.

Pritchard, D.W. (1959), "Computation of the Longitudinal Salinity Distribution in the Delaware Estuary for Various Degrees of River Inflow Regulation", Technical Report XVIII, Chesapeake Bay Institute, The Johns Hopkins University, September 1959.

Richtmeyer, R.D. and Morton, K.W. (1967), Difference Methods for Initial-Value Problems, Interscience Publishers, New York, Second Edition.

Shinohara, K., Tsubaki, T., Awaya, Y., and Furumato, K. (1969), "Numerical Analysis on the Salinity Intrusion in the Tidal Estuary of Well-Mixed Type", Proceedings of 13th Congress, IAHR, Volume 3c.

Stigter, C. and Siemons, J. (1967), "Calculation of Longitudinal Salt-Distribution in Estuaries as Function of Time", Publication No. 52, Delft Hydraulics Laboratory, October 1967.

Stone, H.L. and Brian, P.L.T. (1963), "Numerical Solution of Convective Transport Problems", Journal of the American Institute of Chemical Engineers, Vol. 9, No. 5, September 1963.

Stroup, E.D. and Lynn, R.J. (1963), "Atlas of Salinity and Temperature Distributions in Chesapeake Bay, 1952-1961 and Seasonal Averages 1949-1961", Chesapeake Bay Institute, The Johns Hopkins University.

Taylor, G.I. (1954), "The Dispersion of Matter in Turbulent Flow Through a Pipe", Proceedings, Royal Society of London, Series A, Vol. 223, No. 1155, pp. 446-468, May 1954.

Tide Tables, Revised Annually, National Ocean Survey (formerly Coast and Geodetic Survey), Department of Commerce, Washington, D.C.

Ward, P.R.B. and Fischer, H.B. (1971), "Some Limitations on Use of the One-Dimensional Dispersion Equation, with Comments on Two Papers by R.W. Paulson", Water Resources Research, Vol. 7, No. 1, February 1971.

Wicker, C.F. (1955), "The Prototype and Model Delaware Estuary", Proceedings of 6th General Meeting of the IAHR.

DATA SOURCE REFERENCES

1. "Table of Accumulated Mid-Tide Volumes", Philadelphia District, U.S. Army Corps of Engineers, 25 September 1951.

2. "Mean Tide Curves - 1948", Philadelphia District, U.S. Army Corps of Engineers, Drawer 151, File No. 22811.

3. Delaware River Model Study, Report No. 2, "Salinity Tests of Existing Channel", Technical Memorandum No. 2-337, U.S. Army Corps of Engineers, Vicksburg, Mississippi, June 1954.

4. Jaworski, N.A. and Clark, L.J., "Physical Data Potomac River Tidal System Including Mathematical Model Segmentation", Technical Report No. 43, Chesapeake Technical Support Laboratory, Federal Water Quality Administration, (about 1970).

5. Whaley, R.C., Carpenter, J.H., and Baker, R.L. (1966), "Data Summary Potomac River Nutrient Cruises 1965-1966", Special Report 11, Chesapeake Bay Institute, The Johns Hopkins University, August 1966.

6. Nutrient Transport Study: Data in the form of computer output from an Information Retrieval File on the Potomac River. This data was furnished by Chesapeake Tech. Support Lab., EPA (formerly FWQA).

7. "Observed Flows, Potomac River near Washington, D.C.", Preliminary report, U.S. Geological Survey, for year ending September 30, 1969.

8. Tidal Bench Marks, New York - Part I, Hudson River and New York Harbor, U.S. Coast and Geodetic Survey, U.S. Department of Commerce 2/4/69 and Tides and Currents in the Hudson River, by Paul Schumann, U.S. Coast and Geodetic Survey, Special Publication No. 180, 1934.

9. KYMA Survey, Data File. 1964 Salinity Intrusion Survey conducted by Quirk, Lawler and Matusky Engineers during November 19 - 24, 1964.

10. "Calculation of Average Lower Hudson River Net Flow of 3500 c.f.s. for period of time during KYMA survey." Calculation based on study of Hudson Flow made by Quirk, Lawler and Matusky Engineers.

11. Delaware River Model Study, Report No. 1, "Hydraulic and Salinity Verification", Technical Memorandum No. 2-337, U.S. Army Corps of Engineers, Vicksburg, Mississippi, May 1956.

12. "Delaware River, Fresh Water Flow Data in C.F.S. Pertinent to Salinities on Plate 55", [of Data Source Reference 11], furnished by Waterways Experiment Station, U.S. Army Corps of Engineers, Vicksburg, Mississippi.

13. "Salinity Movements, Year 1932", Drawing C-47 by the Sanitary Water Board, Commonwealth of Pennsylvania.

14. High Water Slack Chloride Profiles, March-May 1966, Figure D-15 from the files of Quirk, Lawler and Matusky, Engineers.

15. Hudson River Flow at Green Island and Tributaries, U.S. Geological Survey, Year 1966.

LIST OF FIGURES AND TABLES

TABLES

LIST OF SYMBOLS

A	cross-sectional area of the estuary
A_{core}	conveyance as core area of the estuary's cross-section
A_{total}	total cross-sectional area of the estuary
a	tidal amplitude
	pipe radius in Taylor's formula
B	seaward excursion from ocean boundary to point where salinity is constant through tidal cycle
b	total estuary width
b_{core}	width of core area
$b_{storage}$	width of storage area
b_{total}	total estuary width = $b_{core} + b_{storage}$
b'	$b'(z)$, width at elevation z above the horizontal datum
C	Chezy resistance coefficient
c	wave speed (shallow)
D	longitudinal turbulent diffusion coefficient
D'	apparent longitudinal diffusion coefficient
D_m	molecular diffusion coefficient
d	depth of core area
d_c	depth from surface to centroid of core area
d'	depth of storage volume = $\frac{V_{storage}}{b_{storage}\Delta x}$
E	longitudinal dispersion coefficient, $E(x,t)$
E_o	longitudinal dispersion coefficient at ocean where $E(x) = E_o(1-x/L)^3$

E_T - longitudinal dispersion coefficient in fresh water region or for a completely mixed estuary, $E_T(x,t)$

E_{Ψ} - longitudinal dispersion coefficient similar to E_T but with Shinohara's transformation of variable $E(\Psi,t)$

E^{SL} - longitudinal dispersion coefficient, $E^{SL}(x)$ defined by the slack water assumption

E^{TA} - longitudinal dispersion coefficient, $E^{TA}(x)$ defined by the time-average over-a-tidal-cycle assumption

$\mathbb{E}$ - estuary number, $\frac{P_T \mathbb{F}_o^2}{Q_f T}$

$\mathbb{E}_D$ - estuary number, $\frac{P_T \mathbb{F}_D^2}{Q_f T}$, where densimetric Froude number is used

e_x, e_y, e_z - turbulent diffusion coefficients

$\bar{e}_x, \bar{e}_y, \bar{e}_z$ - turbulent diffusion coefficients for equations which have been averaged over a tidal cycle

F_x - force in x-direction

$[F_f]_x$ - x-component of boundary frictional resistance force

$\mathbb{F}_o$ - Froude number evaluated at the entrance to the estuary $= \frac{u_o}{\sqrt{gh}}$

$\mathbb{F}_D$ - densimetric Froude number evaluated at the entrance to the estuary $= \frac{u_o}{\sqrt{gh\ \Delta\rho/\rho}}$

G - rate of tidal energy dissipation per unit mass of fluid

g - acceleration of gravity

h - depth of water in $\sqrt{gh}$

depth from water surface to a horizontal datum in defining the tidal dynamics equations

J - rate of gain of potential energy per unit mass of fluid

K - longitudinal dispersion parameter

L - total length of the estuary

Preddy's mixing length, specified in his method

L_{ex} - length of tidal excursion

n - Manning's resistance coefficient

P - hydrostatic pressure on a vertical cross-section

$(P_w)_x$ - x component of pressure force due to convergent boundaries

P_1 and P_2 - proportional factors in Preddy's method

P_T - the tidal prism, defined as the total volume of water entering the estuary on the flood tide

Q - the instantaneous local discharge, $Q(x,t)$

Q_f - the fresh water inflow just above the salinity intrusion region

$Q_{trib}]_x$ - total inflow due to tributaries entering between sections $x + \Delta x$ and $x - \Delta x$, $= q(2\Delta x)$

q - lateral inflow due to tributaries (per unit length)

R_h - hydraulic radius

S - net amount of salt above a station in Preddy's method

slope of trapezoidal channel

s - salinity concentration, $s(x,t)$ for one-dimensional model

local salinity in any dimensional notation

$\bar{s}$ - time-average over a tidal cycle salinity in salt balance equation

s'' - spacial deviation of salinity over the cross-section

$\overset{\circ}{s}$ - dimensionless one dimensional salinity, $\overset{\circ}{s}(x,t) = s/s_o$

s_o - ocean salinity or maximum salinity at the downstream entrance

T - the duration of the tidal period

t - time

u - the x-component of velocity in several dimensions

the cross-sectional average velocity in a one-dimensional case

$\bar{u}$ - time-average over a tidal cycle cross-sectional velocity

u'' - spacial deviation of longitudinal velocity over the cross-section

u_o - the maximum cross-sectional velocity at the mouth of the estuary

u^* - the friction velocity

u_f - the fresh water velocity, or net velocity over a tidal period

$V_{storage}$ - the volume of the storage in a schematized reach

V_{total} - the total volume in a schematized reach

V_j - the wind velocity at segment j

$\forall$ - volume of Shinohara $= \int_o^x A(x,t)dx$

x - longitudinal axis

$\overset{\circ}{x}$ - dimensionless longitudinal distance = x/L

y - vertical axis for two and three dimensional cases

z - lateral axis for two and three dimensional models

vertical axis for one-dimensional models

z_o - distance from horizontal reference datum to bottom of schematized channel

z' - height of local mean water level above mean water level at the downstream section

α - proportionality factor for assigning shoal area to the core or storage

β_w - wind resistance coefficient

γ - specific weight of fluid

η - surface elevation with respect to mean water level

ρ - density of fluid

ρ_a - air density

Notation Applicable only to Development of the Finite Difference Scheme

A_w - constant depending on w

a - arbitrary weighting coefficient in difference equations

b - arbitrary weighting coefficient in difference equations

c - concentration

D - diffusion coefficient, a constant

d - arbitrary weighting coefficient in difference equations

g - arbitrary weighting coefficient in difference equations

m - arbitrary weighting coefficient in difference equations

V - velocity, a constant

w - harmonic number

β - $\frac{V\Delta t}{\Delta x}$

ε_T - truncation error of the difference equation

$\epsilon/2$ - arbitrary weighting coefficient in difference equations

$\theta/2$ - arbitrary weighting coefficient in difference equations

ρ - decay factor

ϕ - velocity factor